Spontaneous and Induced Radiation by Relativistic Particles in Natural and Photonic Crystals. Crystal X-ray Lasers and Volume Free Electron Lasers (VFEL)

V.G. Baryshevsky

Abstract

The mechanisms of spontaneous and induced radiation produced by relativistic particles passing through natural and photonic crystals are reviewed. The theory of Volume Free Electron Lasers based on spontaneous radiation in natural and photonic crystals is presented.

Contents

Introduction

Current development of Free Electron Lasers (FELs) operating in various ranges of wavelengths – from microwave to optical and even X-ray – which is carried out in some research centers gives reason to return to the problem of the possibility to design the FEL on the basis of the interaction between relativistic electron (positron) beams and either natural or artificial (photonic) crystals. In the X-ray range of wavelengths, operation of this type of crystal X-ray FELs is based on several spontaneous radiation mechanisms: parametric X-ray radiation [17,85,123,124,139], diffracted radiation from relativistic channeled particles [17,19,22,139,142,143,144,145,153], generation of X-ray radiation by particles moving in a crystal undulator [13,17,23,139,155,156,157,158]. It was shown that despite serious difficulties, the law of radiative instability of relativistic beams passing through the crystal, which was discovered in [49], enables achieving the generation threshold for induced X-ray radiation even at the beam current density $j \sim 10^8$ A/cm^2, while the current density required for X-ray laser generation in crystals by means of channeling X-ray radiation or radiation in a crystal undulator is $j \sim 10^{12} \div 10^{13}$ [139].

Below, a brief review of the theory of the crystal FEL (based on either a natural or a photonic crystal) is presented. The review emphasizes the general significance of the law of radiative instability discovered in [49], which finally led to formulating the idea of the possibility to develop a new type of FELs, called Volume Free Electron Lasers [25].

1 Diffraction phenomena accompanying spontaneous and stimulated radiation from relativistic particles in crystals ([139])

The emission of photons by relativistic particles in media has been calling attention for a long time. The main reason why this phenomenon arises such interest is because a wide variety of tasks can be solved by using different radiation mechanisms, such as bremsstrahlung, transition and Cherenkov radiations and so on. The last decades have seen a growing interest in the study of radiation by relativistic particles in both natural and artificial (photonic) crystals. A number of new radiation mechanisms associated with a periodic structure of crystals have been considered theoretically and confirmed experimentally [9,117,139,140,141].

All characteristic properties of radiation are in this case determined by the periodic structure of a crystal. The medium can influence radiation processes under passing of relativistic charged particles through crystals in two ways. First of all, it is well known that the trajectory of a charged particle incident on a crystal at a small angle relative to crystallographic planes or axes is formed by a series of grazing collisions with the atoms of a crystal. As a result, the particle moves in an averaged potential of crystallographic planes or axes. In this case we speak about the channeling phenomenon and can consider the motion of channeled particles as the motion inside a potential well – one-dimensional (for plane channeling) or two-dimensional (for axial channeling). According to quantum mechanics a particle moving inside a potential well has a discrete energy spectrum, which is the spectrum of the particle transverse motion. Consequently, such particles can be considered as one-dimensional or two-dimensional atoms (oscillators) characterized by a spectrum of bound

states (zones) of transverse energy ε_n, ε_f. The number of bound states and their characteristics depend on the longitudinal particle energy. One can conclude that many phenomena observed for ordinary atoms will manifest themselves when channeled particles pass through crystals. It is obvious that thus excited atoms should emit photons with the energy equal to the difference between atomic state energies ε_n and ε_f. The frequency of transition $\Omega_{nf} = \varepsilon_n \varepsilon_f$ and depends, in a laboratory frame, on the total particle energy. By analogy with an ordinary moving oscillator, the frequency of the emitted photons is evaluated by the Doppler effect and determined by the following expression:

$$\omega = \frac{\Omega_{nf}}{1 - \beta n(\omega) \cos\theta}, \tag{1}$$

where θ is the radiation angle, $\beta = u/c$, u is the longitudinal particle velocity, $n(\omega)$ is the refraction index of the photon with a frequency ω in the medium.

The relativistic oscillator can be formed not only by an unperturbed crystal channel, but also by an external ultrasonic or laser wave which propagates in the crystal, creating a bent crystal channel [13,17,123,139,155,156,157,158]

On the other hand, when the wavelength of the emitted photons is of the order of the interplanar spacing of atoms in the crystal, radiation diffraction can essentially modify the photon state [123]. In this case the radiation process is characterized by several indices of refraction $n_i(\omega)$ dependent on the direction of the photon momentum, which, in turn, leads to the modification of all mechanisms of radiation formation by relativistic particles in the X-ray range of spectrum. For example, radiation at a large angle relative to the direction of particle motion becomes possible. As a result, the diffraction pattern characterizing a given crystal is formed. The analysis of dielectric properties of a

crystal under diffraction conditions shows that at least one of several indices of refraction $n_i(\omega)$, characterizing the crystal under this condition, becomes greater than unity within a frequency interval. As a consequence, the Vavilov-Cherenkov condition can be fulfilled. In this case spontaneous and induced X-ray radiation analogous to optical Cherenkov radiation appears as well as diffracted transition radiation [123]. Spontaneous quasi-Cherenkov radiation, currently referred to as parametric (quasi-Cherenkov) X-ray radiation (PXR), is thoroughly investigated both theoretically and experimentally (see [85]).

Under diffraction conditions, the radiation of a relativistic oscillator also modifies essentially. Now the periodic structure of a crystal affects both the particle motion and the particle state. This leads to the formation of diffracted radiation of oscillator (DRO), which cannot be reduced to the sequence of two independent processes: radiation by oscillator and diffraction of radiated photons. In this case the process of photon emission and its diffraction are developing simultaneously and coherently and result in the radiation with new properties. Radiation produced by channeled particles is often called the diffracted channeling radiation (DCR).

These types of X-radiation (DRO, DCR), also associated with a change in the indices of refraction under diffraction conditions, was considered in [19] and then in [11,12,20]. Currently, there is an increased interest in DCR (see [142,143,144,145,153]). If, in the absence of diffraction, the X-ray spectrum of the oscillator is determined by the complex Doppler effect ($n(\omega) < 1$), then, under diffraction, the index of refraction can become greater than unity and, consequently, the anomalous Doppler effect is possible. In this case the photon emitted by the oscillator is accompanied by the excitation of the oscillator itself. This is one of the important features of diffracted radiation of

the oscillator (DRO).

So, the modification of refractive properties in periodic media under diffraction leads to the appearance of two types of radiation with angular distribution forming a diffraction pattern determined by the parameters of the periodic medium. Depending on the excited reflex, the spectrum of PXR and DRO for crystals with lattice parameters of the order of Å lies in the range of X-ray and even higher frequencies.

It is well known that in an amorphous medium, the ordinary Cherenkov radiation can be considered as a specific case of radiation of the oscillator with zero eigenfrequency [18]. Similarly, in a periodic medium, the frequency of PXR can be expressed by (1) in the specific case of $\Omega_{nf} = 0$, i.e., $1 - \beta n_i(\omega)\cos\theta = 0$, where $n_i(\omega)$ is the refraction index of the crystal under diffraction conditions.

2 Dispersion characteristics of parametric X-ray radiation (PXR) and diffracted radiation of oscillator (DRO)

Under diffraction the index of refraction depends on the direction of particle motion and the frequency of radiated photon, therefore equation (1) determining the radiated photon spectrum is the equation with several solutions [11,19,20,21,22].

For example, let us consider the case of two-wave diffraction, when the diffraction condition is fulfilled only for a reciprocal lattice vector $\vec{\tau}$. It means that two strong waves with wave vectors $\vec{k}$ and $\vec{k}_{\vec{\tau}} = \vec{k} + \vec{\tau}$ are excited under diffraction. For the simplicity of analysis of photon frequencies, let us represent (1)

in the form:

$$n(\omega) = \frac{\omega - \Omega_{nf}}{\omega\beta\cos\theta}, \tag{2}$$

In this case the index of refraction in a crystal under diffraction conditions is characterized by two dispersion branches $n_{1,2}$. Using a well-known expression for $n_{1,2}$, one can rewrite (2) as follows:

$$\begin{aligned} &\frac{1}{\beta\cos\theta} - \frac{\Omega_{nf}(1-\delta)}{\omega_B\beta\cos\theta} \\ &= 1 - \frac{\omega_L^2}{4/\omega^2}\left\{(1+\beta_1) - A\beta_1\frac{\delta}{|g_0|} \mp \sqrt{\left[(\beta_1-1) - A\beta_1\frac{\delta}{|g_0|}\right]^2 + 4\beta_1\frac{|g_\tau|^2}{g_0^2}}\right\} \end{aligned} \tag{3}$$

for the diffracted radiation of the oscillator (DRO) and

$$\begin{aligned} &\frac{1}{\beta\cos\theta} \\ &= 1 - \frac{\omega_L^2}{4/\omega^2}\left\{(1+\beta_1) - A\beta_1\frac{\delta}{|g_0|} \mp \sqrt{\left[(\beta_1-1)^2 - A\beta_1\frac{\delta}{|g_0|}\right]^2 + 4\beta_1\frac{|g_\tau|^2}{|g_0|^2}}\right\} \end{aligned} \tag{4}$$

for parametric quasi-Cherenkov radiation (PXR), generated by a particle passing through a crystal at constant velocity.

We have introduced the following notations:

$$\alpha = \frac{2(\vec{k}\vec{\tau}) + \tau^2}{\omega^2/c^2},$$

is the deviation from the exact Bragg conditions,

$$\alpha \cong \alpha_{\omega_B} + \left(\frac{\partial\alpha}{\partial\omega}\right)_{\omega_B}(\omega - \omega_B) = \frac{\tau^2c^2}{\omega_B^3}(\omega - \omega_B) = -A\delta,$$

where

$$A = \frac{\tau^2c^2}{\omega_B^2} > 0$$

$\delta = \omega - \omega_B/\omega_B$, $\omega_B = \tau^2 c^2/2|\vec{\tau}\vec{\beta}|$ is the Bragg frequency, corresponding to $\alpha = 0$, $\beta_1 = k_z/k_z + \tau_z$ is the geometry factor of diffraction asymmetry, the z-axis is chosen as a normal to the target surface directed inward the crystal. Let us assume that the particle with a mean velocity $\vec{u}$ moves along the z-axis, $\beta = u/c$, g_0, g_τ are the coefficients in a series expansion in terms of the reciprocal lattice vectors of the crystal susceptibility. For simplicity, we shall assume that a crystal is center-symmetric and absorption is neglected, $\omega_L^2 = 4\pi e n_0/m_c$ is the Langmuir frequency of the medium.

Let us consider in detail the conditions of the existence of parametric X-ray radiation. Indeed, for the existence of this radiation it is sufficient that relation (4) be fulfilled at least for one of the two indices of refraction characterizing the crystal at a given frequency. On the left-hand side of (4), there is a term greater than unity ($\beta < 1$ and $|\cos\theta| < 1$). Consequently, for the existence of the solution of equation (4), the expression between the braces on the right-hand side of (4) should be less than zero. Far from Bragg conditions $\delta \to \infty$, and we transit to a well-known case of amorphous medium., i.e., to the index of refraction $n(\omega) = 1 - \omega_L^2/2\omega^2 < 1$ for any frequencies within the X-ray range. As a result, in this range Cherenkov radiation is impossible. The analysis of (4) near Bragg condition $|\alpha| \leq |g_0|$ shows that the expression between the braces is always positive for one dispersion branch corresponding to the sign $(-)$; consequently, the fulfilment of (4) is impossible. For the second branch corresponding to the sign $(+)$, this expression can be negative at $|\alpha| \geq |g_0|$. For example, in the case of

$$\left|(\beta_1 - 1) - A_{\beta_1}\frac{\delta}{|g_0|}\right| \gg 4\beta_1\left|\frac{g_\tau}{g_0}\right|^2,$$

we can approximately write

$$\frac{1}{\beta\cos\theta} \cong 1 - \frac{\omega_L^2}{2\omega^2}\beta_1\left[1 - A\frac{\delta}{|g_0|}\right]$$

and, obviously, the fulfilment of the Cherenkov condition is possible for Laue diffraction case ($\beta_1 > 0$) at frequencies for which

$$\left|A\frac{\delta}{|g_0|}\right| > 1.$$

In Bragg diffraction case ($\beta_1 < 0$), the Cherenkov condition can be fulfilled not only for one dispersion branch but even for two branches at the degeneration point.

Comparison of (4) and (3) shows that the relation (3) can be satisfied for both dispersion branches at $\Omega_{nf} > 0$, i.e., for radiation accompanied by the transition of the channeled particle to a lower energy level ($\varepsilon_n > \varepsilon_f$). This means that photons with two different frequencies are radiated at a given angle. In this situation we observe a normal complex Doppler effect. In this case, equation (3) is satisfied for radiation angles larger than the angle of parametric (quasi-Cherenkov) radiation. At the same time, the fulfilment of (3) leads to the strong limitation of the particle energy, the radiation angle and the value of deviation from the exact Bragg condition α for the radiation accompanied by the oscillator excitation $\Omega_{nf} < 0$ ($\varepsilon_n < \varepsilon_f$). In this case, according to (3), radiation of a photon (anomalous Doppler effect) with the wave vector directed at a smaller angle relative to the direction of the particle motion than the angle of parametric (quasi-Cherenkov) radiation is possible for one of the dispersion branches.

Equation (3) can be analytically treated for a specific case when

$$2\frac{\omega_L^2}{\Omega^2}\phi(\omega,\theta)(1-\beta\cos\theta)\ll 1, \tag{5}$$

where

$$\phi(\omega,\theta)=\frac{1}{2}\left\{1+\beta_1-A\beta_1\frac{\delta}{|g_0|}\mp\sqrt{\left(\beta_1-1-A\beta_1\frac{\delta}{|g_0|}\right)^2+4\beta_1\left|\frac{g_\tau}{g_0}\right|^2}\right\} \tag{6}$$

Let us represent (3) in the form:

$$\omega=\frac{\Omega_{nf}}{2(1-\beta\cos\theta)}\left(1\pm\sqrt{1-2\frac{\omega_L^2}{\Omega^2}\phi(\omega,\theta)(1-\beta\cos\theta)}\right) \tag{7}$$

In view of (5), (7) splits into two independent equations corresponding to the upper and the lower radiation branches in the absence of diffraction.

$$\omega_I=\frac{\Omega_{nf}}{1-\beta\cos\theta}-\frac{\omega_L^2}{2\Omega_{nf}}\phi(\omega,\theta), \tag{8}$$

$$\omega_{II}=\frac{\omega_L^2}{2\Omega_{nf}}\phi(\omega,\theta). \tag{9}$$

Neglecting the dependence of β_1 on ω, one can obtain the frequency solutions of (8) and (9) as a function of a radiation angle:

$$\begin{aligned}\omega_{I\pm}=\omega_m-\omega_0\Bigg[&\frac{1+\beta_1}{2}-\frac{x}{2}\left\{1+\frac{\omega_m-\omega_B}{\omega_0}\right.\\&\left.\pm\sqrt{\left(\frac{1-\beta_1}{x}+1-\frac{\omega_m-\omega_B}{\omega_0}\right)^2-4\left|\frac{g_\tau}{g_0}\right|^2\frac{1}{x}}\right](1-x)^{-1}\Bigg],\end{aligned} \tag{10}$$

$$\begin{aligned}\omega_{II\pm}=\omega_0\Bigg[&\frac{1+\beta_1}{2}+\frac{x}{2}\left\{1+\frac{\omega_B}{\omega_0}\right.\\&\left.\pm\sqrt{\left(\frac{1-\beta_1}{x}+1-\frac{\omega_B}{\omega_0}\right)^2+4\left|\frac{g_\tau}{g_0}\right|^2\frac{1}{x}}\right](1+x)^{-1}\Bigg],\end{aligned} \tag{11}$$

where

$$\omega_0 = \frac{\omega_L^2}{2\Omega}, \quad \omega_m = \frac{\Omega}{1-\beta\cos\theta}; \quad {}_B = \frac{\tau^2}{2}\left\{|\vec{\tau}_\parallel|\cos\theta - |\vec{\tau}_\perp|\sin\theta\cos\varphi\right\}^{-1}$$

$$x = \frac{\beta_1}{\Omega}\left(|\vec{\tau}_\parallel|\cos\theta - |\vec{\tau}_\perp|\sin\theta\cos\varphi\right),$$

$\vec{\tau}_\parallel$ and $\vec{\tau}_\perp$ are the projections of the reciprocal lattice vector onto the direction of the particle mean velocity and onto the plane perpendicular to particle velocity, respectively; φ is the angle between $\vec{\tau}_\perp$ and $\vec{k}_\perp$. The dependence $\omega = \omega(\theta)$ for the case of symmetric diffraction $\beta_1 = 1$ is shown in Figure 1

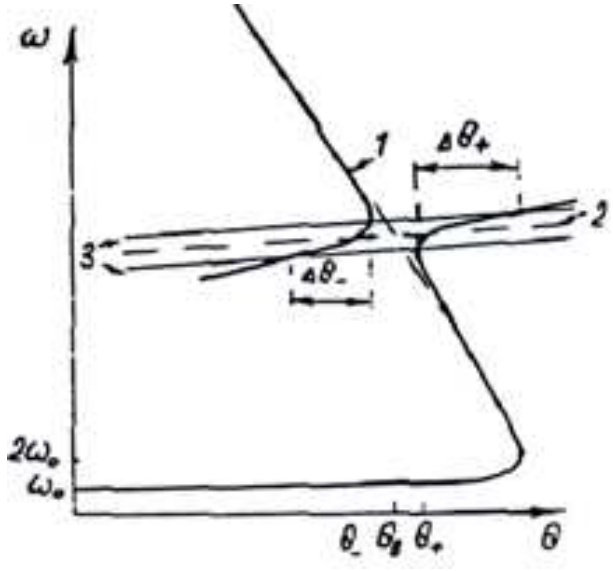

Figure 1. The dependence $\omega = \omega(\theta)$ for the case of symmetric diffraction $\beta_1 = 1$

According to Figure 1 and (10) and (11), the spectrum of radiated photons essentially modifies under diffraction. In the absence of diffraction, each radiation branch splits into two subbranches. Thus, diffraction results in the excitation of an additional branch in the complex Doppler effect with the frequency close to the Bragg frequency ω_B, and in the formation of a radiation non-transparency range in the angular distribution $\Delta\theta = \theta_+ - \theta_- = 10^{-5} \div 10^{-6}$ rad. When the angle θ changes, the solution is first realized for one dispersion

branch and then for the other. Figure 1 shows the angular range in which $|\alpha| \leq |g_0|$. It should be noted that the radiation frequency of the additional diffraction branch changes a little with the change in the radiation angle. As a result, the angular range, in which $|\alpha| \leq |g_0|$, may considerably exceed the ordinary angular interval, characterizing diffraction of an X-ray external monochromatic wave, when $\Delta\theta$ is of the order of several angular minutes (in Figure 1, this is the angular interval $\Delta\theta = \Delta\theta_+ + \Delta\theta_-$). As it is rather complicated to obtain the analytical solution, the numerical calculation of the dependence of $|\alpha|/|g_0|$ on the radiation angle θ near the Bragg angle θ_B was made for the oscillator moving along the crystal direction $\langle 110 \rangle$ and photon diffraction by crystallographic planes (400) in Si. According to these calculations, the magnitude of $\Delta\theta$ weakly depends on the energy and eigenfrequency of the oscillator and retains within the interval $10^{-4} - 10^{-3}$. In Figure 2, the magnitude of $|\alpha|/|g_0|$ is shown as a function of the angle θ at the following parameters of the oscillator: $\Omega = 1$ eV, $\gamma = 2 \cdot 10^3$. As one can see, $\Delta\theta_- \approx 4 \cdot 10^{-3}$ rad, $\Delta\theta_+ = 5.2 \cdot 10^{-3}$ rad and the total interval $|\alpha| \leq |g_0|$, $\Delta\theta = 9.2 \cdot 10^{-3}$ rad.

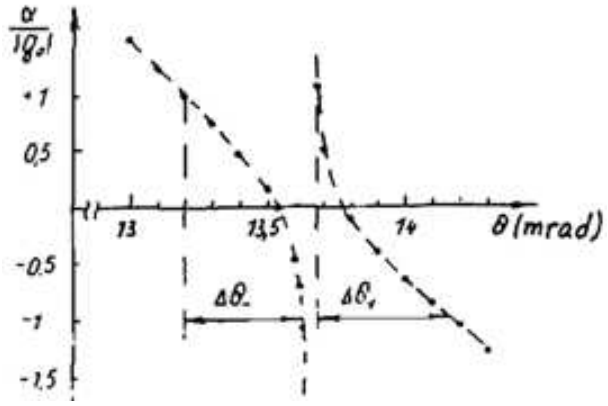

Figure 2.

The values of the angles $\theta_\pm$ at $\alpha = 0$ are determined from the equation

$$\omega_B = \omega_m - \omega_0 \left(1 \pm \frac{g_\tau}{g_0}\right). \tag{12}$$

A similar picture is also observed for the second branch (see (11)). So, if $\omega_0 \neq \omega_B$, and the second term in the radicand of (11) is negligible, then, for example, $\omega_{II+} = \omega_B$ and $\omega_{II-} = \omega_0$ at $\omega_0 < \omega_B$. This means that, as in the previous case, we have the excitation of the wave with the frequency close to the Bragg frequency in addition to the solution far from diffraction at a given radiation angle θ. As the calculation shows, the magnitude of α does not depend on the frequency of the diffracted wave and keeps practically constant, being determined by the oscillator eigenfrequency within the whole interval of radiation angles corresponding to the fulfilment of the condition (5). Although the parameter α depends on the eigenfrequency of the oscillator Ω and equals zero at

$$\Omega_{\pm} = \frac{\omega_L^2}{2\omega_B}\left(1 \pm \frac{g_\tau}{g_0}\right), \tag{13}$$

it remains small ($|\alpha| \leq |g_0|$) within rather a wide interval of eigenfrequencies. For example, in the case considered above $\Omega_{\pm} = 0.092$ eV and $|\alpha| \leq |g_0|$ for the interval $\Omega_{+\min} = 0.08$ eV and $\Omega_{+\max} = 0.15$ eV.

It should be noted that the equality (11) also has the solution for the negative eigenfrequency of the oscillator (at the frequency close to ω_B) that corresponds to the anomalous Doppler effect, i.e., the radiation of the oscillator is accompanied by its excitation. Such a process is possible because under diffraction condition the index of refraction can be greater than unity.

The analysis of the dispersion expression for radiation propagating at a large angle and for arbitrary geometry was made in [24]. Here we discuss the spectra of DRO and PXR only in the two-wave diffraction case. However, due to crystal symmetry, the diffraction condition can be satisfied for many waves, that is,

the case of multi-wave diffraction can be realized. In this case several indices of refraction $n_i(\omega)$ corresponding to different dispersion branches can be greater than unity. It appears that the possibility of new effects in radiation, such as the effect of excitation of radiation in a roundabout way takes place. This means that the PXR intensity in a diffraction peak may differ from zero even in the case when a given reflection is forbidden because of the lattice symmetry. The particular properties in the angular distribution of radiation are observed in the vicinity of the point of degeneration of dispersion branches.

2.1 General expression for spectral-angular distribution of radiation generated by a particle in a photonic crystal

Both the spectral-angular density of radiation energy per unit solid angle $W_{\vec{n}\omega}$ and the differential number of emitted photons $dN_{\vec{n}\omega}\omega = 1/\hbar\omega \cdot W_{\vec{n}\omega}$ can be easily obtained if the field $\vec{E}(\vec{r},\omega)$ produced by a particle at a large distance $\vec{r}$ from the crystal is known [17]

$$W_{\vec{n}\omega} = \frac{er^2}{4\pi^2}\overline{\left|\vec{E}(\vec{r},\omega)\right|^2}, \tag{14}$$

The vinculum here means averaging over all possible states of the radiating system. In order to obtain $\vec{E}(\vec{r},\omega)$, Maxwell's equation describing the interaction of particles with the medium should be solved. The transverse solution can be found with the help of Green's function of this equation, which satisfies the expression:

$$G = G_0 + G_0\frac{\omega^2}{4\pi c^2}(\hat{\varepsilon} - 1)G, \tag{15}$$

G_0 is the transverse Green's function of Maxwell's equation at $\hat{\varepsilon} = 1$. It is given, for example, in [6].

Using G, we can find the field we are concerned with

$$E_n(\vec{r},\omega) = \int G_{ne}(\vec{r},\vec{r}',\omega)\frac{i\omega}{c^2}j_{0e}(\vec{r},\omega)d^3r', \tag{16}$$

where $n, e = x, y, z$, $j_{0e}(\vec{r},\omega)$ is the Fourier transformation of the e-th component of the current produced by a moving beam of charged particles (in the linear field approximation, the current is determined by the velocity and the trajectory of a particle, which are obtained from the equation of particle motion in the external field, by neglecting the influence of the radiation field on the particle motion). Under the quantum-mechanical consideration the current j_0 should be considered as the current of transition of the particle-medium system from one state to another.

According to [17,85], Green's function is expressed at $r \to \infty$ through the solution of homogeneous Maxwell's equations $E_n^{(-)}(\vec{r},\omega)$ containing incoming spherical waves:

$$\lim_{r\to\infty} G_{ne}(\vec{r},\vec{r}',\omega) = \frac{e^{ikr}}{r}\sum_S e_n^s E_{\vec{k}e}^{(-)s*}(\vec{r}',\omega), \tag{17}$$

where $\vec{e}^s$ is the unit polarization vector, $s - 1, 2$, $\vec{e}^1 \perp \vec{e}^2 \perp \vec{k}$.

If the electromagnetic wave is incident on a crystal of finite size, then at $r \to \infty$

$$\vec{E}_k^{s(-)}(\vec{r},\omega) = \vec{e}^s e^{i\vec{k}\vec{r}} + \text{const}\frac{e^{ikr}}{r},$$

and one can show that the relation between the solution $\vec{E}_k^{s(-)}$ and the solution of Maxwell's equation $\vec{E}^{(+)}(\vec{k},\omega)$ describing scattering of a plane wave by the target (crystal), is given by:

$$\vec{E}_{\vec{k}}^{s(-)*} = \vec{E}_{-\vec{k}}^{s(+)} \tag{18}$$

Using (16), we obtain

$$E_n(\vec{r},\omega) = \frac{e^{ikr}}{r}\frac{i\omega}{c^2}\sum_S e_n^s \int E_{\vec{k}}^{s(-)*}(\vec{r},\omega)\vec{j}_0(\vec{r}',\omega)d^3r'. \tag{19}$$

As a result, the spectral energy density of photons with polarization s can be written in the form:

$$W_{\vec{n},\omega}^s = \frac{\omega^2}{4\pi^2c^2}\overline{\left|\int \vec{E}_{\vec{k}}^{s(-)*}(\vec{r},\omega)\vec{j}_0(\vec{r},\omega)d^3r\right|^2}, \tag{20}$$

$$\vec{j}_0(\vec{r},\omega) = \int e^{i\omega t}\vec{j}_0(\vec{r},\omega)dt = eQ\int e^{i\omega t}\vec{v}(t)\delta(\vec{r}-\vec{r}(t))dt, \tag{21}$$

where eQ is the charge of the particle, $\vec{v}(t)$ and $\vec{r}(t)$ are the velocity and the trajectory of the particle at moment t. By introducing (21) into (20) we get

$$dN_{\vec{n},\omega}^s = \frac{e^2Q^2\omega}{4\pi^2\hbar c^3}\overline{\left|\int \vec{E}_{\vec{k}}^{(-)s*}(\vec{r}(t),\omega)\vec{v}(t)e^{i\omega t}d\right|^2}t. \tag{22}$$

Integration in (22) is carried out over the whole interval of the particle motion. It should be noted that the application of the solution of a homogeneous Maxwell's equation instead of the inhomogeneous one essentially simplifies the analysis of the radiation problem and enables one to consider various cases of radiation emission taking into account multiple scattering.

3 Parametric X-ray radiation (PXR)

Using equations (20)–(22), one can easily obtain the explicit expression for the radiation intensity and that for the effect of multiple scattering on the process under study [2,17,85].

Consider, for example, the PXR radiation. Let a particle moving with a uniform velocity be incident on a crystal plate with the thickness L being $L \ll L_c$, where $L_c = (\omega q)^{-1/2}$ is the coherent length of bremsstrahlung $q = \overline{\theta}^2/4$ and $\overline{\theta}^2$ is the mean square angle of multiple scattering. The latter requirement allows neglecting the multiple scattering of particles by atoms. A theoretical method describing multiple scattering affect on the radiation process is given in [125].

According to (22), in order to determine the number of quanta emitted by a particle passing through the crystal plate, one should first find the explicit expressions for the solutions $\vec{E}^{(-)s}_{\vec{k}}$. As was mentioned above, the field $\vec{E}^{(-)s}_{\vec{k}}$ can be found from the relation $\vec{E}^{(-)s}_{\vec{k}} = (\vec{E}^{(+)s}_{-\vec{k}})^*$ if one knows the solution $\vec{E}^{(+)s}_{\vec{k}}$ describing the photon scattering by the crystal.

In the case of two strong waves excited under diffraction (the so-called two-beam diffraction case [3]), one can obtain the following set of equations for determining the wave amplitudes (see [146]):

$$\left(\frac{k^2}{\omega^2} - 1 - \chi_0^*\right) \vec{E}^{(-)s}_{\vec{k}} c_s \chi^*_{-\vec{\tau}} \vec{E}^{(-)s}_{\vec{k}_\tau} = 0$$
$$\left(\frac{k^2}{\omega^2} - 1 - \chi_0^*\right) \vec{E}^{(-)s}_{\vec{k}_\tau} c_s \chi^*_{\vec{\tau}} \vec{E}^{(-)s}_{\vec{k}} = 0. \qquad (23)$$

Here $\vec{k}_{\vec{\tau}} = \vec{k} + \vec{\tau}$, $\vec{\tau}$ is the reciprocal lattice vector, χ_0, $\chi_{\vec{\tau}}$ are the Fourier components of the crystal susceptibility. It is well known that the crystal is

described by a periodic susceptibility (see, for example, [3]:

$$\chi(\vec{r}) = \sum_{\vec{\tau}} \chi_{\vec{\tau}} \exp(i\vec{\tau}\vec{r}). \tag{24}$$

$c_s = \vec{e}^s\vec{e}^s_{\vec{\tau}}$, $\vec{e}^s(\vec{e}^s_{\vec{\tau}})$ are the unit polarization vectors of the incident and diffracted waves, respectively.

The condition for the linear system (23) to be solvable leads to a dispersion equation that determines the possible wave vectors $\vec{k}$ in a crystal. These wave vectors are convenient to present in the form:

$$\vec{k}_{\mu s} = \vec{k} + \vec{\kappa}^*_{\mu s}\vec{N}, \qquad \kappa^*_{\mu s} = \frac{\omega}{c\gamma_0}\varepsilon^*_{\mu s},$$

where $\mu = 1, 2$; $\vec{N}$ is the unit vector of a normal to the entrance crystal surface which is directed into the crystal,

$$\varepsilon_{1(2)s} = \frac{1}{4}\left[(1+\beta_1)\chi_0 - \beta_1\alpha_B\right] \pm \frac{1}{4}\left\{\left[(1-\beta_1)\chi_0 + \beta_1\alpha_B\right]^2 \right.$$
$$\left. +4\beta_1 C_s^2 \chi_{\vec{\tau}}\chi_{-\vec{\tau}}\right\}^{-1/2}. \tag{25}$$

$\alpha_B = (2\vec{k}\vec{\tau} + \tau^2)k^{-2}$ is the off-Bragg parameter ($\alpha_B = 0$ if the exact Bragg condition of diffraction is fulfilled),

$$\gamma_0 = \vec{n}_\gamma \cdot \vec{N}, \quad \vec{n}_\gamma = \frac{\vec{k}}{k}, \quad \beta_1 = \frac{\gamma_0}{\gamma_1}, \quad \gamma_1 = \vec{n}_{\gamma\tau} \cdot \vec{N}, \quad \vec{n}_{\gamma\tau} = \frac{\vec{k} + \vec{\tau}}{|\vec{k} + \vec{\tau}|}.$$

The general solution of (23) inside a crystal is:

$$\vec{E}^{(-)s}_{\vec{k}}(\vec{r}) = \sum_{\mu=1}^{2} \left[\vec{e}^s A_\mu \exp(i\vec{k}_{\mu s}\vec{r}) + \vec{e}^s_\tau A_{\tau\mu} \exp(i\vec{k}_{\mu s\tau}\vec{r})\right]. \tag{26}$$

By matching these solutions with the solutions of Maxwell's equations for the vacuum area, one can find the explicit form of $\vec{E}^{(-)s}_{\vec{k}}(\vec{r})$ throughout the space.

It is possible to discriminate several types of diffraction geometries, namely, the Laue (a) and the Bragg (b) schemes are most well known.

(a) Let us consider the PXR in the Laue case.

In this case, the electromagnetic waves emitted by a particle in both the forward and the diffracted directions leave the crystal through the same surface ($k_z > 0, k_z + \tau_z > 0$), the z-axis is parallel to the normal N (where N is the normal to the crystal surface being directed inside a crystal). By matching the solutions of Maxwell's equations on the crystal surfaces with the help of (23), (25), (26), one can obtain the following expressions for the Laue case:

$$\begin{aligned}
\vec{E}^{(-)s}_{\vec{k}} = &\left\{ \vec{e}^{s} \left[-\sum_{\mu=1}^{2} \xi^{0*}_{\mu s} e^{-i\frac{\omega}{\gamma_0}\varepsilon^{*}_{\mu s} L} \right] e^{i\vec{k}\vec{r}} \right. \\
&\left. + e^{s}_{\vec{\tau}} \beta_1 \left[\sum_{\mu=1}^{2} \xi^{\tau*}_{\mu s} e^{-i\frac{\omega}{\gamma_0}\varepsilon^{*}_{\mu s} L} \right] e^{i\vec{k}_\tau \vec{r}} \right\} \theta(-z) \\
&+ \left\{ \vec{e}^{s} \left[-\sum_{\mu=1}^{2} \xi^{0*}_{\mu s} e^{-i\frac{\omega}{\gamma_0}\varepsilon^{*}_{\mu s}(L-z)} \right] e^{i\vec{k}\vec{r}} \right. \\
&\left. + e^{s}_{\vec{\tau}} \beta_1 \left[\sum_{\mu=1}^{2} \xi^{\tau*}_{\mu s} e^{-i\frac{\omega}{\gamma_0}\varepsilon^{*}_{\mu s}(L-z)} \right] e^{i\vec{k}_\tau \vec{r}} \right\} \\
&\times \theta(L-z)\theta(z) + \vec{e}^{s} e^{i\vec{k}\vec{r}} \theta(z-L),
\end{aligned} \tag{27}$$

where

$$\begin{aligned}
\xi^{0}_{1,2s} &= \mp \frac{2\varepsilon_{2,1s} - \chi_0}{2(\varepsilon_{2s} - \varepsilon_{1s})}; \\
\xi^{\tau}_{1,2s} &= \mp \frac{c_s \chi_{-\tau}}{2(\varepsilon_{2s} - \varepsilon_{1s})}.
\end{aligned} \tag{28}$$

$\theta(z) = 1$ if $z \geq 0$ and $\theta(z) = 0$ if $z < 0$.

Substitution of (27) into (22) gives for the Laue case the differential number of quanta of the forward directed parametric X-rays with the polarization vector

$\vec{e}_s$:

$$\frac{d^2N_{0s}^L}{d\omega d\Omega} = \frac{e^2Q^2\omega}{4\pi^2\hbar c^3}(\vec{e}^s\vec{v})^2 \left| \sum_{\mu=1,2} \xi_{\mu s}^0 e^{i\frac{\omega}{c\gamma_0}\varepsilon_{\mu s}L} \left[\frac{1}{\omega - \vec{k}\vec{v}} - \frac{1}{\omega - \vec{k}_{\mu s}^*\vec{v}} \right] \right.$$
$$\left. \times [e^{i(\omega - \vec{k}_{\mu s}^*\vec{v})T} - 1] \right|^2, \qquad (29)$$

where $T = L/c\gamma_0$ is the particle time of flight; $\vec{e}_1 \parallel [\vec{k}\vec{\tau}]$; $\vec{e}_2 \parallel [\vec{k}\vec{e}_1]$.

One can see that formula (29) looks like the formula which describes the spectral and angular distribution of the Cherenkov and transition radiations in the matter with the index of refraction $n_{\mu s} = k_{z\mu s}/k_z = 1 + \kappa_{\mu s}/k_z$.

The spectral angular distribution for photons in the diffraction direction $\vec{k}_\tau = \vec{k} + \vec{\tau}$ can be obtained from (29) by a simple substitution

$$\vec{e}_s \to \vec{e}_{s\tau}, \qquad \xi_{\mu s}^0 \to \beta_1 \xi_{\mu s}^\tau,$$
$$\xi_{1(2)s}^\tau = \pm \frac{\chi_\tau c_s}{2(\varepsilon_{1s} - \varepsilon_{2s})}$$
$$\vec{k} \to \vec{k}_\tau, \quad \vec{k}_{\mu s} \to \vec{k}_{\tau\mu s} = \vec{k}_{\mu s} + \tau.$$

(b) Now let us consider PXR in the Bragg case. In this case, side by side with the electromagnetic wave emitted in the forward direction, the electromagnetic wave emitted by a charged particle in the diffracted direction and leaving the crystal through the surface of the particle entrance can be observed. By matching the solutions of Maxwell's equations on the crystal surface with the help of (23), (25), (26), one can get the formulas for the Bragg diffraction schemes.

It is interesting that the spectral angular distribution for photons emitted in the forward direction can be obtained from (29) by the following substitution, $\xi_{\mu s}^0 \to \gamma_{\mu s}$,

$$\gamma^0_{1(2)s} = \left[2\varepsilon_{2(1)s} - \chi_0\right]\left[(2\varepsilon_{2(1)s} - \chi_0) - (2\varepsilon_{1(2)s} - \chi_0)\right.$$
$$\left.\times \exp\left[i\frac{\omega}{\gamma_0}(\varepsilon_{2(1)s} - \varepsilon_{1(2)s})L\right]\right]^{-1} \tag{30}$$

The spectral angular distribution of photons emitted in the diffracted direction can be obtained from (29) by substitution

$$\vec{e}_s \to \vec{e}_{s\tau}, \quad \vec{k} \to \vec{k}_\tau, \quad k_{\mu s} \to \vec{k}_{\mu\tau s},$$
$$\xi^0_{\mu s} \exp\left[i\frac{\omega}{\gamma_0}\varepsilon_{\mu s}L\right] \to \gamma^\tau_{\mu s},$$

where

$$\gamma^\tau_{1(2)s} = -\beta_1[c_s\chi_\tau]\left[(2\varepsilon_{2(1)s} - \chi_0) - (2\varepsilon_{1(2)s} - \chi_0)\right.$$
$$\left.\times \exp\left[i\frac{\omega}{\gamma_0}(\varepsilon_{2(1)s} - \varepsilon_{1(2)s})L\right]\right]^{-1}.$$

The angular distribution for the photons emitted at large angles in the the Bragg case was derived in [125]. From (29), (30) we can obtain the angular distribution for the photons emitted in the forward direction:

$$dN^B_{0s} = \frac{e^2Q^2}{4\hbar c}|\beta_1||r_s|^2$$
$$\times\left|\left\{(\gamma^{-2} + \vartheta^2 - \chi_0)^2 - |\beta_1|r_s \ \exp\left[-i\frac{\omega_B}{2\gamma_0 c}\frac{(\gamma^{-2} + \vartheta^2 - \chi_0)^2 - |\beta_1|r_s}{\gamma^{-2} + \vartheta^2 - \chi_0}L\right]\right\}\right|^{-2}$$
$$\times\left|\frac{(\gamma^{-2} + \vartheta^2 - \chi_0)^2 - |\beta_1|r_s|}{(\gamma^{-2} + \vartheta^2 - \chi_0)^2}\right|\frac{\omega_B T}{\sin^2\vartheta_B}\vartheta^3 d\vartheta. \tag{31}$$

According to (31), the PXR angular distribution for this case oscillates as a function of ϑ, L, ω_B. If $\vartheta^2 \gg \gamma^{-2}$, χ_0, the oscillation period is $\vartheta_{0s} = \sqrt{c/\omega_B L_0}$. For $k_B = (\omega_B/c) = 10^9$ cm^{-1}, $L_0 = L/\gamma_0 = 10^{-2}$ cm, we have $\vartheta_{0s} = 3\times10^{-4}$.

For low energy electrons, oscillations in N^B_{0s} disappear. Let us note that the PXR photon number is proportional to Q^2. As a result, the PXR intensity is

very high for heavy nuclei.

For example, for Pb the photon number may be 1 per nucleus for $L = 1$ cm. It can be used for the detection of particles and for the precise measurement of their energy.

4 Surface parametric X-ray (quasi-Cherenkov) radiation (SPXR) and DRO

When a particle travels in a vacuum near the surface of a spatially periodic medium, new kinds of radiation arise [25,26] – surface parametric (quasi-Cherenkov) X-ray radiation (SPXR) and surface DRO (see Figure 3). This phenomenon takes place under the condition of uncoplanar surface diffraction, first considered in [4].

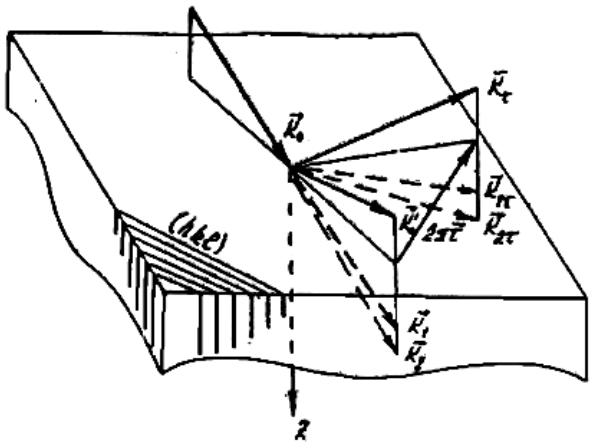

Figure 3.

The solution of Maxwell's equation $\vec{E}^{(+)}_{\vec{k}}(\vec{r})$ in this case of uncoplanar surface diffraction was obtained in [4]. It was shown that the surface diffraction in the two-wave case is characterized by two angles of total reflection (several angles in the case of multi-wave diffraction [27]). The solution obtained in [27]

contains the component, which describes the state that damps with growing distance from the surface of the medium, both within the material and in the vacuum, and which describes a surface wave, i.e., a wave in which the energy flux is directed along the boundary of the surface of a spatially periodic target (see review [28]). According to [4], this solution, which describes scattering of a plane wave by the target under the surface diffraction geometry, can be written in the form:

$$\vec{E}^{(+)s}_{\vec{k}} = e_s e^{i\vec{k}\vec{r}} + A_s(\vec{k},\omega)e^{i\vec{k}_1\vec{r}} + B_s(\vec{k},\omega)e^{i\vec{k}_2\vec{r}}, \tag{32}$$

where the wave vector in a vacuum $\vec{k} = (\vec{k}_t, \vec{k}_\perp)$, $\vec{k}_1 = (\vec{k}_t - \vec{k}_\perp)|\vec{k}_{2\perp}| = \sqrt{k^2 - k_{2t}^2}$, $\vec{k}_2 = (\vec{k}_{2t} - \vec{k}_{2\perp})$, $\vec{k}_{2t} = \vec{k}_t + 2\pi\vec{\tau}$, $\vec{k}_t$ is the component of the wave vector that is parallel to the surface, $\vec{\tau}$ is the reciprocal lattice vector, ω is the photon frequency. The amplitudes A_s and B_s are given in [5,26]. Substituting the solution $\vec{E}^{(-)s}_{\vec{k}} = (\vec{E}^{(+)s}_{-\vec{k}})^*$ into (16), we can find the spectral-angular distribution of SPXR and DRO. For example, in the case of DRO, the differential number of emitted photons for a particle moving parallel to the crystal surface is [25]

$$\frac{d^2N_s}{d\omega d\Omega} = \frac{e^2\omega T}{2\pi\hbar c^3}\left|\vec{u}\vec{B}_s(\vec{k},\omega)\right|^2 \delta(\vec{k}_t\vec{u} + 2\pi\vec{\tau}\vec{u} - \omega)e^{-2\mathtt{Im}k_{2\perp}|z_0|}. \tag{33}$$

Here we assume that a particle moves parallel to the target surface at a distance Z_0 at a constant velocity $\vec{u}$; T is the flight time. The argument of δ-function in (33) is equal to zero for the frequencies

$$\omega_u = \frac{|2\pi\vec{\tau}\vec{u}|}{1 - \vec{n}_t\vec{u}/c},$$

where $\vec{n}_t$ is the component of the unit vector in the direction of $\vec{k}$, which is parallel to the surface.

After integrating (33) over the frequencies, the angular distribution of radiation takes the form:

$$\frac{d^2N_s}{d\Omega} = \frac{e^2\omega_u T}{2\pi\hbar c^3}\left|\vec{u}\vec{B}_s(\vec{k},\omega_u)\right|^2 e^{-2\mathtt{Im}k_{2\perp}|z_0|}. \tag{34}$$

The spectral-angular distribution of SPXR generated by a particle incident on the crystal at a small angle relative to the crystal surface was obtained in [29,30,31,32].

It should be noted that, according to the analysis made in [25], the formation of circularly polarized quanta under the surface diffraction is possible and, as a consequence, such circularly polarized quanta can be produced in the SPXR process [32].

Let now an oscillator with the vibration frequency Ω in the laboratory system move along the surface. In this case we also obtain the expression similar to equation (33) with the following replacements made in the exponent: ω by $\omega\pm\Omega$ and v by the velocity amplitude at frequency Ω. As a result, the integrals appearing in equation (33) will give δ-functions of the form $\delta(\vec{k}_t\vec{v}-\omega\pm\Omega)$, $\delta(\vec{k}_{2t}\vec{v}-\omega\pm\Omega)$. Now all three integrals are non-zero. The first one describes the normal Doppler effect, the second one, the same effect including the influence of a mirror reflected wave on radiation. Of greatest interest is the third integral. In this case the δ-function leads to the equality $\omega = (2\pi\tau_t\vec{v}\pm\Omega)(1-\vec{n}_t\vec{v}/c)^{-1}$. If $2\pi\tau_T\vec{v} > \Omega$, then both signs of the frequency Ω are allowed for radiation. From the quantum viewpoint, one sign corresponds to the emission of quantum by the oscillator (or atom) when it drops to a lower energy level, and the opposite sign corresponds to the inverse process: of the quantum emission when the oscillator (or atom) rises to a higher energy level. In other words,

the phenomenon of surface diffraction results in the appearance of the vacuum anomalous Doppler effect [25].

Let now a beam of charged particles (or oscillators) move along the surface of a natural or a photonic crystal in a vacuum. The phenomenon of spontaneous radiation causes the beam's instability relative to the photon emission and the formation of the charge density wave in the beam. The processes considered above also leads to the appearance of such instability. According to [25], multi-wave diffraction of emitted photons in this case also leads to a different reduction of the generation threshold similar to that appearing when a beam passes through a crystal [47,48,49,50,51,122].

Due to such instability the beam radiates photons collectively and its longitudinal energy decreases. The presence of the external field (in our case - excitation of surface diffraction by the external field) can accelerate the beam. Note that the instability studied in [47,48,49,50,51,122] is a particular case of instabilities caused by the processes of the emission of waves (instability may be caused by, for example, the parametric process of the pump wave splitting into two waves, the Mandelstam-Brillouin effect, four-wave processes) [159]. In all these cases, the power of the root dependence of the instability increment changes in the periodic medium if at least for one of the waves, the diffraction conditions are chosen according to the requirements of [122] of the coincidence of the roots of the dispersion equation characterizing the periodic medium.

4.1 Parametric X-ray radiation in crystals under action of high frequency ultrasonic waves

According to [5,17], in the presence of an external variable field (for example, an ultarsonic field), a crystal is characterized by an effective index of refraction, depending on external field parameters. By varying these parameters, one can change the properties of parametric radiation.

As the characteristics and yield of PXR depend on the solution $\vec{E}^{(-)}(\vec{r},\omega)$ of the homogeneous Maxwell's equation describing the diffraction process in crystals, the investigation of the influence of an external ultrasonic (US) field on diffraction of X-ray points to the strong influence of a US external field on the PXR process. In [33] it was pointed to the essential modification of scattering process and X-ray radiation process under the diffraction condition in crystals. Due to a dynamical character of PXR formation, according to [34], the influence of a US wave on this process will be maximum when the US wavelength coincides with the period of extinction beatings.

The theory of PXR under the action of an external US wave on a crystal target was derived in [35,36,37,38,39]. The boundary problem of diffraction of X-rays by a crystal target subjected to an external US wave was solved for the case of two-wave diffraction in [40,41,42]. Here we do not give the expressions for photon wave functions $\vec{E}^{(-)}(\vec{k},\vec{r})$ because they are very clumsy. The spectral-angular PXR distribution in the presence of a US wave was obtained in [36,37] (for detail see [139]). Experimental observation of the effect of the US wave on parametric radiation was performed in [160,161]. Experimentally observed features of the PXR in the US wave were explained in [162].

5 Diffracted X-ray radiation from channeling particle (DCR)

As we discussed above, the X-ray radiation of a relativistic oscillator in a crystal essentially modifies under diffraction conditions of emitted photons. A new diffracted radiation of oscillator (DRO) appears as a result of coherent summation of two processes – photon radiation and photon diffraction, but it cannot be reduced to a sequence of these two processes. The relativistic oscillator itself can be a relativistic atom or a relativistic charged particle channeled in the potential well of averaged crystallographic potential of axes (planes), or an oscillator formed by an external electromagnetic field (ultrasonic, laser). It was shown in [17,19,20,21,22] that the DRO spectrum is rather complex and is determined by the complex and anomalous Doppler effect (see Sections 1, 2).

It is known that the transverse energy of channeled electrons (positrons) is discrete and state-to-state transitions result in radiation, i.e., in this case a channeled particle is like a one-dimensional or two-dimensional oscillator with the eigenfrequency in the laboratory frame $\Omega_{nf} = \varepsilon_n - \varepsilon_f$, where ε_n and ε_f are the eigenvalues of corresponding one- or two-dimensional Schrödinger equation, in which the particle rest mass is replaced by the total energy $m\gamma$.

For the analysis of DRO characteristics, it is necessary to obtain the spectral-angular distribution. The description of the channeled particle motion with the help of one- or two-dimensional Bloch functions was given in [10]. The expressions for spectral-angular DRO distribution for different cases of photon dynamical diffraction were obtained in [11,12,20]. For example, in the case of two-wave Laue diffraction the spectral-angular distribution of DRO can be

written in the following way [11,12,20]:

$$\frac{d^2N_s^\tau}{d\omega d\Omega} = \frac{e^2\beta_1\omega}{\pi^2\hbar c^3}\sum_{nf} Q_{nn}|\vec{e}_{0s}\vec{g}_{nf}|^2 \left|\sum_{\mu=1,2}\zeta_{\mu s}^\tau \frac{1-e^{-iq_{znf}^{\mu s}L}}{q_{znf}^{\mu s}}\right|^2, \tag{35}$$

where

$$q_{znf}^{\mu s} = \omega(1-\beta_\parallel\cos\theta) - \Omega_{nf} - \frac{\omega}{\gamma_0}\delta_{\mu s}, \tag{36}$$

θ is the angle between the photon wave vector $\vec{k}_\tau$ directed at a small angle relative to the particle velocity and the z-axis. In the dipole approximation, which is true for the X-ray radiation, we have

$$\vec{g}_{nf} = -i\left[\beta_\parallel\vec{n}_z(\vec{k}_\perp\vec{\rho}_{nf}) + \Omega_{nf}\vec{\rho}_{nf}\right]$$

in an arbitrary nondipole case $\vec{g}_{nf}$ is defined in [11,12],

$$\vec{\rho}_{nf} = \int\limits_\Delta = \varphi_{n\vec{k}}(\vec{\rho})\varphi^*_{f\vec{k}}(\vec{\rho})d^2\rho,$$

$\varphi_{n\vec{k}}$ and $\varphi_{f\vec{k}}$ are the two-dimensional Bloch functions satisfying the equation similar to the Schrödinger equation (see [11,12,20]), L is the crystal target length, Q_{nn} is the population probability of the particle transverse energy state n.

According to (35), the maximum intensity should be observed at the angles and frequencies that satisfy the equation

$$\omega(1-\beta_\parallel\cos\theta) - \Omega_{nf} - \frac{\omega}{\gamma_0}\delta_{\mu s} = 0 \tag{37}$$

The solutions of this equation were obtained above.

In the case of rather thick crystals, the angular distribution of DRO was obtained in [17,12,20]. For example, the angular distribution of radiation generated by plane-channeled particles can be written as [14]:

$$\frac{dN_\tau^s}{d\Omega} = \frac{e^2 L_{\rm eff}\beta_1^2}{2\pi}\sum_{nf} Q_{nn}|x_{nf}|^2 \sum_\mu \frac{(\omega_{nf}^{\mu s})^2}{\Omega_{nf}}\left|\zeta_\tau^{\mu s}(\omega_{nf}^{\mu s})\right|^2$$
$$\times\left[1-\frac{(\omega_{nf}^{\mu s})^2}{\gamma_1\Omega_{nf}}\mathtt{Re}\left(\frac{\partial\delta_{\mu s}}{\partial\omega}\right)\right]^{-1}_{\omega=\omega_{nf}^{\mu s}} F_s(\theta,\varphi) \qquad (38)$$

for r-polarization:

$$F_r(\theta,\varphi) = \left\{\beta_1\omega_{nf}^{\mu\sigma}\sin^2\theta\cos\varphi\frac{\tau_y\cos\varphi-\tau_x\sin\varphi}{|\vec{\tau}_\perp|}+\Omega_{nf}\frac{\tau_z\sin\theta\sin\varphi-\tau_y\cos\theta}{|\vec{\tau}_\perp|}\right\}^2$$

and for π-polarization

$$F_\pi(\theta,\varphi) = \left[\frac{\beta_1\omega_{nf}^{\mu\sigma}\sin\theta\cos\varphi[\cos\theta(\vec{n},\vec{\tau})-\tau_2]}{|\vec{\tau}_\perp|}+\Omega_{nf}\frac{[\sin^2\theta\cos\varphi(\vec{n}_1\vec{\tau})-\tau_x]}{|\vec{\tau}_\perp|}\right]^2$$

where

$$\omega_{nf}^{\mu s} = \Omega_{nf}(1-\beta\cos\theta-\gamma_1^{-1}\mathtt{Re}\delta_{\mu s}(\omega_{nf}^{\mu s}))^{-1},$$

x_{nf} is the matrix element obtained from one-dimensional Bloch functions, $L_{\rm eff}$ is the effective length (at $L < L_{\rm abs}$, $L_{\rm eff} = L$, $L \gg L_{\rm abs}$, $L_{\rm eff} = L_{\rm abs}$, where $L_{\rm abs}$ is the absorption length). The term in square brackets takes account of the influence of the dispersion of the medium on the angular distribution. As the frequency, satisfying dispersion equation (37), goes over from one dispersion branch to another with changing the radiation angle θ, the summation over μ means that we select the corresponding root of the dispersion equation for each definite radiation angle θ; $\vec{n}_1$ is the unit vector directed along the wave vector of the photon propagating at a small angle relative to the mean velocity of a channeled particle.

Numerical calculation of the angular DCR distribution taking into account the dispersion characteristics of the medium under diffraction conditions, was made in [24]. According to Figure 4, the angular distribution has a fine structure which corresponds to the region of transition from one dispersion branch to another.

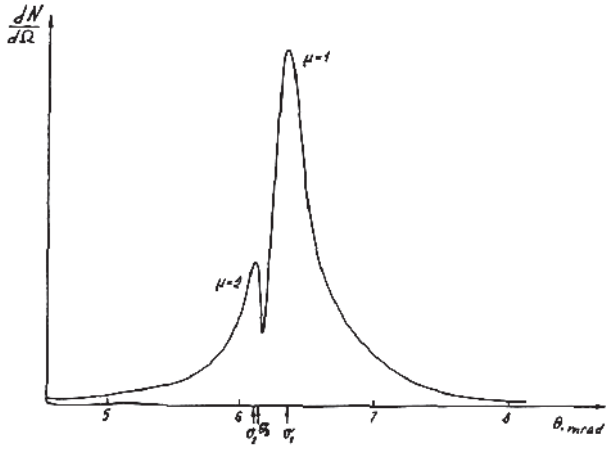

Figure 4.

One can see that the DCR distribution looks like two narrow rings – one of which corresponds to the solution $\mu = 2$, the other, to $\mu = 1$ (in the case of PXR generation, only one solution satisfies the Cherenkov condition). The angular position of the DCR distribution maxima can be estimated in the first approximation as:

$$\theta_{1,2} = \sqrt{\theta_D^2 \pm \frac{\sqrt{\beta r_s'}}{\sqrt{1 + 2\sin^2\theta_B}/\frac{\Omega}{\omega_B}}}, \tag{39}$$

where θ_D is the angle that satisfies the following equation

$$\theta^2 + \gamma^2 + \frac{\omega_L^2}{\omega_B^2} - \frac{2\Omega_{nf}}{\omega_B} = 0$$

θ_B and ω_B are the angle and the frequency satisfying the exact Bragg condition. For example, according to Figure 4, the values of these angles are

$\theta_1 = 6.1 \cdot 10^{-3}$ rad and $\theta_2 = 6.2 \cdot 10^{-3}$ rad. The ratio of the angular width to the value of the angle θ is about $\Delta\theta/\theta_D \cong 0.1$. The expressions for the angular distribution of radiation are simplified essentially if the particle energy is rather small ($1 - \beta \gg 1/\gamma_{0,1}\mathtt{Re}\delta_{\mu s}$). In this case we can consider that the frequency corresponding to the maximum intensity does not depend on the dielectric properties of the crystal, being determined by the radiation angle alone. The DRO characteristics for this case were considered in [43].

In [44] the possibility of experimental observation of the DRO by measuring the angular distribution was analyzed. It was shown that for such experiments particle beams of high quality are required because the radiation characteristics are very sensitive to the parameters of a particle beam. Indeed, the DRO angular distribution shown in Figure 4 takes place only for a particle beam whose characteristics satisfy the following inequality:

$$\frac{\Delta\gamma}{\gamma} + \frac{(\Delta\theta_{\text{eff}}\gamma)^2}{2} + \frac{2\pi\gamma^2}{k_B L_0} < \frac{\gamma^2\sqrt{\beta r_s'}}{2}, \tag{40}$$

where γ is the Lorentz factor, $\Delta\theta_{\text{eff}}$ is the angular spread, $\Delta\gamma/\gamma$ is the energy spread, $\Delta\Omega = 2\pi c/L$ is the divergence of the oscillator eigenfrequencies.

In the opposite case, the angular width of the maxima is equal to

$$\Delta\theta = +\frac{1}{\gamma}\left(\frac{2\Delta\gamma}{\gamma} + (\theta_{\text{eff}}\gamma)^2 + \frac{4\pi\gamma^2}{k_B L_0}\right)^{1/2} \tag{41}$$

As an example, the dependence of DRO angular distribution characteristics on the energy divergence of the particle beam is shown in Figure 5 one can see that this dependence is rather sharp indeed.

The dependence of the angular density of radiation on the energy of a rela-

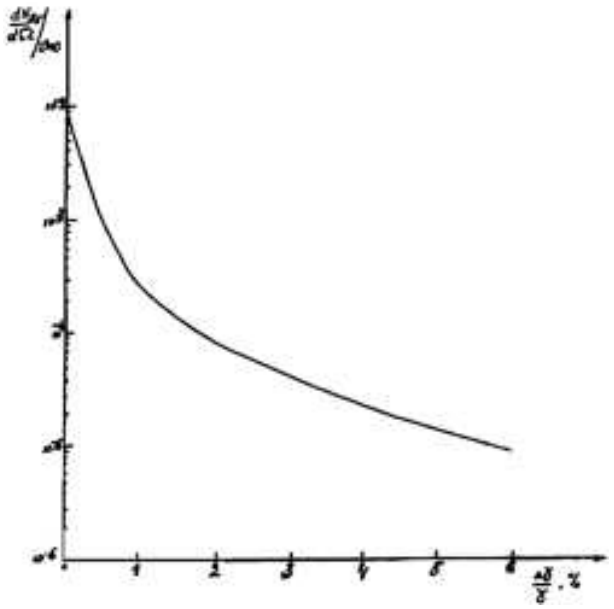

Figure 5.

tivistic oscillator, which has a "resonance" character at a given angle of radiation observation, was also considered in [44]. If the observation angle is equal to zero, the maximum of the angular distribution sharply increases with $\gamma \to \gamma^R = (\omega_B/2\Omega)^{1/2}$. When the frequency ω_B equals $\omega_B = \omega_m\theta_x = 2\Omega\gamma^2$, the maximum value of the radiation density is observed at γ being a little larger than γ_R. The angular distribution in this case looks like a bell and its width decreases sharply with $\gamma \to \gamma_R$ (see Figure 6).

In the range of $\gamma > \gamma_R$ ($\omega_B < \omega_{\max}$), the single narrow maximum splits into two peaks (φ is fixed), which shift to the range of larger radiation angles θ with increasing particle energy E. In [44], the relative estimation was given for the contributions from different radiation mechanisms to the total radiation angular distribution which can be observed in a definite reflex. It was shown that at $\Delta\gamma/\gamma \sim 1\%$, the ratio of the DRO angular density of diffracted

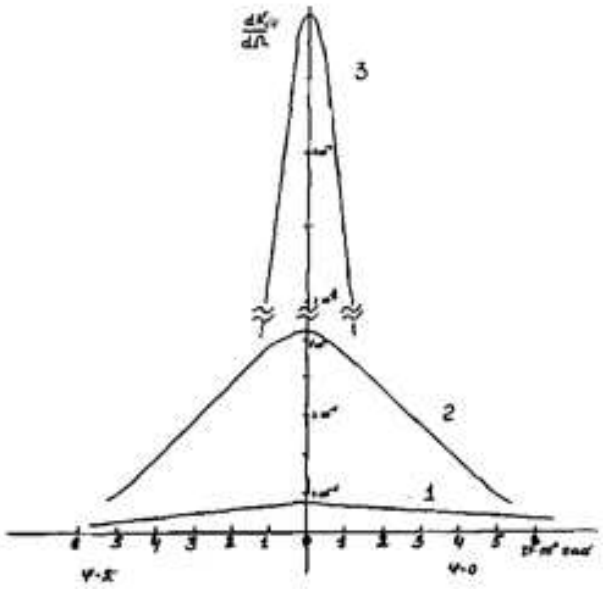

Figure 6.

bremsstrahlung at $\theta = 0$ is

$$R_1 = \frac{R_{\rm DRO}}{I_{DB}} = \frac{Q_{nn}\theta_L^2(\sin^2\psi + \cos^2 2\theta_B \cos^2\psi)}{(1+\cos^2 2\theta_B)4\overline{\theta_s^2}L(\Delta\gamma/\gamma)^2}, \tag{42}$$

where the estimation is given for a channeled electron (positron), θ_L is the Lindhard angle, ψ is the angle between the particle oscillation plane and the diffraction plane, $\overline{\theta_s^2}$ is the mean square angle of multiple scattering per unit length, $1/4\,\theta_L^2$ is the classical estimation of the magnitude of $|x_{nf}|^2\Omega^2c^{-2}$. For a Si crystal and the channeled electron with the energy $E = 23.6$ MeV ($\gamma \approx \gamma_R$; planes of channeling (100), $\theta = 0$, diffraction plane (220)) the value of the ratio is $R_1 = 25$, that is, the DRO intensity is 25 times larger than the intensity of the diffracted bremsstrahlung at $\Delta\gamma/\gamma \cong 1\%$ and $\Delta\psi^2\gamma^2 < \Delta\gamma/\gamma$. If the diffracted radiation is observed at the angle $\theta \neq 0$, we should compare it with the contribution from the parametric (quasi-Cherenkov) radiation. In this case the analogous ratio is estimated as [44,139]

$$R_2 = \frac{R_{\rm DRO}}{I_{RxR}} \cong Q_{nn} \left(\frac{\theta_L}{4\frac{\Delta\gamma}{\gamma}\theta_D} \right)^2 \times \frac{(1+\theta_D^2\gamma^2+\gamma^2\gamma_n^{-2})^2(\sin^2\psi+\cos^2\psi\cos^2 2\theta_B)}{(\sin^2\varphi+\cos^2\varphi\cos^2 2\theta_B)}, \quad (43)$$

where φ is the angle between the wave vector $\vec{k}$ and the diffraction plane, $\gamma_n = \omega_B/\omega_L$ is the Lorentz factor corresponding to the threshold magnitude of the energy $E = mc^2(g_0')^{-1/2}$. One can see that this ratio essentially depends on the value of the azimuthal angle φ. For example, for a Si crystal this ratio is estimated as $R_2 \cong 5$ when the electron with the energy $E = 34$ MeV is channeled between the planes (100) and the diffraction plane is (220).

Thus, the experimental observation of the diffracted radiation of oscillator is possible with the help of the particle beams of high quality.

A relativistic oscillator can be formed not only by an unperturbed crystal channel but also by an external ultrasonic or laser field [13,25,123]. A more detailed treatment of particle radiation in crystals under the laser wave was given in [45]. In [45] the radiation of electrons (positrons) in a crystal subjected to a laser wave, which forms an oscillator, was considered. The intensity of such radiation was estimated. A relativistic oscillator can be a channeled particle, which moves in a plane channel bent by a variable external field (ultrasonic or laser wave), i.e., in some crystal undulator [13]. In this case, the oscillator frequency in the laboratory frame is $\Omega' = \kappa_z u - \Omega$, where $\vec{\kappa}$ is the wave vector of an external wave in a crystal, Ω is its frequency (the z-axis is chosen along the direction of the average particle velocity $\vec{u}$). Diffracted radiation of the oscillator formed by an external ultrasonic wave was considered in [23].

According to [13], the trajectory of a particle moving in the dynamic ultrasonic

undulator is written in the form (see Figure 7)

$$\vec{r}(t) = \vec{r}_{\rm ch}(t) + \vec{r}^{s}(t) = \vec{r}_{\rm ch}(t) + \vec{a}\cos(\Omega' t + \delta), \tag{44}$$

where $\vec{r}_{\rm ch}(t)$ is the radius vector describing the motion of an ordinary high-frequency channeled particle, and $\vec{r}^{s}(t)$ is the radius vector describing the motion of a particle in the dynamic undulator.

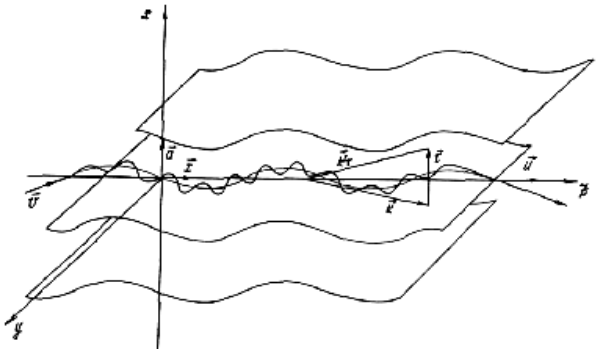

Figure 7.

Assuming that the frequency of an ultrasonic wave is much smaller than the frequency of particle oscillations in a crystal channel, we can consider these two kinds of particle motion independently: the motion of an ordinary channeled particle and the motion of the equilibrium trajectory center of particle gravity inside the bent channel formed under the action of the external variable field. $\vec{a}$ and δ are the amplitude and the initial phase of particle oscillation in the ultrasonic channel. It should be noted that if the amplitude of the ultrasonic wave satisfies the condition $a \ll uU(Ed\kappa^2)^{-1}$ (E is the particle energy, d is the width of the crystal channel, and V is the depth of a potential well for a crystal channel), then the radius of the crystal curvature due to the action of the ultrasonic wave is much larger than the radius of the trajectory curvature for the channeled particle incident on the crystal at the Lindhard angle. In this case, the equilibrium trajectory of a positively charged particle gravity center

corresponds to the trajectory of a stable channeling regime, and the curvature of the crystal channel caused by the action of the ultrasonic wave leads only to the displacement Δ of the equilibrium trajectory center of gravity during the particle passage through the crystal. That is why for positively charged particles, for which $a_f + \Delta \leq d/2$, one can take into account the dechanneling effect, which is due to the channel curvature, by considering the mean square angle of multiple scattering in this bent channel in the same way as in an amorphous medium [23] (a_f is the amplitude of particle oscillation for the ordinary channeling regime).

In the case under consideration, an essential difference arises in comparison with the case of diffracted radiation from the oscillator caused by a channeled particle. This is that the atomic (nuclear) oscillations, resulting in the formation of the ultrasonic undulator, will simultaneously lead to the dielectric constant modulation in a crystal and, consequently, can change the diffraction process itself. As a result, the photon wave function changes. Maxwell's equations describing this situation are given in [23]. The case when the influence of an ultrasonic wave on the X-ray diffraction process can be reduced to the change of the magnitude of the Fourier components of the crystal dielectric susceptibility alone was considered in detail. The spectral-angular distribution was obtained and the contributions of parametric (quasi-Cherenkov) radiation and of DRO itself were separated. The spectral and angular characteristics were analyzed and the total number of photons in a diffraction peak was estimated.

It was shown that if the following inequality $(a\Omega')^2 > (a_f\Omega_f)^2$ is fulfilled, the diffracted radiation from a particle in the external field will be more intensive than the DRO from an ordinary channeled particle (a_f and Ω_f are the am-

plitude and the frequency of particle oscillations in an unperturbed channel). According to [13], this inequality can be realized for a standard ultrasonic field source and, as shown by the estimations, the influence of this wave on dechanneling process can be ignored in this situation.

In conclusion it should be noted that the diffracted radiation can also be forced under the motion of the oscillator over the crystal surface, by analogy with the surface parametric (quasi-Cherenkov) radiation [25]. Radiation from particles moving in crystal undulators is now being actively studied both theoretically and experimentally (see [154,155,156,157,158]).

6 X-ray radiation from a spatially modulated relativistic beam in a crystal ([147])

As was mentioned in the Introduction, in our works we suggested a new type of the free electron laser based on volume multi-wave distributed feedback. It was shown that multi-wave distributed feedback enables reducing the generation threshold from the values of the current densities of a relativistic beam, such as 10^{13} A/cm^2, which are practically unavailable, to acceptable values, such as $10^7 - 10^8$ A/cm^2. This reduction can be achieved even in the X-ray range (10-100 keV).

One of the most important ways of reducing the generation threshold in free electron lasers consists in prior modulation of the density of a beam of relativistic particles. In particular, modulation gives rise to radiation coherent to the beam, which appears alongside with spontaneous radiation of electrons as the beam gets into the undulator.

According to [25,49,51,59,119,137], one of the schemes of the X-ray laser is based on using parametric quasi-Cherenkov radiation, diffracted radiation of a relativistic oscillator in the crystal (or radiation in a crystal undulator). In this case the relativistic electrons (positrons) move not in the vacuum, but in the crystal. Interaction of particles with the atoms of matter result in multiple scattering, which will apparently diminish the beam's modulation amplitude and, hence, the intensity of coherent radiation.

In [147], the spectral angular distribution of the intensity of parametric X-ray (quasi-Cherenkov) radiation was obtained as well as the radiation of a relativistic oscillator formed by a spatially modulated beam under multiple scattering. The conditions were determined under which multiple scattering does not affect the intensity of coherent radiation. It was shown that the number of quanta coherently emitted by the beam in the X-ray range with reasonable requirements to the value of the current density of the beam of relativistic particles, such as $\approx 10^8$ A/cm^2, is too small in comparison with the number of spontaneously emitted quanta. For this reason, the experimental observation of the effect of coherent radiation of quanta in the X-ray range should be carried out in a rather narrow spectral angular range. In this case, in the wavelength range of 50 – 100 Å, it is possible to observe the effect when the degree of beam modulation is as small as $\mu \simeq 10^{-5}$.

In our case of relativistic particles, their energy is much greater than the energy of emitted γ-quanta. So one can consider the radiation process within the framework of classical electrodynamics. Let a beam of charged particles (electrons or positrons) traverse the area occupied by matter. The spectral density $W^s_{\vec{n}\omega}$ of the radiation energy per unit solid angle of photons characterized by the polarization vector $\vec{e}^s$ ($\vec{n} = \vec{k}/k$, $\vec{k}$ is the photon wave vector) can

be found when one knows the Fourier transform in time of the electric field strength in the produced electromagnetic wave $\vec{E}(\vec{r},\omega)$. According to [7,5], at long distances from the target

$$E_i(\vec{r},\omega)\frac{e^{ikr}}{r}\frac{i\omega}{c^2}\sum_i e_i^s\int \vec{E}_{\vec{k}}^{(-)s^*}(\vec{r}',\omega)\vec{\jmath}(r',\omega)d^3r', \tag{45}$$

where $\vec{E}_{\vec{k}}^{(-)s}(\vec{r},\omega)$ is the solution of the homogeneous Maxwell's equations, which describes scattering by this wave of the photon with wave vector $\vec{k}$ and polarization s. The scattering asymptotics has a form of an incident plane wave plus a converging spherical wave. In this case $\vec{E}_{\vec{k}}^{s(-)*} = \vec{E}_{-\vec{k}}^{s(+)}$, where $\vec{E}_{-\vec{k}}^{s(+)}$ is the ordinary solution of the homogeneous Maxwell's equations with asymptotic behavior containing a diverging spherical wave;

$$\vec{\jmath}(\vec{r},\omega) = \int e^{i\omega t}\vec{\jmath}(\vec{r},\omega)dt$$

is the Fourier transform of the beam's current, which equals

$$\vec{\jmath}(\vec{r},\omega) = e\sum_i \vec{v}_i(t)\delta(\vec{r}-\vec{r}'(t)),$$

$\vec{r}_i(t)$ is the coordinate of the i-th particle of the beam at moment t, $\vec{v}_i(t)$ is the particle velocity; e is the particle's electric charge. Using (45), we obtain the following expression for spectral-angular energy distribution of radiation generated by the particle beam in the target:

$$W_{\vec{n}\omega}^s = \frac{\omega^2}{4\pi^2c^3}\overline{\left|\int \vec{E}_{\vec{k}}^{(-)s^*}(\vec{r},\omega)\vec{\jmath}(\vec{r},\omega)d^3r\right|^2}. \tag{46}$$

The vinculum in (46) denotes averaging over the distribution of the coordinates and velocities of the particles in the beam (allowing for multiple scattering in the target). With the help of the distribution function $w(\vec{r}_l,\vec{v}_l,t;\,\vec{r}'_m,\vec{v}'_m,t')$

defining the joint probability density of finding in the l-th particle the coordinate $\vec{r}_l$ and velocity $\vec{v}_l$ at moment t, and finding in the m-th particle the coordinate $\vec{r}'_m$ and velocity $\vec{v}'_m$ at moment t', (46) can be written as follows:

$$W^s_{\vec{n}\omega} = \frac{e^2\omega^2}{4\pi^2c^3}\sum_l\sum_m e^{i\omega t}e^{-i\omega t'}\vec{v}_l\vec{E}^{s(-)*}_{\vec{k}}(\vec{r}_l,\omega)$$
$$\times\vec{v}'_m\vec{E}^{s(-)}_{\vec{k}}(\vec{r}'_m,\omega)w(\vec{r}_l,\vec{v}_l,t;\,\vec{r}'_m,\vec{v}'_m,t')d^3r_l d^3v_l d^3r'_m d^3v'_m dt dt'. \qquad (47)$$

According to (47), the spectral-angular distribution of energy $W^s_{\vec{n}\omega}$ can be represented as follows:

$$W^s_{\vec{n}\omega} = \sum_l \overline{|\mu_l|^2} + \sum_{l\neq m}\overline{\mu_l\mu^*_m}, \qquad (48)$$

where

$$\mu_l = \frac{e\omega}{2\pi c}\int \vec{E}^{s(-)*}_{\vec{k}}(\vec{r}_l(t),\omega)\vec{\beta}_l(t)e^{i\omega t}dt$$

has a meaning of the amplitude of photon emission by the l-electron; $\vec{\beta}_l = \vec{v}/c$.

In the case when correlations in the positions of different particles can be neglected, $w(\vec{r}_l,\vec{v}_l,t;\,\vec{r}_m,\vec{v}_m,t') = w_1(\vec{r}_l,\vec{v}_i,t)w_1(\vec{r}_m,\vec{v}_m,t')$ $(l\neq m)$. As a result, (48) can be recast as

$$W^s_{\vec{n}\omega} = \sum_l(\overline{|\mu_l|^2} - \overline{|\mu_l|^2}) + \left|\sum_l\overline{\mu^2}\right|^2. \qquad (49)$$

The first sum in (49) describes spontaneous incoherent radiation of photons, the second one – which is proportional to the squared modulus of the sum of averaged emission amplitudes – describes coherent across the beam photon emission. To define the conditions under which the distribution of coordinates and velocities in the beam has no effect on the process of coherent radiation of a photon, let us take into account that when a photon is emitted

in a homogeneous medium (e.g., due to the Cherenkov effect), $\vec{E}^{s(-)}_{\vec{k}}$ has a form of a plane wave, while in the case when parametric X-ray radiation or diffracted radiation of the oscillator is generated in the crystal (in a medium with spatially-periodic dielectric permittivity), the expression for $\vec{E}^{s(-)}_{\vec{k}}$ has a form of a superposition of plane waves [5,17,20,85]. In particular, in the space region occupied by the target, $\vec{E}^{s(-)}_{\vec{k}}$ can be represented in the form:

$$\vec{E}^{s(-)}_{\vec{k}}(\vec{r}_l(t),\omega) = \sum_n A_n e^{i\vec{k}_n \vec{r}_l(t)},$$
$$\vec{r}_l(t) = \vec{r}_{l0} + \vec{u}_l t + \delta\vec{r}_l(t). \tag{50}$$

Here $\vec{r}_{l0}$ is the electron coordinate at time $t = 0$; $\vec{u}_l$ is the electron velocity in a vacuum; $\delta\vec{r}_l(t)$ describes the variation of the electron trajectory under the action of the forces (in particular, those leading to multiple scattering) that affect the particle in the area occupied by the target. Let us assume that $\vec{u}_l = \vec{u} + \Delta\vec{u}_l$, where $\Delta\vec{u}_l \ll \vec{u}$. To be more specific, take the z-axis as directed along $\vec{u}$.

Now, let us determine the conditions under which the distribution of the coordinates and velocities in the beam has no effect on the intensity of coherent radiation.

Let the crystal surface through which the electrons enter the target be located at point $z = 0$. At the moment of time $t = 0$, their coordinates were $\vec{r}_{0l}$ and were located in the area $z < 0$. Consequently, the l-electron reaches the surface $z = 0$ at time $t_l = |z_{l0}|/u_{zl}$. During this time, the electron will move over the distance $\delta\vec{r}_{l\perp} = \vec{u}_{l\perp}|\vec{z}_{l0}|/u_{zl}$ in the transverse direction. As a result, the electron's transverse coordinate at entering the target will be

$$\vec{r}_{l\perp} = \vec{r}_{l0\perp} + \vec{u}_{l\perp}\frac{|z_{l0}|}{u_{zl}} = \vec{r}_{l0\perp} - \vec{u}_{l\perp}\frac{z_{l0}}{u_{zl}}.$$

The major contribution to the amplitude μ_l comes from integration over the interval corresponding to particle motion inside the target [8]. We shall consider this very contribution. In the integral over time involved in the amplitude μ_l, we shall shift the zero-time position corresponding to the particle motion in the target area to point $t = 0$.

As a result, the amplitudes μ_l can be represented in the form:

$$\mu_l = A_l l^{-i\vec{k}_\perp \vec{r}_{l0\perp}} e^{-i\frac{\omega}{u_{zl}} z_{l0}} e^{i\vec{k}\vec{u}_{l\perp}\frac{z}{u_{zl}}}, \tag{51}$$

where A_l is the amplitude of radiation in the crystal of the l-electron, which entered the target at point $r = 0$ at time $t = 0$. If the additional phase shift occurring during the time T of the electron motion in the crystal is small due to velocity distribution Δu_l, i.e., $\vec{k}\vec{\Delta}\vec{u}_l T < 1$, then multiple scattering has no effect on the amplitude of radiation. Here, in the case of parametric (quasi-Cherenkov) radiation, all the amplitudes A_l equal one another, while in the case of diffracted radiation of the oscillator (radiation of channeled particles), the amplitudes A_l depend on the the particle entry point into the channel, which should be taken into account in averaging the amplitudes. It is known that the root mean square angle of multiple scattering $\langle\vartheta^2\rangle = g\frac{E_s^2}{E^2}\frac{l}{L}$, where E_s =21 MeV, E is the particle energy, l is the traveled path length, L is the radiation length, g is the coefficient for the difference between $\langle\vartheta^2\rangle$ and $\langle\vartheta^2\rangle_{\rm am}$ in an amorphous medium. For positrons moving in the regime of planar channeling, the magnitude of g can be much less than unity. When $e^\pm$ move at small angles relative to the axes, the magnitude of g can become much greater than unity. Two requirements follows from inequality $\vec{k}\Delta\vec{u}_l T < 1$: $k_\perp\sqrt{\langle\vartheta^2\rangle}$, $l < 1$ and $kl\langle\vartheta^2\rangle < 1$. The former can always be chosen with the help of the

observation angle. The latter yields the requirement $l < \frac{1}{\sqrt{k\langle\vartheta^2\rangle_1}}$, where $\langle\vartheta^2\rangle_1$ is the root mean square angle of multiple scattering over the unit length ($l \sim \gamma$, γ is the particle Lorentz factor). This leads to the fact that even for quite hard radiation with the quantum energy of the order of 100 keV, the target thickness required to avoid the effect of multiple scattering on the radiation process, appears rather large ($l \leq 10^{-3}$ cm) for electrons with the energy of 1 GeV. We shall further assume that this condition is fulfilled. So from (49) we have the following expression for the spectral angular distribution of the number of emitted quanta $d^2N/d\omega d\Omega = W^s_{\vec{n}\omega}/\hbar\omega$:

$$\frac{d^2N}{d\omega d\Omega} = \frac{d^2N_1}{d\omega d\Omega}N_l + \frac{d^2N_1}{d\omega d\Omega}\sum_{l\neq m}\overline{e^{-i\vec{K}\vec{r}_l}e^{i\vec{K}^*\vec{r}_m}}, \tag{52}$$

where

$$\vec{r}_l = \left(\vec{r}_{0\perp l} - \vec{u}_{l\perp}\frac{z_{0l}}{u_{zl}}, \frac{u}{u_{zl}}z_{0l}\right), \quad \vec{K} = \left(\vec{k}_\perp, \frac{\omega}{u}\right)$$

in the case of parametric radiation; if radiation is produced by a relativistic oscillator (radiation from channeled particles, diffracted radiation of the oscillator) with the vibration frequency Ω in the laboratory system of coordinates, vector $\vec{K} = \left(\vec{k}_\perp, \frac{\omega\pm\Omega}{u}\right)$. From (52) follows that to achieve the conditions under which the velocity distribution Δu_l in a beam has no effect on (52), the longitudinal dimensions L_b of the bunch of particles should satisfy the relations:

$$\frac{\omega}{u}\frac{\Delta u_{zl}}{u}L_b < 1 \quad \text{and} \quad k_\perp\frac{\Delta u_\perp}{u}L_b < 1,$$

i.e.,

$$L_b < \frac{1}{k\nu^2} \quad \text{and} \quad L_b < \frac{1}{k\nu_\gamma\nu},$$

where ν is the characteristic angular distribution of particles' velocities in the beam; ν_γ is the quantum emission angle. When the longitudinal dimensions of the bunch satisfy these conditions, the magnitude of $\vec{r}_l$ in (52) can be taken equal to $\vec{r}_{0l}$. Now averaging in (52) is easy to perform. Since the double sum in (52) does not depend on velocities of particles, averaging is reduced to averaging over the initial distribution of the coordinates of particles in the beam. Let us introduce the beam density $\rho(\vec{r})$; $\int_{V_b} \rho(\vec{r}) d^3r = N_e$ (V_b is the bunch volume, N_e is the number of particles in the bunch). Upon averaging (52) with the distribution $\rho(r)$, we obtain

$$\frac{d^2N}{d\omega d\Omega} = \frac{d^2N_1}{d\omega d\Omega} N_e + \frac{d^2N_1}{d\omega d\Omega} \left| \int e^{-i\vec{K}\vec{r}} \rho(\vec{r}) d^3r \right|^2, \tag{53}$$

where $d^2N_1/d\omega d\Omega$ is the spectral angular distribution of quanta formed as a result of spontaneous radiation by a single electron. Let us consider a beam modulated as $\rho(\vec{r}) = \rho_0 + \rho_1 \cos(\vec{\tau}\vec{r})$. As a result, (54) will include rapidly oscillating integrals, which can be replaced by δ-functions with good accuracy. This enables writing (53) in the form

$$\frac{d^2N}{d\omega d\Omega} = \frac{d^2N_1}{d\omega d\Omega} N_e + \frac{d^2N_1}{d\omega d\Omega} \frac{\pi}{2} N_e \mu^2 \rho_0 \delta(\vec{K} - \vec{\tau}), \tag{54}$$

where $\mu = \rho_1/\rho_0$. From (54) follows that the total number of quanta emitted by the bunch equals

$$N = N_e \left(N_1 + c \left. \frac{d^2N_1}{d\omega d\Omega} \right|_{\vec{K}=\vec{\tau}} \frac{\pi}{2} \mu^2 \frac{\rho_0}{k_0^2} \right). \tag{55}$$

Here N_1 is the number of quanta of incoherent spontaneous radiation, which are produced by a single electron traversing the target under study; $k_0 = |\vec{\tau}| = \frac{2\pi}{\lambda_0}$, λ_0 is the radiation wavelength equal to the spatial modulation period d of the beam.

Note that (55) is easy to obtain from the following quantitative considerations: In performing integration over $d\omega d\Omega$ in (53), the characteristic range of values, where the second term in (53) is nonzero is: $\Delta k_\perp \sim 1/L_{\perp b}$ for the transverse dimension and $\Delta\omega/c \sim 1/L_b$, for the longitudinal dimension. As a result, we have

$$\int \frac{d^2N_1}{d\omega d\Omega}\left|\int e^{-i\vec{K}\vec{r}}\rho(r)d^3r\right|^2 d\omega d\Omega \simeq \left.\frac{d^2N_1}{d\omega d\Omega}\right|_{K=\tau} N_e^2\mu^2 c\frac{\Delta^2 k_\perp \Delta k_\parallel}{k_0^2}$$
$$\simeq c\left.\frac{d^2N_1}{d\omega d\Omega}\right|_{K=\tau} N_e^2\frac{1}{L_{\perp b}^2}\frac{1}{L_b}\frac{\mu^2}{k_0^2} \simeq N_e c\left.\frac{d^2N_1}{d\omega d\Omega}\right|_{K=\tau}\frac{\rho_0\mu^2}{k_0^2}, \tag{56}$$

i.e., the expression appearing in (55). The ratio of the total number of coherently emitted quanta to that of incoherently emitted quanta is

$$\frac{N_{\rm coh}}{N_{\rm incoh}} \simeq \frac{\pi}{2}\frac{\mu^2\rho_0}{k_0^2\Delta k\Delta\Omega}. \tag{57}$$

Here $\Delta k(\Delta\Omega)$ is the characteristic range k (of solid angles), where the quantum is emitted through incoherent spontaneous radiation; $\Delta k/k \sim 1/\gamma$, $\Delta\Omega \sim 1/\gamma^2$; γ is the particle Lorentz factor. In obtaining (57), the estimate $N_1 \simeq \frac{d^2N_1}{dkd\Omega}\Delta k\Delta\Omega$ was used; (57) can also be recast as

$$\frac{N_{\rm coh}}{N_{\rm incoh}} \simeq \frac{\mu^2\rho_0}{k_0^3}\gamma^3. \tag{58}$$

Note that according to [8], in the case of parametric radiation when $1/\gamma^2 < n_{\rm eff}-1$ ($n_{\rm eff}$ is the effective index of refraction in the radiation area), the characteristic range of radiation angles (the frequency distribution) $\Delta\vartheta$, $\Delta\omega/\omega \sim \sqrt{n_{\rm eff}-1}$. As a result, with growing γ, the ratio (58) tends to the limit $N_{\rm coh}/N_{\rm incoh} \simeq (\mu^2\rho_0/k_0^3)(n_{\rm eff}-1)^{-3/2}$. Recall that in the X-ray range of $10\div100$ keV, $n_{\rm eff}-1 \simeq 10^{-5}\div10^{-7}$. From (57), (58) follows that with other conditions being equal, the ratio $N_{\rm coh}/N_{\rm incoh}$ decreases rapidly with growing k (with

the decrease in the radiation wavelength). Thus for example, even at current densities in a beam as high as 10^8 A/cm^2, which corresponds to $\rho_0 \simeq 10^{17}$ and at $\mu = 1$, the ratio $N_{\rm coh}/N_{\rm incoh} \leq 10^{-1}$ for quantum energy of 10 keV and $\gamma = 10^3$. At the same time, the ratio of the spectral densities of radiation within the range of the emission angles $\Delta\vartheta \sim 1/kL_{\perp b} \ll 1/\gamma$ of coherent radiation is $\mu^2 N_e$.

Thus, within this range of emission angles, the intensity of coherent spontaneous radiation exceeds that of incoherent spontaneous radiation when the modulation depth is $\mu \geq 1\sqrt{N_e}$. For example, when the number of electron in the bunch is $N_e \simeq 10^{12}$, it is sufficient that $\mu \geq 10^{-6}$, which enables one to appreciably simplify the problem of experimental observation of coherent radiation in the X-ray range of 10-100 keV. Note that the formulas derived here are also applicable when the target is irradiated by the laser pulse of length greater than L_b. Indeed, let us divide the whole pulse length into the bunches, each of length L_b, i.e., we have (54), (55), where N_e stands for the number of electrons in the entire pulse.

Now let us estimate the number of quanta which can be produced coherently, e.g., in the case of parametric (quasi-Cherenkov) radiation mechanism. From general formulas (52) for parametric radiation in the Laue case follows the below expression for spectral-angular distribution of quanta emitted in the direction of diffraction:

$$\left.\frac{d^2N_1}{dkd\Omega}\right|_{\vec{K}=\vec{\tau}} \simeq \frac{e^2}{\hbar c\pi^2}\left|\frac{\chi_{\tau_1}}{\vartheta_B}\right|^2 k_0 N^2, \tag{59}$$

where L is the crystal thickness; χ_{τ_1} is the Fourier component of the crystal susceptibility for quantum diffraction by the system of planes defined by the

crystal reciprocal lattice vector r_1, ϑ_B is the Bragg diffraction angle.

According to (59), (55), for the number of coherently emitted quanta per electron we have

$$N_{1\mathrm{coh}} \simeq 10^{-3} \left| \frac{\chi_{\tau_1}}{\vartheta_B} \right|^2 \mu^2 \frac{\rho_0 L^2}{k_0}. \tag{60}$$

For radiation generated in Si, $\chi_\tau \sim 10^{-5}$ for (400) plane, $k_0 = 10^9$, $\vartheta_B \simeq 45^\circ$, $\rho_0 \simeq 10^{17}$, $L = 10^{-1}$ cm, we have $N_{1\mathrm{coh}} \simeq 10^{-7}\mu^2$.

In the case of PXR generation in a layered medium (i.e. in NiC) in the range of wavelengths $\simeq 50 \div 100$ Å, $\chi_\tau \sim 10^{-2}$, $k_0 = 10^7$, $L \simeq 10^{-4}$ cm, we have $N_{1\mathrm{coh}} \simeq 10^{-5}\mu^2$. At the same time, in the case of generation of surface PXR, when the quantum absorption length in the medium does not restrain the radiation intensity, which is proportional to the path length traveled over the grating [25], $N_{1\mathrm{coh}} \simeq 10^3\mu^2$ for $L = 1$ cm. When PXR is generated in the optical range $k_0 = 10^5$, $\chi_\tau = 10^{-1}$, $L \simeq 10^{-1}$ cm, we have $N_{1\mathrm{coh}} \simeq 10^5\mu^2$. Note here that the obtained estimates increase by two-three orders of magnitude in the case of Bragg diffraction because of the increase in d^2N_1 in narrow spectral ranges [138].

For the oscillator mechanism of radiation [20]

$$\frac{dN_{1\mathrm{osc}}}{dk d\Omega} \simeq \frac{e^2}{\hbar c \pi} \left(\frac{v_\perp}{c} \right)^2 k_0 L^2, \tag{61}$$

$v_\perp$ is the velocity amplitude of the transverse vibrations of the particle. For this reason, to obtain the estimates, $|\chi_\tau/\vartheta_B|^2$ in (60) is replaced by $(v_\perp/c)$. In particular, for positrons channeled in Si, the characteristic values of $v_\perp/c \simeq 10^{-5}$ and of $dN_{1\mathrm{osc}} \simeq dN_{1\mathrm{PXR}}$.

Thus, it follows from the above analysis that using a spatially modulated beam, one can observe coherent parametric X-ray radiation. Moreover, in a soft X-ray range, under the condition when the surface parametric radiation is generated [25], coherent radiation can be observed even when the degree of beam modulation is not very high (e.g., for $\mu \simeq 10^{-5}$, we have $N_{1\mathrm{coh}} \simeq 10^{-7}$). As a result, when the transmitted pulse contains $N_e \simeq 10^{12}$, we obtain $N_\gamma \simeq 10^5$, which is quite acceptable. The possibility to use modulated beams for generating coherent radiation in crystal undulators has recently been considered in [148].

7 Crystal X-ray Free Electron Lasers on the basis of PXR and DRO (DCR)

High spectral and angular densities of parametric (quasi-Cherenkov) and diffracted radiation of the oscillator as well as narrow spectral and angular widths of radiation reflex give a basis for application of considered spontaneous mechanisms of X-ray radiation for the construction of an X-ray coherent radiation source by using beams of relativistic particles in crystals. Such a system can be considered as a crystal X-ray free electron laser (FEL). The idea of X-ray FELs based on spontaneous parametric and DRO (DCR) radiation in crystals was first expressed in [46,47,48]. In [46,47,48,49,50], the dispersion equation for the eigenstates of the system consisting of electromagnetic radiation, a beam of relativistic oscillators and a crystal was obtained. The increment of the beam instability was also analyzed. The possibility in principle of obtaining X-ray coherent radiation with the help of a beam of relativistic oscillators in crystals was shown. In [51], the parametric (PXR) relativistic beam instability in a crystal was considered and the corresponding increment was obtained.

Radiative instability caused by spontaneous radiation in crystal undulators and by a laser wave propagating through a crystal was studied in [60]. Thus, in [46,47,48,49,50,51,60], a new kind of the X-ray FEL – the solid X-ray free electron laser (SXFEL) was suggested. As we have pointed out above, several mechanisms of spontaneous X-ray radiation generated by a relativistic electron beam in crystals can constitute the basis for such SXFELs: parametric (quasi-Cherenkov) X-ray radiation and diffracted radiation of oscillators formed in crystals, for example, by channeling [46,47,48,49,50,56,57,58,59] or under the action of an external field [58,60].

The main feature of such an X-ray generator is that the crystal target, in this case, not only forms the mechanism of spontaneous radiation, but also acts as a three-dimensional resonator for X-ray radiation which produces a distributed feedback (DFB). The construction of the X-ray generator by using channeled electron beams in crystals was also considered in [61,62,63,64,65] and the construction of the X-ray generator on the basis of resonance transition radiation was discussed in [66,67]. The possibility of using the crystal as a resonator that produces a one-dimensional distributed feedback for an X-ray coherent generator was first expressed in [68]. This idea was used for the formation of a one-dimensional DFB in a solid X-ray FEL on the basis of channeled particles in [64,65]. However, in all these works, the DFB was traditionally considered in a one-dimensional geometry when the radiated and diffracted waves propagate along one line in opposite directions. The authors of [64,65] obtained a low generation threshold for such a system with a one-dimensional DFB only due to ignoring the radiation self-absorption inside the crystal. The correct consideration of absorption, as it was shown in [59], leads to the threshold beam density of the order of $j^{th} \sim 10^{12}$ A/cm^2 for this DFB

geometry.

In the solid X-ray free electron laser, suggested
in [46,47,48,49,50,51,52,53,54,55,56,57,58,59,60], the crystal resonator produces a three-dimensional DFB that allows one to optimize the system and to essentially decrease the generation threshold. The analysis showed that the process of amplification and generation in such a crystal (natural or photonic) solid resonator essentially modifies and, under definite conditions, develops more intensively. It was shown that the interaction between the particle beam and the electromagnetic field is the strongest near the region of degeneration of roots of diffraction dispersion equation, particularly, in the case of multi-wave diffraction.

Let us consider in detail PXR and DRO (DCR) crystal X-ray FELs

8 Parametric (Quasi-Cherenkov) X-ray FEL

The quasi-Cherenkov instability of a relativistic electron (positron) beam in a three-dimensional periodic medium in the X-ray range was first considered in [51,139]. The authors formulated the problem of X-ray parametric radiation amplification in an infinite medium caused by quasi-Cherenkov instability of a beam of relativistic particles. The dispersion equation for the case of two-beam diffraction and the increment of instability was obtained. It was shown that the strongest interaction between the particle beam and radiation was close to the region of degeneration of the dispersion equation roots. The boundary problem of amplification of radiation in a finite parallel-plane crystal target was solved, and the generation threshold for the particle density was obtained. It was

assumed that a relativistic particle beam with a mean velocity $\vec{u}$ was incident at a definite angle ψ_0 on the parallel-plane crystal target with the length L. The orientation of the particle beam relative to crystallographic planes was made in such a way that spontaneous photons radiated by a particle beam were under diffraction conditions for planes with low indices. The fulfillment of diffraction condition not only brings about the possibility of quasi-Cherenkov radiation in the X-ray range itself but also produces a three-dimensional distributed feedback.

The closed set of equations describing the interaction of a radiating beam with a crystal, in the general case, consists of Maxwell's equations for the electromagnetic field and the equation for particle motion in the field (for a "cold" particle beam, $\theta\psi < (kL)^{-1}$, where θ is the radiation angle, ψ is the angular spread of particles in a beam, $\vec{k}$ is the photon vector) or the equation for the distribution function (in the case of a "hot" particle beam). For example, in the case of a "cold" beam we have:

$$\begin{aligned}
&\vec{\nabla}\times\vec{\nabla}\times\vec{E}(\vec{r},\omega)=\frac{4\pi i\omega}{c^2}\vec{j}(\vec{r};\omega)+\frac{\omega^2}{c^2}\vec{D}(\vec{r},\omega),\\
&\frac{d\vec{v}_\alpha(t)}{dt}=\frac{e}{m\gamma}\left\{\vec{E}(\vec{r}_\alpha(t),t)+\left[\frac{\vec{v}_\alpha(t)}{c}\vec{H}(\vec{r}_\alpha(t),t)\right]\right.\\
&\left.-\frac{\vec{v}_\alpha(t)}{c}\left(\frac{\vec{v}_\alpha(t)}{c}\vec{E}(\vec{r}_\alpha(t),t)\right)\right\},
\end{aligned}\tag{62}$$

where $\vec{j}(\vec{r},t)=e\sum\limits_\alpha\vec{v}_\alpha(t)\delta(\vec{r}-\vec{r}_\alpha(t))$ is the microscopic current density of particles in a beam, $n(\vec{r},t)=e\sum\limits_\alpha\delta(\vec{r}-\vec{r}_\alpha(t))$ is the corresponding charge density, $\vec{r}_\alpha(t)$ and $\vec{v}_\alpha(t)$ are the trajectory and the velocity of the α-th particle in a beam, $\vec{E}(\vec{r},t)$ and $\vec{H}(\vec{r},t)$ are the electric and magnetic strengths of the field, $\vec{D}(\vec{r},\omega)=\varepsilon(\vec{r},\omega)\vec{E}(\vec{r},\omega)$, $\varepsilon(\vec{\pi},\omega)=\sum\limits_\tau\varepsilon_\tau(\omega)e^{-i\vec{\tau}\vec{r}}$ is the crystal dielectric constant, $\varepsilon_0=1+g_0\cong 1-\omega_L^2/\omega^2$, $\omega_L^2=4\pi e^2n_0/m_e$, n_0 is the electron density

in a crystal, $g_\tau \equiv \varepsilon_\tau$ is the Fourier component of the dielectric constant, $\vec{\tau}$ is the reciprocal lattice vector.

For the case of two-wave generation, with the trajectory and velocity of a particle represented as $\vec{r}_\alpha(t) = \vec{r}_{0\alpha} + \vec{u}t + \delta\vec{r}_\alpha(t)$ and $\vec{v}_\alpha(t) = \vec{u} + \delta\vec{v}_\alpha(t)$, where $\vec{\tau}_{0\alpha}$ is the position of the α-th particle in a beam at the moment of intersection of the crystal boundary, the system (62) can be written as a system of Maxwell's equations for electromagnetic fields $\vec{E}(\vec{k},\omega)$ and $\vec{E}_\tau(\vec{k},\omega)$ in the following way [52,53,54,55]

$$\begin{aligned}\left(k^2c^2 - \omega^2\varepsilon_0 + \frac{\tilde{\omega}_L^2}{\gamma} - \omega^2\varepsilon_b(\vec{k})\right)E_\sigma - \omega^2 g_\tau E_\sigma^\tau = 0\\ -\omega^2 g_{-\tau}E_\sigma + \left(k_\tau^2c^2 - \omega^2\varepsilon_0 + \frac{\tilde{\omega}_L^2}{\gamma} - \omega^2\varepsilon_b(\vec{k}_\tau)\right)E_\sigma^\tau = 0,\end{aligned} \tag{63}$$

where $\vec{k}_\tau = \vec{k} + \vec{\tau}$, $E_\sigma = \vec{E}(\vec{k},\omega)\vec{e}_\sigma$, $E_\sigma^\tau = \vec{E}(\vec{k}_\tau,\omega)\vec{e}_\sigma$, $\vec{e}_\sigma \parallel [\vec{k}\vec{\tau}]$. The set of equations (63) is written for σ-polarization of radiation because it is excited with maximum probability at parametric (quasi-Cherenkov) radiation, $\tilde{\omega}_L^2 = 4\pi e^2\tilde{n}_0/m_e$, $\tilde{n}_0$ is the mean density of the unperturbed particle beam.

Comparison of (63) and the ordinary set of Maxwell's equations describing X-ray dynamical diffraction in a crystal allows one to conclude that the boundary problem of X-ray amplification (generation) under penetration of a particle beam through a periodic medium can be reduced to the problem of X-ray diffraction by an "active" periodic medium, which consists of the crystal + radiating particle beam and is characterized by the following dielectric constant:

$$\tilde{\varepsilon}_0(\vec{k}_\tau,\omega) = \varepsilon_0 - \frac{\tilde{\omega}_L^2}{\gamma\omega^2} - \frac{\tilde{\omega}_L^2}{\gamma\omega^2}\frac{(\vec{u}\vec{e}_\sigma)^2}{c^2}\frac{k^2c^2 - \omega^2}{(\omega - \vec{k}\vec{u})^2},$$

$$\tilde{\varepsilon}_0(\vec{k},\omega) = \varepsilon_0 - \frac{\tilde{\omega}_L^2}{\gamma\omega^2} - \frac{\tilde{\omega}_L^2}{\gamma\omega^2}\frac{(\vec{u}\vec{e}_\sigma)^2}{c^2}\frac{k_\tau^2 c^2 - \omega^2}{(\omega - \vec{k}_\tau\vec{u})^2}. \tag{64}$$

As the electron density in a beam is much smaller than that in a crystal, the second term on the right-hand side of (64) can be neglected. The last term has a resonance behavior under the fulfillment of synchronism condition between the particle beam and the electromagnetic field $\omega - \vec{k}\vec{u} \cong 0$. In the X-ray range, the fulfillment of this condition for a diffracted wave is impossible, that is why it is possible to consider $\vec{\varepsilon}_0(\vec{k}_\tau,\omega) \cong \varepsilon_0$.

In the case of a "hot" beam, the dielectric constant of such an "active" medium is represented as:

$$\tilde{\varepsilon}_0(\vec{k}_\tau,\omega) = \varepsilon_0 - \frac{\tilde{\omega}_L^2}{\gamma\omega^2}\frac{xe^{-x^2}\theta^2}{(\psi_1\cos\varphi + \psi_2\sin\varphi + \psi_\parallel/\gamma^2\theta)^2},$$

where $x = \omega - \vec{k}\vec{u}$, ψ_1, ψ_2, $\psi_\parallel$ are the transverse and longitudinal divergences of the particle velocities in a beam, φ is the azimuthal angle of a photon, θ is the angle between the photon wave vector and the z-axis, directed inside the crystal as a normal to the crystal surface.

Thus, the reduction of the analysis of amplification and generation processes in an X-ray FEL to the solution of a boundary problem of X-ray dynamical diffraction by an "active" crystal target of length L enables one to find generation thresholds of such a system for different regimes of FEL operation and to perform the optimization of parameters [54,55].

The dispersion relation determining the solutions for the electromagnetic wave vector inside the "active" medium in the case of two-wave generation is as follows:

$$(\omega - \vec{k}\vec{u})^2 \left\{ (k^2c^2 - \omega^2\varepsilon_0)(k_\tau^2 c^2 - \omega^2\varepsilon_0) - \omega^4 g_\tau g_{-\tau} \right\}$$
$$= -\frac{\tilde{\omega}_L^2}{\gamma} \frac{(\vec{u}\vec{e}_\sigma)^2}{c^2} (k^2c^2 - \omega^2)(k_\tau^2 c^2 - \omega^2\varepsilon_0). \quad (65)$$

and the general solution of the set of equations (63) can be represented in the form

$$\vec{E} = \sum_{\mu=1}^{4} \vec{e}_\sigma C_\mu e^{i\vec{k}_0\vec{r}} (1 + S_\mu e^{i\vec{\tau}\vec{r}}) e^{i\delta_\mu z}, \quad (66)$$

where

$$S_\mu = \frac{\omega^2 g_{-\tau}}{k_\mu^2 c^2 - \omega^2\varepsilon_0}, \quad \vec{k}_\mu = \vec{k}_0 \delta_\mu \vec{n}_z$$

are the roots of dispersion equation (65). The wave amplitudes C_μ are found from the matching conditions for the electromagnetic field (66) on the boundaries of the crystal target and are given in [55].

As a result, the generation conditions for the case of a two-wave distributed feedback and different cases of "cold" and "hot" beams as well as for different regimes (weak and high gain regimes) were obtained. It was shown that in all cases the generation threshold has a simple meaning: on the left-hand side of equality there is always the term describing the "production" of radiation inside the crystal; on the right-hand side, there are two terms describing the radiation losses. Particularly, the first of these terms refers to the radiation losses through the crystal boundaries, while the second term corresponds to self-absorption of radiation inside the crystal.

The analysis showed that the conditions of generation threshold are optimal near the region of degeneration of roots of dispersion equation (65). This region corresponds to the edge of a nontransparency region in the dynamical diffrac-

tion theory, and the interaction of the electromagnetic field with a particle beam and with a crystal is most effective here.

It should be noted that the condition of the degeneration of dispersion equation roots leads to the requirement for the photon radiation angle $\theta^2 = (-\beta_1)^{-1/2}|g_\tau| - |g'_0| - \gamma^2$, and this, in turn, gives the restriction for the possible geometry of Bragg diffraction in the X-ray range $-\frac{r'}{|g'_0|+\gamma^2} < \beta_1 < 0$, where $r = g_\tau g_{-\tau}$.

The estimations of the threshold magnitude of the beam current density showed that the case of a two-wave solid distributed feedback is not an optimal case for achieving the generation regime in the X-ray range. If for a "cold" particle beam in LiH and $\psi_\perp < 10^{-6}$ rad, $\psi_\parallel < 10^{-8}$ rad, the threshold current is of the order of 10^9 A/cm^2 at $l \sim 0.1$ cm, then multiple scattering of electrons makes the beam "hot" and leads to the increase in the threshold density of a particle beam up to $j_{th} \geq 10^{10}$ A/cm^2.

Because of the destructive influence of multiple scattering process on the quality of a beam of relativistic particles and, consequently, on the threshold conditions, the crystal target length should be to reduced as much as possible. As is known from the optical laser theory, the mirror resonator, similar to a Fabry-Perot resonator, is used for this purpose. In the X-ray range, mirrors can be replaced by crystal plates that are oriented in such a way that the radiation wave vector is under the Bragg condition. Due to radiation, the generation process takes place in a narrow angular and spectral interval $\Delta\omega/\omega \sim \Delta\theta \leq 10^{-5}$; high effectiveness of the radiation reflection under diffraction conditions by an external crystal resonator can be obtained under the corresponding coordination of the resonator and the crystal target ("active" medium). This allows

one to essentially reduce the radiation losses through target boundaries. In [54], the generation threshold for the system with the external Braggmirrors was derived, and it was shown that the term connected with losses through the boundaries could be reduced by a factor of $(1 - |R|)$, where R is the reflection coefficient of a Bragg mirror. As a result, we can shorten the crystal length to the size necessary for achieving the generation threshold. However, the estimation showed that the threshold magnitude holds rather high.

As the analysis in [54] showed, the transition to the distributed feedback under the surface uncoplanar diffraction when the radiating particle beam is incident on a crystal at a small angle $\psi \sim \sqrt{g_0'}$ relative to the crystal surface (see Figure 3), allows one to step down the generation threshold. First of all, the destructive influence of multiple scattering on the particle beam is suppressed. Besides, the behavior of dispersion equation roots changes, which modifies the process of radiation amplification.

The disadvantage of the case of two-wave diffraction distributed feedback is that the coordination between the degeneration condition of dispersion equation roots and the requirement of Cherenkov synchronism hardly fixes the geometry of distributed feedback and leads to small magnitudes of the diffraction asymmetry factor β_1. This, in turn, leads to the enhancement of self-absorption of radiation inside the crystal target. In [48] was pointed out that the transition to the multi-wave diffraction allows one to modify the functional dependence of the increment of the particle beam instability and, consequently, to step down the threshold density of a beam as well. The dispersion equation for the three-wave coplanar diffraction geometry of distributed feedback was obtained, and the rule for writing the dispersion equation for an arbitrary multi-wave diffraction distributed feedback was formulated. In [54], the expression for the

generation threshold in the case of three-wave coplanar diffraction was also derived. It was shown that in this case the Cherenkov condition was fulfilled for two dispersion branches, which provided the possibility of the coincidence of diffraction roots with Cherenkov synchronism condition near the exact Bragg condition and, consequently, the possibility of optimization of the threshold magnitude. In the case of the Laue-Bragg diffraction geometry, the threshold density of the beam can be reduced to $j_{th} \sim 10^8$ A/cm^2, at $\psi \sim 5 \cdot 10^{-5}$ rad in the vicinity of the double degeneration of dispersion equation roots. It should be noted that even in the case of three-wave generation, it becomes possible to apply the phenomenon of anomalous X-ray penetration under diffraction condition and, as a result, to step down self-absorption of radiation inside the crystal.

Thus, we can conclude that the most suitable geometry for the achievement of the generation regime of quasi-Cherenkov X-ray radiation with the help of relativistic electron (positron) beams in crystals is the grazing geometry of the particle beam incidence on a target with the distributed feedback formed by multi-wave surface diffraction.

The spectral-angular distribution of the coherent PXR near the generation threshold was obtained in [55].

In [52], the spectral-angular distribution of coherent radiation far from the generation threshold was derived within the framework of the perturbation theory, and the possibility of experimental observation of the coherent PXR in existing accelerators was analyzed. It was shown that observation of coherent parametric (quasi-Cherenkov) radiation far from the generation threshold was a very complicated problem for the X-ray range, but it was possible to observe

the coherent radiation in an optical range nowadays.

9 The X-ray generator on the basis of diffracted channeling radiation (DCR)

The second type of a crystal generator is based on the application of diffracted radiation by the oscillator (DRO) as a spontaneous radiation mechanism [56,57,58,59,60]. As stated above, the radiating oscillator can be formed in different ways. This can be electrons channeled in an averaged crystallographic potential of planes or axes, or electrons moving in an electrostatic wiggler [58] or, for example, an oscillator formed by an external ultrasonic (optical) wave in a crystal [60]. It is obvious that the general approach to the consideration of the generation problem with the help of a relativistic oscillator beam does not depend on the formation mechanism of the oscillator itself. Since the oscillator is a quantum system, it is more accurate to perform the calculation of the polarizability tensor of a particle beam within the framework of quantum electrodynamics. Reduction of the problem of radiation application (generation) by a particle beam in a finite crystal target to the problem of diffraction of X-rays by an "active" medium, consisting of a crystal and a beam of radiating oscillator, holds true in this case as well.

The expression for the polarizability of such an "active" medium in the case of channeled particles in unperturbed averaged crystal potential was obtained in [57]:

$$\tilde{\varepsilon}_0(\vec{k},\omega) = \varepsilon_0 - \frac{\tilde{\omega}_L^2}{\gamma\omega^2} - \frac{4\pi e^2 n_0}{\omega^2}(W_2 - W_1)\frac{\left|\vec{a}(\vec{k})_{21}\vec{e}_\sigma\right|^2}{\omega - \vec{u}\vec{k} - \Omega_{21} + i\Gamma}; \qquad (67)$$

where $\vec{\alpha}_{21}(\vec{k})$ is the matrix element of the operator $\hat{\alpha}\exp(i\vec{k}\vec{r})$, which in the dipole approximation takes the form

$$\vec{\alpha}(\vec{k})_{21} = -ix_{21}(\Omega_{21}\vec{n}_x + k_x\vec{u}_z).$$

The axis $\vec{n}_x$ is chosen so that it lies along the transverse particle oscillations in a channel, $\vec{u}_\parallel$ is the longitudinal velocity parallel to the channeling planes, ($k_x = \vec{k}\vec{n}_x$, $\vec{u}_\parallel\vec{n}_x = 0$), Ω_{21} is the frequency of the transition, $\vec{e}_\sigma \parallel [\vec{k}\vec{\tau}]$, W_1 and W_2 are the population of the states 1 and 2, Γ is the phenomenological constant, taking into account inelastic oscillations; its order of magnitude estimate gives $(L_d)^{-1}$, where L_d is the dechanneling length. In obtaining (67), it was taken into account that the synchronism condition could be fulfilled only for the wave propagating at a small angle relative to the longitudinal velocity of the particle. The fulfillment of the synchronism condition for the diffracted wave is impossible in the X-ray range. As the analysis showed [57], although there were a lot of zones (states) of transverse energy of a channeled particle, the main contribution to the polarizability tensor was made by a certain transition with the frequency Ω_{21}. This means that the consideration is reduced to the two-level problem.

Indeed, the contribution to the beam polarizability from the transition between the levels m and n is determined by the deviation from the exact synchronism condition of the radiation field with the oscillator, i.e., $\mathtt{Re}(\omega - \vec{u}\vec{k} - \Omega_{mn}) = 0$. This contribution should be taken into account only if

$$\left|\mathtt{Re}(\omega - \vec{u}\vec{k} - \Omega_{mn}) \leq \left|\mathtt{Im}(\vec{k}\vec{u} - \omega) + \Gamma_{mn}\right|\right| \tag{68}$$

If the magnitudes of $\mathtt{Re}\omega$ and the angle between $\vec{u}$ and $\vec{k}$ are fixed, the number

of transitions contributing to the polarizability depends on the relationship between $\Delta\Omega$ and $\left|\mathtt{Im}(\vec{k}\vec{u}-\omega)+\Gamma_{mn}\right|$, where $\Delta\Omega$ determines the typical value of the difference $\Omega_{n+1,n}-\Omega_{n,n-1}$ which characterizes the unharmonism of the averaged potential (for a harmonic potential $\Delta\Omega = 0$). The analysis of the magnitude of $\Delta\Omega$ for different kinds of averaged crystallographic plane potentials shows that

$$\Delta\Omega \gg \left|\mathtt{Im}(\vec{k}\vec{u}-\omega)+\Gamma_{mn}\right|,$$

and, consequently, the synchronism condition can be fulfilled only for a certain transition Ω_{21}. Other terms in a polarizability tensor can be neglected as nonresonant. It was shown that the most effective interaction between the oscillator beam and the radiated wave takes place near the degeneration region of roots of the dispersion equation determining the eigenstates of the field in an "active" medium. But, as contrasted to the parametric (quasi-Cherenkov) generator, for which the radiation condition is realized only at large deviation from the exact Bragg condition, now there is a possibility to overlap the synchronism condition with the exact diffraction condition. As a result, in the case under consideration the manifestation of the effect of anomalous X-ray penetration through the resonator under dynamic diffraction (Borman effect) is possible. This circumstance is very important because of strong absorption of X-rays inside a crystal target. In [57] the boundary problem of X-ray diffraction by an "active" medium of a finite size was solved, and the generation condition was obtained. It was shown that the beam can be in synchronism with one of the modes of the "active" medium. These modes correspond to the waves with the wave vectors being the roots (δ_1 and δ_2) of the dispersion equation. According to [57], the generation condition can be realized in two

cases: for the wave corresponding to the root δ_2 at the positive magnitude of $\alpha = \alpha_+$ and for the wave corresponding to the root δ_1 for the negative deviation from the exact Bragg condition $\alpha = \alpha_-$. It was shown that the solutions of the generation equation for different modes are identical in structure. All of them lead to the phase condition

$$\delta_1^{(0)} - \delta_2^{(0)} = \frac{2\pi n}{\omega L} \tag{69}$$

where $\delta_1^{(0)}$ and $\delta_2^{(0)}$ are the solutions of the diffraction dispersion equation. The conditions of generation are written for the case of a channeled particle in [57] and for the case of electrostatic and magnetostatic wiggler in [58].

If the condition (69) is fulfilled, the longitudinal structure of the modes turns out to be close to the structure of a standing wave. That is, $|E|^2$ and $|E_\tau|^2$ are proportional to $\sim \cos^2 \frac{2\pi n}{\omega L}(z - L)$. This condition is similar to a well known phase condition of the stand wave appearance in a mirror resonator of an ordinary laser [60]. The meaning of amplitude conditions is the same as in the case of the quasi-Cherenkov X-ray generator. The field amplification, due to the radiation process, should be equal to the radiation losses caused by absorption inside the crystal and the output of radiation through the boundaries of the crystal target. Because the gain in the weak-gain regime is proportional to the current density of a beam, the formula for the threshold gain sets requirements for the current density. The invariant characteristics of a particle beam are often used instead of the current density, that is, the current I, the normalized emittance $\varepsilon_n = \gamma r \langle\psi\rangle$ and the normalized brightness $B_n = I/\pi^2\varepsilon_n^2$, where r is the beam radius, $\langle\psi\rangle$ is the angular spread. The angular spread corresponds to the divergence of the longitudinal velocity $\sigma_\varepsilon \cong u\langle\psi^2\rangle/2$, and the corresponding divergence of the particle energy is $\left(\frac{\Delta\gamma}{\gamma}\right)_e = \gamma_\parallel^2 \frac{\langle\psi^2\rangle}{2}$. For a LiH crystal, the

diffraction plane (220) the values of the threshold normalized brightness of the beam, which correspond to the generation threshold for magnetic, optical undulators and channeled particles, are given in Table 1. According to Table 1, the value of brightness in the case of two-wave distributed feedback is rather high. But, as it was shown for a parametric quasi-Cherenkov generator, using the surface multi-wave diffraction for the formation of disturbed feedback, one can decrease the threshold characteristics of a particle beam and provide the achievement of the generation regime.

In [57] the underthreshold spectral-angular distribution of radiation was analyzed and it was shown that the observation of collective radiation by relativistic oscillators was a very complicated problem in the X-ray spectral range.

Thus, the parallel consideration of two kinds of crystal three-dimensional X-ray generators, which are distinguished by the mechanisms of spontaneous radiation, shows that three-dimensional distributed feedback allows one to decrease the current density of the particle beam by several orders of magnitude in comparison with the results obtained in [61,62,63,64,65]. This enables one to consider the construction of the FEL in the hard X-ray range as a scientific problem of nowadays, which can be analyzed both theoretically and experimentally.

10 Crystal X-ray FEL based on a natural crystal or an electromagnetic undulator

Crystal X-ray FELs based on a natural crystal and on an electromagnetic undulator were first considered in [60]. The English version of this paper is

Table 1

Parameters	Magnetostatic Wiggler	Optical Wiggler	Channeled Particle
Accelerator			
Energy	$= 5$ GeV	$= 290$ MeV	$= 500$ MeV
Normalized brightness	$= 3.5 \cdot 10^{9}$	$= 1.7 \cdot 10^{10}$	$= 5 \cdot 10^{9}$
Energy spread	$= 2.4 \cdot 10^{-3}$	$1.2 \cdot 10^{-5}$	
Density of current	$= 5.3 \cdot 10^{7}$	$= 1.3 \cdot 10^{6}$	$= 3.3 \cdot 10^{8}$
Wiggler			
Wavelength	$= 1$ mm	$= 5\,\mu m$	
Magnetic field strength	$= 17.5$ kG		
Laser energy		$= 0.75$ gW	
Crystal			
Wavelength of radiation	$= 0.05$ Å	$= 0.15$ Å	$= 1$ Å
Asymmetry parameter	$= 9$	$= 1$	
Diffraction plane	(220)	(220)	(100)

given below.

Let a relativistic electron (or positron) beam of velocity $\vec{u}_0$ and the beam velocity distribution $\Delta\vec{u}$ move in a spatially periodic medium (e.g., in a crystal).

Let a linearly polarized laser pump wave be incident onto the beam along the direction $\vec{n}_p$. Let the wave have the wave vector $\vec{k}_p = \vec{k}_p n$, frequency ω_p, and the field strength $\vec{E}_p = \vec{E}_p^0 \cos(\vec{k}_p \vec{r} - \omega_p t + \delta)$, where δ is the initial vibration phase. The z-axis is chosen directed along the beam's average velocity $\vec{u}_0$. The presence of the electromagnetic pump wave induces radiation leading to various sorts of instability. The most known of them is the so-called the three-wave parametric instability, which emerges due to the conversion of the pump wave into the Doppler-shifted electromagnetic wave and the charge density wave: $\omega_p = \omega + \omega_{ch}$, $\vec{k}_p = \vec{k} + \vec{k}_{ch}$ (ω, $\vec{k}$ are the frequency and the wave vector of the high-frequency wave, respectively, ω_{ch}, $\vec{k}_{ch}$ are the frequency and the wave vector of a charge density wave). This process is scrutinized for the case of homogeneous matter [120].

In the case of a 3 D-periodic medium that we are considering here, the situation is basically different from that studied earlier because for ω and $\vec{k}$ satisfying the Bragg condition, the wave scattered by the beam is diffracted.

Maxwell's equations and the equations of particle motion, which describe the process under study, have the form:

$$
\begin{aligned}
&\mathrm{rot}\vec{H} = \frac{1}{c}\frac{\partial \vec{D}}{\partial t} + \frac{4\pi}{c}\vec{j}, \qquad \vec{D}(\vec{r},t) = \int\limits_{-\infty}^{\infty} \varepsilon(\vec{r}, t-t')\vec{E}(\vec{r},t')dt', \\
&\mathrm{rot}\vec{E} = -\frac{1}{c}\frac{\partial \vec{H}}{\partial t}, \qquad \mathrm{div}\vec{E} = 4\pi\rho, \qquad \frac{\partial \rho}{\partial t} + \mathrm{div}\vec{j} = 0, \\
&\vec{j}(\vec{r},t) = e\sum_i \vec{v}_i(t)\delta(\vec{r} - \vec{r}_i(t)), \\
&\rho(\vec{r},t) = e\sum_i \delta(\vec{r} - \vec{r}_i(t)), \\
&\frac{d\vec{v}_i(t)}{dt} = \frac{e}{m\gamma_i}\vec{E}(\vec{r}_i(t),t) + \frac{e}{mc\gamma_i}\left[\vec{v}_i(t)\vec{H}(\vec{r}_i(t),t)\right] \\
&-\frac{e}{mc^2\gamma_i}(\vec{v}_i(t)(\vec{v}_i(t)\vec{E}(\vec{r}_i(t),t))),
\end{aligned}
\tag{70}
$$

where $\vec{E}(\vec{r}_i(t)),t)$, $\vec{H}(\vec{r}_i(t),t)$ are the electric and magnetic field strengths at moment t at the location point of the i-th electron $\vec{r}_i(t)$, $\vec{D}$ is the electric induction, $\varepsilon(\vec{r},t)$ is the dielectric permittivity of the crystal at point $\vec{r}$, $\varepsilon(\vec{r},t) = 0$ at $t<0$, $\vec{v}_i(t)$ is the velocity of the i-th electron of the beam at time t, $\vec{j}(r,t)$ is the beam's current density at point $\vec{r}$ at time t, $\rho(\vec{r},t)$ is the density of the beam's electron charge, e is the electron charge of the particle ($e = \pm|e|$), $\gamma_i = (1 - v^2/c^2)^{-1/2}$ is the particle Lorentz factor, c is the velocity of light.

For the Fourier transforms $\vec{D}(\vec{r},\omega)$ and $\vec{E}(\vec{r},\omega)$, we have the relation $\vec{D}(\vec{r},\omega) = \varepsilon(\vec{r},\omega)\vec{E}(\vec{r},\omega)$, where the crystal's spatially periodic dielectric permittivity can be represented as the Fourier series: $\varepsilon(\vec{r},\omega) = \sum \varepsilon_\tau(\omega)e^{i\vec{\tau}r}$, $\vec{\tau}$ is the reciprocal lattice vector. Studying the possibility of occurrence of induced radiation, one should first of all determine the gain coefficient or, which is the same, the beam instability increment. To find them, in solving (70) we may confine ourselves to linear approximation, finding the dielectric permittivity of the beam+crystal system in the presence of the given pump wave. Take the Fourier transform in time of (70). To be more specific, let us further consider the case when a single diffracted wave $\vec{k}_\tau = \vec{k}+\vec{\tau}$ appears through diffraction. Let us also assume that the scattering plane of the wave, i.e., the plane defined by vectors $\vec{k}_p$ and $\vec{k}$ coincides with the diffraction plane defined by $\vec{k}$, $\vec{k}_\tau$. In a similar way as in the case of dynamical diffraction of X-rays, the generation of π- and σ-polarized waves in the crystal in the absence of the beam can be considered separately. Recall that the polarization vector of σ-polarized waves is orthogonal to the diffraction plane

$$\vec{e}_\sigma \parallel \vec{e}_0^{\vec{r}} \parallel \frac{[\vec{k}\vec{\tau}]}{|[\vec{k}\vec{\tau}]|}.$$

We also assume that the polarization vector $\vec{e}_p$ of the pump wave is parallel

to $\vec{e}_\sigma$. In this case, upon taking the Fourier transform, (70) takes the form:

$$\begin{cases} (k^2c^2 - \varepsilon_0\omega^2)E_\sigma(\vec{k},\omega) - \varepsilon_\tau\omega^2 E_\sigma(\vec{K}_\tau,\omega) = 4\pi i\omega j_\sigma(\vec{k},\omega), \\ (k_\tau^2c^2 - \varepsilon_0\omega^2)E_\sigma(\vec{k}_\tau,\omega) - \varepsilon_{-\tau}\omega^2 E_\sigma(\vec{k},\omega) = 0, \\ \omega E_\parallel(\vec{k},\omega) = -4\pi i j_\parallel(\vec{k},\omega), \end{cases} \tag{71}$$

where $\parallel$ denotes the component of the field and current strength parallel to the wave vector $\vec{k}$, $\vec{E}_\sigma = (\vec{E}\vec{e}^{\nu})$. In writing (71), the components $j_\sigma(\vec{k}_\tau,\omega)$ and $j_\parallel(\vec{k}_\tau,\omega)$ of the current, for which the synchronism condition does not hold in the X-ray range and whose contribution is therefore small, are discarded. Without channeling, the particle velocity in the beam can be represented as a sum:

$$\vec{v}_i(t) = \vec{u}_i + \vec{v}_{pi}(t) + \delta\vec{v}_{i\sigma}(t) + \delta\vec{v}_{i\parallel}(t),$$

where $\vec{u}_i$ is the particle's longitudinal velocity in the absence of the electromagnetic wave.

$$\vec{v}_{pi}(t) = -\frac{e\vec{E}_p^0}{m\gamma_i\omega_p}\sin(\vec{k}_p\vec{r}_{0i} - \overline{\omega}_p t + \delta) \equiv \vec{v}_p^0\sin(\vec{k}_p\vec{r}_{0i} - \overline{\omega}_p t + \delta)$$

is the velocity of the i-th particle under the external electromagnetic pump wave, $\overline{\omega}_p = \omega_p - (\vec{k}_p\vec{u}_i)$, $\delta\vec{v}_{i\sigma}(t)$ is the velocity disturbance of the i-th particle in the field of a transverse scattered electromagnetic wave, $\delta\vec{v}_{i\parallel}(t)$ is the velocity disturbance induced by a longitudinal wave. The position of the i-th particle at time t is written accordingly $\vec{r}_i(t) = \vec{r}_{0i} + \vec{u}_i(t) + \delta\vec{r}_i(t)$, where $\vec{r}_{0i}$ is the position of the i-th particle ($e^\pm$) in the beam at time $t = 0$, $\delta\vec{r}_i(t)$ is the time change of the position of the i-th ($e^\pm$) in the beam.

The Fourier components of the transverse and the longitudinal current in the linear approximation with respect to perturbation can be presented as follows:

$$j_\sigma(\vec{k},\omega) = \frac{i(\vec{e}_\sigma\langle\vec{u}_i\rangle)}{4\pi}(\vec{k}\vec{E}(k,\omega)) + \left\langle \frac{i(\vec{e}_\sigma\vec{v}_p^0)}{4\pi}((\vec{k}-\vec{k}_p)\vec{E}(\vec{k}-\vec{k}_p,\omega-\omega_p)) \right.$$
$$\left. +e\langle\sum_i \delta v_{i\sigma}(\omega-\vec{k}\vec{u}_i)e^{-i\vec{k}\vec{r}_{0i}}\right\rangle, \tag{72}$$

$$j_\parallel(\vec{k},\omega) = \frac{i(\vec{k}\langle\vec{u}_i\rangle)}{4\pi}E_\parallel(\vec{k},\omega) + e\langle\sum_i \delta v_{i\parallel}(\omega-\vec{k}\vec{u}_i)e^{-i\vec{k}\vec{r}_{0i}}\rangle$$
$$+\begin{cases} e(\vec{v}_p^0\vec{n}_k)n_0, & \vec{k}=\vec{k}_p, \\ \\ \frac{i(\vec{v}_p^0\vec{n}_k)}{4\pi}((\vec{k}-\vec{k}_p)\vec{E}(\vec{k}-\vec{k}_p,\omega-\omega_p)), & \vec{k}\neq\vec{k}_p. \end{cases} \tag{73}$$

$\langle\quad\rangle$ denotes averaging over the velocity distribution in the beam.

To obtain a closed system of equation, let us take the Fourier transform of the equation of particle motion (70) and separate the transverse components of the velocity and the perturbation field from the longitudinal ones. The linear approximation to the disturbance of the particle velocity gives

$$\langle\sum_i \delta v_{i\sigma}(\overline{\omega})e^{-i\vec{k}\vec{r}_{0i}}\rangle = \left\langle\frac{ie^2n_0}{m\omega\gamma_i}\delta E_\sigma(\vec{k},\omega)\right\rangle + \left\langle\frac{ie^2n_0}{4m\overline{\omega}\gamma_i}\right.$$
$$\times\left\{\left[\frac{(\vec{e}_\sigma\vec{k}_p)}{\omega_p-\omega}+(\vec{v}_p^0\vec{e}_\sigma)-\frac{2(\vec{v}_p^0(\vec{k}-\vec{k}_p))}{\omega-\omega_p}\right]\delta E_\sigma(\vec{k}-\vec{k}_p,\omega-\omega_p)\right. \tag{74}$$
$$\left.+2(\vec{v}_p^0\vec{e}_\sigma)\langle(\vec{n}_k\vec{v}_i)\rangle\delta E_\parallel(\vec{k}-\vec{k}_p,\omega-\omega_p)\right\} - \frac{ie^2n_0}{mc^2\overline{\omega}\gamma_i}\left[(\vec{u}_i\vec{e}_\sigma)^2\delta E_\sigma(\vec{k},\omega)\right.$$
$$\left.\left.+(\vec{u}_i+\vec{e}_\sigma)(\vec{u}_i\vec{n}_K)\delta E_\parallel(\vec{k},\omega)\right]\right\rangle,$$

$$\left\langle \sum_i \delta v_{i\|}(\overline{\omega}) e^{-i\vec{k}\vec{r}_{0i}} \right\rangle = \left\langle \frac{ien_0(1-(\vec{u}_i\vec{n}_k)^2)}{m\overline{\omega}\gamma_i}\delta E_\|(\vec{k},\omega) \right.$$
$$+\frac{ien_0}{m\overline{\omega}\gamma_i}\left[\frac{k}{\omega}-\frac{(\vec{u}_i\vec{n}_k)}{c^2}\right](\vec{u}_i\vec{e}_\sigma)\delta E_\sigma(\vec{k},\omega)+\frac{ien_0}{mc\overline{\omega}\gamma_i} \qquad (75)$$
$$\left.\times\left[\frac{\vec{k}_p-\vec{k}}{\omega_p-\omega}-\frac{(\vec{u}_i\vec{n}_{k_p-k})}{c}\right](\vec{v}_p^0\vec{e}_\sigma)\delta E_\sigma(\vec{k}-\vec{k}_p,\omega-\omega_p),\right.$$

where $\overline{\omega}=\omega-\vec{k}\vec{u}_i$, $\langle\ldots\rangle$ is averaging over $\vec{u}$.

Substitution of the obtained expressions for the velocity disturbance into (72), (73) and then into (71) gives a closed system of equations for transverse and longitudinal fields under two-wave dynamical diffraction of scattered radiation:

$$\begin{aligned}&(k^2c^2-\varepsilon_0\omega^2-\langle\omega_{p\perp}^2\rangle)\delta E_\sigma(\vec{k},\omega)-\varepsilon_\tau\omega^2\delta E_\sigma(\vec{k}_\tau,\omega)\\&=G_1\delta E_\sigma(\vec{k},\omega)+G_2\delta E_\sigma(\vec{k},\omega),\\&(k_\tau^2c^2-\varepsilon_0\omega^2-\langle\omega_{p\perp}^2\rangle)\delta E_\sigma(\vec{k}_\tau,\omega)-\varepsilon_{-\tau}\omega^2\delta E_\sigma(\vec{k},\omega)=0,\end{aligned} \qquad (76)$$

where

$$\langle\omega_{p\perp}^2\rangle=\frac{\omega_L^2}{\langle\gamma\rangle}=\frac{4\pi e^2n_0}{m_e\langle\gamma\rangle},\quad \omega_{p\|}^2=\frac{\omega_L^2}{\langle\gamma\rangle^3},$$

n_0 is the unperturbed particle density in the beam, m_e is the mass of $e^\pm$,

$$\begin{aligned}G_1=&\left\langle\frac{\omega_{p\perp}^2(\vec{e}_\sigma\vec{u})^2}{4c^2(\overline{\omega}^2-\omega_{p\|}^2)}(\omega^2-k^2c^2)\right\rangle,\\G_2=&\left\langle\frac{(\vec{v}_p^0\vec{e}_\sigma)^2\omega_{p\perp}^2((\vec{k}-\vec{k}_p)\vec{n}_k)}{4c^2[(\overline{\omega}-\overline{\omega}_p)^2-\omega_{p\|}^2]}\left[(\vec{k}_p\vec{n}_{k_p-k})c-\omega_p(\vec{\beta}\vec{n}_{k_p-k})\right.\right.\\&\left.\left.+(kc-\omega(\vec{\beta}\vec{n}_k))\right]\right\rangle.\end{aligned} \qquad (77)$$

The determinant of (76) defines the dispersion equation that specifies the relation between $\vec{k}$ and ω and enables finding the instability increment of the beam. We shall describe the beam by Maxwell's velocity distribution $f(\vec{u})$ with the effective temperatures T_1, T_2, T_3 over the x, y , z axes, respectively

or, which is the same, with thermal-induced velocity dispersions characterized by average thermal velocities $v_{\alpha T} = \sqrt{\frac{2T_\alpha}{m}}$:

$$f(\vec{u}) = \frac{1}{\pi^{3/2} v_{1T} v_{2T} v_{3T}} e^{-\frac{(u_x - u_{0x})^2}{v_{1T}^2}} e^{-\frac{(u_y - u_{0y})^2}{v_{2T}^2}} e^{-\frac{(u_z - u_{0z})^2}{v_{3T}^2}}. \tag{78}$$

Upon averaging (77) with the function (78), we obtain

$$G_1 = -\frac{\omega_{p\perp}^2 (\vec{e}_\sigma \vec{u}_0)^2 (\omega^2 - k^2 c^2)}{2c^2 \Omega^2} \left\{ 1 + i \frac{\sqrt{\pi}\overline{\omega}}{\Omega} W\left(\frac{\overline{\omega}}{\Omega}\right) \right\}, \tag{79}$$

$$G_2 = -\frac{(\vec{v}_p^0 \vec{e}_\sigma)^2 \omega_{p\perp}^2 ((\vec{k} - \vec{k}_p)\vec{n}_k)}{2c^2 \Omega_1^2} \left[((\vec{k}_p \vec{n}_{k_p - k}) c - \omega_p (\vec{\beta} \vec{n}_{k_p - k})) \right.$$
$$\left. + (kc - \omega(\vec{\beta}\vec{n}_k)) \right] \left\{ 1 + i \frac{\sqrt{\pi}(\overline{\omega} - \overline{\omega}_p)}{\Omega_1} W\left(\frac{\overline{\omega} - \overline{\omega}_p}{\Omega_1}\right) \right\}, \tag{80}$$

where $W(\xi) = \left(1 + \frac{2i}{\sqrt{\pi}} \int\limits_0^\xi e^{x^2} dx\right) e^{-\xi^2}$ is the Kramp function (it is tabulated in [121]), $\overline{\omega} = \omega - \vec{k}\vec{u}_0$, $\overline{\omega}_p = \omega_p - \vec{k}_p \vec{u}_0$, $\Omega^2 = k_x^2 v_{1T}^2 + k_y^2 v_{2T}^2 + k_z^2 v_{3T}^2$, $\Omega_1^2 = (k_x - k_{px})^2 v_{1T}^2 + (k_y - k_{py})^2 v_{2T}^2 + (k_z - k_{pz})^2 v_{3T}^2$.

Equations (76) together with functions (79), (80) determine the parametric Cherenkov instability and parametric decay instability of the thermal beam. From (79), (80) follows that in the case when the parameters ω and $\vec{k}$ are such that $\zeta \gg 1$, the velocity distribution in the beam appears insignificant, and so one can analyze an appreciably simpler case of a cold beam. Since in radiation of a relativistic particle quanta are emitted in a narrow angular range in the direction of the particle motion, then k_x, $k_y \ll k_z$. As a result, at the given values of Ω and Ω_1, the beam's velocity distribution in transverse direction can exceed that in the longitudinal direction. Of particular interest is the radiation pattern for parametric decay instability, in which case there is a possibility in principle to make the differences $k - x - k_{px}$ and $k_y - k_{yp}$, appearing in the

expression for Ω_1, go to zero. The transverse velocity distribution in this case appears to be insufficient at all.

In a real situation, due to the finite dimensions of the system and non-monochromaticity of radiation, these differences cannot vanish, though they can be reduced appreciably. Let us estimate the maximum possible magnitude of the increment. Suppose that the parameter $\zeta \gg 1$. As stated above, in this case we go over to the approximation of a cold beam and can use the expression $f(\vec{u}) = \delta(\vec{u} - \vec{u}_0)$ for the distribution function. The parametric Cherenkov instability for this case was considered in [51] (see Section above). The term proportional to G_2 leads to parametric decay instability of the beam in a periodic medium. In the general case, the Cherenkov and decay instabilities develop at different frequencies and can therefore be considered separately. So here we shall focus on the decay instability, omitting the term containing G_1 in (76) for corresponding $\vec{k}$ and ω. In the case of a cold beam, using (76), (77), we have the following equation for decay instability:

$$[(k^2c^2 - \omega^2\varepsilon_0)(k_\tau^2c^2 - \omega^2\varepsilon_0) - \omega^4\varepsilon_\tau\varepsilon_{-\tau}](\overline{\omega} - \overline{\omega}_p)^2 = A_2(k_\tau^2c^2 - \omega^2\varepsilon_0), \quad (81)$$

where A_2 is the factor of the term $[(\overline{\omega} - \overline{\omega}_p)^2 - \omega_{p\prime\prime}^2]^{-1}$ in G_2; $\omega_{p\prime\prime}^2$ is dropped as it is small for the particle densities $n_0 \simeq 10^{15} \div 10^{17}$ cm^{-1} in the beam that are of interest to us.

The solution of dispersion equation (81) can be found in the weakly-coupled waves approximation, which is applicable in this case because a non-linear right-hand side of (81) is small. In this approximation, the solution of dispersion equation (81) is sought near the intersection of solutions of the dispersion equations for coupled waves into which (81) is split when its right-hand side

equals zero, i.e.,

$$\begin{cases} (k^2c^2 - \omega^2\varepsilon_0)(k_\tau^2c^2 - \omega^2\varepsilon_0) - \omega^4\varepsilon_\tau\varepsilon_{-\tau} = D(k_z, \vec{k}_\perp, \omega) = 0, \\ ((\omega - \vec{k}\vec{u}_0) - \omega_p)^2 = 0. \end{cases} \tag{82}$$

Using weakly-coupled waves approximation of the perturbation theory and assuming that ε_0, $\varepsilon_{\pm\tau}$ are real values (i.e., neglecting the intrinsic absorption of the medium), the upper estimate of the increment of the beam's parametric decay instability when a pump wave is scattered in a 3D periodic medium can be obtained from (81):

$$\eta \simeq \frac{\omega_B}{c}\sqrt[4]{\frac{\omega_{p\perp}^2}{4\omega_B^2}\frac{|\vec{v}_p^0|^2}{c^2}\frac{\overline{\omega}_p}{\omega_B}|\varepsilon_\tau|}, \tag{83}$$

where $\frac{|v_p|^2}{c^2} = \frac{e^2|E_p^0|^2}{m_e^2c^2\langle\gamma\rangle^2\omega_p^2}$, ω_B is the Bragg frequency. Equation (83) is obtained in the assumption that the synchronism condition is fulfilled exactly and that $D(k_z, \vec{k}_\perp, \omega) = 0$ in the degeneration point of the eigensolutions of the dispersion equation of diffraction. In this case the multiplicity of the root, determining the increment, is greater by one than in the case of modified decay in the absence of diffraction of a scattered wave. This results in the decrease in the instability threshold, depending on the beam density and the intensity of the external electromagnetic pump wave [118,119]. According to (83), the numerical estimate of the maximum increment of the parametric decay instability of a cold relativistic beam is as follows: $\eta \sim 0.5$ at $E_p^0 \sim 10^5$ in CGS, $\gamma = 2 \cdot 10^2$, $\omega_\sigma = 1.6 \cdot 10^{19}$ s^{-1}, $\omega_p = 10^{14}$ s^{-1} $n_0 \sim 10^{15}$ cm^{-3}, $\varepsilon_0 - 1 = 5 \cdot 10^{-6}$, $\varepsilon_\tau \simeq 10^{-6}$.

In the above theoretical analysis we did not actually use the explicit form of v_p^0 and the direct relation between ω_p and $\vec{k}_p$. This theory is therefore fully ap-

plicable to the case when, instead of the electromagnetic wave, crystal planes bent under the ultrasonic wave act as a dynamic wiggler. A detailed treatment of the particle motion in such an ultrasonic wiggler was given in [13]. The corresponding dispersion equation is obtained from (76), (77), (81) by substituting for v_p^0 the corresponding expression for the case of the ultrasonic wiggler $|\vec{v}_p^s| = (\vec{e}_\sigma \vec{r}_{0\perp}^s)\Omega_s'$ (where $\Omega_s' = \kappa_z u_0 - \Omega_s$, $\vec{\kappa}$ is the wave vector of the ultrasonic wiggler, Ω_s is its frequency, $\vec{r}_{0\perp}^s$ is the amplitude of the particle's transverse vibrations in the ultrasonic wiggler [13]) and by substituting $\vec{\kappa}$ for k_p; Ω_s, for ω_p; Ω_s', for $\overline{\omega}_p$. Upon this substitution, for the instability increment in an ultrasonic wiggler, we obtain the expression similar to (83). This enables readily obtaining the following ratio of the instability increment in an ultrasonic wiggler to that in a light wiggler:

$$R = \frac{\eta_s}{\eta} = \left(\frac{|v_p^s|^2\Omega_s'}{|v_p^0|^2\Omega_s}\right)^{1/4} = \left(\frac{(r_{0\perp}^s)^2(\Omega_s')^3 m_e^2\gamma^3\omega_p^3}{e^2E_p^{02}\overline{\omega}_p}\right)^{1/4}. \qquad (84)$$

The analysis shows that (84) can be greater than unity. In a real situation, absorption can always reduce by one or two orders of magnitude the upper limiting estimate given above, but the conclusion about a significant magnitude of the gain coefficient holds true.

11 Volume Free Electron Laser

As has been stated, the features of radiation from relativistic particles in crystals, which were considered earlier in this review, have a general character and are also manifested when radiation is generated in artificial crystals (at present termed "photonic crystals") [25,60,87,88,89,117,164,181,176].

In contrast to generation in the X-ray range, generation of radiation in microwave and optical ranges does not require such high particle current densities. As a result, application of photonic crystals made it possible to develop a new type of generator, called the Volume Free Electron Laser (VFEL). Its main features will be considered below.

12 Generation equations and threshold conditions in the case of two-wave diffraction

Using multi-wave diffraction in a VFEL for the formation of a volume distributed feedback enables one, on the one hand, to appreciably reduce the length of the interaction area, and, on the other hand, to employ electron beams with a large transverse cross-section for pulse generation, which improves the electrical endurance of the generator and prevents burning of the glass in the discharge tubes during high-power lasing. Besides, multi-wave diffraction provides the selection of radiation modes in oversized systems [105].

When radiation is generated in an FEL, the electrons interact with the electromagnetic wave in a finite spatial region, and release energy into the wave. Depending on the length of the spatial region, different generation regimes are realized. At $|\mathtt{Im}k_zL| \gg 1$, generation occurs in a strong (exponential) amplification regime, which is mainly employed in amplifiers. The regime of weak single-passage amplification ($|Imk_zL| \leq 1$) is chiefly used in generators. In order to determine the structure of the fields and to describe the evolution of instability in such systems, in addition to the knowledge of the dispersion equations and their solutions, one should match the fields at the boundaries of the regions (joining solutions). This procedure gives the field distribution

in the system.

Now we shall formulate the boundary problem. Let an electron beam with mean velocity $\vec{u}$ be incident onto a plane-parallel spatially periodic plate of thickness L. The electron beam is oriented so that the radiation generated by the beam will be under diffraction conditions. Under two-wave diffraction, two fundamentally different geometries are possible. In the first case (Laue geometry (see Figure 8) both waves are emitted through one and the same boundary of the periodic structure ($\gamma_0\gamma_1 > 0$,where $\gamma_0 = \frac{(\vec{k}\vec{n})}{k}$ and $\gamma_1 = \frac{(\vec{k}_\tau\vec{n})}{k}$ are the cosines made by the wave vectors $\vec{k}$ and $\vec{k}_\tau$ with the normal vector to the surface of the periodic medium). In this geometry the amplifying regime is possible.

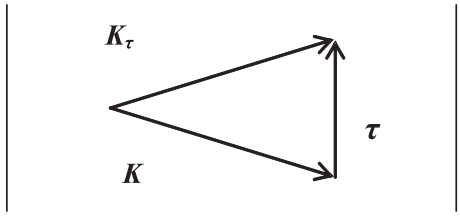

Figure 8. The geometry of two-wave Laue diffraction $\vec{k}, \vec{k}_\tau$ are the wave vectors of the incident and diffracted waves, $\vec{\tau}-$ is the reciprocal lattice vector of the periodic structure. The projections of both wave vectors onto the direction of the normal to the surface have the same sign.

In the latter case (Bragg geometry (see Figure 9)), the incident and diffracted waves leave the plate through the opposite surfaces ($\gamma_0\gamma_1 < 0$), when the electron current emits photons, positive feedback appears, and the generation regime is available.

Let us write the expression for the fields appearing in the system described here

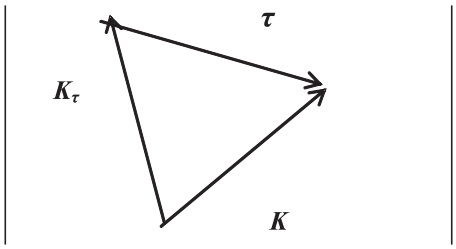

Figure 9. The geometry of two-wave Bragg diffraction. $\vec{k}, \vec{k}_\tau$ are the wave vectors of the incident and diffracted waves, respectively; $\vec{\tau}$ is the reciprocal lattice vector of the periodic structure. The projection of the wave vectors onto the direction of the normal to the surface are opposite in sign.

$$\begin{aligned} & a\vec{e}\exp\left(i\vec{k}_0\vec{r}\right) + b\vec{e}_\tau \exp\left(i\vec{k}_{0\tau}\vec{r}\right) \qquad (I) \\ & \sum_i c_i \exp\left(i\vec{k}_i\vec{r}\right)\left(\vec{e} + s_i\vec{e}_\tau \exp\left(i\vec{\tau}\vec{r}\right)\right) \qquad (II) \\ & f\vec{e}\exp\left(i\vec{k}_0\vec{r}\right)\exp\left(-ik_{0z}L\right) + \vec{e}_\tau \exp\left(i\vec{k}_{0\tau}\vec{r}\right)\exp\left(-ik_{0\tau z}L\right) \qquad (III)\,, \end{aligned} \tag{85}$$

$$\begin{aligned} & a\vec{e}\exp\left(i\vec{k}_0\vec{r}\right) + g\vec{e}_\tau \exp\left(i\vec{k}^{(-)}_{0\tau}\vec{r}\right) \qquad (I) \\ & \sum_i c_i \exp\left(i\vec{k}_i\vec{r}\right)\left(\vec{e} + s_i\vec{e}_\tau \exp\left(i\vec{\tau}\vec{r}\right)\right) \qquad (II) \\ & f\vec{e}\exp\left(i\vec{k}_0\vec{r}\right)\exp\left(-ik_{0z}L\right) + b\vec{e}_\tau \exp\left(i\vec{k}^{(-)}_{0\tau}\vec{r}\right)\exp\left(ik_{0\tau z}L\right) \qquad (III) \end{aligned} \tag{86}$$

In (85), (86) (I) and (III) denote the fields before and after the periodic structure. In Laue geometry (85), in the general case two waves with specified amplitudes are incident on the system: one along the direction with the wave vector $\vec{k}$ and amplitude b and the other one along the direction with the wave vector $\vec{k}_\tau$ and amplitude b. They propagate from one side (in this case to the surface $z = 0$). In Bragg diffraction geometry (86), the waves are incident on the system from opposite sides (the incident wave of amplitude a falls onto the surface $z = 0$, and the diffracted wave with amplitude b, onto the surface $z = L$). Wave vectors $\vec{k}_0$ and $\vec{k}_{0r}$ satisfy the standard dispersion equation describing propagation of electromagnetic waves in vacuum ($k^2c^2 - \omega^2 = 0$).

(II) denotes the field in a periodic medium. The dispersion relation in the medium is defined by (100).

$$s_i = \frac{\omega^2 \chi_{-\tau}}{\left[\left(\vec{k}_i + \vec{\tau}\right)^2 c^2 - \omega^2 \varepsilon_0\right]}$$

is the coupling coefficient between the diffracted and the incident waves for the i-th mode determined from equations (85), (86) and dispersion equation (100).

In the case of a "cold" electron beam, dispersion equation (100) takes the form:

$$\begin{aligned}\left(\omega - \vec{k}\vec{u}\right)^2 \left\{\left(k^2c^2 - \omega^2\varepsilon_0^{(1)}\right)\left(k_\tau^2 c^2 - \omega^2 \varepsilon_0^{(2)}\right) - \omega^4 r\right\} \\ = -\frac{\omega_l^2}{\gamma}\left(\frac{\vec{u}\vec{e}}{c}\right)^2 \left(k^2c^2 - \omega^2\right)\left(k_\tau^2 c^2 - \omega^2\varepsilon_0^{(2)}\right)\end{aligned} \tag{87}$$

As a result, sum (II) consists of six terms because equation (86) is of the sixth order with respect to k_z. But if the radiation geometry is not plane and the dielectric susceptibility is small, then the two waves mirror-reflected from the target surface may be ignored. In the case of a "hot" electron beam dispersion equation (100) reads:

$$\begin{aligned}&\left(k^2c^2 - \omega^2\varepsilon_0^{(1)}\right)\left(k_\tau^2 c^2 - \omega^2 \varepsilon_0^{(2)}\right) - \omega^4 r \\ &= -\frac{\sqrt{\pi}\omega_l^2}{\delta_0^{(i)}\gamma}\left(\frac{\vec{u}\vec{e}}{c}\right)^2 x_i \exp\left(-x_i^2\right) \qquad \left(k^2c^2 - \omega^2\right)\left(k_\tau^2 c^2 - \omega^2\varepsilon_0^{(2)}\right)\end{aligned} \tag{88}$$

Sum (II) now contains only four terms because the corresponding dispersion equation is of the fourth order. With the mirror-reflected waves being neglected, only two terms remain, and the system of the boundary conditions for defining the unknown coefficients takes a very simple form: the field in the periodic structure is completely determined by the two boundary conditions

for the fields of the incident and diffracted waves at the boundaries of the periodic structure.

$$\begin{aligned} a &= c_1 + c_2 \\ b &= s_1 c_1 + s_2 c_2 \end{aligned} \tag{89}$$

$$\begin{aligned} a &= c_1 + c_2 \\ b &= s_1 c_1 \exp\left(ik_{1z}L\right) + s_2 c_2 \exp\left(ik_{2z}L\right). \end{aligned} \tag{90}$$

Equation (89) gives the continuity conditions for the incident and diffracted waves at the boundary $z = 0$ for the Laue diffraction case. For the case of Bragg diffraction, equation (90) gives the boundary conditions for the incident and diffracted waves, respectively when $z = 0$ and $z = L$. In the regime of a "cold" electron beam, provided the mirror-reflected waves are neglected, dispersion equation (86) has four solutions. To define the structure of the field appearing in a periodic plate, four boundary conditions should be used. Two of them have the same form as those in the case of a "hot" beam: the continuity of the incident and diffracted waves at the target boundaries. Two additional conditions are the continuity of the charge and current densities at the input boundary. As a result, the system of equations defining the fields in this case

has the form

$$\begin{cases} \sum\limits_{i=1}^{4} c_i = a \\ \sum\limits_{i=1}^{4} \frac{c_i}{\delta_i} = 0 \\ \sum\limits_{i=1}^{4} \frac{c_i}{\delta_i^2} = 0 \\ 1\,) \sum\limits_{i=1}^{4} s_i c_i = b \qquad \text{or} \qquad 2\,) \quad \sum\limits_{i=1}^{4} s_i c_i \exp\{ik_{iz}L\} = b. \end{cases} \tag{91}$$

The first equation in (91) expresses the continuity of the incident wave at the front boundary, the third and second ones describe the continuity of the charge and current densities at the front boundary, $\delta_i = \frac{\vec{k}_i\vec{u}-\omega}{ku_z}$. The fourth equation expresses the continuity of the diffracted wave value at the front boundary in Laue geometry (denoted by figure 1 in line four of (91) or at the back boundary in the case of Bragg geometry (figure 2 in line 4 of (91)). It is easy to see (see (89), (91)) that in Laue diffraction geometry, the electromagnetic field in the interaction area will also be absent if the amplitudes of the incident waves equal zero.

The situation is different in Bragg geometry. From (90), (91) follows that in this case, under certain conditions it is possible that the field in the medium exists at nonzero amplitudes of the incident fields. The generation equations defining these conditions are obtained by equating the determinants of the systems (90) and (91) to zero. For a "hot" electron beam, the generation equation takes the form:

$$s_2 \exp(ik_{2z}L) - s_1 \exp(ik_{1z}L) = 0. \tag{92}$$

A similar equation for a "cold" electron beam reads

$$
\begin{aligned}
&s_1 \exp\{ik_{1z}L\}\delta_1^2 (\delta_2-\delta_3)(\delta_2-\delta_4)(\delta_3-\delta_4)\\
&-s_2 \exp\{ik_{2z}L\}\delta_2^2 (\delta_1-\delta_3)(\delta_1-\delta_4)(\delta_3-\delta_4)\\
&+s_3 \exp\{ik_{3z}L\}\delta_3^2 (\delta_1-\delta_2)(\delta_1-\delta_4)(\delta_2-\delta_4)\\
&-s_4 \exp\{ik_{4z}L\}\delta_4^2 (\delta_1-\delta_2)(\delta_1-\delta_3)(\delta_2-\delta_3)=0.
\end{aligned} \tag{93}
$$

Upon solving these equations, one may determine the threshold generation conditions, i.e., the electron current and other parameters of the beam, marking the starting point from which radiation prevails over the losses. Besides, radiation generation takes place when some phase relations are fulfilled: phase shift between the two diffraction modes traversing the interaction area should be a multiple of 2π (the field at the output should be similar to that at the input):

$$
\mathtt{Re}\,(k_{1z}-k_{2z})\,L = 2\pi n. \tag{94}
$$

In the region, where these conditions are fulfilled, the solution of (93), (94) has the form:

$$
\omega'' = \frac{\omega}{2(1-\beta)}\left\{ G^{(b)} - \chi_0''\left(1-\beta \mp \frac{\sqrt{-\beta}r''}{|\chi_\tau|\chi_0''}\right) - \left(\frac{\gamma_0 c}{\vec{n}\vec{u}}\right)^3 \frac{16\pi^2 n^2}{-\beta\,(k\chi_\tau L_*)^2\, kL_*}\right\}. \tag{95}
$$

ω'' in (95) is the increment of absolute instability, which describes the increase of the field amplitude in time in the field linear regime,

$$
G^{(b)} = \begin{cases}
-\frac{\sqrt{\pi}}{\gamma}\frac{\omega_l^2}{\omega^2}\frac{(\vec{u}\vec{e})^2}{u^2}\frac{k^2c^2-\omega^2}{\delta_0^2}x^{(t)}\exp(-x^{(t)2}) & \text{for a "hot" beam}\\
\\
\\
\frac{\pi^2 n^2}{4\gamma}\left(\frac{\omega_l}{\omega}\right)^2\frac{(\vec{u}\vec{e})^2}{u^2}(k^2c^2-\omega^2)k^2L_*^2 f(y) & \text{for a "cold" beam}
\end{cases}
$$

$$
f(y) = \sin y \frac{(2y+\pi n)\sin y - y\,(y+\pi n)\cos y}{y^3\,(y+\pi n)^3} \tag{96}
$$

is the profile function depending on the detuning from synchronism conditions $y = \frac{\delta\omega}{2u_z} L_*$.

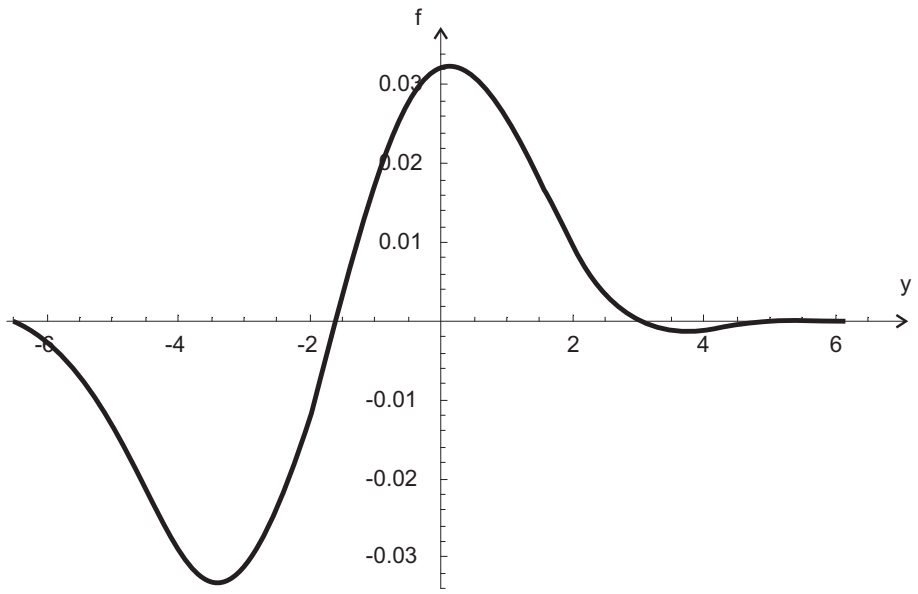

Figure 10. The profile generation function in the root degeneration region versus the detuning from synchronism conditions y

The profile function of detuning is plotted in Figure 10. As follows from (96) and Figure 10, one of the peculiarities of generation in the region of degeneration of the roots of the diffraction equation is that stimulated radiation is nonzero at zero detuning. This peculiarity appears due to the interference of contributions to radiation coming from the two branches of the diffraction equation. In a standard classical FEL, generation does not occur at the exact fulfillment of the synchronism condition. This is due to the fact that the gain coefficient is proportional to the difference between spontaneous radiation and absorption. In the case when these branches overlap each other, the gain coefficient becomes proportional to the derivative of the spectral function, while at zero detuning from synchronism conditions the spectral intensity of spontaneous radiation reaches its maximum, and the derivative at this point equals zero.

Equation (95) has an obvious physical meaning: the first term between the braces is proportional to the intensity of radiation produced by the electron beam (in the unit length). The next two terms describe losses of radiation appearing through absorption and due to the fact that radiation leaves the area of interaction with electrons. The values of the electron beam parameters, at which the radiation generation equals radiation losses (ω'') mark the starting point for the generation process. From the obtained expression (95) follows that at given values of the size of the interaction area and absorption, there is an optimal diffraction geometry in which the losses Γ_{loss} are minimum. In the general case, the optimal geometry is not at all plane. Figure 11 plots the relation $\Gamma_{\text{loss}}(\beta)/\Gamma_{\text{loss}}(\beta=-1)$ against the asymmetry factor for diffraction in the millimeter wavelength range ($\lambda \sim 4$ mm).

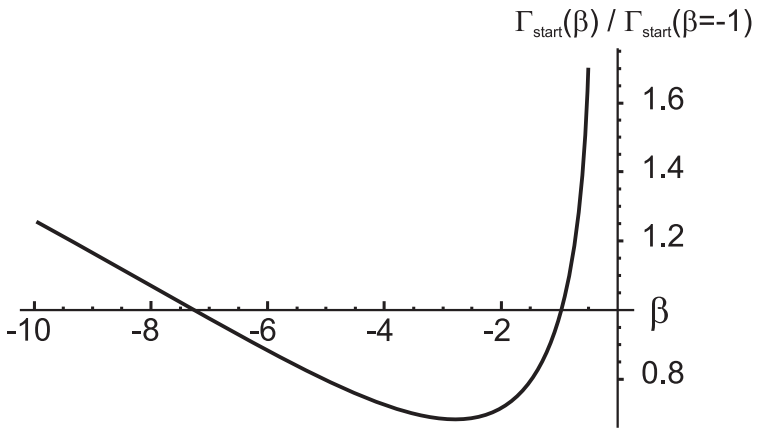

Figure 11. The relation $\Gamma_{loss}(\beta)/\Gamma_{loss}(\beta=-1)$ as a function of the asymmetry factor of diffraction for $\lambda \sim 4$ mm and $L = 10$ cm

13 Generation equations and threshold conditions in the geometry of three-wave Bragg diffraction

Above we have considered the theory of a volume distributed feedback generator in the geometry of two-wave Bragg diffraction. It has been shown that the transition to a volume distributed feedback opens up wider perspectives for the optimization of the system. Transition to a multi-wave distributed feedback provides additional possibilities. Here we shall mention some of them. For example, in a hard X-ray range, where the susceptibility has a negative value $\chi_0' < 0$, the condition of fulfillment of Cherenkov synchronism imposes restrictions on the asymmetry factor of diffraction $|\beta| > \left(\left|\chi_0^{'}\right| + \gamma^{-2}\right) / |\chi_\tau|^2$. In the X-ray spectral range, where the absorption is large, radiation losses under the condition of two-wave dynamical diffraction will be rather large at such values of the asymmetry factor. Moreover, strict requirements are set for the parameters of the starting generation current. One of the ways to diminish the losses is using supplementary external mirrors. Transition to multi-wave diffraction also enables one to reduce losses because the parameters of the system required to initiate the generation process change due to the rearrangement of the field structure in the interaction area. Synchronism conditions in this case contain additional parameters as compared to the two-wave dynamical diffraction, which enables one to match the Cherenkov conditions to the parameters corresponding to the regions with smaller absorption of radiation.

The possibility of generation at the point of degeneration of several diffraction roots is another important feature of multi-wave diffraction. At this point the functional change of the threshold characteristics occurs (e.g., the coincidence of the two roots gives the doubly degenerate case and $s = 2$) and, as a result,

it becomes possible to reduce the length of the generation area (at a given operating current) or the operating current (at a given length of the generation area).

Application of multi-wave diffraction for generating in a microwave range has one more remarkable feature – the possibility of selecting modes in oversized waveguides and resonators. Production of microwave power pulses requires high electric strength of the generator and radiation resistance of the output window. To reduce load on these elements, the transversal (with respect to the direction of the electron beam velocity) dimension of the resonator should be large (much larger than the wavelength). As a rule this leads to a multi-mode generation regime and low efficiency. In the presence of n-wave diffraction, selection of modes can be effectively carried out due to the requirement of fulfillment of $n-1$ Bragg condition.

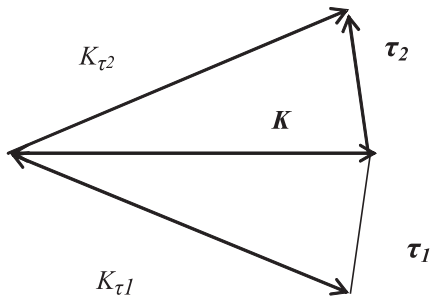

Figure 12. Figure Three-wave diffraction in Laue-Laue geometry. Projection of wave vectors $\vec{k}, \vec{k}_{\tau 1}, \vec{k}_{\tau 2}$ onto the normal to the surface have the same sign. $\vec{\tau}_1, \vec{\tau}_2$ are the reciprocal lattice vectors of the periodic structure.

To illustrate the potential of the multi-wave distributed feedback, we shall give a more detailed consideration of three-wave diffraction. In this case, volume distributed feedback (VDF) can be realized in three different geometries:

(1) Laue-Laue diffraction, when the three waves exit through the same surface ($\gamma_0, \gamma_1, \gamma_2 > 0$, Figure 12;

(2) diffraction in Bragg-Bragg geometry, when $\gamma_0 > 0$, while $\gamma_1, \gamma_2 < 0$. That is, the wave vector satisfying the synchronism condition is directed along the normal to the surface of the slow-wave structure, and the two vectors corresponding to diffracted waves point in the opposite direction;

(3) Bragg-Laue diffraction, when $\gamma_0, \gamma_1 > 0$, $\gamma_2 < 0$. Vector $\vec{k}$ corresponding to the synchronous wave and one of the vectors $\vec{k}_1 = \vec{k} + \vec{\tau}_1$ corresponding to the diffracted wave point in the same direction, while vector $\vec{k}_2 = \vec{k} + \vec{\tau}_2$ points in different direction (see Figure 13).

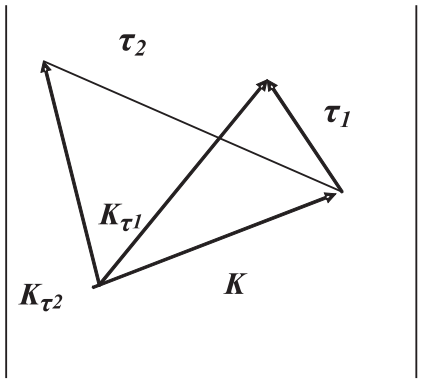

Figure 13. Figure Three-wave diffraction in Laue-Bragg geometry. The projection of wave vectors $\vec{k}, \vec{k}_{\tau 1}$ onto the surface normal and the projection of vector $\vec{k}_{\tau 2}$ are opposite in sign. $\vec{\tau}_1$, $\vec{\tau}_2$ are the reciprocal lattice vectors of the periodic structure.

Similarly to the two-wave case, the problem of the beam interaction with the target field may be reduced to the problem of three-wave diffraction of an electromagnetic wave incident onto the active medium. The active medium here is the system "spatially-periodic structure + electron beam".

The system of equations describing the process of three-wave coplanar diffraction by such an active medium takes the form:

$$\begin{aligned} D_\sigma^{(0)} E_\sigma^{(0)} - \omega^2 \chi_1 E_\sigma^{(1)} - \omega^2 \chi_2 E_\sigma^{(2)} = 0 \\ -\omega^2 \chi_{-1} E_\sigma^{(0)} + D_\sigma^{(1)} E_\sigma^{(1)} - \omega^2 \chi_{2-1} E_\sigma^{(2)} = 0 \\ -\omega^2 \chi_{-2} E_\sigma^{(0)} - \omega^2 \chi_{1-2} E_\sigma^{(1)} + D_\sigma^{(2)} E_\sigma^{(2)} = 0, \end{aligned} \tag{97}$$

where the terms

$$D^{(i)} = k_i^2 c^2 - \omega^2 \varepsilon_0^{(i)} + \frac{\omega_l^2}{\gamma} + \Gamma_i \left(\left(\vec{k}_i - \vec{k}_o \right)^2 c^2 - (\omega - \omega_o)^2 \right) \tag{98}$$

that contain the contributions due to resonance interaction of electrons with the wave,

$$\Gamma_i = \begin{cases} \frac{\omega_l^2}{\gamma} \frac{\Omega^2}{(\omega - \vec{k}_i \vec{u} - \omega_o)^2} & \text{in the case of a "cold" electron beam} \\ \\ \frac{\sqrt{\pi} \omega_l^2}{\gamma} \frac{\Omega^2}{\delta_0^{(i)}} x_i \exp(-x_i^2) & \text{in the case of a "hot" electron beam} \end{cases} \tag{99}$$

The values of Γ_i in equation (99) are given for two generation regimes: in the regime of a "cold" electron beam all the electrons have the same velocity and the velocity spread is small ($\frac{\vec{k}\Delta\vec{u}}{\Delta\omega} \ll 1$, where $\Delta\vec{u}$ is the thermal straggling of the electron beam, $\Delta\omega$ is the width of the emission line). In this case all the electrons participate in the interaction with the electromagnetic wave. In the regime of a "hot" electron beam the relation $\frac{\vec{k}\Delta\vec{u}}{\Delta\omega} \geq 1$ is fulfilled. In this case only a part of the electron beam participates in the interaction process. The explicit form of Ω and ω_0 depends on the generation mechanism. For the Cherenkov mechanism $\Omega = \left(\frac{\vec{u}\vec{e}_i}{c} \right)^2$, where $\vec{e}_i$ is the polarization vector, $\omega_o = 0$. In (97)–(99)

$$\omega_l^2 = \frac{4\pi n_e}{m_e}, \quad x_i = \frac{\omega - \vec{k}_i \vec{u} - \omega_o}{\sqrt{2}\delta_0^{(i)}}, \quad \delta_0^{(i)2} = k_{i1} \psi_x^2 + k_{iy}^2 \psi_y^2 + k_{iz}^2 \psi_z^2, \quad \psi_i$$

are the thermal straggling for a "hot" electron beam in the distribution function:

$$f_{(0)} = \frac{n_e}{(2\pi)^{3/2}\,\psi_1\psi_2\psi_3} exp\left\{-\frac{v_1^2}{2u^2\psi_1^2} - \frac{v_2^2}{2u^2\psi_2^2} - \frac{v_3^2}{2u^2\psi_3^2}\right\}$$

is the distribution function describing the velocity spread of the electrons in a beam before the interaction with the electromagnetic wave.

In the case of two-wave Bragg diffraction, when only two wave vectors satisfy the Bragg condition [3] and two strong waves are excited, the dispersion equation for Cherenkov instability takes the form

$$\left(k^2c^2 - \omega^2\varepsilon_0^{(1)} + \frac{\omega_l^2}{\gamma} + \Gamma_1\left(k^2c^2 - \omega^2\right)\right)$$
$$\times\left(k_\tau^2c^2 - \omega^2\varepsilon_0^{(2)} + \frac{\omega_l^2}{\gamma} + \Gamma_\tau\left(k_\tau^2c^2 - \omega^2\right)\right) - \omega^4 r = 0. \qquad (100)$$

Here $r = \chi_\tau\chi_{-\tau}$

As it was noted in [49,50], the functional relationship between the imaginary part of the solution k_z and the electron beam density may change appreciably at the points of degeneration of roots k_z of the diffraction equation (the dispersion equation without the electron beam describing the dispersion of electromagnetic waves in a periodic medium). This occurs, in particular, at the point of s-fold degeneration of roots: $\mathtt{Im}k_z \sim n_e^{1/(2+s)}$. In the Compton generation regime, this quantity significantly exceeds in magnitude a similar parameter for $\mathtt{Im}k_{zz} \sim n_e^{1/3}$ beyond the root degeneration region. From this fact the authors of [49,50] concluded that the instability increment in the degeneration region grows sharply.

The dispersion equation corresponding to the system (97) for the three-wave

case of coplanar diffraction reads:

$$F_{\sigma}^{(3)}\left(\vec{k},\vec{k}_1,\vec{k}_2\right)=-\Gamma F_{\sigma}^{(2)}\left(\vec{k}_1,\vec{k}_2\right), \tag{101}$$

where

$$\begin{aligned}
&F_{\sigma}^{(3)}\left(\vec{k},\vec{k}_1,\vec{k}_2\right)=\left(k^2c^2-\omega^2\varepsilon_0\right)\left(k_1^2c^2-\omega^2\varepsilon_0\right)\left(k_2^2c^2-\omega^2\varepsilon_0\right)\\
&-\omega^4\left(k^2c^2-\omega^2\varepsilon_0\right)\chi_{1-2}\chi_{2-1}-\omega^4\left(k_1^2c^2-\omega^2\varepsilon_0\right)\chi_2\chi_{-2}\\
&-\omega^4\left(k_2^2c^2-\omega^2\varepsilon_0\right)\chi_1\chi_{-1}-\omega^6\left(\chi_1\chi_{-2}\chi_{2-1}+\chi_2\chi_{-1}\chi_{1-2}\right),\\
&F_{\sigma}^{(2)}\left(\vec{k}_1,\vec{k}_2\right)=\left(k_1^2c^2-\omega^2\varepsilon_0\right)\left(k_2^2c^2-\omega^2\varepsilon_0\right)-\omega^4\chi_{1-2}\chi_{2-1}.
\end{aligned}$$

In deriving (101), we based on the assumption that the electrons are synchronous to the wave with wave vector $\vec{k}$. The field in the three-wave system is written as follows:

(1) in Laue-Laue geometry

$$\begin{aligned}
&a^{(0)}\vec{e}\exp\left(i\vec{k}_0\vec{r}\right)+a^{(1)}\vec{e}_1\exp\left(i\vec{k}_{01}\vec{r}\right)+a^{(2)}\vec{e}_2\exp\left(i\vec{k}_{02}\vec{r}\right)\\
&\sum_i c_i\exp\left(i\vec{k}_i\vec{r}\right)\left(\vec{e}+s_i\vec{e}_{\tau}\exp\left(i\vec{\tau}\vec{r}\right)\right)\\
&b\vec{e}\exp\left(i\vec{k}_0\vec{r}\right)\exp\left(-ik_{0z}L\right)+b^{(1)}\vec{e}_1\exp\left(i\vec{k}_{01}\vec{r}\right)\exp\left(-ik_{01z}L\right)\\
&+b^{(2)}\vec{e}_2\exp\left(i\vec{k}_{02}\vec{r}\right)\exp\left(-ik_{02z}L\right),
\end{aligned}$$

(2) in Bragg-Bragg geometry

$$\begin{aligned}
&a^{(0)}\vec{e}\exp\left(i\vec{k}_0\vec{r}\right)+b^{(1)}\vec{e}_1\exp\left(i\vec{k}_{01}^{(-)}\vec{r}\right)+b^{(2)}\vec{e}_2\exp\left(i\vec{k}_{02}^{(-)}\vec{r}\right)\\
&\sum_i c_i\exp\left(i\vec{k}_i\vec{r}\right)\left(\vec{e}+s_i\vec{e}_{\tau}\exp\left(i\vec{\tau}\vec{r}\right)\right)\\
&b\vec{e}\exp\left(i\vec{k}_0\vec{r}\right)\exp\left(-ik_{0z}L\right)+a^{(1)}\vec{e}_1\exp\left(i\vec{k}_{01}^{(-)}\vec{r}\right)\exp\left(ik_{01z}L\right)\\
&+a^{(1)}\vec{e}_1\exp\left(i\vec{k}_{01}^{(-)}\vec{r}\right)\exp\left(ik_{01z}L\right),
\end{aligned}$$

(3) in Bragg-Laue geometry

$$
\begin{aligned}
&a^{(0)}\vec{e}\exp\left(i\vec{k}_0\vec{r}\right)+a^{(1)}\vec{e}_1\exp\left(i\vec{k}_{01}\vec{r}\right)+b^{(2)}\vec{e}_2\exp\left(i\vec{k}_{02}^{(-)}\vec{r}\right)\\
&\sum_i c_i\exp\left(i\vec{k}_i\vec{r}\right)\left(\vec{e}+s_i\vec{e}_\tau\exp\left(i\vec{\tau}\vec{r}\right)\right)\\
&b\vec{e}\exp\left(i\vec{k}_0\vec{r}\right)\exp\left(-ik_{0z}L\right)+b^{(1)}\vec{e}_1\exp\left(i\vec{k}_{01}\vec{r}\right)\exp\left(ik_{01z}L\right)\\
&+a^{(1)}\vec{e}_1\exp\left(i\vec{k}_{01}^{(-)}\vec{r}\right)\exp\left(ik_{01z}L\right),
\end{aligned}
$$

In the above expressions the waves incident on the structure have the amplitudes $a^{(i)}$, while the exit waves have the amplitudes $b^{(i)}$. In the expression for the field in a periodic structure, summation is made over the diffraction modes. In the case of a "cold" beam, the sum contains five terms, and in the case of a "hot" beam, three terms.

$$
s_i^{(1)}=\frac{\lambda_i\lambda_{i2}-r_2}{\lambda_{i2}\chi_1+\chi_2\chi_{1-2}}\qquad\text{and}\qquad s_i^{(2)}=\frac{\lambda_i\lambda_{i1}-r_1}{\lambda_{i1}\chi_2+\chi_1\chi_{2-1}}
$$

are the coupling coefficients between the diffracted waves and the incident wave; their form is obtained by the system of equations (97), $\lambda_{i\alpha}=\{\left(\vec{k}_i+\vec{\tau}_\alpha\right)^2c^2-\omega^2\varepsilon_0\}/\omega^2, r_\alpha=\chi_\alpha\chi_{-\alpha}$.

By analogy with a two-wave case, we shall join the fields at the system boundaries and write the system of equations defining the field in the interaction area:

(1) in the case of Laue-Laue geometry:

$$
\begin{aligned}
&\sum_{i=1}^5 c_i=a\qquad\sum_{i=1}^5 s_i^{(1)}c_i=a_1\qquad\sum_{i=1}^5 s_i^{(2)}c_i=a_2\\
&\sum_{i=1}^5\frac{c_i}{\delta_i}=0\qquad\sum_{i=1}^5\frac{c_i}{\delta_i^2}=0,
\end{aligned}
\tag{102}
$$

(2) for Bragg-Bragg geometry

$$\sum_{i=1}^{5} c_i = a \qquad \sum_{i=1}^{5} s_i^{(1)} c_i \exp\left(ik_{iz}L\right) = a_1 \qquad \sum_{i=1}^{5} s_i^{(2)} c_i \exp\left(ik_{iz}L\right) = a_2$$
$$\sum_{i=1}^{5} \frac{c_i}{\delta_i} = 0 \qquad \sum_{i=1}^{5} \frac{c_i}{\delta_i^2} = 0, \tag{103}$$

(3) for Bragg-Laue geometry

$$\sum_{i=1}^{5} c_i = a \qquad \sum_{i=1}^{5} s_i^{(1)} c_i = a_1 \qquad \sum_{i=1}^{5} s_i^{(2)} c_i \exp\left(ik_{iz}L\right) = a_2$$
$$\sum_{i=1}^{5} \frac{c_i}{\delta_i} = 0 \qquad \sum_{i=1}^{5} \frac{c_i}{\delta_i^2} = 0. \tag{104}$$

In all three of these systems (102)–(102) the first three equalities are obtained from the requirement of the continuity of fields at the boundary. In the Laue-Laue case the boundary conditions are written for the boundary $z = 0$. In Bragg-Bragg geometry one condition for the incident wave is written for the boundary $z = 0$, two others, for diffracted waves for the boundary $z = L$. In Laue-Bragg geometry two conditions are defined at $z = 0$, and one, at $z = L$. The last two equations of the obtained systems follow from the requirement of continuity of the current and charge densities at the boundary $z = 0$. In the three-wave case of Laue geometry, as well as in the case of a two-wave VDF, only the amplification regime is possible. In Bragg-Bragg and Bragg-Laue geometry both the amplification regime and the generation regime accompanied by radiation from spontaneous noise at zero amplitude of the incident field are possible. Using the systems (103) and (104), write the generation equations for these two geometries.

Bragg-Bragg geometry

$$\begin{aligned}
&\left(s_1^{(1)}s_2^{(2)}-s_2^{(1)}s_1^{(2)}\right)\delta_1\delta_2\left(\delta_3-\delta_4\right)\exp\{i\left(k_{1z}+k_{2z}\right)L\}\\
&-\left(s_1^{(1)}s_3^{(2)}-s_3^{(1)}s_1^{(2)}\right)\delta_1\delta_3\left(\delta_2-\delta_4\right)\exp\{i\left(k_{1z}+k_{3z}\right)L\}\\
&+\left(s_1^{(1)}s_4^{(2)}-s_4^{(1)}s_1^{(2)}\right)\delta_1\delta_4\left(\delta_2-\delta_3\right)\exp\{i\left(k_{1z}+k_{4z}\right)L\}\\
&+\left(s_2^{(1)}s_3^{(2)}-s_3^{(1)}s_2^{(2)}\right)\delta_2\delta_3\left(\delta_1-\delta_4\right)\exp\{i\left(k_{2z}+k_{3z}\right)L\}\\
&-\left(s_2^{(1)}s_4^{(2)}-s_4^{(1)}s_2^{(2)}\right)\delta_2\delta_4\left(\delta_1-\delta_3\right)\exp\{i\left(k_{2z}+k_{4z}\right)L\}\\
&+\left(s_3^{(1)}s_4^{(2)}-s_4^{(1)}s_3^{(2)}\right)\delta_3\delta_4\left(\delta_1-\delta_2\right)\exp\{i\left(k_{3z}+k_{4z}\right)L\}=0.
\end{aligned}\tag{105}$$

Bragg-Laue geometry

$$\begin{aligned}
&s_1^{(2)}\exp\left(ik_{1z}L\right)\delta_1\{s_2^{(1)}\delta_2\left(\delta_4-\delta_3\right)-s_3^{(1)}\delta_3\left(\delta_4-\delta_2\right)+s_4^{(1)}\delta_4\left(\delta_3-\delta_2\right)\}\\
&-s_2^{(2)}\exp\left(ik_{2z}L\right)\delta_2\{s_1^{(1)}\delta_1\left(\delta_4-\delta_3\right)-s_3^{(1)}\delta_3\left(\delta_4-\delta_1\right)+s_4^{(1)}\delta_4\left(\delta_3-\delta_1\right)\}\\
&+s_3^{(2)}\exp\left(ik_{3z}L\right)\delta_3\{s_1^{(1)}\delta_1\left(\delta_4-\delta_2\right)-s_2^{(1)}\delta_2\left(\delta_4-\delta_1\right)+s_4^{(1)}\delta_4\left(\delta_2-\delta_1\right)\}\\
&-s_4^{(2)}\exp\left(ik_{4z}L\right)\delta_4\{s_1^{(1)}\delta_1\left(\delta_3-\delta_2\right)-s_2^{(1)}\delta_2\left(\delta_3-\delta_1\right)+s_3^{(1)}\delta_3\left(\delta_2-\delta_1\right)\}=0
\end{aligned}\tag{106}$$

Similar generation equations in these geometries may be written for a "hot" electron beam [105].

Before we proceed to the analysis of generation equations, let us examine the behavior of the roots of the dispersion equation for three-wave diffraction. It is known that the most effective interaction of the electron beam and the electromagnetic wave takes place at the root degeneration point when the synchronism condition is fulfilled. Thus, the parameters for the generation threshold can be determined by the weakly-coupled mode method [106]. According to this method, we first find the solutions of the dispersion equation without the electron beam, then the additional synchronism condition is imposed on these solutions. To complete the procedure, one should substitute the value of $\vec{k}=\vec{k}_0$ that satisfies the condition $\omega-\vec{k}_0\vec{u}=0$ into the dispersion equation describing three-wave diffraction. Making use of the form of $F_\sigma^{(3)}\left(\vec{k},\vec{k}_1,\vec{k}_2\right)$ in

(101), we get:

$$\begin{aligned} &ll_1l_2 - lr_{12} - l_1r_2 - l_2r_1 - f = 0 \\ &\beta_1\beta_2 l_1 l_2 + l\left(\beta_1 l_1 + \beta_2 l_2\right) - \beta_1\beta_2 r_{12} - \beta_1 r_1 - \beta_2 r_2 = 0. \end{aligned} \tag{107}$$

In (106)

$$l = \left(k_0^2c^2 - \omega^2\varepsilon_0\right)/\omega^2 = \sin^2\theta + \left(\frac{c}{u\gamma}\right)^2 - \chi_0,$$

$$l_{1,2} = l + \alpha_{1,2}, \qquad \alpha_{1,2} = \frac{2\vec{k}_0\vec{\tau}_{1,2} + \tau_{1,2}^2}{\omega^2/c^2}$$

are the two parameters of deviation from Bragg diffraction conditions, $f = \chi_1\chi_{-2}\chi_{2-1} + \chi_2\chi_{-1}\chi_{1-2}$, $\beta_{1,2} = \gamma_0/\gamma_{1,2}$ are the asymmetry factors of diffraction, $\gamma_0, \gamma_1, \gamma_2$ are the direction cosines of diffraction. In (107) the first equation is the requitement for simultaneous fulfillment of the synchronism conditions and the dispersion equation of diffraction $F_\sigma^{(3)}\left(\vec{k}, \vec{k}_1, \vec{k}_2\right) = 0$. The second equation in (107) appears due to the requirement for root degeneration of the diffraction equation. Introducing new variables $z_1 = l_1/l$ and $z_2 = l_2/l$, we obtain from (107):

$$\begin{aligned} &z_1z_2 - \frac{r_2z_1 + r_1z_2}{l^2} - \frac{r_{12}}{l^2} - \frac{f}{l^3} = 0 \\ &\beta_1\beta_2 z_1 z_2 + \beta_1 z_1 + \beta_2 z_2 - \beta_1\beta_2\frac{r_{12}}{l^2} - \frac{\beta_1 r_1 - \beta_2 r_2}{l^2} = 0. \end{aligned} \tag{108}$$

Solve (108) for z_i:

$$\begin{aligned} z_1 &= \frac{r_1 - \beta_2\chi_1\chi_2\frac{\chi_{1-2}}{l} \pm \chi_{1-2}\left(1 + \frac{\chi_1\chi_2}{\chi_{1-2}l}\right)\sqrt{-\frac{\beta_2}{\beta_1}\left(l^2 + \beta_1 r_1 + \beta_2 r_2\right)}}{l^2 + \beta_2 r_2} \\ z_2 &= \frac{r_2 - \beta_1\chi_1\chi_2\frac{\chi_{1-2}}{l} \mp \chi_{1-2}\left(1 + \frac{\chi_1\chi_2}{\chi_{1-2}l}\right)\sqrt{-\frac{\beta_1}{\beta_2}\left(l^2 + \beta_1 r_1 + \beta_2 r_2\right)}}{l^2 + \beta_1 r_1}. \end{aligned} \tag{109}$$

Thus, at the point of intersection of roots, the parameters of deviation from the Bragg conditions $a_{1,2}$ appear to be expressed in terms of the angle of the radiation wave vector with respect to the velocity vector (recall here that $l = \sin^2\theta + (c(u\gamma))^2 - \chi_0$), the asymmetry factors of diffraction (β_i) and the polarizability (χ_i) of the periodic structure. From (109) follows that at the point of degeneration of diffraction roots and simultaneous fulfillment of Cherenkov synchronism, the following condition should hold:

$$\beta_1\beta_2\left(l^2 + \beta_1 r_1 + \beta_2 r_2\right) < 0. \tag{110}$$

From (110) follows that there are no degeneration points in Laue geometry ($r_1, r_2 > 0$, while for the Laue case doth asymmetry factors β_1 and β_2 are positive values). In Bragg-Bragg geometry, a critical angle exists:

$$sin\theta_{thr} = \sqrt{\sqrt{-\beta_1 r_1 - \beta_2 r_2} + \chi_0 - \left(\frac{c}{u\gamma}\right)^2}. \tag{111}$$

The degeneration region occurs at radiation angles $\theta < \theta_{\text{thr}}$. So, in the X-ray spectral range in Bragg-Bragg geometry at least one of the asymmetry factors should be large. In Bragg-Laue geometry there is the opposite situation, when the degeneration region occurs at $\theta > \theta_{\text{thr}}$. In three-wave geometry there is a possibility of threefold degeneration of roots. At the point of threefold degeneration, there is a strong relationship among the direction of the photon emission, asymmetry factors, and the polarizabilities of the periodic structure.

The conditions for the threshold current values are obtained by through solving equations (105) and (106). In a weak single-stage amplification regime ($|Imk_zL| \ll 1$), this conditions in the region of two-fold degeneration have the

form:

$$G^{(b)} = |a|\chi_0'' + \frac{16}{|\beta_1\beta_2|}\left(\frac{\gamma_0 c}{\vec{n}\vec{u}}\right)^3 \frac{\pi^2 n^2}{\left(klL_*\right)^2 kL_*}|\eta_{BL(BB.)}| \tag{112}$$

In (112) the following notations are used:

$$a = \frac{z_1 z_2 + z_1 + z_2 - \frac{r_1+r_2+r_{12}}{l^2} + \frac{r_{12}+z_1 r_2''+z_2 r_1''}{l\chi_0''} + \frac{f"}{l^2\chi_0''}}{z_1 z_2 - \frac{r_{12}}{l^2}},$$

$$a = \frac{z_1 z_2 + z_1 + z_2 - \frac{r_1+r_2+r_{12}}{l^2} + \frac{r_{12}+z_1 r_2^{//}+z_2 r_1^{//}}{l\chi_0^{//}} + \frac{f"}{l^2\chi_0^{//}}}{z_1 z_2 - \frac{r_{12}}{l^2}},$$

$$\eta_{BL} = X\frac{\left(s_3^{(1)} - s_1^{(2)}\right)\varsigma_1 + s_1^{(2)}\varsigma_2 - s_3^{(2)}\varsigma_2 cos\{k\left(\delta_1^{/} - \delta_3^{/}\right)L\}}{s_1^{(2)}\left(s_3^{(1)} - s_1^{(1)}\right)\left(z_1 z_2 - \frac{r_{12}}{l^2}\right)},$$

$$\eta_{BB} = X\frac{s_3^{(1)}\varsigma_1 - s_3^{(2)}\varsigma_2 + \left(s_2^{(1)}\varsigma_1 - s_1^{(2)}\varsigma_2\right)cos\{k\left(\delta_1^{/} - \delta_3^{/}\right)L\}}{\left(s_3^{(2)}s_1^{(1)} - s_3^{(1)}s_1^{(2)}\right)\left(z_1 z_2 - \frac{r_{12}}{l^2}\right)},$$

$$\varsigma_1 = \frac{(1+\beta_1 z_1)\left(\frac{z_1\chi_2}{l} + \frac{\chi_1\chi_2 - 1}{l^2}\right) - \left(z_1 - \frac{r_1}{l^2}\right)\frac{\chi_2}{l}}{\beta_1\left(\frac{z_1\chi_2}{l} + \frac{\chi_1\chi_2-1}{l^2}\right)^2},$$

$$\varsigma_2 = \frac{(1+\beta_2 z_2)\left(\frac{z_2\chi_1}{l} + \frac{\chi_2\chi_1 - 2}{l^2}\right) - \left(z_2 - \frac{r_2}{l^2}\right)\frac{\chi_1}{l}}{\beta_2\left(\frac{z_2\chi_2}{l} + \frac{\chi_2\chi_1-2}{l^2}\right)^2}.$$

$G^{(b)}$ is defined in (95), (96).

The threshold condition in equation (112) holds true in the region of the two-fold degeneration of roots k_{1z}, k_{2z}, and as the modes corresponding to these roots pass through the interaction area, their relative phase shift should satisfy the condition $(k_{1z} - k_{2z})\,L = 2\pi n$ (here the roots are "almost" degenerated if $(2\pi n)/k|\chi_\tau|L) \ll 1$). The third diffraction root is located at a distance $|k_{3z} - k_{1z}| \sim |\chi_\tau|$, $|k_{3z} - k_{2z}| \sim |\chi_\tau|$ from the degenerated roots.

The dependence of the threshold conditions on the length of the interaction

area at the point of three-fold degeneration changes appreciably:

$$G = A\chi_0'' + \frac{B}{kL}\left(\frac{2\pi}{klL}\right)^4 \quad . \tag{113}$$

Realization of this regime requires that the following phase conditions be fulfilled: $(k_{1z} - k_{2z})\,L = 2\pi n$, $(k_{2z} - k_{3z})\,L = 2\pi m$, $n \neq m$. The coefficients A, B in (113) depend on the polarizabilities, z_1, z_2 and the indices m, n. Since they are awkward, they are dropped here. From (113) follows that in the region of three-fold degeneration of roots, the functional dependence of the losses at the boundaries on L changes significantly. According to (113), for a "cold" electron beam, when absorption is not important, $j_{\text{thr}} \sim \frac{1}{(kL)^3}\left(\frac{2\pi}{klL}\right)^4$ (it would be recalled here that in the regime of a "cold" electron beam $G \sim jL^2$ (see (96)). Under dynamical diffraction, when inequality $\frac{4\pi}{klL} \ll 1$ holds, this dependence leads to an appreciable reduction of the threshold current. Under multi-wave (s-wave) VDF, the threshold current depends on L as

$$j_{thr} \sim \frac{1}{(kL)^3}\left(\frac{2\pi}{klL}\right)^{2(s-1)}, \tag{114}$$

so the transition to multi-wave diffraction enables one to significantly reduce the longitudinal dimension of the generating system.

As follows from the above results, the volume distributed feedback (VDF) has a number of advantages that make its application beneficial for generating stimulated radiation in a wide spectral range (with the wavelengths from centimeters and millimeters to angströms). Moreover, in a short-wave spectral range, the size of the radiating system reduces appreciably due to the change of the functional dependence under multi-wave VDF. A short-wave spectrum corresponds to greater values of the wave number k, so at a given operating

current, due to the presence of the factor $\left(\frac{2\pi}{klL}\right)^{2(s-1)}$, L can be appreciably reduced. In optical and X-ray ranges, where the requirements for the current density and the quality of the beam are very strict, there appears the possibility to noticeably reduce the threshold values of the current for a given beam propagation area. In this case the VFEL is a unique system providing lasing at relatively small interaction lengths. In a microwave range, VFELs are beneficial for both the reduction of the generator size and selection of modes when producing high-power radiation pulses in oversized generators.

14 Application of volume diffraction gratings for terahertz lasing in Volume FELs (VFELs)

Generation of radiation in millimeter and far-infrared range with nonrelativistic and low-relativistic electron beams is a complicated task. Gyrotrons and cyclotron resonance facilities are used as sources in millimeter and submillimeter range, but for their operation a magnetic field of several tens of kiloGauss $\left(\omega \sim \frac{eH}{mc}\gamma\right)$ is necessary. Slow-wave devices (TWT, BWT, orotrons) in this range require application of dense and thin (< 0.1 mm) electron beams because only electrons passing near the slowing structure at distance $d \leq \lambda\beta\gamma/(4\pi)$ can effectively interact with electromagnetic waves. It is difficult to guide thin beams near a slowing structure with desired accuracy. And electrical endurance of resonator limits radiation power and density of the acceptable electron beam. Conventional waveguide systems are essentially restricted by the requirement for transverse dimensions of a resonator, which should not significantly exceed the radiation wavelength. Otherwise, the generation efficiency decreases abruptly due to the excitation of plenty of modes.

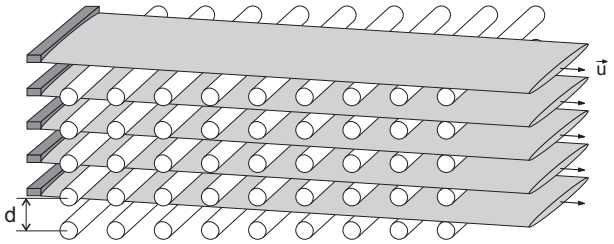

Figure 14. General view of Volume Free Electron Laser formed by metal threads with several sheet electron beams.

Most of the above problems can be overcome in Volume Free Electron Lasers (VFEL)

In volume FELs, the greater part of the electron beam interacts with an electromagnetic wave due to volume distributed interaction. Transverse dimensions of a VFEL resonator could significantly exceed radiation wavelength $D \gg \lambda$. In addition, the electron beam and the radiation power are distributed over the whole volume, which is beneficial for electrical endurance of the system. Multi-wave Bragg dynamical diffraction provides mode discrimination in VFELs.

14.1 Amplification and generation in a photonic crystal

Let us consider an electron beam with velocity $\vec{u}$ passing through a periodic structure composed of either dielectric or metal threads (see Figure 14) Fields, appearing while an electron beam passes through a volume spatially periodic medium, are described by the set of equations given in [105] Instability of electron beam is described by the dispersion equation [105]:

$$(k^2c^2 - \omega^2\varepsilon)(k_\tau^2c^2 - \omega^2\varepsilon + \chi_\tau^{(b)}) - \omega^2\chi_\tau\chi_{-\tau} = 0. \qquad (115)$$

$\vec{k}_\tau = \vec{k} + \vec{\tau}$ is the wave vector of the diffracted photon, $\vec{\tau} = \left\{\frac{2\pi}{a}l; \frac{2\pi}{b}m; \frac{2\pi}{c}n\right\}$ are the reciprocal lattice vectors, a, b, c are the translation periods, $\chi_\alpha^{(b)}$ is the part of dielectric susceptibility caused by the presence of the electron beam. As synchronism conditions are incompatible with those of Bragg, in the instability range $k^2 \neq k_\tau^2$. At the same time, two different types of instability exist, depending on radiation frequency. Amplification takes place when the electron beam is in synchronism with the electromagnetic component $\vec{k} + \vec{\tau}$, which has a positive projection k_z. If the projection k_z is negative and generation threshold is reached, then generation evolves. In the first case, radiation propagates along the transmitted wave which has positive projection of group velocity $v_z = \frac{c^2 k_z^{(0)}}{\omega} \quad (k_z^{(0)} = \sqrt{\omega^2\varepsilon - k_\perp^2})$, and beam disturbance moves along it. In the second case, the group velocity has negative projection $v_z = -\frac{c^2 k_z^{(0)}}{\omega}$, and radiation propagates along the back-wave and the electromagnetic wave comes from the range of the greatest beam disturbance to the place, where electrons come into the interaction area. For a one-dimensional structure such a mechanism is realized in a backward-wave tube. In amplification case, equation (115) gives for the increment of instability: $\mathtt{Im}k_z' = -\frac{\sqrt{3}}{2}f$, where

$$f = \sqrt[3]{\frac{h\omega_L^2(\vec{u}\vec{e}^{\tau})^2\omega^4 r}{2k_z^{(0)}c^4u_z^2\left(k_\tau^2c^2 - \omega^2\varepsilon_0\right)}},$$

if the condition $2k_z'f \gg \frac{\omega^2\chi_0"}{c^2}$ is fulfilled. Here $r = \chi_\tau\chi_{-\tau}$, $h(\vec{u}\vec{e}^{\tau})^2/c^2 = 1/\gamma^3$ if the electron beam propagates in a strong guiding magnetic field, otherwise, $h = 1/\gamma$. In case $2k_z'f \ll \frac{\omega^2\chi_0"}{c^2}$ a dissipative instability evolves. Its increment is

$$\mathtt{Im}k_z = -\frac{c}{\omega}\sqrt{\frac{k_z^{(0)}f^3}{\chi_0}}.$$

If inequalities $k_z^{`2} \gg 2k_z k_z^{`}$ and $k_z^{`2} \gg \frac{\omega^2 \chi_0"}{c^2}$ are fulfilled, the spatial increment of instability can be expressed as

$$\mathtt{Im}k_z^{`} = -\left(\frac{h\omega_L^2(\vec{u}\vec{e^r})^2\omega^4 r}{c^4\left(k_\tau^2 c^2 - \omega^2\varepsilon_0\right)u_z^2}\right)^{1/4},$$

but the parameters providing such dependence correspond to the conversion from the amplification to the generation regime (for the Compton instability this situation takes place at $k_z^{(0)} \approx 0$). The frequency of amplified radiation is defined as:

$$\omega = \frac{\vec{\tau}\vec{u}}{1 - \beta_x\eta_x - \beta_y\eta_y - \beta_z\sqrt{\varepsilon - \eta_x^2 - \eta_y^2}}. \tag{116}$$

The instability in the generation regime is described by the temporal increment and cannot be described by the spatial increment. The increment of absolute instability can be found by solving the equation $\mathtt{Im}k_z^{(+)}(\omega) = \mathtt{Im}k_z^{(-)}(\omega)$ with respect to the imaginary part of ω. Calculated dependence of temporal increment on the parameter of detuning is presented in Figure 15.

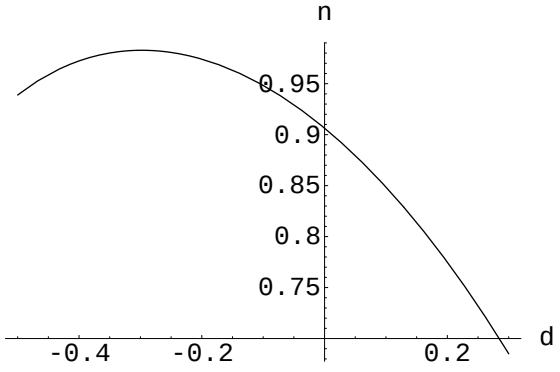

Figure 15. Calculated dependence of temporal increment on tuning out parameter

Axes in Figure 15are denoted as:

$$d = \frac{a_1 + k_z^{(0)}}{f}, \quad n = \frac{\frac{\omega"}{u_z} + \frac{2\omega\omega"\varepsilon_0 + \omega^2\chi_0"}{c^2 k_z^{(0)}}}{f}.$$

It follows from Figure 15 that at a certain value of the parameter of detuning:

$$\frac{a_1 + k_z^{(0)}}{f} \approx -0.3 \tag{117}$$

the increment of instability has a maximum

$$\frac{\frac{\omega"}{u_z} + \frac{2\omega\omega"\varepsilon_0 + \omega^2\chi_0"}{c^2 k_z^{(0)}}}{f} \approx 0.98. \tag{118}$$

The increment of absolute instability can be found from (118). The absolute instability can evolve if current exceeds start value, which is determined by dissipation. The amplification regime has no threshold and decisive influence of dissipation causes dissipative instability. Frequencies, corresponding to the generation regime, are defined by an expression different from (116):

$$\omega = \frac{\vec{\tau}\vec{u}}{1 - \beta_x\eta_x - \beta_y\eta_y + \beta_z\sqrt{\varepsilon - \eta_x^2 - \eta_y^2}}. \tag{119}$$

Thus, it follows from (116), (119) that the change of a radiation angle causes smooth frequency tuning. As a result, the generation frequencies are less than those corresponding to the amplification regime. Hence, using the system as an amplifier, one should add dispersion elements in it to raise dissipation in the frequency range, where generation occurs.

The use of Bragg multi-wave distributed feedback increases generation efficiency and provides discrimination of generated modes. If the conditions of synchronism and Bragg conditions are not fulfilled simultaneously, photonic crystals (diffraction structures) with different periods can be applied [107]. One of them provides the synchronism of the electromagnetic wave with the electron beam $\omega - \vec{k}\vec{u} = \vec{\tau}_1\vec{u}$. The second photonic crystal (diffraction structure) evolves distributed Bragg coupling $|\vec{k}| \approx |\vec{k} + \vec{\tau}_j|$, $\vec{\tau}_j$ $(j = 2 \div n)$ are

the reciprocal lattice vectors of the second structure. Threshold conditions for s-wave diffraction are converted to:

$$G^{(s)} = \frac{a_s^3}{(k\chi L_*)^{2s} k L_*} + \chi_0'' b_s. \tag{120}$$

For dynamical diffraction, when $k|\chi|L_* \gg 1$, either the generation start current or the length of the generation zone at certain current value can be reduced.

Each Bragg condition holds one of free parameters. For example, for certain geometry and electron beam velocity, two conditions for three-wave diffraction entirely determine transverse components of wave vectors k_x and k_y, and therefore generation frequency (see (116), (119)). Hence, volume photonic crystal (diffraction system) provides mode discrimination due to multi-wave diffraction.

The above results affirm that a photonic crystal (volume diffraction structure) provides both amplification and generation regimes even in the absence of dynamical diffraction. In the latter case, generation evolves with backward wave, similar to the backward-wave tube. The frequency in such structures is changed smoothly either by a smooth variation of the radiation angle (variation of k_x and k_y) or by the rotation of the diffraction grating or the electron beam (change of $\vec{\tau}\vec{u}$) (see (116)). For certain geometry and reciprocal lattice vector, amplification corresponds to higher frequencies than generation. Rotation of either the diffraction grating or the electron beam also changes the value of the boundary frequency, which separates generation and amplification ranges. The use of multi-wave distributed feedback owing to Bragg diffraction allows one either to increase the generation efficiency or to reduce

the length of the interaction area (120). In this case, generation is available with both backward and following waves. In particular, the proposed volume structure can be used for generation of sub-millimeter radiation by accelerator LIU-3000. The parameters of this setup are: electron beam energy $E = 800$ keV, beam current $I = 100 \div 200$ A. To generate radiation with wavelength of 0.3 mm in such a system, a volume structure composed of strained threads should have a period ~ 2 mm, and a period of diffraction grating providing Bragg coupling ~ 0.16 mm. Generation of radiation in the terahertz range can also be obtained in a photonic crystal using higher harmonics of the Fourier expansion of the dielectric permittivity of the crystal [163].

15 Dependence of VFEL threshold conditions on undulator parameters

A sharp increase of amplification caused by volume distributed feedback (VDFB) yields a noticeable reduction of threshold currents necessary for the lasing start. This fact is particularly important for lasing in sub-millimeter and visible ranges and for shorter wavelengths. Explicit expressions of the VFEL threshold currents were obtained in [105]. Here we shall consider the dependence of VFEL starting current on the undulator parameters [149].

The set of equations describing the interaction of a relativistic electron beam, which propagates in the spatially periodic structure of the undulator is [105]:

$$DE - \omega^2\chi_1 E_1 - \omega^2\chi_2 E_2 - ... = 0$$
$$-\omega^2\chi_{-1}E + D_1 E_1 - \omega^2\chi_{2-1}E_2 - ... = 0 \quad (121)$$
$$-\omega^2\chi_{-2}E - \omega^2\chi_{1-2}E_1 + D_2 E_2 = 0 - ..., \quad (122)$$

where $D_\alpha = k_\alpha^2 c^2 - \omega^2 \varepsilon + \chi_\alpha^{(b)}$, $\vec{k}_\alpha = \vec{k} + \vec{\tau}_\alpha$ are the wave vectors of photons diffracted by the crystal planes with corresponding reciprocal vectors $\vec{\tau}_\alpha$, $\varepsilon_0 = 1 + \chi_0$, χ_α are the dielectric constants of a periodic structure; $\chi_\alpha^{(b)}$ is the part of dielectric susceptibility appearing from the interaction between an electron beam propagating in the undulator and radiation. Setting the determinant of the linear system (121) equal to zero, one can obtain the dispersion equation for the system "electromagnetic wave + undulator + electron beam + periodic structure". In the case of two-wave dynamical diffraction, this equation has the following form:

$$DD_1 - \omega^4 \chi_1 \chi_{-1} = 0 \tag{123}$$

For the system with finite interaction length, the solution of the boundary problem can be presented as a sum:

$$\vec{E} + \vec{E}_1 = \sum_i c_i \exp\{i\vec{k}_i\vec{r}\}(\vec{e} + \vec{e}_1 s_1^{(i)} \exp i\vec{\tau}\vec{r}) \tag{124}$$

In (124) $s_1^{(i)} = (k_i^2 c^2 - \omega^2 \varepsilon_0)/(\omega^2 \chi_1)$ and $\vec{k}_i$ are the coupling coefficients between the diffracted and transmitted waves and the solutions of dispersion equation (123), respectively. The coefficients c_i are defined by boundary conditions at the system ends $z = 0$ and L. The part of the electron beam energy converting into radiation can be expressed by:

$$\begin{aligned} I &\sim \gamma_0 |E(z = L)|^2 + |\gamma_1||E_1(z = 0)|^2 \\ &= (\gamma_0 |a|^2 + |\gamma_1||b|^2) \left(\frac{\gamma_0 c}{\vec{n}\vec{u}}\right)^3 \frac{16\pi^2 n^2}{-\beta(k|\chi_1|L_*)^2 k L_* (\Gamma_{\text{start}} - \Gamma)}, \end{aligned} \tag{125}$$

where L is the length of interaction in the undulator

$$\Gamma_{\text{start}} = \left(\frac{\gamma_0 c}{\vec{n}\vec{u}}\right)^3 \frac{16\pi^2 n^2}{-\beta(k|\chi_1|L_*)^2} - \chi'' \left(1 - \beta \pm \frac{r''\sqrt{-\beta}}{|\chi_1|\chi''}\right)$$

$$\Gamma = \frac{\pi^2 n^2}{4} \frac{\pi \Theta_s^2 j_0 c^2}{\gamma_z^2 \gamma I_A \omega^2} k^2 L_*^2 f(y),$$

$f(y)$ is the function describing the dependence of generation on detuning from the synchronism condition, $y = (\omega - \vec{k}\vec{v}_w - \Omega)L/(2u_z)$ is the detuning factor, $\beta = \gamma_0/\gamma_1$ is the diffraction asymmetry factor, γ_0, γ_1 are diffraction cosines, $\chi'' = \mathtt{Im}\chi_0$, $\Theta_s = eH_w/(mc^2\gamma k_w)$, $\gamma_z^{-2} = \gamma^{-2} + \Theta_s^2$, $k_w = 2\pi/\lambda_w$, λ_w is the undulator period, H_w is the undulator field. It follows from (125) that:

1. the starting current in the case of two-wave diffraction is proportional to $j_{\text{start}} \sim (kL)^{-1}(k\chi_1 L)^{-2}$;

2. the non-one dimensional VDFB provides the possibility to decrease the starting current of generation by varying the angles between the waves.

3. if the electron beam current is less than the starting value $j < j_{\text{start}}$, the energy of the electromagnetic wave at the system entrance can be written in the form:

$$E/(\gamma_0|a|^2 + |\gamma_1||b|^2) = 1 - \beta \frac{\pi^2 n^2}{4} \frac{\pi \Theta_s^2 j_0 c^2}{\gamma_z^2 \gamma I_A \omega^2} (kL)^3 \left(\frac{k\chi_\tau L}{4\pi}\right)^2 f(y) \qquad (126)$$

The conventional FEL gain is proportional to $(kL)^3$ [104], but as follows from (126) in the case of two-wave diffraction, the gain gets an additional factor $\sim \left(\frac{k\chi_\tau L}{4\pi}\right)^2$, which noticeably exceeds unity in conditions of dynamical diffraction. Such an increase of the radiation output at the degeneration point can be explained by the reduction of the wave group velocity, which can be written as:

$$v_g = -\left(\frac{\partial D}{\partial k_z}\right) / \left(\frac{\partial D}{\partial \omega}\right) \sim \prod_{i<j} (k_{zi} - k_{zj}) \qquad (127)$$

It follows from (127) that for multi-wave dynamical diffraction at the s-fold-degeneration point $v_g \sim v_0/(kL)^s$, the starting current $j_{\rm start} \sim (kL)^{-3}(k\chi_1 L)^{-2s}$ and the amplification are proportional to $(kL)^3(k\chi_1 L)^{2s}$. It should be noted that the considered effects take place in a wide spectral range for wavelengths from centimeters to X-ray, and the influence of the effect increases with frequency growth.

The generation threshold in the undulator VFEL in the case of VDFB can be achieved at a lower electron beam current and a shorter undulator length when special conditions of degeneration of roots are fulfilled. Changing the VDFB conditions by varying the volume geometry parameters (for example, the angle between the wave vectors) gives the possibility to increase the Q-factor and to decrease the starting current (see Figure **??**). Hence, the generation efficiency can be increased.

16 Use of a dynamical undulator mechanism to produce short wavelength radiation in VFELs

Here we shall consider VFEL lasing in a system with a dynamical undulator [150]. In this system radiation of long wavelengths creates the undulator for lasing at a shorter wavelength. Two diffraction gratings with different spatial periods form a VFEL resonator. The grating with longer period pumps the resonator with the long wavelength radiation to provide the necessary amplitude of the undulator field. The grating with the shorter period is used to select the mode for the short wavelength radiation. Lasing of such a system in the terahertz frequency range is discussed below.

Numerous applications can benefit from the development of powerful electromagnetic generators with frequency tuning in millimeter, sub-millimeter and terahertz wavelength range using low-relativistic electron beams. One of the ways to create such generators is to use VFEL principles. The main distinction of VFEL in comparison with the traditional FEL is the use of the non one-dimensional distributed feedback, which allows wide range tuning of frequency, decreases starting currents of generation, and allows one to use a wide electron beam (or several beams) [55,105]. In the VFEL the generation evolves in a large volume, which increases the electrical strength of the resonator (the electromagnetic power and electron beam are distributed over a greater volume). This peculiarity of the VFEL is essential for generation of power and super-power electromagnetic pulses. The mode discrimination in such an oversized system is carried out by multi-wave dynamical diffraction [105]. Low relativistic electron beams in the undulator system can be used for radiation of short wavelength radiation, but it requires manufacturing of undulators with a small period. For example, to obtain radiation with the wavelength of $0.3-1$ mm at the beam energy $E = 800$ KeV-1 MeV an undulator with the period $\sim 0.3-1$ cm is necessary. This is an extremely complicated problem. The use of a two-stage FEL with the dynamical wiggler generated by an electron beam [104] is a possible solution to this problem.

The dynamical wiggler can be created with the help of any radiation mechanism: Cherenkov, Smith-Purcell, quasi-Cherenkov [55], undulator. VFEL principles provide advantages of the two-stage generation scheme and, in particular, allow one to smoothly tune the period of dynamical wiggler by rotating the diffraction grating. There is the possibility of smooth frequency tuning for both the pump wave and the signal wave either by variation of geometric

parameters of the volume diffraction grating or by their rotation. Moreover, the VFEL allows one to create the dynamical wiggler in a large volume, that is a great problem for a static wiggler.

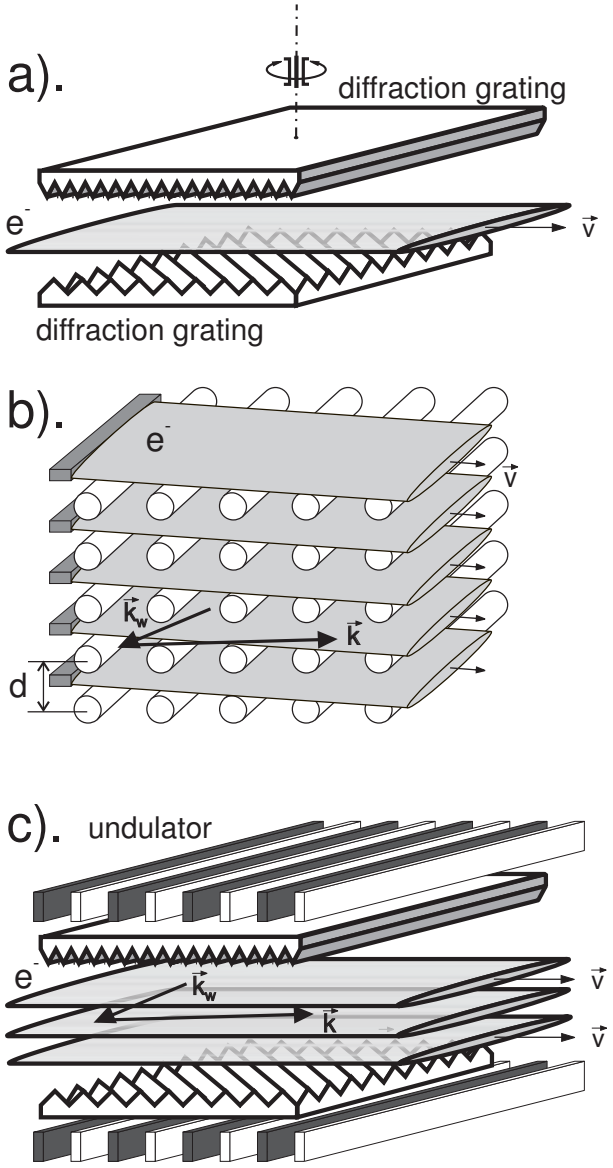

Figure 16. The schemes of dynamic wiggler. Rotation of diffraction grating (schemes a). and c).) changes the period of dynamic wiggler

There are two stages in the generation scheme proposed above:

(a) creation of the dynamical wiggler in a system with two-dimensional (three-

dimensional) gratings (in other words, during this stage, the electromagnetic field, which exists inside the VEFL resonator, is used to create the dynamical wiggler). Smooth variation of the orientation of the diffraction grating in the VEFL resonator provides means for a smooth change of the dynamical wiggler parameters;

(b) radiation is generated by an electron beam interacting with the dynamical wiggler, which is created during the previous stage (stage a).
Both stages evolve in the same volume.

The idea of a two-stage tunable VFEL described above can be realized in different ways. Let us consider some examples (Figure 16a-c). Figure 16 a displays the two-stage device in which the dynamical wiggler is realized on the basis of a VEFL generator using the Smith-Purcell radiation mechanism. This generation scheme was considered in [107], when experimentally realized, first lasing of a VFEL was observed [181]

In this case only a part δl_x of an electron beam participates in the generation process during the first stage: $\frac{\delta l_x}{l_x} \sim \lambda_w \beta\gamma/(4\pi l_x)$, here δl_x is the transverse size of the part of the electron beam participating in the interaction, l_x is the transverse size of the electron beam, λ_w is the wavelength, $\beta = u/c$, u is the electron velocity, γ is the Lorentz factor. The resonator in Figure 16a consists of two diffraction gratings [164,181]. The lower grating provides the Smith-Purcell generation mechanism. The period d_1 of this grating is determined by $d_1 \sim \beta\gamma^2\lambda_w \cos\varphi$ (d_1 is the period of the Smith-Purcell grating, φ is the angle between the direction of the electron velocity and the direction of the grating periodicity). The upper grating provides the distributed feedback [55,105] by multi-wave dynamical diffraction. The conditions of dynamical diffraction

$|\vec{k}_w| \approx |\vec{k}_w + \vec{\tau}_i|$ are fulfilled in this case ($\vec{\tau}_i$ are the reciprocal wave (lattice) vectors of this grating). It should be noted that the period of the upper grating does not coincide with that of the lower one. Radiation accumulated in the resonator during the described first stage creates the dynamical wiggler. Beam electrons oscillate in this electromagnetic wiggler and radiate just as in a conventional FEL (this is not necessarily the same electron beam that participates in the first stage. It can be another beam of higher energy). The field inside the resonator is a standing wave. Traveling waves, which form this standing wave are actually the pump waves. They are scattered by the electron beam according to the synchronism condition $\omega - (\vec{k}\vec{u}) \approx \omega_w - (\vec{k}_w\vec{u})$. The resulting wave has the wavelength $\lambda \sim \frac{1-\beta}{1+\beta}\lambda_w$ (in the last estimation it is supposed that the wave vector $\vec{k}_w$ of the pump wave is antiparallel to the velocity, and the wave vector $\vec{k}$ is parallel to it. For a relativistic beam, this relation has the form $\lambda \sim \lambda_w/(4\gamma^2)$. It should be emphasized that in this case there is one more possible way to create the dynamical wiggler in the resonator shown in Figure 16a. It is based on the excitation of a slow wave, which is diffracted by the lower grating (surface VFEL). The electron beam oscillates in this wiggler and radiates. In this case the upper grating forms the distributed feedback which provides VFEL lasing at shorter wavelength. The change of the radiated frequency is provided by the rotation of both the upper and lower gratings. Figure 16b presents the variant of the volume diffraction grating which can provide the generation mechanism and distributed feedback simultaneously [55,105]. Let us note that in these examples the generation mechanism during the first stage is based on the slowing of the electromagnetic wave and only a part of the electron beam participates in the creation of the dynamical wiggler. The whole electron beam participates in the generation process during

the second stage. The larger the part of the beam that does not participate in the the first stage interaction, the more unperturbed electrons appear during the second stage and, therefore, they radiate more effectively. The dynamical wiggler in Figure 16c uses the undulator radiation mechanism during the first stage. In this case the dynamical wiggler is formed during the first stage due to the interaction between the electron beam and a conventional magnetostatic undulator. The frequency of the pump wave is $\omega_w \sim \frac{2\pi\beta}{d_u(1-\beta\cos(\theta))}$, where d_u is the period of the magnetostatic undulator. During this stage the lower diffraction grating is used to provide the distributed feedback for the wave with frequency ω_w and operation of the VFEL at this frequency. During the second stage, electrons oscillate in the field of this wave, which plays the role of the dynamical wiggler. As a result, during the second stage of the process the wave with the frequency $\omega \sim 4\gamma^2\omega_w$ is generated and the distributed feedback is provided by the upper grating, the period of which corresponds to the wave with the frequency ω. The rotation of diffraction gratings provides frequency tuning.

It is clear that the time τ_w of the dynamical wiggler creation is a very important characteristic of the proposed system. This time is determined by $\tau_w \sim Q/\omega_w$, where ω_w is the frequency of the pump wave.

The Q factor of resonator for the frequency ω_w should be sufficient to create a magnetic field amplitude of about 100 G - 1 kG. It follows from the energy balance equation in the resonator, $(\omega_w/Q)V(H_m^2/8\pi) = W_0$, ($W_0$ is the power of the pump wave formed by the electron beam) that $Q = (\omega_w/W_0)V(H_m^2/8\pi)$, where V is the cavity volume, H_m is the amplitude of the magnetic field of the dynamical wiggler. It follows from the above that to create the magnetic field of about $100 - 1000$ G, the time $\tau_w \sim 10^{-10} - 3 \times 10^{-9}$ s is necessary

($V = 30$ cm^3, $W \sim 30$ MW). As one can see, this time is small enough for the wiggler to evolve while the electron beam passes through the system. When the pump field achieves the necessary magnitude, stage (b) begins.

Dynamics of the signal electromagnetic wave and the electron beam in the system (volume diffraction grating + pump electromagnetic wave) in this case is described by equations

$$\begin{array}{r} D_0\ E - \omega^2\chi_1 E_1 - \omega^2\chi_2 E_2 - \omega^2\chi_3 E_3 - \ldots = 0 \\ -\omega^2\chi_{-1}\, E + D_1 E_1 - \omega^2\chi_{2-1} E_2 - \omega^2\chi_{3-1} E_3 - \ldots = 0, \\ -\omega^2\chi_{-2}\, E - \omega^2\chi_{1-2} E_1 + D_2 E_2 - \omega^2\chi_{3-2} E_3 - \ldots = 0. \end{array} \tag{128}$$

In (128) $D_\alpha = k_\alpha^2 c^2 - \omega^2\varepsilon + \chi_\alpha^{(b)}$, $\vec{k}_\alpha = \vec{k} + \vec{\tau}_\alpha$ is the vector of the diffracted wave, $\chi_\alpha^{(b)}$ is the part of the dielectric susceptibility corresponding to the interaction of the electron beam with radiation

$$\chi_\alpha^{(b)} = \frac{q_\alpha^{(w)}}{\left\{\omega - (\vec{k}_\alpha \vec{v}_w) \mp (\omega_w - (\vec{k}_w \vec{v}))\right\}^2}$$

$$\begin{aligned} q_\alpha^{(w)} = {} & \frac{a_w^2}{4\gamma^3}\frac{\omega_L^2}{(k_w v)^2}\left\{\left[\frac{(\vec{u}\vec{e}_\alpha)}{c(k_w v)}(\omega_w \vec{u} - \vec{k}_w c^2)(\vec{k}_\alpha - \vec{k}_w)\right.\right. \\ & \left.\left. -(\vec{k}_\alpha \vec{e}_w)c\right]\frac{(\vec{u}\vec{e}_\alpha)}{c} - (\vec{k}_w \vec{e}_\alpha)(\vec{u}\vec{e}_w) - (\vec{e}_\alpha \vec{e}_w)(k_w v)^2\right\}^2 \\ & \times \left\{(\vec{k}_\alpha - \vec{k}_w)^2 c^2 - (\omega - \omega_w)^2\right\}, \end{aligned}$$

$\vec{k}, \omega, \vec{e}$ and $\vec{k}_w, \omega_w, \vec{e}_w$ are the wave vectors, frequencies and polarization vectors of both the signal and pump waves, respectively, $v = (c, \vec{u})$, $k_w = (\omega_w/c, \vec{k}_w)$, $a_w = eH_w/mc\omega_w$. The dispersion equation corresponding to equation (128) has the following schematic form

$$F^{(n)} = -\chi_\alpha^{(b)} F^{(n-1)}, \tag{129}$$

where the term $F^{(n)}$ on left-hand side of (129) corresponds to the n-wave Bragg dynamical diffraction (equation $F^{(n)} = 0$ is the dispersion equation defining diffraction modes in the n-wave case). The continuity of the current densities, charge densities, and transverse components of fields on the boundaries and dispersion equation (129) give the equation for the generation threshold [105]. From (128) we obtain that for the n-fold degeneration point of the roots of the dispersion equation (when $n+1$ roots of the equation $D^{(m)} = 0$ at $m \geq n+1$ coincide), the equation for the generation threshold has the following form

$$\frac{1}{\gamma^3}\left(\frac{\omega_L}{\omega}\right)^2 a_w^2 k^3 L_*^3 = \frac{a_n}{(k|\chi|L_*)^{2n}} + b_n k \chi'' L_*. \tag{130}$$

In (130) $k = \omega/c$, L_* is the length of the interaction area of the electron beam with electromagnetic radiation, χ'' is the imaginary part of the dielectric susceptibility, which describes absorption, a_n, b_n are the parameters depending on the geometric parameters of the system (except L_*). The equality (130) has an obvious physical meaning: the left-hand side of (130) contains the term describing generation of radiation by the electron beam, and the right-hand side includes the terms describing losses on the boundaries (the first term) and absorption losses (the second term) in the medium. One of the peculiarities of the VFEL with multi-wave distributed feedback is the possibility of a sharp decrease of losses at the boundaries (the first term on the right-hand side of (130) decreases with the increase of s due to the condition $k|\chi|L_* \gg 1$ under dynamical diffraction). Let us express the synchronism condition for the above generation mechanism $\omega - \vec{k}\vec{v} = \Omega_w$, where $\Omega_w = \omega_w - \vec{v}\vec{k}_w$. Then, the frequency of the signal wave is equal to (if the pump wave is oncoming)

$$\omega = \frac{2\omega_w(\vec{\tau}_1, \ldots \vec{\tau}_n, \vec{n}_u, S)(1 - \beta\cos(\Theta_w))}{1 - \beta\cos(\Theta)}. \tag{131}$$

In (131) the explicit dependence of the pump wave frequency on the geometry of the multi-wave diffraction $(\vec{\tau}_1, \ldots \vec{\tau}_n)$ and the set of resonator parameters S is marked out (if a resonator is not oversized, then the dependence on S disappears). Smooth change of the VFEL geometry also varies the Q factor and, therefore, varies the generation efficiency. For example the dependence of Q on the diffraction asymmetry factor $f = \gamma_0/\gamma_1$ is shown in Figure 17 (γ_0, γ_1 are diffraction cosines [55]).

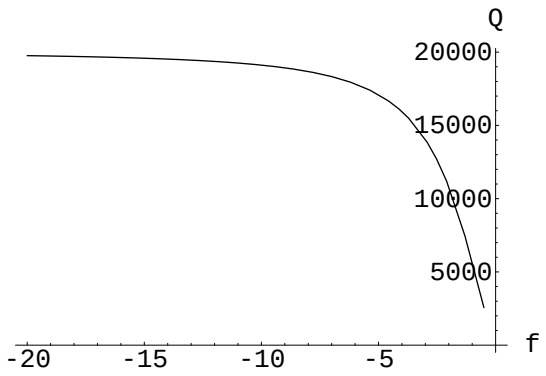

Figure 17. Calculated dependence of Q factor on diffraction asymmetry factor f

It should be noted that the distributed feedback can be used for both the first and the second stages. To optimize the resulting radiation output, Q factor can be controlled at both stages. Thus, for radiation angle $\Theta = 0$ the frequency $\omega \sim 4\gamma^2\omega_w$, even the moderately relativistic electron beam ($E \sim 1$ MeV) gives a frequency multiplication ~ 35 times. If during the first stage the undulator mechanism is used (undulator period $\sim$ 8 cm), then the wavelength of the pump wave is $\lambda_w \sim 1$ cm. Thus the signal wave is generated in the teraHertz range (Figure 17).

Thus,

(1) the principles of VFEL can be used for creation of a dynamical wiggler with variable period in a large volume,

(2) the two-stage scheme of generation can be used for lasing in the teraHertz frequency range using low-relativistic beams,
(3) the two-stage scheme of generation combined with the volume distributed feedback opens up the possibility of creating powerful generators with wide electron beams (or system of beams).

17 Formation of distributed feedback in a FEL under multi-wave diffraction

We shall further consider the boundary problem for a quasi-Cherenkov FEL for the case in which a distributed feedback is provided by three-wave coplanar diffraction of the emitted photons [105]. As compared with a two-wave distributed feedback, in the three-wave case the appropriate choice of parameters enables reducing the interaction region between a particle beam and the electromagnetic wave necessary to reach the oscillation threshold as well as radiation losses inside the medium. For example, it allows a reduction in the size of an FEL and the construction of more compact coherent radiation sources in any spectral range.

Here we show that the two-wave DFB (in which only two waves are strongly excited) is not optimal because the region of root degeneration often coincides with the region of strong radiation absorption inside the medium. This is especially important for solid FELs. The most effective resonator is one with a multi-wave DFB, where the distributed feedback is formed by multi-wave dynamical diffraction. The advantages of a multi-wave DFB are analyzed in detail for the solid quasi-Cherenkov FEL with three-wave coplanar DFB because this analysis can be conducted analytically. Consider, for example, the

specific case of a solid X-ray quasi-Cherenkov FEL where the crystal medium provides both a spontaneous radiation mechanism in the X-ray spectral range [8] and diffraction of the emitted X-rays by the crystal forming the three-dimensional distributed feedback. For the X-ray spectral range, the crystal target is a radiator and a resonator simultaneously. It should be mentioned that the analysis derived below will be appropriate for other spectral ranges as well. For example, a three-dimensional optical grating can be formed inside a solid target by a laser. Moreover, a multi-wave distributed feedback can be formed by surface dynamical diffraction if a particle beam moves over a three-dimensional periodic structure at a distance not larger than λ_γ (where λ is the radiation wavelength, γ is the Lorentz factor). In this way the multi-wave DFB can be used with an ordinary undulator FEL.

Let a relativistic particle beam be incident on a crystal plate ($0 \leq z \leq L$) at an arbitrary angle Ψ_0. The set of Maxwell's equations which describes the interaction of an electromagnetic wave with a crystal and with a particle beam passing through a crystal target can be written in the following form [55]:

$$\begin{aligned} D_\sigma^{(0)} E_\sigma^{(0)} - \omega^2 \chi_1 E_\sigma^{(1)} - \omega^2 \chi_2 E_\sigma^{(2)} &= 0, \\ -\omega^2 \chi_{-1} E_\sigma^{(0)} + D_\sigma^{(1)} E_\sigma^{(1)} - \omega^2 \chi_{2-1} E_\sigma^{(2)} &= 0, \\ -\omega^2 \chi_{-2} E_\sigma^{(0)} - \omega^2 \chi_{1-2} E_\sigma^{(1)} + D_\sigma^{(2)} E_\sigma^{(2)} &= 0, \end{aligned} \tag{132}$$

where $D_\sigma^{(\alpha)} = k_\alpha^2 c^2 - \omega^2 \varepsilon_0^{(\alpha)} + \chi_b^{(\alpha)}$. We assume that a particle beam and a crystal plate are oriented so that the three-wave coplanar diffraction condition is satisfied for emitted photons. In this case only three strong waves with the σ-polarization are excited inside the crystal medium. (see [55] for two-wave diffraction geometry). The subscript α ($\alpha = 0 - 2$) labels the transmitted wave ($\alpha = 0$) and diffracted waves ($\alpha = 1, 2$); $E_\sigma^{(\alpha)}$ are the σ components of the amplitudes of electromagnetic waves, $\vec{k}_1 = \vec{k}_0 + \vec{\tau}_1$, $\vec{k}_2 = \vec{k}_0 + \vec{\tau}_2$ are

the wave vectors of photons diffracted by crystal planes with corresponding reciprocal vectors $\vec{\tau}_1$ and $\vec{\tau}_2$; $\epsilon_0^{(\alpha)} = 1 + \chi_\alpha$ are the dielectric constants of a crystal for transmitted and diffracted waves.

$$\chi_b^{(\alpha)} = \frac{1}{\gamma}(\omega_L/\omega^2)(\vec{u}\vec{e}_\sigma/c)^2 \frac{k_\alpha^2 c^2 - \omega^2}{(\omega - \vec{k}_\alpha\vec{u})^2 - \frac{\hbar^2}{4m^2c^4\gamma^2}(k^2c^2 - \omega^2)^2} \tag{133}$$

for the "cold" beam limit and

$$\chi_b^{(\alpha)} = -\frac{i\sqrt{\pi}}{\gamma}(\omega_L/\omega)^2(\vec{u}\vec{e}_\sigma/c)^2 \frac{k_\alpha^2 c^2 - \omega^2}{\delta_\alpha^2} x_\alpha^t \exp[-(x_\alpha^t)^2]$$

for the "hot" beam limit. χ_b represents the part of the dielectric susceptibility produced by the interaction of a particle beam with radiation, $x_\alpha^t = (\omega - \vec{k}_\alpha\vec{u})/\sqrt{2}\delta_\alpha$, $\delta_\alpha^2 = (k_{\alpha 1}^2\Psi_1^2 + k_{\alpha 2}^2\Psi_2^2 + k_{\alpha 3}^2\Psi_3^2)u^2$, and $\Psi = \Delta\overline{V}/|\overline{V}|$ is the velocity spread. As was shown in [55], comparison of a standard equation of X-ray dynamical diffraction with (132) leads to the conclusion that the combination of a crystal and a particle beam may be considered as an "active" medium with dielectric susceptibility equal to $\chi_\alpha + \chi_b^{(\alpha)}$. It permits the boundary problem of X-ray amplification (lasing) due to the passage of a particle beam through a periodic medium to be reduced to the problem of X-ray diffraction by an "active" periodic medium consisting of a crystal plus radiating particle beam.

The geometry of three-wave diffraction is shown in Figure 18, where $\vec{V}$ is the mean particle beam velocity, $z = 0$ and $z = L$ are the two surfaces of a crystal plate.

The dispersion equation determining the electromagnetic modes inside the "active" medium can be represented in the following form:

$$F_\sigma^{(3)}(\vec{k}_0; \vec{k}_1; \vec{k}_2) = -i\chi_b^{(0)} F_\sigma^{(2)}(\vec{k}_1; \vec{k}_2), \tag{134}$$

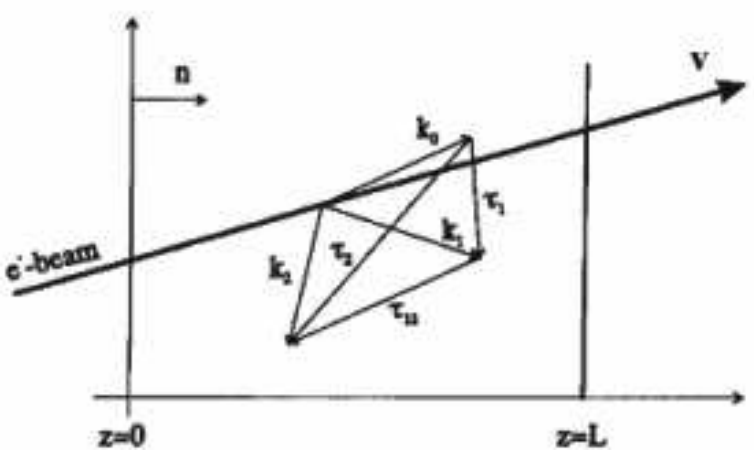

Figure 18. Figure The geometry of three-wave diffraction. $\vec{V}$ is the mean particle beam velocity, and $z = 0$ and $z = L$ are two surfaces of a crystal plate

where

$$F_\sigma^{(3)}(\vec{k}_0;\vec{k}_1;\vec{k}_2) = (k^2c^2 - \omega^2\epsilon_0^{(0)})(k_1^2c^2 - \omega^2\epsilon_0^{(1)})(k_2^2c^2 - \omega^2\epsilon_0^{(2)}) -$$
$$-\omega^4(k^2c^2 - \omega^2\epsilon_0)\chi_{1-2}\chi_{2-1} - \omega^4(k_1^2c^2 - \omega^2\epsilon_0^{(1)})\chi_2\chi_{-2}$$
$$-\omega^4(k_2^2c^2 - \omega^2\epsilon_0^{(2)})\chi_1\chi_{-1} - \omega^6(\chi_1\chi_{-2}\chi_{2-1} + \chi_2\chi_{-1}\chi_{1-2});$$

$$F_\sigma^{(2)}(\vec{k}_1;\vec{k}_2) = (k_1^2c^2 - \omega^2\epsilon_0^{(1)})(k_2^2c^2 - \omega^2\epsilon_0^{(2)}) - \omega^4\chi_{1-2}\chi_{2-1}$$

.

From (134) follows that the root degeneration (the strongest interaction is in the root degeneration region) and the fulfillment of the Cherenkov condition are possible simultaneously only under the following conditions:

$$l_0l_1l_2 - l_0r_{12} - l_1r_2 - l_2r_1 - f = 0,$$
$$\beta_1\beta_2l_1l_2 + l_0(\beta_1l_1 - \beta_2l_2) - \beta_1\beta_2r_{12} - \beta_1r_1 - \beta_2r_2 = 0, \qquad (135)$$

where $l_0 = \theta^2 - \chi_0 + \gamma^{-2}$, $l_{1,2} = l_0 + \alpha_{B1,2}$; $\alpha_{B1,2} = (2\vec{k}\vec{\tau}_{1,2} + \vec{\tau}_{1,2}^2)/k^2$.

It is straightforward to show that for the fulfillment of (135), the system

parameters should satisfy the following relationship:

$$\beta_1\beta_2(l_0^2 + \beta_1 r_1 + \beta_2 r_2) < 0, \tag{136}$$

where $f = \chi_1\chi_{-2}\chi_{2-1} + \chi_2\chi_{-1}\chi_{1-2}$, $\beta_{1,2} = \gamma_0/\gamma_{1,2}$ are the asymmetry factors of diffraction $\gamma_\alpha = (\vec{k}_0\vec{n})/|\vec{k}_\alpha|$, $r_1 = \chi_1'\chi_{-1}'$ and $r_2 = \chi_2'\chi_{-2}'$. Expression (136) is more restrictive than the equivalent relation for the two-wave case [55].

In the case of Bragg-Bragg diffraction in the X-ray spectral range there is a restriction on the radiation angle

$$\theta_{B-B}^{\max} = (\sqrt{-\beta_1 r_1 - \beta_2 r_2} + \chi_0' - \gamma^{-2})^{1/2}. \tag{137}$$

This relation leads to a large value of the diffraction asymmetry factor, which, in turn, leads to strong radiation absorption inside the medium in the vicinity of the root degeneration point – just as in the two-wave DFB case [55]. The situation changes in the Bragg-Laue geometry. In this case the inequality (136) can be satisfied at angles $\theta \geq \theta_{B-B}$, which makes it possible to reduce the asymmetry factors β_1 and β_2 and, consequently, radiation absorption inside the crystal.

The solution of the corresponding boundary problem is presented as a sum:

$$\vec{E} = \sum_i c_i \exp i\vec{k}_i\vec{r}(\vec{e}_0 + \vec{e}_1 s_i^{(1)} \exp i\vec{\tau}_1\vec{r} + \vec{e}_2 s_i^{(2)} \exp i\vec{\tau}_2\vec{r}), \tag{138}$$

where $s^{(1)} = (\lambda\lambda_2 - r_2)/(\lambda_2\chi_1 + \chi_2\chi_{1-2})$, $s^{(2)} = (\lambda\lambda_1 - r_1)/(\lambda_1\chi_2 + \chi_1\chi_{2-1})$, and $\vec{k}_i$ are the solutions of the dispersion equation and the coefficients of coupling between the transmitted and diffracted waves, $E^{(1)} = s^{(1)}E$, $E^{(2)} = s^{(2)}E$, $\lambda_\alpha = [(\vec{k} + \vec{\tau})^2c^2 - \omega^2\epsilon_0]/\omega^2$. To determine the unknown coefficients,

it is necessary to solve the boundary conditions for the waves on the crystal surfaces. These can be written in the following form for the Bragg-Laue case:

$$\sum_i^3 c_i = 1, \quad \sum_i^3 s_i^{(1)} c_i = 0, \quad \sum_i^3 s_i^{(2)} c_i l_i = 0. \tag{139}$$

The condition (139) is written for the "hot" beam limit. For the "cold" beam limit the corresponding expression can be found in [54].

It is well known [116] that the oscillation threshold can be determined from the condition that $\Delta = 0$, where Δ is the determinant of the system (139).

Solving the equation $\Delta = 0$, we obtain the threshold in the form

$$G = a\chi_0'' + \frac{16}{|\beta_1\beta_2|}\left[\frac{\gamma_0 c}{\vec{n}\vec{u}}\right]^3 \frac{\pi^2 n^2}{(kl_0 L_*)^2 kL_*}\eta_{B-L} \tag{140}$$

with the phase condition $(k_{1z} - k_{2z})L = 2\pi n$ (n is an integer), $r_{12} = \chi_{1-2}\chi_{2-1}$, where

$$G = -\frac{\pi^2 n^2}{4\gamma}\left\{\frac{\omega_L}{\omega}\right\}^2 k^2 L_*^2(\chi_0' \pm \sqrt{-\beta}|\chi_\tau| - \gamma^{-2})(\chi_0' \pm \sqrt{-\beta}|\chi_\tau|)\sin\phi^2$$
$$\times \sin y[(2y + \pi n)\sin y - y(y + \pi n)\cos y]y^3(y + \pi n)^{-3}$$

for the "cold" beam limit and

$$G = -\sqrt{\pi}\frac{\omega_L^2}{\gamma\omega^2}\frac{(l_0 + \chi_0' - \gamma^{-2})(l_0 + \chi_0')\sin\phi^2}{\delta_0^2/k^2}x^t e^{-(x^t)^2}$$

for the "hot" beam limit. a and η_{BL} are smooth functions depending on the diffraction geometry and usually are of the order unity, $y = k\delta L/2$ and δ is the deviation from the exact Cherenkov synchronism condition.

The analysis shows that in the coplanar Bragg-Laue diffraction geometry of DFB radiation, absorption inside the medium can be reduced in the region of

root degeneration. For example, under dynamical diffraction by the (111) and $(11\overline{1})$ planes with a symmetry factor $\beta_1 = -\beta_2 = \beta = 0.16$, the current density required to achieve the threshold can be reduced by approximately one order of magnitude in comparison with a two-wave DFB FEL using LiH and an electron energy of 750 MeV with a transverse angular spread $\Psi_\perp = 5 \times 10^{-6}$ rad [55].

18 Distributed feedback under the multi-wave diffraction

In principle, in the general case of the n-wave diffraction DFB, it is possible to achieve the degeneration of n roots. In this case the threshold condition has the form:

$$G = \frac{a_n}{(k|\chi'_\tau|L)^{2(n-1)}kL} + b_n\chi''_0, \tag{141}$$

where a_n and b_n are the functions weakly dependent on the diffraction type.

The energy loss through target surfaces can be reduced due to the fulfillment of the inequality $k|\chi_\tau|L \gg 1$ under dynamical diffraction. As the degree of dispersion root degeneration increases, radiation remains inside the target longer because the group velocity decreases and is proportional to $\sim L^{n-1}$, where n is the degree of dispersion root degeneration. As a result, the region of interaction between the particle beam and the emitted radiation can be reduced. This leads to the possibility of reducing the FEL's dimensions, i.e., of constructing a compact source of coherent radiation.

19 Parametric X-ray FEL operating with external Bragg reflectors

This section is devoted to the application of external Bragg reflectors in a volume parametric X-ray FEL [151]. It is shown that external Bragg reflectors permit not only a reduction of electromagnetic energy losses through target boundaries but also a reduction of the radiation self-absorption inside the target by modifying radiation modes excited in the active medium containing a particle beam plus a crystal. As a result, the starting beam current can be reduced by more than a factor of ten. It is also shown that the best conditions for lasing are realized when the diffracted wave is reflected by the external Bragg reflector.

19.1 Generation threshold for parametric X-ray FEL with external reflectors

The scheme of an X-ray volume FEL using spontaneous X-ray parametric radiation has been considered in [55]. Following the remarks mentioned above, the scheme under consideration differs from the case described in [55] by the addition of external Bragg reflectors which can be placed in the direction of both transmitted and diffracted waves. For example, in the case of a three-crystal scheme of diffracted wave reflection, the geometry of a volume FEL can be represented in the following way:

Here $\vec{V}$ is the mean velocity of electrons, $\vec{k}$ and ω are the wave vector and the frequency of the emitted photon, $\vec{k}$ and ω are the wave vector and the frequency of the diffracted photon, a, b, c, d are the crystal targets. We assume that the crystal (a) in Fig.19 is oriented relative to the particle beam so that only two strong waves are excited inside the crystal under diffraction (two-wave

diffraction).

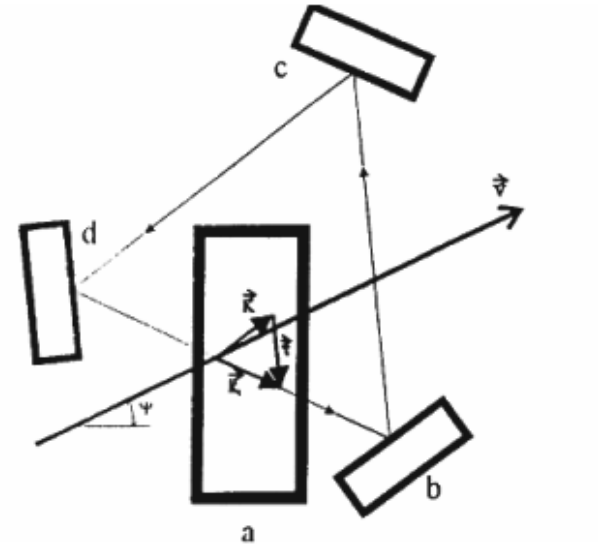

Figure 19.

The closed system of Maxwell's equations, including the equation describing the motion of electrons, and the method of its solution were described in [55].

The introduction of external Bragg reflections modifies only the boundary conditions where the reflection coefficients for diffracted and transmitted waves appear. Besides, the analysis shows that there appears the possibility of realization of lasing regime under a Laue diffraction scheme (see Figure 19) which is impossible, in principle, without external Bragg reflectors.

Let us restrict ourselves to the analysis of Laue geometry for distributed feedback. Solving the boundary conditions while taking into account the phase relation for the main crystal target (a) and for the external reflectors we can obtain the generation equations for two cases.

Case (1) The "cold" beam limit and weak amplification:

$$G = \begin{cases} (1-|\alpha|)(1-\frac{\beta l_1'}{l_0'})\frac{\gamma_0 V}{V_z} + k[x_1'' + \frac{\beta l_1'}{l_0'}x_2'']L_* = \Gamma_{\rm th}^{(1)}, \quad (1) \\ (1-|\alpha|)(1-\frac{\beta l_0'}{l_1'})\frac{\gamma_0 V}{V_z} + k[x_1'' + \frac{l_0'}{\beta l_1'}x_2'']L_* = \Gamma_{\rm th}^{(2)}, \qquad (2) \end{cases} \tag{142}$$

where

$$\begin{aligned} G &= \frac{\beta}{4\gamma}k^2 L_*^3 \left(\frac{\omega_L}{\omega}\right)^2 (l_0' + \chi_0' - \gamma^{-2})(l_0' + \chi_0')l_1'(l_0' + \beta l_1')^{-1}\sin^2\Phi f(\chi), \\ f(x) &= \frac{\sin x}{x}\frac{x\cos x - \sin x}{x^2}, \\ l_0' &= 1/2[-\alpha_B \pm \sqrt{\alpha_B^2 + 4r}], \quad l_1' = 1/2[+\alpha_B \pm \sqrt{\alpha_B^2 + 4r}], \\ x_{1(2)}'' &= \frac{1}{4}\chi_0''\left\{1 + \beta \pm \frac{(l_0' - \beta l_1')(\beta - 1) + 2\beta r''/\chi_0''}{[(l_0' - \beta l_1')^2 + 4\beta r]^{1/2}}\right\}, \end{aligned} \tag{143}$$

the prime means the real part of the magnitude and the double prime means its imaginary part; equation (1) of the system (142) describes the case of diffracted wave reflection, and equation (2) corresponds to the case of transmitted wave reflection. The quantity $\alpha = |\alpha|\exp i\phi$ is the reflection coefficient for transmitted (2) or for diffracted (1) waves respectively.

The value of $(1-|\alpha|)$ can be very small for a narrow interval of angles $(1-|\alpha|) = -\chi_0''|\chi_\tau|^{-1}(1-\exp(-W))$, where W is the Debye-Waller factor. For example, for a LiH crystal $(1-|\alpha|) < 10^{-3}$ at $\sim 1-10$ keV photoenergies.

As a result, the radiation losses through crystal boundaries can be essentially reduced. This means that the threshold condition will be determined mainly by radiation absorption. In this case (142) can be represented in the form:

$$\begin{aligned} (1) \qquad j_{\rm th} &= \frac{4}{\beta}\left(\Lambda_2'' + \frac{b_0}{\beta b_1}\Lambda_1''\right)\frac{b_0 + \beta b_1}{(b_0 - a_F)(b_0 - a_F^{(1)})b_1} = \frac{m\gamma c^3}{b_0 e L_*^2}\frac{\chi_0''}{|\chi\tau|^2}g_1(a,\beta), \\ (2) \qquad j_{\rm th} &= \frac{4}{\beta}\left(\Lambda_1'' + \frac{b_0}{\beta b_1}\Lambda_2''\right)\frac{b_0 + \beta b_1}{(b_0 - a_F)(b_0 - a_F^{(1)})b_1}\frac{m\gamma c^3}{b_0 e L_*^2}\frac{\chi_0''}{|\chi\tau|^2}g_2(a,\beta), \end{aligned} \tag{144}$$

here $b_{0(1)} = \mp a + [a^2+1]^{1/2}$, $a = \frac{\alpha_B}{2|\chi\tau|}$, $\Lambda''_{1(2)} = \frac{x''_{1(2)}}{\chi''_0}$, $a_F = \frac{(|\chi'_0|+\gamma^{-2})}{|\chi\tau|}$, $a_F^{(1)} = \frac{|\chi'_0|}{|\chi\tau|}$.

The dependence of g_1 and g_2 on the parameter of deviation from the exact Bragg condition is shown in Figure 20 (a) and (b) for a LiH crystal, the (111) diffraction plane, $E = 700$ MeV, $\beta = 1$, $\omega = 3 \times 10^{-18}$ c^{-1} and the angular divergence of electrons in the beam $\Delta\Psi_\perp = 10^{-6}$ rad.

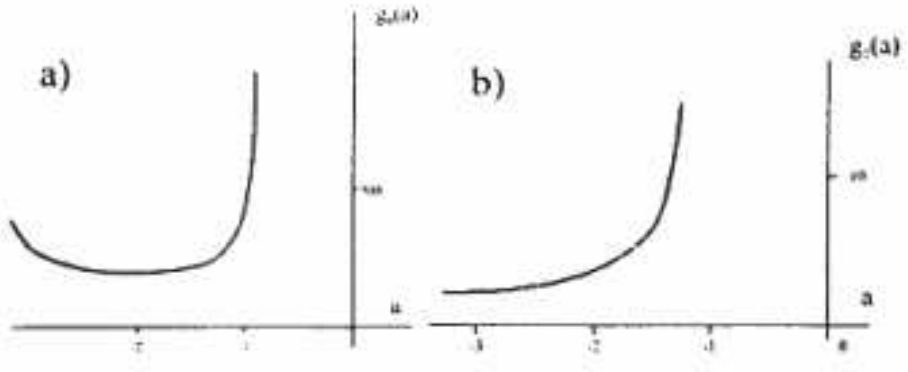

Figure 20.

From Figure 20 (a) it can be seen that $g_2(a)$ has a minimum of ~ 200 at a definite deviation parameter $a = -2$. At the same time, $g_1(a)$ does not have a definite optimal value. It depends weakly on the asymmetry factor and approaches 2 as the absolute value of the deviation parameter a increases.

A detailed comparative analysis of these figures shows that under the same conditions, the threshold current in the first case is 100 times larger than in the second case. It follows from Figure 20 (b) and (144) that

$$j_{\rm th}^{\rm opt} \simeq 2\frac{m\gamma c^3}{b^0 e L_*^2}\frac{\chi''_0}{|\chi\tau|^2}.$$

This can be explained by the fact that the growth rate of the electromagnetic field is maximum at the deviation parameter $\alpha_B/2|\chi_\tau| \sim -10$. The analysis shows that in this case the main part of radiated electromagnetic energy turns

out to be accumulated in the diffracted wave. This means that for achieving the best condition for lasing, the Bragg reflector should be placed in the direction of the diffracted wave.

Case(2). The "hot" beam limit.

The boundary condition in this case is simpler, and for the diffracted wave reflection we can obtain the dispersion equation in the form:

$$\frac{\Gamma^t}{4}\left(1-\frac{(l_0'-\beta l_1')}{[(l_0'-\beta l_1')^2+4\beta r]^{1/2}}\right)=\Gamma_{\rm th}^{(1)}, \tag{145}$$

where

$$\Gamma^t=-\sqrt{\pi}\frac{\omega_L^2}{\gamma}\frac{(l_0+\chi_0'-\gamma^{-2})(l_0+\chi_0')\sin^2\phi}{\delta_0^2}x^t\exp(-(x_t)^2),$$
$$x^t=\frac{(\omega-k'U)}{\sqrt{2}\delta_0},\quad l_0=\Theta^2-\chi_0-\gamma^{-2},\quad \delta_0=\omega\Theta\Delta\Psi_\perp, \tag{146}$$

Θ is the radiation angle, $\Delta\Psi_\perp$ is the transverse angular divergence of electron velocities in the beam.

At a small value of $(1-|\alpha|)$, when the threshold condition is determined by the radiation absorption, the relation analogous to (144) for the "cold" particle beam can be represented as: $j_{\rm th}\sim Ag_3(a,\,\beta)$, where a is the function similar to that in (144). It weakly depends on the asymmetry factor, the particle energy, and the crystal parameters. The dependence of g_3 on the deviation parameter a is shown in Figure 21.

We can see that in this case there is an optimal value of α_B at which the magnitude of g_3 is minimum. At the same parameters as in the case of a "cold" particle beam and at $\Delta\Psi_\perp=5\cdot10^{-6}$ rad $j_{\rm th}=2\cdot10^9$ A/cm^2.

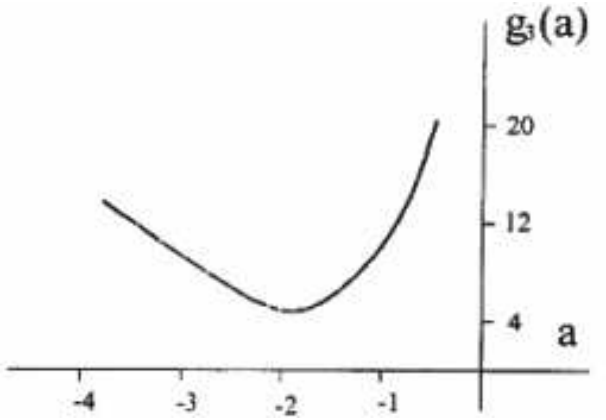

Figure 21.

So, from the above analysis we can conclude that the application of external Bragg reflectors allows one to lower the threshold electron beam current density of the electron beam necessary for achieving lasing in the X-ray spectral range by more than a factor of ten. The best situation is realized when the Bragg reflector is placed in the direction of the diffracted wave. In this case the value of the starting beam current can be $j_{\rm th} \simeq 2 \cdot 10^9$ A/c for the "hot" particle beam and $j_{\rm th} \simeq 10^8$ A/c for the "cold" particle beam and the generation frequency $\omega \simeq 3 \cdot 10^{18}$ c^{-1} in LiH, $E = 700$ MeV, $\beta = 1$ and $L_* \leq 5 \cdot 10^{-3}$ cm.

20 Theory of induced PXR in a crystal plate (general formulas) ([55])

Let an ultra-relativistic electron (positron) beam of velocity $\vec{u}$ enter, at a certain angle, a crystal plane-parallel plate with length L (the z-axis is perpendicular to the crystal surface, and the plate lies in the interval $(0 < z < L)$. The set of equations describing the interaction of an electromagnetic wave with the "crystal-beam" system consists of Maxwell's equations and those of

particle motion in the electromagnetic field. The dielectric susceptibility of a crystal has the form $\varepsilon(\vec{r};\omega) = \sum_{\vec{\tau}} \varepsilon_\tau(\omega) \exp(-i\vec{\tau}\vec{r})$, where $\vec{\tau}$ is the reciprocal lattice vector. Perturbations of the current density and charge density in the linear field approximation may be written in the form:

$$\begin{aligned}
&\delta\vec{j}(\vec{k};\omega) = e\sum_\alpha \exp(-i\vec{k}\vec{r}_{\alpha 0}) \left\{\delta\vec{v}_\alpha(\omega - \vec{k}\vec{u})\right. \\
&\left. -i\vec{u}[\vec{k}\delta\vec{r}_\alpha(\omega - \vec{k}\vec{u})]\right\} \delta n(\vec{k};\omega) \qquad (147)\\
&= e\sum_\alpha \exp(-i\vec{k}\delta\vec{r}_{\alpha 0}) \left\{-i[\vec{k}\vec{r}_\alpha(\omega - \vec{k}\vec{u})]\right\},
\end{aligned}$$

where $\delta\vec{j}(\vec{k};\omega)$ and $\delta n(\vec{k};\omega)$ are the Fourier transformations of the expressions

$$\begin{aligned}
\vec{j}(\vec{r};t) &= e\sum_\alpha \vec{v}_\alpha(t)\delta[\vec{r} - \vec{r}_\alpha(t)] \\
n(\vec{r};t) &= \sum_\alpha \delta[\vec{r} - \vec{r}_\alpha(t)].
\end{aligned}$$

$\vec{u}$ is the unperturbed electron (positron) velocity; $\delta\vec{v}_\alpha$ and $\delta\vec{r}_\alpha$ are perturbations of the velocity and radius vectors, respectively, due to the interaction with the radiation field:

$$\begin{aligned}
\vec{v}_\alpha(t) &= \vec{u} + \delta\vec{v}_\alpha(t) \\
\vec{r}_\alpha(t) &= \vec{r}_{\alpha 0} + \vec{u}t + \delta\vec{r}_\alpha(t).
\end{aligned}$$

The subscript α denotes the number of the particle.

Deriving the perturbations of velocity and radius vectors by the particle motion equation and using (147) for the current density, one can obtain a set of Maxwell's equations, which describes the interaction of an electromagnetic wave with a crystal, and a particle beam penetrating through it, in the following form:

$$k_\tau^2\vec{E}(\vec{k}_{\tau'},\omega) - \vec{k}_{\tau'}[\vec{k}_{\tau'}\vec{E}(\vec{k}_{\tau'},\omega)] - \frac{\omega^2}{c^2}\sum_\tau \varepsilon_\tau(\vec{k}_{\tau'},\vec{\omega})\vec{E}(\vec{k}_{\tau+\tau'},\omega)$$

$$= -\frac{\omega_L^2}{\gamma c^2}\vec{E}(\vec{k}_{\tau'},\omega) - \left(\frac{\omega_L^2\vec{k}_{\tau'}}{\gamma c^2(\omega-\vec{k}_{\tau'}\vec{u})} + \frac{\omega_L^2(\vec{k}_{\tau'}C^2-\omega^2)}{\gamma C^4(\omega-\vec{k}_{\tau'}\vec{u})^2}\right) \tag{148}$$
$$\times\left[(\vec{u}\vec{E}(\vec{k}_{\tau'},\omega)) - \left(\frac{\omega_L^2\vec{u}}{\gamma c^2(\omega-\vec{k}_{\tau'}\vec{u})}\right)(\vec{k}_{\tau'}\vec{E}(\vec{k}_{\tau'},\omega))\right],$$

$\vec{\tau}' = 0, \vec{\tau}_1, \vec{\tau}_2, \ldots$.

The set of equations (148) describes the situation when a distributed feedback is formed by many diffracted waves (it is the analogy of the case of multi-wave X-ray diffraction in crystals [3]). However, the analysis of such a general situation is very complicated. So we only consider here a two-wave distributed feedback. This allows us to obtain all the main characteristics of X-ray FELs analytically and also to show the advantages of three-dimensional geometry of distributed feedback in comparison with the one-dimensional case.

So, let us consider specifically the generation of a σ-polarized wave, i.e., the wave polarized in the diffraction plane. For the geometry of the so-called two-beam diffraction [190], where two strong waves are excited and diffraction occurs by the set of crystallographic planes, determined by a reciprocal lattice vector. In this case one can obtain a set of Maxwell's equations describing two-wave diffraction in a crystal, having a beam penetrating through it, in the following way:

$$\left(k^2c^2 - \omega^2\varepsilon_0 + \frac{\omega_L^2}{\gamma} + \frac{\omega_L^2}{\gamma}\frac{(\vec{u}\vec{e}'_\sigma)^2}{c^2}\frac{k^2c^2-\omega^2}{(\omega-\vec{k}\vec{u})^2}\right)E_\sigma - \omega^2\varepsilon_\tau E_\sigma^\tau = 0$$
$$-\omega^2\varepsilon_{-\tau}E_\sigma + \left(K_r^2c^2 - \omega^2\varepsilon_0 + \frac{\omega_L^2}{\gamma} + \frac{\omega_L^2}{\gamma}\frac{(\vec{u}\vec{e}_\sigma)^2}{e^2}\frac{k_\tau^2c^2-\omega^2}{(\omega-\vec{k}_\tau\vec{u})^2}\right)\vec{E}_\sigma^\tau = 0. \tag{149}$$

In (149) $E_\sigma = \vec{E}(\vec{k},\omega)\cdot\vec{e}_\sigma$, $E_\sigma^\tau = \vec{E}(\vec{k}+\vec{\tau},\omega)\cdot\vec{e}_\sigma$, $\vec{e}\parallel[\vec{k}\vec{\tau}]$, $\omega_L^2 = 4\pi e^2 n_0/m$, where n_0 is the average electron (positron) density in a beam. Comparing

(149) with the standard equation of X-ray dynamical diffraction, one can see that the system of a crystal and particle beam may be considered as an active medium with dielectric susceptibility:

$$\tilde{\varepsilon}_0(\vec{k},\omega) - 1 = \varepsilon_0 - 1 - \frac{\omega_L^2}{\gamma\omega^2} - \frac{\omega^2 - L}{\gamma\omega^2}\frac{(\vec{u}\vec{e}_\sigma)^2}{c^2}\frac{k^2c^2 - \omega^2}{(\omega - \vec{k}\vec{u})^2},\ \tilde{\varepsilon}_{\tilde{\tau}} = \varepsilon_\tau$$

$$\tilde{\varepsilon}_0(\vec{k}_\tau,\omega) - 1 = \varepsilon_0 - 1 - \frac{\omega_L^2}{\gamma\omega^2} - \frac{\omega_L^2}{\gamma\omega^2}\frac{(\vec{u}\vec{e}_\sigma)^2}{c^2}\frac{\vec{k}_\tau^2c^2 - \omega^2}{(\omega - \vec{k}_\tau\vec{u})^2},\ \tilde{\varepsilon}_{-\tau} = \varepsilon_{-\tau}$$

Further, we shall analyze the generation of the wave with a wave vector $\vec{k}$, which makes a small angle with the particle velocity vector $\vec{u}$. In this case the wave vector $\vec{k}_\tau = \vec{k} + \vec{\tau}$ is directed at a large angle relative to $\vec{u}$, and consequently the magnitude of $(\omega - \vec{k}_\tau\vec{u})$ cannot become small. As a result, the terms containing the expression $(\omega - \vec{k}_\tau\vec{u})$ in their denominators will be small and can be ignored. We shall also neglect the term ω_L^2/γ – this is justified for real beam densities. It is well known that in order to provide non-zero solutions for the equation set (149), its determinant should be equal to zero. This also defines the dispersion equation, and for the σ-polarized wave it can be written in the form:

$$(\omega - \vec{k}\vec{u})^2\left[(k^2c^2 - \omega^2\varepsilon_0)(k_\tau^2c^2 - \omega^2\varepsilon_0) - \omega^4\varepsilon_\tau\varepsilon_{-\tau}\right] = -\frac{\omega_L^2}{\gamma}\frac{(\vec{u}\vec{e}_\sigma)^2}{c^2}(k^2c^2 - \omega^2)(k_\tau^2c^2 - \omega^2\varepsilon_0). \tag{150}$$

The dispersion equation in such a form was derived in [51]. To solve the boundary problem, we use field continuity, the beam density and the beam current density at the boundaries. For the last two conditions we apply the following expressions, obtained from the equations of particle motion and the expression for the particle beam current

$$\delta j_\sigma = \frac{ie^2 n_0}{m\gamma\omega}\frac{(\vec{u}\vec{e}_\sigma)^2}{c^2}\frac{k^2c^2-\omega^2}{(\omega-\vec{k}\vec{u})^2}E_\sigma$$
$$j_\sigma = e(\vec{u}\vec{e}_\sigma)n_0 - \frac{ie^2 n_0}{m\gamma}\frac{(\vec{u}\vec{e}_\sigma)^2}{c^2(\omega-\vec{k}\vec{u})}E_\sigma. \qquad (151)$$

The dispersion equation (150) is sixth-order and, hence six solutions correspond to it. However, the two solutions corresponding to mirror reflected waves can be neglected due to the small value of $\varepsilon_\tau(\omega)$ in the X-ray range, $\varepsilon_0 - 1 \equiv g_0$; $\varepsilon_\tau \sim 10^{-5}$. Small values of ε_τ and g_0 will also be utilized when performing joining (we only join electric field strengths at boundaries).

The general solution for the field in a crystal is written as

$$\vec{E} = \sum_{i=1}^{4} \vec{e}_\sigma c_i \exp(i\vec{k_i}\vec{r})[1 + s_i \exp(i\vec{\tau}\vec{r})], \qquad (152)$$

where $\vec{k}_i$ is the i-th solution of the dispersion equation (150) and $\vec{k}_{i\tau} = \vec{k}_i + \vec{\tau}$; $\vec{\tau}$ is the reciprocal lattice vector corresponding to the planes of diffraction reflection.

Taking into account the remarks made, the boundary conditions may be written as:

$$\begin{aligned}
&c_1 + c_2 + c_3 + c_4 = 1,\\
&f_1c_1 + f_2c_2 + f_3c_3 + f_4c_4 = 0,\\
&g_1c_1 + g_2c_2 + g_3c_3 + g_4c_4 = 0,\\
&s_1c_1e^{iK_{1z}L} + s_2c_2e^{iK_{2z}L} + s_3c_3e^{iK_{3z}L} + s_4c_4e^{iK_{4z}L} = 0,\\
&s_i = \frac{\omega^2\varepsilon_{-\tau}}{k_{i_\tau}^2c^2 - \omega^2\varepsilon_0}, \qquad f_i = \frac{(\vec{u}\vec{e}_\sigma)^2}{(\omega-\vec{k}_i\vec{u})}, \qquad g_i = \frac{k_i^2c^2-\omega^2}{(\omega-\vec{k}_i\vec{u})^2}\frac{(\vec{u}\vec{e}_\sigma)^2}{c^2}.
\end{aligned} \qquad (153)$$

In (153), only those boundary conditions are written that determine the field inside a crystal. The first equation corresponds to the continuity of an incident wave at the boundary $z = 0$; the second and the third conditions correspond to vanishing of the beam density and the beam current density at the crystal

entrance. The last condition corresponds to the vanishing of the diffracted wave at the exit boundary $z = L$ (we consider Bragg diffraction geometry), $\vec{k}_i$ and k_{iz} ($i = 1 \div 4$) are the solutions of the dispersion equation (150). The linear system (153), defining the coefficients c_i placed ahead of i-modes in (152), has the solution $c_i = \Delta_i/\Delta$, where Δ is the determinant of the system (153), Δ_i is the i-th minor, obtained as a result of replacement of the i-th column by

$$\begin{pmatrix} 1 \\ 0 \\ 0 \\ 0 \end{pmatrix}.$$

Hence, at $\Delta \to 0$, the field amplitudes inside a crystal will increase, and thus a condition occurs when the field is nonzero though the incident wave is equal to zero. The condition $\Delta = 0$ with $\Delta_i \neq 0$ is called the generation threshold condition [116]. Substituting the expressions

$$\begin{aligned} &\vec{k}_i = \vec{k}_0 + \vec{k}\delta_i\vec{n}, \qquad k_{0z} = \frac{\omega - \vec{k}_\perp\vec{u}_\perp}{u_z}, \\ &k = \omega/c, \qquad \delta_i \ll 1, \end{aligned} \tag{154}$$

(where $\vec{n}$ is the normal to the crystal surface, $\vec{k}_0 = (k_{0z}, \vec{k}_\perp)$) into the determinant Δ, we can represent the generation threshold condition $\Delta = 0$ as

$$\begin{aligned} &\frac{(\delta_1-\delta_2)(\delta_1-\delta_3)(\delta_2-\delta_3)}{\delta_1^2\delta_2^2\delta_3^2}s_4e^{ik\delta_4L} - \frac{(\delta_1-\delta_2)(\delta_1-\delta_4)(\delta_2-\delta_4)}{\delta_1^2\delta_2^2\delta_4^2}s_3e^{ik\delta_3L} \\ &+\frac{(\delta_1-\delta_3)(\delta_1-\delta_4)(\delta_3-\delta_4)}{\delta_1^2\delta_3^2\delta_4^2}s_2e^{ik\delta_2L} - \frac{(\delta_2-\delta_3)(\delta_2-\delta_4)(\delta_3-\delta_4)}{\delta_2^2\delta_3^2\delta_4^2}s_1e^{ik\delta_1L} = 0 \end{aligned} \tag{155}$$

In (155), the terms containing nonresonance f_i and g_i $(i = 1 \div 4)$ were neglected.

Further investigation will be based on a common consideration of (150) and (155). We substitute (154) into (150) and transform the dispersion equation as follows:

$$\frac{(\vec{u}\vec{n})^2}{c^2}\delta^2[4\gamma_0\gamma_1\delta^2 + 2(\gamma_1 l + \gamma_0 l_\tau)\delta + l l_\tau - \tau] = \\ -\frac{1}{\gamma}\left(\frac{\omega_L}{\omega}\right)^2 \theta^2 \sin^2\varphi(l + g_0)l_\tau. \qquad (156)$$

In (156) θ is the angle between $\vec{k}$ and $\vec{u}$; φ is the angle between $\vec{k}_{\perp_u}$ and $\vec{\tau}_{\perp_u}$, where the symbol $\perp_u$ denotes the projection onto a plane perpendicular to the velocity, $r = \varepsilon_\tau\varepsilon_{-\tau}$; $l = \theta^2 + g_0 + \gamma^{-2}$; $l_\tau = l + \alpha$; $\alpha = (2\vec{k}_0\vec{\tau} + \tau^2)/k^2$ is the departure from the Bragg condition.

$$\gamma_0 = \frac{(\vec{k}_0\vec{n})}{K}, \qquad \gamma_1 = -\frac{(\vec{k}_{0\tau}\vec{n})}{K}$$

are the cosines of the angles, made by the wave vectors of the transmitted and diffracted waves with the normal vector.

21 Spontaneous and induced parametric and Smith-Purcell radiation from electrons moving in a photonic crystal built from the metal threads ([117])

Research and development of microwave generators using radiation from an electron beam in a periodic slow-wave circuit (traveling wave tubes, backward wave oscillators, etc.,) has a long history [69,70]. First generators operated in the centimeter wavelength range.

In 1953 Smith and Purcell [71] made the next step and observed generation of incoherent radiation at visible wavelengths by using a finely-focused electron beam propagating close to the surface of a metal diffraction grating (at the distance $\delta \leq \frac{\lambda\beta\gamma}{4\pi}$, δ is the so-called beam impact parameter, λ is the radiation wavelength, $\beta = v/c$, v is the electron beam velocity, γ is the electron Lorentz-factor). Beam current densities were insufficient to produce significant amplification of the spontaneous emission. However, as it was shown in [72,73], to change this spontaneous radiation process into a stimulated one, the generator should be supplied with a feedback cavity formed by a pair of reflectors.

After the discovery of the Smith-Purcell effect, it soon became clear that it might be used as a radiation source in the millimeter to visible range, for which tunable sources were hardly or not available at that time [74,75].

The Smith-Purcell effect belongs to the general class of diffracted radiation effects induced by electron interaction with a medium. Diffraction of waves associated with the electromagnetic field of the electron by an obstacle leads to the so-called diffracted radiation [76]. Diffracted radiation in periodical structures is in the basis of operation of traveling wave tubes [69,70] and such devices as the orotron [77,78,79] and the ledatron [80] (see also [81,82,83,84]).

All the above devices use feedback, which is formed by either two parallel mirrors placed on both sides of the working area or a one-dimensional diffraction grating, in which incident and diffracted (reflected) waves move along the electron beam (one-dimensional distributed feedback).

The conception of volume distributed feedback [49] was first originated in view of prediction and experimental study of spontaneous parametric and diffracted

transition X-ray radiation from charged particles in crystals (PXR) [85]. The detailed analysis of the induced PXR and channeling radiation revealed unique possibilities provided by volume distributed feedback [49]. It was shown that dynamical diffraction in a volume spatially periodic medium evokes the peculiar conditions, corresponding to degeneration of the eigenmodes that results in a new law of electron beam instability. Within these peculiar conditions the electron beam interacts with the electromagnetic wave more effectively [49].

Thus, for example, even in the X-ray range the electron beam current density necessary for running up to the generation threshold in conditions of non-one-dimensional distributed feedback [49,25] appears significantly reduced (10^8 A/cm^2 for LiH crystal against 10^{13} A/cm^2 required in [86]) that even makes possible to reach generation threshold for the induced X-ray radiation in crystals i.e. to create an X-ray laser.

Moreover, all the conclusions are valid for a beam moving in vacuum close to the surface of the periodic medium either in the presence or absence of the undulator [25].

The originated law is universal and valid for all wavelength ranges (from X-ray to microwave) regardless the spontaneous radiation mechanism [25,49,55,87,88,105,110,181,182]. Radiation generators using non-one-dimensional distributed feedback, which is created with the aid of either natural or artificial (photonic) crystals, is called Volume Free Electron Laser (VFEL).

Use of the volume distributed feedback makes available:

1. frequency tuning at fixed energy of the electron beam in the significantly wider range than conventional systems can provide;

2. significant reduction of the threshold current of the electron beam due to more effective interaction of the electron beam with the electromagnetic wave allows and, as a result, miniaturization of generators;

3. reduction of limits for the available output power by the use of wide electron beams and diffraction gratings (photonic crystals) of large volumes;

4. simultaneous generation at several frequencies;

5. effective modes selection in oversize systems, in which the radiation wavelength is significantly smaller than the resonator dimensions.

Studies of the two-dimensional distributed feedback application in millimeter-wave FEL-oscillators began in the 90s in [94,95,96,97,98].

One of the VFEL types uses a "grid" volume resonator ("grid" photonic crystal) that is formed by a periodic structure built from either dielectric or metal threads (see Figure 22) [89,110,112].

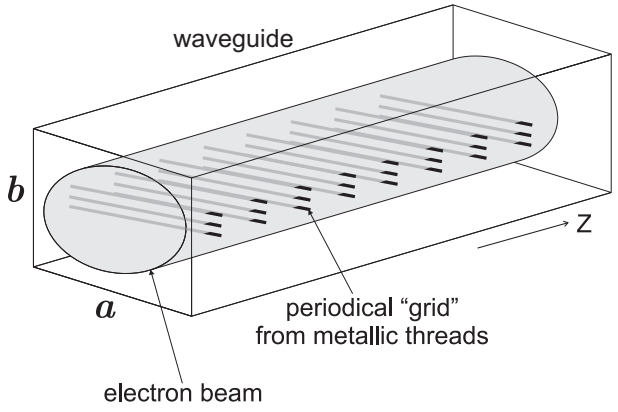

Figure 22. VFEL "grid" resonator ("grid" photonic crystal)

The "grid" structure formed by periodically strained dielectric threads was experimentally studied in [110], where it was shown that "grid" photonic crystals have sufficiently high Q factors ($10^4 - 10^6$). Lasing from VFELs with the "grid"

resonator formed by periodically strained metal threads was observed in [112].

Propagation of waves through a photonic crystal is the subject of numerous theoretical and experimental studies [90,91,92,93].

In [117] the properties of a "grid" photonic crystal built from metal threads were considered along with its frequency characteristics in view of their importance for VFEL lasing. A challenge, which appears when considering interaction of an electromagnetic wave with such a photonic crystal, is as follows. In contrast to the case of wave interaction with a thin dielectric thread, the interaction of the electromagnetic wave with a single metal thread of the "grid" (i.e., the diffraction grating unit cell) cannot be described in terms of the perturbation theory.

The approach developed in [117] provides the description of diffraction in a "grid" grating in terms of the amplitude of the wave scattering by a single thread. Methods for calculation of scattering amplitudes are well-developed [100,101]. This approach enables developing the theory of diffraction in a "grid" photonic crystal similar to the dynamical theory of diffraction for X-rays [3,15] and using the results obtained therein. The equations describing lasing of VFEL with such a resonator have been obtained.

22 Scattering by a set of metal threads in free space

Suppose a plane electromagnetic wave $\vec{E} = \Psi_0 \vec{e} = e^{i\vec{k}\vec{r}}\vec{e}$ falls onto a metal thread. Here $\vec{e}$ is the polarization vector of the wave, $\vec{k}$ is the wavevector, $\vec{r}$ is the coordinate. Suppose the wave falls perpendicular to the cylinder axis i.e. along OZ. The metal thread looks like a cylinder placed into the origin of

coordinates and the cylinder axis coincides with the axis x Figure (23).

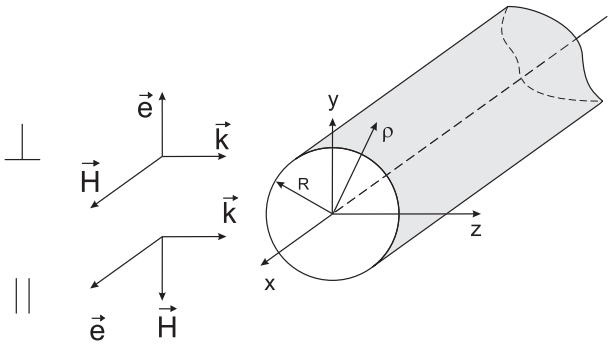

Figure 23. Coordinates and vectors

Two orientations of $\vec{e}$ should be considered: $\vec{e}$ is parallel to the cylinder axis x and $\vec{e}$ is perpendicular to the cylinder axis x. The solution of the problem of the wave scattered by a cylinder is well-known [100,101]. Below the case when the radiation wavelength λ exceeds the thread radius R ($\lambda \gg R$) is considered.

For clarity, suppose that $\vec{e} \parallel 0x$. In this case the expression, which describes the wave appearing due to scattering, can be expressed as a superposition of the incident Ψ_0 and scattered Ψ_{sc} waves as follows [100,101]:

$$\Psi = \Psi_0 + \Psi_{sc} = e^{ikz} + a_0 H_0^{(1)}(k\rho), \tag{157}$$

here ρ is the transverse coordinate $\rho = (y, z)$, $H_0^{(1)}$ is the Hankel function of zero order, k is the wave number, a_0 is the amplitude of the scattered wave.

$$a_{0(\parallel)} = \frac{-J_0(k_t R)J_0'(kR) + \sqrt{\varepsilon_t}J_0'(k_t R)J_0(kR)}{J_0(k_t R)H_0^{(1)\prime}(kR) - \sqrt{\varepsilon_t}J_0'(k_t R)H_0^{(1)}(kR)}\ , \tag{158}$$

$$a_{0(\perp)} = \frac{-J_0(k_t R)J_0'(kR) + \frac{1}{\sqrt{\varepsilon_t}}J_0'(k_t R)J_0(kR)}{J_0(k_t R)H_0^{(1)\prime}(kR) - \frac{1}{\sqrt{\varepsilon_t}}J_0'(k_t R)H_0^{(1)}(kR)}\ , \tag{159}$$

where ε_t is the dielectric permittivity of the thread material, $k_t = \sqrt{\varepsilon_t}k$. Note that for $\lambda \gg R$ the amplitude a_0 does not depend on the scattering angle.

Let us now consider a wave, which is scattered by a set of threads placed at the points with the coordinates $\rho_n = (y_n, z_n)$. The scattered wave can be expressed as a superposition of waves scattered by separate threads:

$$\Psi = e^{ikz} + a_0 \Sigma_n H_0^{(1)}(k\,|\vec{\rho} - \vec{\rho}_n|) e^{ikz_n} \tag{160}$$

or, using the integral representation for the Hankel function, $H_0^{(1)}(k\rho)$

$$\Psi = e^{ikz} + A_0 \Sigma_n \int\limits_{-\infty}^{\infty} \frac{e^{ik\sqrt{|\vec{\rho}-\vec{\rho}_n|^2 - x^2}}}{\sqrt{|\vec{\rho} - \vec{\rho}_n|^2 - x^2}} dx e^{ikz_n}, \tag{161}$$

where $A_0 = -\frac{ia_0}{\pi}$, $|\vec{\rho} - \vec{\rho}_n|^2 = (y - y_n)^2 + (z - z_n)^2$.

Note that in (161) we neglected the contributions from rescattered waves.

Let us consider a wave passing through a layer of cylinders whose axes are distributed in the plane $x0y$ with the distance d_y between them. Suppose that the transversal size of the layer $L_\perp$ is much larger than both d_y and the radiation wavelength ($L_\perp \gg d_y$ and $L_\perp \gg \lambda$). This assumption enables considering the ideal case when the layer is supposed to have an infinite size in the plane $x0y$. In this case summation over the coordinates y_n provides the following expression for Ψ:

$$\Psi = e^{ikz} + \frac{2\pi i A_0}{k d_y} e^{ikz} = (1 + \frac{2\pi i A_0}{k d_y}) e^{ikz}. \tag{162}$$

This expression reflects a well-known fact that a plane wave scattered by a plane layer of the scatterers is expressed as a plane wave with the modified amplitude.

Thus, after passing m planes spaced d_z apart from each other, the scattered

wave can be expressed as:

$$\Psi = \left(\sqrt{\left(1 - \frac{2\pi \ \mathrm{Im}A_0}{k \ d_y}\right)^2 + \left(\frac{2\pi \ \mathrm{Re}A_0}{k \ d_y}\right)^2} \right)^m e^{i\varphi m} e^{ikz}, \tag{163}$$

where

$$\varphi = \mathrm{arctg} \left(\frac{\frac{2\pi \ \mathrm{Re}A_0}{k \ d_y}}{1 - \frac{2\pi \ \mathrm{Im}A_0}{k \ d_y}} \right),$$

$m = L_z/d_z$ inside the photonic crystal formed by threads and L_z is the length of the photonic crystal. This expression can be easily converted to the form $\Psi = e^{iknz}$, where n is the index refraction defined as

$$\begin{aligned} n = n' + in'' = \left(1 + \tfrac{\lambda}{2\pi d_z} \arctan\left(\frac{\frac{\lambda}{d_y}\mathrm{Re}A_0}{1 - \frac{\lambda}{d_y}\mathrm{Im}A_0}\right)\right) - \\ -i\tfrac{\lambda}{2\pi d_z} \ln\left(\sqrt{\left(\tfrac{\lambda}{d_y}\mathrm{Re}A_0\right)^2 + \left(1 - \tfrac{\lambda}{d_y}\mathrm{Im}A_0\right)^2}\right), \end{aligned} \tag{164}$$

here $\lambda = 2\pi/k$ is used, n' and n'' denotes the real and imaginary parts of n, respectively, $\mathrm{Re}A_0$ and $\mathrm{Im}A_0$ are the real and imaginary parts of A_0.

Let us consider now the parameter $|\frac{\lambda}{d_y}A_0|$ and suppose it to be small. When $|\frac{\lambda}{d_y}A_0| \ll 1$, (164) can be rewritten as:

$$n = 1 + \frac{2\pi}{d_y d_z k^2} A_0. \tag{165}$$

The same expression can also be obtained for the index of refraction of the wave with polarization orthogonal to the thread axis ($\vec{e} \perp 0x$).

When the parameter $|\frac{\lambda}{d_y}A_0|$ grows with the growth of the density of scatterers (i.e., with decreasing d_y), the rescattered waves become important and the difference between the mean and local fields should be considered similarly to

Clausius-Mossoti (Lorentz-Lorenz) relation [99]. Calculations show that the parameter $|\frac{\lambda}{d_y}A_0|$ behaves differently for different polarizations (see Figure 24) and for the wave with polarization parallel to the threads, this parameter can appear greater than 1. In this case formula (165) for parallel polarization is not valid and the expressions considering wave rescattering should be applied (see [117]).

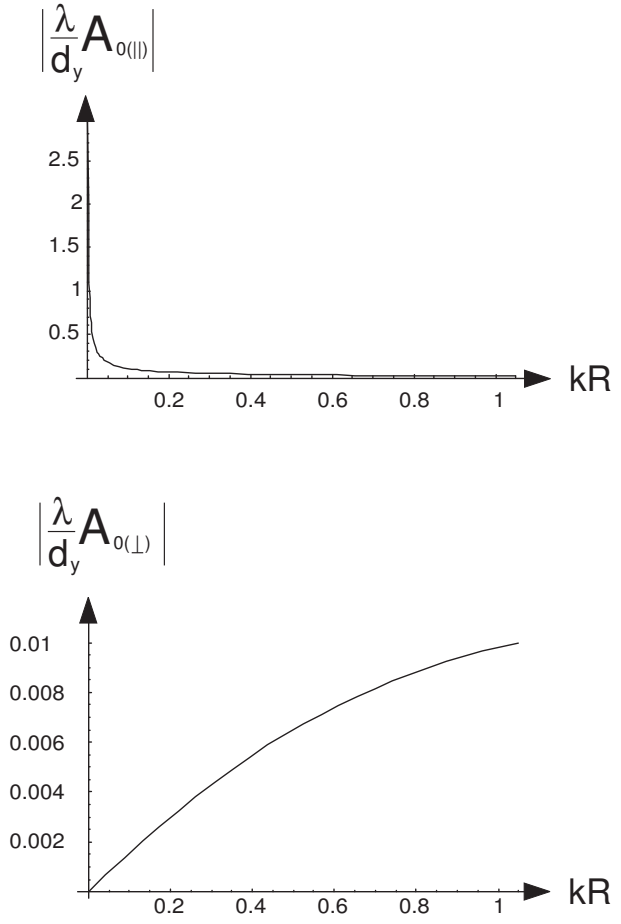

Figure 24. Dependence of parameter $|\frac{\lambda}{d_y}A_0|$ on kR for parallel and orthogonal polarizations ($d_y = 0.5$ cm, $d_z = 1.6$ cm)

It is important to remind that the conception of the refraction index is applicable even to considering waves of different types (X-rays, particles) passing through matter when the distance between scatterers exceeds many times the wavelength, i.e., $kd \gg 1$ [1]. At that, if the wavelength is either comparable or

smaller than the size of the scatterer, then the refraction index is determined by the amplitude of the wave scattering at zero angle. In the considered case of the wave scattering by the thread the amplitude A_0 in (165) should be replaced by the amplitude of forward scattering of the wave by the thread. The explicit expression for this amplitude see in [100,101].

Radiation wavelengths of our interest are $\lambda \leq 3$ cm. In this wavelength range, the skin depth δ is about 1 micron for most metals (for example, $\delta_{Cu} = 0.66$ μm, $\delta_{Al} = 0.8$ μm, $\delta_W = 1.16$ μm, and so on). Thus, in this wavelength range the metal threads can be considered as perfectly conducting.

From (158), (159) follows that the amplitude A_0 for a perfect conducting cylinder for polarization of the electromagnetic wave parallel to the cylinder axis can be expressed as:

$$A_{0(\|)} = \frac{1}{\pi}\frac{J_0(kR)\,N_0(kR)}{J_0^2(kR)+N_0^2(kR)} + i\frac{1}{\pi}\frac{J_0^2(kR)}{J_0^2(kR)+N_0^2(kR)}\ . \tag{166}$$

Using the asymptotic values for these functions for $kR = \frac{2\pi R}{\lambda} \ll 1$

$$\begin{aligned} &J_0(x\to 0)\approx 1,\ N_0(x\to 0)\approx -\tfrac{2}{\pi}\ln\tfrac{2}{1.781\cdot x}, \\ &J_0'(x\to 0) = -J_1 \approx -\tfrac{x}{2},\ N_0'(x\to 0) = -N_1 \approx \tfrac{2}{\pi}\tfrac{1}{x}, \end{aligned} \tag{167}$$

one can obtain:

$$\mathrm{Re}A_{0(\|)} \approx -\frac{1}{\pi}\ \frac{\frac{2}{\pi}\ln(\frac{2}{1.781\cdot kR})}{1+(\ln(\frac{2}{1.781\cdot kR}))^2}\ ,\ \mathrm{Im}A_{0(\|)} \approx \frac{1}{\pi}\ \frac{1}{1+(\ln(\frac{2}{1.781\cdot kR}))^2}\ , \tag{168}$$

From (168) it can be seen that for $kR \ll 1$, the values $\mathrm{Re}A_{0(\|)} < 0$, therefore,

the real part of the index of refraction in this limit can be expressed as:

$$n'_{(\|)} = 1 - \frac{2\pi}{d_y d_z k^2} |\mathrm{Re} A_{0(\|)}|, \tag{169}$$

From (169) follows that the growth of the wavelength (reduction of k) makes $n'_{\|} \to 0$, and $n'_{\|}$ can even become negative. However, it should be reminded that (169) is valid only when $|n'_{\|} - 1| \ll 1$ (i.e $\frac{2\pi}{d_y d_z k^2} |\mathrm{Re} A_{0(\|)}| \ll 1$). It is interesting to compare $n'_{\|}$ calculated by formulas (164) and (169): in the range of large wavelength they yield different results because the condition $|n'_{\|} - 1| \ll 1$ is violated. In this case the expressions given in [117] should be applied. Note also that $n'_{\|} = 0$ corresponds to the threshold of the wave total reflection from the medium surface.

Let us consider a particular example: suppose the radiation wavelength is $\lambda = 3$ cm and the thread radius $R = 50$ μm, then

$$ReA_{0(\|)} = -0.096, \; ImA_{0(\|)} = 0.032, \tag{170}$$

Suppose $d_y = 0.5$ cm, $d_z = 1.6$ cm, therefore, the parameter $|\frac{\lambda}{d_y} A_0| \ll 1$ for both polarizations and (165) gives:

$$n_{\|} = 0.828 + i \cdot 0.058, \tag{171}$$

The above analysis does not include the contribution to the index of refraction from rescattered waves. Their contribution was investigated in [89,103,112,117,152,165]. It was shown, in particular, that the the index of refraction $n_{\perp}$ for a wave with the polarization vector orthogonal to the threads can be greater than unity, i.e., in such photonic crystals, the Cherenkov effect is possible.

23 Complex anomalous Doppler effect in the "grid" photonic crystal

Let us now study Smith - Purcell (diffracted) radiation in a photonic crystal when an electron beam of velocity $\vec{v}$ passes through the "grid".

The radiation condition can be expressed as

$$\omega - \vec{k}n(k)\vec{v} = \vec{\tau}\vec{v} \ , \tag{172}$$

where $\vec{\tau}$ is the reciprocal lattice vector and $n(k)$ is the index of refraction. Suppose the electron beam velocity is directed along the axis OZ, then (172) can be presented in the form:

$$k - \tau_z\beta = k\, n(k)\, \beta \cos\theta, \tag{173}$$

where $\beta = \frac{v}{c}$, the angle between $\vec{k}$ and the electron beam velocity is denoted by θ and $\tau_z = \frac{2\pi m_h}{d_z}$, where $m_h = 1, 2, ...$ is the harmonic number. From (173) follows the equation

$$(\frac{k - \tau_z\beta}{\beta\cos\theta})^2 = k^2 + \eta \ , \tag{174}$$

which is similar to the equation for the complex and anomalous Doppler effect [18].

The roots of this equation give the spectrum of frequencies of diffracted (Smith-Purcell) radiation, which is induced by a particle moving in the above volume "grid" structure. In the case under consideration $\frac{\eta}{\tau_z^2} \ll 1$. For β providing $\frac{\eta}{\tau_z^2\beta^2} \ll 1$, the roots of (174) can be easily found:

$$k_1 = \frac{\tau_z \beta}{1-(\beta\cos\theta)^2}\left(1-\beta\cos\theta\sqrt{1+\frac{\eta}{\tau_z^2}\frac{1-(\beta\cos\theta)^2}{\beta^2}}\right),$$
$$k_2 = \frac{\tau_z \beta}{1-(\beta\cos\theta)^2}\left(1+\beta\cos\theta\sqrt{1+\frac{\eta}{\tau_z^2}\frac{1-(\beta\cos\theta)^2}{\beta^2}}\right), \quad (175)$$

where η is taken at $k = \frac{\tau_z \beta}{1-(\beta\cos\theta)^2}$.

It should be reminded here that $\tau_z = \frac{2\pi m_h}{d_z}$, where $m_h = 1, 2, ...$ is the harmonic number. From (176) follows that higher harmonics provide getting radiation with higher frequencies. For example, for the electron beam with the energy 200 keV, considering $\theta \sim 20^\circ$ and $d_z = 1.6$ cm, the first harmonic ($m_h = 1$) gives radiation frequencies ~ 10 GHz and ~ 40 GHz for the roots 1 and 2 of equation (173), respectively, the 30-th harmonic ($m_h = 30$) provides ~ 230 GHz and ~ 1 THz.

Let us now study diffracted radiation in a metal waveguide of rectangular cross-section with the "grid" structure ("grid" photonic crystal) placed inside it (see Figure 22). Suppose that the lateral dimensions a and b of the waveguide noticeably exceed the distance between the next threads of the "grid" photonic crystal ($a, b \gg d_y, d_z$). This makes possible to consider a waveguide with the "grid" photonic crystal inside as a waveguide filled with matter with the effective dielectric permittivity $\varepsilon = n^2$.

Remember that in the waveguide with the axis parallel to OZ, the x and y components of the wavevector are not continuous, but quantized. And only the wavenumber k_z changes continuously. The wave field inside the waveguide represents a wave standing in the transversal directions (OX and OY), but traveling along OZ.

In the waveguide there is the discrete set of the waves with the eigenvalues κ_{mn} determined by the waveguide transverse dimensions (width a and height b) [16,100,101]

$$\kappa_{mn}^2 = (\frac{\pi m}{a})^2 + (\frac{\pi n}{b})^2 \ . \tag{176}$$

Therefore, in the waveguide the radiation frequency ω is related to the wavenumber k_z as follows [16]:

$$k_z^2(m,n) = (\frac{\omega}{c})^2 \varepsilon - \kappa_{mn}^2 \ . \tag{177}$$

Remembering that $n^2 = \varepsilon = 1 + \chi$ (ε is the permittivity of the "medium" formed by the metal threads and χ is its susceptibility) one can rewrite (177) as follows:

$$k_z^2(m,n) = (\frac{\omega}{c})^2 - (\kappa_{mn}^2 - \eta) \ , \tag{178}$$

here $\eta = \frac{\omega^2}{c^2}\chi$. According to the previous section $n < 1$, therefore both χ and η are negative.

Therefore, addition of the described volume structure to the waveguide "replaces" their own eigenvalues by some effective K_{mn} ($K_{mn}^2 = \kappa_{mn}^2 - \eta$). It is interesting to note here that, as $\eta < 0$, the addition of the volume grid to the waveguide increases the waveguide limiting frequency (i.e., the effective waveguide appears as though having smaller transversal dimensions).

Let us now consider the spontaneous Smith-Purcell radiation from a particle moving along the waveguide axis. The radiation condition for the Smith-

Purcell radiation (172) converts to

$$\omega - k_z v = \tau_z v \ . \tag{179}$$

Combination of (178) and (179) enables one to find the equation for radiation frequencies similar to (174):

$$(\frac{\omega - \tau_z v}{v})^2 = (\frac{\omega}{c})^2 - (\kappa_{mn}^2 - \eta) \ . \tag{180}$$

The roots of this equation for $\frac{\eta}{\tau_z^2 \beta^2} \ll 1$ can be obtained similarly (176):

$$\begin{aligned} \omega_1 (m,n) &= \frac{\tau_z v}{1-\beta^2} \left(1 - \beta \sqrt{1 - \frac{(\kappa_{mn}^2 - \eta)}{\tau_z^2} \frac{1-\beta^2}{\beta^2}} \right) , \\ \omega_2 (m,n) &= \frac{\tau_z v}{1-\beta^2} \left(1 + \beta \sqrt{1 - \frac{(\kappa_{mn}^2 - \eta)}{\tau_z^2} \frac{1-\beta^2}{\beta^2}} \right) . \end{aligned} \tag{181}$$

For a detailed treatment of the theory of VFEL lasing using electron beam radiation in a "grid" photonic crystal, see [117].

24 Generation of radiation in Free Electron Lasers with photonic crystals (diffraction gratings) with the variable spatial period

In this section the equations providing the description of the generation process in FEL with varied parameters of a photonic crystal (diffraction grating) are obtained [152]. It is shown that applying photonic crystals (diffraction gratings) with the variable period, one can significantly increase the radiation output. It is mentioned that photonic crystals (diffraction gratings) can be used for creation of the dynamical wiggler with variable period in the system.

This makes possible to develop double-cascaded FEL with variable parameters changing, which efficiency can be significantly higher that of conventional system.

Generators using radiation from an electron beam in a periodic slow-wave circuit (traveling wave tubes, backward wave oscillators, free electron lasers) are now widespread [111].

Diffracted radiation [76] in periodical structures is in the basis of operation of traveling wave tubes (TWT) [69,70], backward wave oscillators (BWO) and such devices as Smith-Purcell lasers [71,72,73,74,75] and volume FELs using two- or three-dimensional distributed feedback [87,88,181,182].

The analysis shows that during the operation of such devices electrons lose their energy for radiation, therefore, the electron beam slows down and gets out of synchronism with the radiating wave. These limits the efficiency of the generator, which usually does not exceed $\sim 10\%$.

During the first years after the creation of the traveling wave tube, it was demonstrated [70] that synchronism between the electron beam and the electromagnetic wave in a TWT can be retained by changing the phase velocity of the wave. Application of systems with variable parameters in microwave devices significantly increases their efficiency [70,114].

The same methods are widely used for increasing the efficiency of undulator FELs [115].

24.1 Lasing equations for the system with a photonic crystal (diffraction grating) with changing parameters

In the general case the equations, which describe lasing process, follow from the Maxwell equations:

$$\begin{aligned} &\mathrm{rot}\vec{H} = \frac{1}{c}\frac{\partial \vec{D}}{\partial t} + \frac{4\pi}{c}\vec{j},\ \mathrm{rot}\vec{E} = -\frac{1}{c}\frac{\partial \vec{H}}{\partial t}, \\ &\mathrm{div}\vec{D} = 4\pi\rho,\ \frac{\partial \rho}{\partial t} + \mathrm{div}\vec{j} = 0, \end{aligned} \tag{182}$$

here $\vec{E}$ and $\vec{H}$ are the electric and magnetic fields, $\vec{j}$ and ρ are the current and charge densities, the electromagnetic induction $D_i(\vec{r},t') = \int \varepsilon_{il}(\vec{r},t-t')E_l(\vec{r},t')dt'$ and, therefore, $D_i(\vec{r},\omega) = \varepsilon_{il}(\vec{r},\omega)E_l(\vec{r},\omega)$, the indices $i,l = 1,2,3$ correspond to the axes x,y,z, respectively.

The current and charge densities are respectively defined as:

$$\vec{j}(\vec{r},t) = e\sum_{\alpha}\vec{v}_{\alpha}(t)\delta(\vec{r}-\vec{r}_{\alpha}(t)),\ \rho(\vec{r},t) = e\sum_{\alpha}\delta(\vec{r}-\vec{r}_{\alpha}(t)), \tag{183}$$

where e is the electron charge, $\vec{v}_{\alpha}$ is the velocity of the particle α (α numerates the beam particles),

$$\frac{d\vec{v}_{\alpha}}{dt} = \frac{e}{m\gamma_{\alpha}}\left\{\vec{E}(\vec{r}_{\alpha}(t),t) + \frac{1}{c}[\vec{v}_{\alpha}(t)\times\vec{H}(\vec{r}_{\alpha}(t),t)] - \frac{\vec{v}_{\alpha}}{c^2}(\vec{v}_{\alpha}(t)\vec{E}(\vec{r}_{\alpha}(t),t))\right\}, \tag{184}$$

here $\gamma_{\alpha} = (1-\frac{v_{\alpha}^2}{c^2})^{-\frac{1}{2}}$ is the Lorentz-factor, $\vec{E}(\vec{r}_{\alpha}(t),t)$ ($\vec{H}(\vec{r}_{\alpha}(t),t)$) is the electric (magnetic) field at the point of location $\vec{r}_{\alpha}$ of the particle α.

It should be reminded that (184) can also be written as [187]:

$$\frac{d\vec{p}_{\alpha}}{dt} = m\frac{d\gamma_{\alpha}v_{\alpha}}{dt} = e\left\{\vec{E}(\vec{r}_{\alpha}(t),t) + \frac{1}{c}[\vec{v}_{\alpha}(t)\times\vec{H}(\vec{r}_{\alpha}(t),t)]\right\}, \tag{185}$$

where p_α is the particle momentum.

Combining the equations in (182), we obtain:

$$-\Delta\vec{E}+\vec{\nabla}(\vec{\nabla}\vec{E})+\frac{1}{c^2}\frac{\partial^2\vec{D}}{\partial t^2}=-\frac{4\pi}{c^2}\frac{\partial\vec{j}}{\partial t}. \tag{186}$$

The dielectric permittivity tensor can be expressed as $\hat{\varepsilon}(\vec{r})=1+\hat{\chi}(\vec{r})$, where $\hat{\chi}(\vec{r})$ is the dielectric susceptibility. When $\hat{\chi}\ll 1$, (186) can be rewritten as:

$$\Delta\vec{E}(\vec{r},t)-\frac{1}{c^2}\frac{\partial^2}{\partial t^2}\int\hat{\varepsilon}(\vec{r},t-t')\vec{E}(\vec{r},t')dt'=4\pi\left(\frac{1}{c^2}\frac{\partial\vec{j}(\vec{r},t)}{\partial t}+\vec{\nabla}\rho(\vec{r},t)\right). \tag{187}$$

When the grating is ideal $\hat{\chi}(\vec{r})=\sum_\tau\hat{\chi}_\tau(\vec{r})e^{i\vec{\tau}\vec{r}}$, where $\vec{\tau}$ is the reciprocal lattice vector.

Let the photonic crystal (diffraction grating) period be smoothly varied with distance, which is much greater then the diffraction grating (ptotonic crystal lattice) period. It is convenient in this case to present the susceptibility $\hat{\chi}(\vec{r})$ in the form, typical of the theory of X-ray diffraction in crystals with lattice distortion [113]:

$$\hat{\chi}(\vec{r})=\sum_\tau e^{i\Phi_\tau(\vec{r})}\hat{\chi}_\tau(\vec{r}), \tag{188}$$

where $\Phi_\tau(\vec{r})=\int\vec{\tau}(\vec{r}')d\vec{l}'$, $\vec{\tau}(\vec{r}')$ is the reciprocal lattice vector in the vicinity of the point $\vec{r}'$. In contrast to the theory of X-rays diffraction, in the case under consideration $\hat{\chi}_\tau$ depends on $\vec{r}$. Moreover, $\hat{\chi}_\tau$ depends on the volume of the lattice unit cell Ω, which can be significantly varied for diffraction gratings (photonic crystals), as distinct from natural crystals. The volume of the unit cell $\Omega(\vec{r})$ depends on coordinate and, for example, for a cubic lattice it is determined as $\Omega(\vec{r})=\frac{1}{d_1(\vec{r})d_2(\vec{r})d_3(\vec{r})}$, where d_i are the lattice periods. If $\hat{\chi}_\tau(\vec{r})$

does not depend on $\vec{r}$, the expression (188) converts to that usually used for X-rays in crystals with lattice distortion [113].

It should be reminded that for an ideal crystal without lattice distortions, the wave, which propagates in the crystal can be presented as a superposition of plane waves:

$$\vec{E}(\vec{r},t)=\sum_{\vec{\tau}=0}^{\infty}\vec{A}_{\vec{\tau}}e^{i(\vec{k}_{\tau}\vec{r}-\omega t)}, \tag{189}$$

where $\vec{k}_{\tau}=\vec{k}+\vec{\tau}$.

Let us now use the fact that in the case under consideration the typical length for the change of the lattice parameters significantly exceeds the lattice period. Then the field inside the crystal with lattice distortion can be expressed similarly to (189), but with $\vec{A}_{\vec{\tau}}$ depending on $\vec{r}$ and t and changing noticeably at the distances much greater than the lattice period.

Similarly, the wave vector should be considered as a slowly changing function of a coordinate.

According to the above, let us find the solution of (187) in the form:

$$\vec{E}(\vec{r},t)=\mathrm{Re}\left\{\sum_{\vec{\tau}=0}^{\infty}\vec{A}_{\vec{\tau}}e^{i(\phi_{\tau}(\vec{r})-\omega t)}\right\}, \tag{190}$$

where $\phi_{\tau}(\vec{r})=\int_0^{\vec{r}}k(\vec{r})d\vec{l}+\Phi_{\tau}(\vec{r})$, where $k(\vec{r})$ can be found as a solution of the dispersion equation in the vicinity of the point with the coordinate vector $\vec{r}$, integration is made over the quasiclassical trajectory, which describes motion of the wavepacket in the crystal with lattice distortion.

Now let us consider the case when all the waves participating in the diffraction

process lie in a plane (coupled wave diffraction, multiple-wave diffraction), i.e., all the reciprocal lattice vectors $\vec{\tau}$ lie in one plane [3,15]. Suppose the wave polarization vector is orthogonal to the plane of diffraction.

Let us rewrite (190) in the form

$$\vec{E}(\vec{r},t) = \vec{e}\,E(\vec{r},t) = \vec{e}\,\mathrm{Re}\left\{\vec{A}_1 e^{i(\phi_1(\vec{r})-\omega t)} + \vec{A}_2 e^{i(\phi_2(\vec{r})-\omega t)} + ...\right\}, \qquad (191)$$

where

$$\phi_1(\vec{r}) = \int_0^{\vec{r}} \vec{k}_1(\vec{r}')d\vec{l}, \qquad (192)$$

$$\phi_2(\vec{r}) = \int_0^{\vec{r}} \vec{k}_1(\vec{r}')d\vec{l} + \int_0^{\vec{r}} \vec{\tau}(\vec{r}')d\vec{l}. \qquad (193)$$

Then multiplying (187) by $\vec{e}$, one can get:

$$\Delta E(\vec{r},t) - \frac{1}{c^2}\frac{\partial^2}{\partial t^2}\int \hat{\varepsilon}(\vec{r},t-t')E(\vec{r},t')dt' = 4\pi\vec{e}\left(\frac{1}{c^2}\frac{\partial\vec{j}(\vec{r},t)}{\partial t} + \vec{\nabla}\rho(\vec{r},t)\right). \qquad (194)$$

Applying the equality $\Delta E(\vec{r},t) = \vec{\nabla}(\vec{\nabla}E)$ and using (191), we obtain

$$\Delta(\vec{A}_1 e^{i(\phi_1(\vec{r})-\omega t)}) = e^{i(\phi_1(\vec{r})-\omega t)}[2i\vec{\nabla}\phi_1\vec{\nabla}A_1 + i\vec{\nabla}\vec{k}_1(\vec{r})A_1 - k_1^2(\vec{r})A_1], \qquad (195)$$

Therefore, substitution of the above expression into (194) gives the following system:

$$\begin{aligned}
&\frac{1}{2}e^{i(\phi_1(\vec{r})-\omega t)}[2i\vec{k}_1(\vec{r})\vec{\nabla}A_1 + i\vec{\nabla}\vec{k}_1(\vec{r})A_1 - k_1^2(\vec{r})A_1 \\
&+\frac{\omega^2}{c^2}\varepsilon_0(\omega,\vec{r})A_1 + i\frac{1}{c^2}\frac{\partial\omega^2\varepsilon_0(\omega,\vec{r})}{\partial\omega}\frac{\partial A_1}{\partial t} + \frac{\omega^2}{c^2}\varepsilon_{-\tau}(\omega,\vec{r})A_2 \\
&+i\frac{1}{c^2}\frac{\partial\omega^2\varepsilon_{-\tau}(\omega,\vec{r})}{\partial\omega}\frac{\partial A_2}{\partial t}] \\
&+ \text{conjugated terms } = 4\pi\vec{e}\left(\frac{1}{c^2}\frac{\partial\vec{j}(\vec{r},t)}{\partial t} + \vec{\nabla}\rho(\vec{r},t)\right),
\end{aligned}$$

$$\frac{1}{2}e^{i(\phi_2(\vec{r})-\omega t)}[2i\vec{k}_2(\vec{r})\vec{\nabla}A_2 + i\vec{\nabla}\vec{k}_2(\vec{r})A_2 - k_2^2(\vec{r})A_2$$
$$+\frac{\omega^2}{c^2}\varepsilon_0(\omega,\vec{r})A_2 + i\frac{1}{c^2}\frac{\partial\omega^2\varepsilon_0(\omega,\vec{r})}{\partial\omega}\frac{\partial A_2}{\partial t} + \frac{\omega^2}{c^2}\varepsilon_\tau(\omega,\vec{r})A_1$$
$$+i\frac{1}{c^2}\frac{\partial\omega^2\varepsilon_\tau(\omega,\vec{r})}{\partial\omega}\frac{\partial A_1}{\partial t}]$$
$$+ \text{ conjugated terms } = 4\pi\vec{e}\left(\frac{1}{c^2}\frac{\partial\vec{j}(\vec{r},t)}{\partial t} + \vec{\nabla}\rho(\vec{r},t)\right), \qquad (196)$$

where vector $\vec{k}_2(\vec{r}) = \vec{k}_1(\vec{r}) + \vec{\tau}$, $\varepsilon_0(\omega,\vec{r}) = 1 + \chi_0(\vec{r})$, here the notation $\chi_0(\vec{r}) = \chi_{\tau=0}(\vec{r})$ is used, $\varepsilon_\tau(\omega,\vec{r}) = \chi_\tau(\vec{r})$. Note here that for a numerical analysis of (196), if $\chi_0 \ll 0$, it is convenient to take vector $\vec{k}_1(\vec{r})$ in the form $\vec{k}_1(\vec{r}) = \vec{n}\sqrt{k^2 + \frac{\omega^2}{c^2}\chi_0(\vec{r})}$.

For better understanding, let us suppose that the diffraction grating (photonic crystal lattice) period changes along one direction and define this direction as axis z.

Thus, for a one-dimensional case, when $\vec{k}(\vec{(r)}) = (\vec{k}_\perp, k_z(z))$, the system (196) converts to the following:

$$\frac{1}{2}e^{i(\vec{k}_\perp\vec{r}_\perp+\phi_{1z}(z)-\omega t)}[2ik_{1z}(z)\frac{\partial A_1}{\partial z} + i\frac{\partial k_{1z}(z)}{\partial z}A_1 - (k_\perp^2 + k_{1z}^2(z))A_1$$
$$+\frac{\omega^2}{c^2}\varepsilon_0(\omega,z)A_1 + i\frac{1}{c^2}\frac{\partial\omega^2\varepsilon_0(\omega,z)}{\partial\omega}\frac{\partial A_1}{\partial t} + \frac{\omega^2}{c^2}\varepsilon_{-\tau}(\omega,z)A_2$$
$$+i\frac{1}{c^2}\frac{\partial\omega^2\varepsilon_{-\tau}(\omega,z)}{\partial\omega}\frac{\partial A_2}{\partial t}]$$
$$+ \text{ conjugated terms } = 4\pi\vec{e}\left(\frac{1}{c^2}\frac{\partial\vec{j}(\vec{r},t)}{\partial t} + \vec{\nabla}\rho(\vec{r},t)\right),$$
$$\frac{1}{2}e^{i(\vec{k}_\perp\vec{r}_\perp+\phi_{2z}(z)-\omega t)}[2ik_{2z}(z)\frac{\partial A_2}{\partial z} + i\frac{\partial k_{2z}(z)}{\partial z}A_2 - (k_\perp^2 + k_{2z}^2(z))A_2$$
$$+\frac{\omega^2}{c^2}\varepsilon_0(\omega,z)A_2 + i\frac{1}{c^2}\frac{\partial\omega^2\varepsilon_0(\omega,z)}{\partial\omega}\frac{\partial A_2}{\partial t} + \frac{\omega^2}{c^2}\varepsilon_\tau(\omega,z)A_1$$
$$+i\frac{1}{c^2}\frac{\partial\omega^2\varepsilon_\tau(\omega,z)}{\partial\omega}\frac{\partial A_1}{\partial t}]$$
$$+ \text{ conjugated terms } = 4\pi\vec{e}\left(\frac{1}{c^2}\frac{\partial\vec{j}(\vec{r},t)}{\partial t} + \vec{\nabla}\rho(\vec{r},t)\right), \qquad (197)$$

Let us multiply the first equation by $e^{-i(\vec{k}_\perp \vec{r}_\perp + \phi_{1z}(z) - \omega t)}$ and the second by $e^{-i(\vec{k}_\perp \vec{r}_\perp + \phi_{2z}(z) - \omega t)}$. This procedure enables neglecting the conjugated terms, which appear fast oscillating (when averaging over the oscillation period they become zero).

Considering the right-hand side of (197), let us take into account that microscopic currents and densities are the sums of terms, containing delta-functions, therefore, the right-hand side can be rewritten as:

$$e^{-i(\vec{k}_\perp \vec{r}_\perp + \phi_{1z}(z) - \omega t)} 4\pi \vec{e} \left(\frac{1}{c^2} \frac{\partial \vec{j}(\vec{r}, t)}{\partial t} + \vec{\nabla} \rho(\vec{r}, t) \right) \tag{198}$$
$$= -\frac{4\pi i \omega e}{c^2} \vec{e} \sum_\alpha \vec{v}_\alpha(t) \delta(\vec{(r)} - \vec{(r)}_\alpha(t)) e^{-i(\vec{k}_\perp \vec{r}_\perp + \phi_{1z}(z) - \omega t)} \, \theta(t - t_\alpha) \, \theta(T_\alpha - t)$$

here t_α is the time of entrance of particle α to the resonator, T_α is the time of particle leaving the resonator, $\theta-$functions in (199) indicate that for the time moments preceding t_α and following T_α, the particle α does not contribute to the process.

Let us suppose now that a strong magnetic field is applied for beam guiding through the generation area. Thus, the problem appears one-dimensional (components v_x and v_y are suppressed). Averaging the right-hand side of (199) over the particle positions inside the beam, points of particle entrance to the resonator $r_{\perp 0\alpha}$ and time of particle entrance to the resonator t_α one can obtain:

$$e^{-i(\vec{k}_\perp \vec{r}_\perp + \phi_{1z}(z) - \omega t)} 4\pi \vec{e} \left(\frac{1}{c^2} \frac{\partial \vec{j}(\vec{r}, t)}{\partial t} + \vec{\nabla} \rho(\vec{r}, t) \right)$$
$$= -\frac{4\pi i \omega \rho \, \vartheta_1 \, u(t) \, e}{c^2} \frac{1}{S} \int d^2 \vec{r}_{\perp 0} \frac{1}{T} \int_0^t e^{-i(\phi_1(\vec{r}, \vec{r}_\perp, t, t_0) + \vec{k}_\perp \vec{r}_{\perp 0} - \omega t)} dt_0$$
$$= -\frac{4\pi i \omega \rho \, \vartheta_1 \, u(t) \, e}{c^2} \langle\langle e^{-i(\phi_1(\vec{r}, \vec{r}_\perp, t, t_0) + \vec{k}_\perp \vec{r}_{\perp 0} - \omega t)} dt_0 \rangle\rangle, \tag{199}$$

where ρ is the electron beam density, $u(t)$ is the mean electron beam velocity, which depends on time due to energy losses, $\vartheta_1 = \sqrt{1 - \frac{\omega^2}{\beta^2 k_1^2 c^2}}$, $\beta^2 = 1 - \frac{1}{\gamma^2}$, $\langle\langle\ \rangle\rangle$ indicates averaging over the transversal coordinate of the point of particle entrance to the resonator $r_{\perp 0\alpha}$ and time of particle entrance to the resonator t_α.

According to [102], the averaging procedure in (199) can be simplified, when consider that random phases, appearing due to random transversal coordinate and time of entrance, presents in (199) as differences. Therefore, double integration over $d^2\vec{r}_{\perp 0}\, dt_0$ can be replaced by single integration [102].

The system (197) in this case converts to:

$$\begin{aligned}
&2ik_{1z}(z)\frac{\partial A_1}{\partial z} + i\frac{\partial k_{1z}(z)}{\partial z}A_1 - (k_\perp^2 + k_{1z}^2(z))A_1 \\
&+\frac{\omega^2}{c^2}\varepsilon_0(\omega, z)A_1 + i\frac{1}{c^2}\frac{\partial \omega^2\varepsilon_0(\omega, z)}{\partial \omega}\frac{\partial A_1}{\partial t} + \frac{\omega^2}{c^2}\varepsilon_{-\tau}(\omega, z)A_2 \\
&+i\frac{1}{c^2}\frac{\partial \omega^2\varepsilon_{-\tau}(\omega, z)}{\partial \omega}\frac{\partial A_2}{\partial t} = i\frac{2\omega}{c^2}J_1(k_{1z}(z)), \\
&2ik_{2z}(z)\frac{\partial A_2}{\partial z} + i\frac{\partial k_{2z}(z)}{\partial z}A_2 - (k_\perp^2 + k_{2z}^2(z))A_2 \\
&+\frac{\omega^2}{c^2}\varepsilon_0(\omega, z)A_2 + i\frac{1}{c^2}\frac{\partial \omega^2\varepsilon_0(\omega, z)}{\partial \omega}\frac{\partial A_2}{\partial t} + \frac{\omega^2}{c^2}\varepsilon_{\tau}(\omega, z)A_1 \\
&+i\frac{1}{c^2}\frac{\partial \omega^2\varepsilon_{\tau}(\omega, z)}{\partial \omega}\frac{\partial A_1}{\partial t} = i\frac{2\omega}{c^2}J_2(k_{2z}(z)),
\end{aligned} \tag{200}$$

where the currents J_1, J_2 are determined by the expression

$$J_m = 2\pi j\vartheta_m \int_0^{2\pi} \frac{2\pi - p}{8\pi^2}(e^{-i\phi_m(t,z,p)} + e^{-i\phi_m(t,z,-p)})\, dp, \quad m = 1, 2 \tag{201}$$

$$\vartheta_m = \sqrt{1 - \frac{\omega^2}{\beta^2 k_m^2 c^2}}\ ,\ \beta^2 = 1 - \frac{1}{\gamma^2}\ ,$$

$j = en_0 v$ is the current density, $A_1 \equiv A_{\tau=0}$, $A_2 \equiv A_\tau$, $\vec{k}_1 = \vec{k}_{\tau=0}$, $\vec{k}_2 = \vec{k}_1 + \vec{\tau}$. The expressions for J_1 and k_1 independent on z was obtained in [102].

When more than two waves participate in the diffraction process, the system (201) should be supplemented with equations for waves A_m, which are similar to those for A_1 and A_2.

Now we can find the equation for the phase. From (192), (193) follows that

$$\frac{d^2\phi_m}{dz^2} + \frac{1}{v}\frac{dv}{dz}\frac{d\phi_m}{dz} = \frac{dk_m}{dz} + \frac{k_m}{v^2}\frac{d^2z}{dt^2}, \tag{202}$$

Let us introduce a new function $C(z)$ as follows:

$$\frac{d\phi_m}{dz} = C_m(z)e^{-\int_0^z \frac{1}{v}\frac{dv}{dz'}dz'} = \frac{v_0}{v(z)}C_m(z), \tag{203}$$

$$\phi_m(z) = \phi_m(0) + \int_0^z \frac{v_0}{v(z')}C_m(z')dz'$$

Therefore,

$$\frac{dC_m(z)}{dz} = \frac{v(z)}{v_0}\left(\frac{dk_m}{dz} + \frac{k_m}{v^2}\frac{d^2z}{dt^2}\right). \tag{204}$$

In a one-dimensional case, equation (185) can be written as:

$$\frac{d^2z_\alpha}{dt^2} = \frac{e\vartheta}{m\gamma(z_\alpha,t,p)}\mathrm{Re}E(z_\alpha,t), \tag{205}$$

therefore,

$$\frac{dC_m(z)}{dz} = \frac{v(z)}{v_0}\frac{dk_m}{dz} + \frac{k_m}{v_0 v(z)}\frac{e\vartheta_m}{m\gamma^3(z,t(z),p)}Re\{A_m(z,t(z))e^{i\phi_m(z,t(z),p)}\}, \tag{206}$$

$$\frac{d\phi_m(t,z,p)}{dz}|_{z=0} = k_{mz} - \frac{\omega}{v},\ \phi_m(t,z,p)|_{z=0} = p,$$

$$A_1|_{z=L} = E_1^0,\ A_2|_{z=L} = E_2^0,$$

$$A_m|_{t=0} = 0,\ m = 1,2,$$

$t > 0,\ z \in [0, L],\ p \in [-2\pi, 2\pi],\ L$ is the length of the photonic crystal.

These equations should be supplied with the equations for $\gamma(z, p)$. It is well-known that

$$mc^2 \frac{d\gamma}{dt} = e\vec{v}\vec{E}. \tag{207}$$

Therefore,

$$\frac{d\gamma(z, t(z), p)}{dz} = \sum_l \frac{e\vartheta_l}{mc^2} \mathrm{Re}\{\sum_l A_l(z, t(z)) e^{i\phi_l(z, t(z), p)}\}. \tag{208}$$

The above obtained equations (201), (204), (206), (208) enable describing the generation process in a FEL with varied parameters of diffraction grating (photonic crystal). The analysis of the system (206) can be simplified by replacement of the $\gamma(z, t(z), p)$ with its averaged by the initial phase value

$$< \gamma(z, t(z)) >= \frac{1}{2\pi} \int_0^{2\pi} \gamma(z, t(z), p)\, dp.$$

Note that the law of parameters change can be both smooth and stair-step.

Using photonic crystals provide the development of different VFEL arrangements (see Figure 25).

It should be noted that, for example, in the FEL (TWT, BWO) resonator with changing in space parameters of grating (photonic crystal), the electromagnetic wave with a spatial period depending on z is formed. This means that the dynamical undulator with a period depending on z appears along the whole resonator length, i.e., a tapering dynamical wiggler becomes settled. It is well known that a tapering wiggler can significantly increase the efficiency

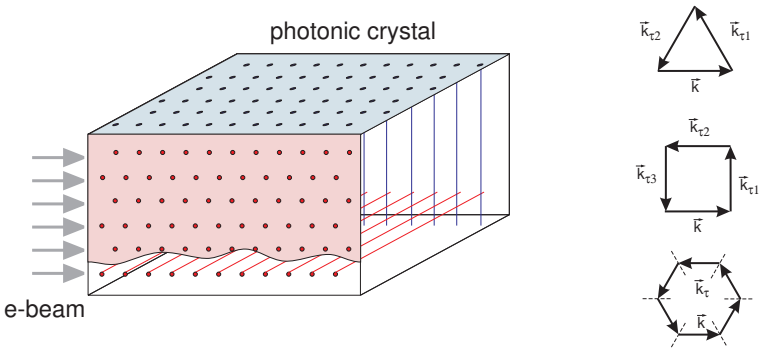

Figure 25. An example of photonic crystal with the thread arrangement providing multi-wave volume distributed feedback. Threads are arranged to couple several waves (three, four, six and so on), which appear due to diffraction in such a structure, in both the vertical and horizontal planes. The electronic beam takes the whole volume of photonic crystal.

of the undulator FEL. The dynamical wiggler with varied period, which is proposed, can be used for development of double-cascaded FEL with parameters changing in space. The efficiency of such a system can be significantly higher that of a conventional system. Moreover, the period of a dynamical wiggler can be made much shorter than that available for wigglers using static magnetic fields.

It should also be noted that the compression of the radiation pulse in such a system is possible because the phase velocity of the electromagnetic wave depends on time.

Thus, the equations providing the description of the generation process in FEL with varied parameters of diffraction grating (photonic crystal) are obtained. It is shown that applying diffraction gratings (photonic crystal) with the variable period one can significantly increase radiation output. It is mentioned that diffraction gratings (photonic crystal) can be used for creation of the dynamical wiggler with variable period in the system. This makes possible

to develop double-cascaded FEL with variable parameters changing, which efficiency can be significantly higher that of conventional system.

In conclusion, it should be noted that in the photonic crystals built from metal (or dielectric) threads, waves are effectively diffracted even when their lengths are much smaller than the distance between the threads. That is why it is possible to generate radiation in the terahertz range using diffraction gratings with a millimeter period alone.

Above, we have studied the features of generation for the sources with transverse dimensions much greater than the radiation wavelength. In the case when the finite dimensions of a resonator should be taken into account, it is necessary to follow the rules given in [87,117,152,163].

24.2 Radiative instability of a relativistic electron beam moving in a finite-dimensional photonic (or natural) crystal

According to the analysis given in [163], the first and most important step in describing the generation process in VFELs (FELs and so on) is the analysis of the problem of the electron beam instability in the resonator. The theoretical study of the instability of electron beams moving in natural and artificial (photonic) crystals was carried out above for the ideal case of an infinite medium (see the review in [87] and [49,102,117,152,181]). The question arising in this regard is how the finite dimensions of the photonic crystal placed inside the resonator affect the law of electron beam instability. It is known, for example, that the discrete structure of the modes in waveguides and resonators is crucial for effective generation in the microwave range [83,84,183,184,185].

In present section the radiative instability of a beam moving in a photonic crystal is studied. The dispersion equation describing instability in this case is obtained. It is shown that the law $\Gamma \sim \rho^{1/(s+3)}$ is also valid and caused by the mixing of the electromagnetic field modes in the finite volume due to the periodic disturbance from the photonic crystal.

The system of equations describing generation of induced radiation in photonic (and natural) crystals can be obtained similarly to those in section 24.1 (equations (182)-(187)).

In the general case, the susceptibility of the photonic crystal reads $\hat{\chi}(\vec{r}) = \sum\limits_i \hat{\chi}_{cell}(\vec{r} - \vec{r}_i)$, where $\hat{\chi}_{cell}(\vec{r} - \vec{r}_i)$ is the susceptibility of the crystal unit cell. The susceptibility of an infinite perfect crystal $\hat{\chi}(\vec{r})$ can be expanded into the Fourier series as follows: $\hat{\chi}(\vec{r}) = \sum\limits_{\vec{\tau}} \hat{\chi}_{\vec{\tau}} e^{i\vec{\tau}\vec{r}}$, where $\vec{\tau}$ is the reciprocal lattice vector of the crystal.

To be more specific, let us consider in details a practically important case when a photonic crystal is placed inside a smooth waveguide of rectangular cross-section.

The eigenfunctions and the eigenvalues of such a waveguide are well-studied [16,188].

Suppose the z-axis to be directed along the waveguide axis. Make the Fourier transform of (186) over time and longitudinal coordinate z . Expanding thus obtained equation for the field $\vec{E}(\vec{r}_\perp, k_z, \omega)$ over a full set of vector eigenfunctions of a rectangular waveguide $\vec{Y}^{\lambda}_{mn}(\vec{r}_\perp, k_z)$ (where $m, n = 1, 2, 3....$, while λ

describes the type of the wave [6], one can obtain for the field $\vec{E}$ the equality

$$\vec{E}\left(\vec{r}_{\perp},k_z,\omega\right)=\sum_{mn\lambda}C^{\lambda}_{mn}\left(k_z,\omega\right)\vec{Y}^{\lambda}_{mn}\left(\vec{r}_{\perp},k_z\right). \tag{209}$$

As a result, the following equation can be written

$$\begin{aligned}&\left[\left(k_z^2+\kappa^2_{mn\lambda}\right)-\tfrac{\omega^2}{c^2}\right]C^{\lambda}_{mn}\left(k_z,\omega\right)-\\&-\tfrac{\omega^2}{c^2}\tfrac{1}{2\pi}\sum_{m'n'\lambda'}\int\vec{Y}^{\lambda^*}_{mn}\left(\vec{r}_{\perp},k_z\right)\hat{\chi}\left(\vec{r}\right)\vec{Y}^{\lambda'}_{m'n'}\left(\vec{r}_{\perp},k'_z\right)e^{-i(k_z-k'_z)z}\,d^2r_{\perp}C^{\lambda'}_{m'n'}\left(k'_z,\omega\right)dk'_zdz=\\&=\tfrac{4\pi i\omega}{c^2}\int\vec{Y}^{\lambda^*}_{mn}\left(\vec{r}_{\perp},k_z\right)\left\{\vec{j}\left(\vec{r}_{\perp},z,\omega\right)+\tfrac{c^2}{\omega^2}\vec{\nabla}\left(\vec{\nabla}\vec{j}\left(\vec{r}_{\perp},z,\omega\right)\right)\right\}e^{-ik_zz}d^2r_{\perp}dz\end{aligned} \tag{210}$$

where $\kappa^2_{mn\lambda}=k^2_{xm\lambda}+k^2_{yn\lambda}$.

The beam current and density appearing on the right-hand side of (210) are complicated functions of the field $\vec{E}$. To study the problem of the system instability, it is sufficient to consider the system in the approximation linear over perturbation, i.e., one can expand the expressions for $\vec{j}$ and ρ over the field amplitude $\vec{E}$ and abridge oneself with the linear approximation.

As a result, a closed system of equations comes out. For further consideration, one should obtain the expressions for the corrections $\delta\vec{j}$ and $\delta\rho$ due to beam perturbation by the field. Considering the Fourier transforms of the current density and the beam charge $\vec{j}\left(\vec{k},\omega\right)$ and $\rho\left(\vec{k},\omega\right)$, one can obtain from (183) that

$$\delta\vec{j}\left(\vec{k},\omega\right)=e\sum_{\alpha=1}^{N}e^{-i\vec{k}\vec{r}_{\alpha_0}}\left\{\delta\vec{v}_{\alpha}\left(\omega-\vec{k}\vec{u}_{\alpha}\right)+\vec{u}_{\alpha}\frac{\vec{k}\delta\vec{v}_{\alpha}\left(\omega-\vec{k}\vec{u}_{\alpha}\right)}{\omega-\vec{k}\vec{u}_{\alpha}}\right\}, \tag{211}$$

where $\vec{r}_{\alpha_0}$ is the original coordinate of the electron, $\vec{u}_{\alpha}$ is the unperturbed velocity of the electron.

For simplicity, let us consider a cold beam, for which $\vec{u}_\alpha \approx \vec{u}$, where $\vec{u}$ is the mean velocity of the beam. The general case of a hot beam is obtained by averaging $\delta\vec{j}\left(\vec{k},\omega\right)$ over the velocity $\vec{u}_\alpha$ distribution in the beam.

According to (184), the velocity $\delta\vec{v}_\alpha$ is determined by the field $\vec{E}\left(\vec{r}_\alpha,\omega\right)$ taken at the electron location point $\vec{r}_\alpha$. The Fourier transform of the field $\vec{E}\left(\vec{r}_\alpha,\omega\right)$ has a form

$$\vec{E}\left(\vec{r}_\alpha,\omega\right) = \frac{1}{\left(2\pi\right)^3}\int \vec{E}\left(\vec{k}',\omega\right) e^{i\vec{k}'\vec{r}_\alpha} d^3k'.$$

As a result, the formula for $\delta\vec{j}\left(\vec{k},\omega\right)$ includes the sum $\sum\limits_\alpha e^{-i\left(\vec{k}-\vec{k}'\right)\vec{r}_\alpha}$ over the particle distribution in the beam. Suppose that the electrons in an unperturbed beam are uniformly distributed over the area occupied by the beam. Therefore

$$\sum_\alpha e^{-i\left(\vec{k}-\vec{k}'\right)\vec{r}_\alpha} = \left(2\pi\right)^3 \rho_0\, \delta\left(\vec{k}-\vec{k}'\right),$$

where ρ_0 is the beam density (the number of electrons per 1 cm^3).

As a result, the following expression for $\delta\vec{j}\left(\vec{k},\omega\right)$ can be obtained [51,60]:

$$\delta\vec{j}\left(\vec{k},\omega\right) = \frac{i\vec{u}e^2\rho\left(k^2-\frac{\omega^2}{c^2}\right)}{\left(\omega-\vec{k}\vec{u}\right)^2 m\gamma\omega}\vec{u}\vec{E}\left(\vec{k},\omega\right). \qquad (212)$$

Using the continuity equation, one immediately obtains the expression for $\rho\left(\vec{k},\omega\right)$. Expression (212), the inverse Fourier transform of $\vec{E}\left(\vec{k},\omega\right)$, and the

expansion (209) enable writing the system of equations (210) as follows:

$$\left[(k_z^2+\kappa_{mn\lambda}^2)-\frac{\omega^2}{c^2}\right]C_{mn}^{\lambda}(k_z,\omega)-$$

$$-\frac{\omega^2}{c^2}\frac{1}{2\pi}\sum_{m'n'\lambda'}\int\vec{Y}_{mn}^{\lambda^*}(\vec{r}_\perp,k_z)\,\hat{\chi}(\vec{r})\,\vec{Y}_{m'n'}^{\lambda'}(\vec{r}_\perp,k_z')\,e^{-i(k_z-k_z')z}\,d^2r_\perp C_{m'n'}^{\lambda'}(k_z',\omega)\,dk_z'dz = \quad (213)$$

$$=-\frac{\omega_L^2\left(k_{mn}^2c^2-\omega^2\right)}{\gamma c^4\left(\omega-\vec{k}_{mn}\vec{u}\right)^2}\left\{\frac{1}{2\pi}\left|\int\vec{u}\,\vec{Y}_{mn}^{\lambda}\left(\vec{k}_\perp,k_z\right)d^2k_\perp\right|^2\right\}C_{mn}^{\lambda}(k_z,\omega),$$

where $\vec{Y}_{mn}^{\lambda}\left(\vec{k}_\perp,k_z\right)=\int e^{-i\vec{k}_\perp\vec{r}_\perp}\vec{Y}_{mn}^{\lambda}(\vec{r}_\perp,k_z)\,d^2r_\perp$.

Note that within the limit where the transverse dimensions of a photonic crystal tend to infinity, the expression between the braces takes the form $(\vec{e}\vec{u})^2$, where $\vec{e}$ is the unit polarization vector of the wave emitted by the beam [51,60].

Now let us consider the integrals on the left-hand side of equation (213). Note that according to [6,16,188], the eigenfunctions $\vec{Y}_{mn}^{\lambda}(\vec{r}_\perp,k_z)$ of a rectangular waveguide include the combinations of sines and cosines of the form $sin\frac{\pi m}{a}x, cos\frac{\pi m}{a}x$ $(sin\frac{\pi n}{b}y, cos\frac{\pi n}{b}y)$, i.e., in fact, the combinations $e^{i\frac{\pi m}{a}x}, e^{i\frac{\pi n}{b}y}$. Hence, the left-hand side of the equation includes the integrals of the type

$$I=\int e^{-i\frac{\pi m}{a}x}\sum_i\hat{\chi}_{cell}(x-x_i,y-y_i,z-z_i)\,e^{i\frac{\pi m'}{a}x}dx.$$

The substitution of variables $x-x_i=\eta$ gives the sums of the form

$$S_x=\sum_i e^{-i\frac{\pi}{a}(m-m')x_i}$$

where $x_i=d_xf_1$, where d_x is the period of the photonic crystal along the x-axis, $f_1=1,2,...N_x$, where N_x is the number of cells along the x-axis.

The above-mentioned sum

$$S_x = \sum_i e^{-i\frac{\pi}{a}(m-m')x_i} = e^{i\frac{\pi}{2a}(m-m')(N_x-1)d_x} \frac{sin\frac{\pi(m-m')d_xN_x}{2a}}{sin\frac{\pi(m-m')d_x}{2a}}. \quad (214)$$

If $m - m' = 0$, then $S_x = N_x$.

Let us now discuss what this sum is equal to when $m - m' = 1$. In the numerator $d_xN_x = a$, hence, the nominator is equal to 1 ($sin\frac{\pi}{2} = 1$), while in the denominator $sin\frac{\pi d_x}{2a} \approx \frac{\pi}{2N_x}$. As a result, the relation $\frac{S_x(m-m'=1)}{S_x(m-m'=0)} = \frac{2}{\pi} \approx 0.6$.

With growing difference $m-m'$, the contribution to the sum of the next terms diminishes until the following equality is fulfilled

$$\frac{\pi\,(m-m')\,d_x}{2a} = \pi \mathrm{P}, \quad (215)$$

where $\mathrm{P} = \pm 1, \pm 2...$ In this case the sum $S_x = N_x$.

The similar reasoning is valid for summation along the y-axis.

It follows from the aforesaid that if the equalities like (214), (215) are fulfilled, that is, the equalities $k_{xm} - k'_{xm'} = \tau_x$ are fulfilled (i.e., $k'_{xm'} = k_{xm} - \tau_x$), where $\tau_x = \frac{2\pi}{d_x}F$ is the x-component of the reciprocal lattice vector of the photonic crystal, $F = 0, \pm 1, \pm 2...$ and $k_{yn} - k'_{yn'} = \tau_y$ (i.., $k'_{yn'} = k_{yn} - \tau_y$), where $\tau_y = \frac{2\pi}{d_y}F'$ is the y-component of the reciprocal lattice vector of the photonic crystal, $F' = 0, \pm 1, \pm 2...$), then the major contribution to the sums comes from the amplitudes $C^{\lambda'}_{m'n'}(k'_z, \omega) \equiv C^{\lambda'}\left(\vec{k}_{\perp mn} - \vec{\tau}_\perp, k_z - \tau_z, \omega\right) = C^{\lambda'}\left(\vec{k}_{mn} - \vec{\tau}, \omega\right)$.

In describing the system we shall further consider only those modes that satisfy the equalities of the type (214), (215). As stated above, the contribution of other modes is suppressed.

As a result, one can rewrite the system of equations (213) as

$$\begin{array}{l}\left(\vec{k}_{mn}^{2}-\frac{\omega^{2}}{c^{2}}\right)C^{\lambda}\left(\vec{k}_{mn},\omega\right)-\frac{\omega^{2}}{c^{2}}\sum\limits_{\lambda'\tau}\chi_{mn}^{\lambda\lambda'}\left(\vec{\tau}\right)C^{\lambda'}\left(\vec{k}_{mn}-\vec{\tau},\omega\right)= \\ -\frac{\omega_{L}^{2}\left(k_{mn}^{2}c^{2}-\omega^{2}\right)}{\gamma c^{4}\left(\omega-\vec{k}_{mn}\vec{u}\right)^{2}}\left\{\frac{1}{2\pi}\left|\int\vec{u}\,\vec{Y}_{mn}^{\lambda}\left(\vec{k}_{\perp},k_{z}\right)d^{2}k_{\perp}\right|^{2}\right\}C^{\lambda}\left(\vec{k}_{mn},\omega\right),\end{array} \tag{216}$$

i.e.,

$$\begin{array}{l}\left(\vec{k}_{mn}^{2}-\frac{\omega^{2}}{c^{2}}\left(1+\chi_{mn}^{\lambda\lambda}\left(0\right)-\frac{\omega_{L}^{2}\left(k_{mn}^{2}c^{2}-\omega^{2}\right)}{\omega^{2}\gamma c^{2}\left(\omega-\vec{k}_{mn}\vec{u}\right)^{2}}\left\{\frac{1}{2\pi}\left|\int\vec{u}\,\vec{Y}_{mn}^{\lambda}\left(\vec{k}_{\perp},k_{z}\right)d^{2}k_{\perp}\right|^{2}\right\}\right)\right)C^{\lambda}\left(\vec{k}_{mn},\omega\right) \\ -\frac{\omega^{2}}{c^{2}}\sum\limits_{\lambda'\tau}\chi_{mn}^{\lambda\lambda'}\left(\vec{\tau}\right)C^{\lambda'}\left(\vec{k}-\vec{\tau},\omega\right)=0\end{array} \tag{217}$$

where $\chi_{mn}^{\lambda\lambda'}\left(\tau\right)=\frac{1}{d_{z}}\int\vec{Y}_{mn}^{\lambda*}\left(\vec{r}_{\perp},k_{z}\right)\hat{\chi}\left(\vec{r}_{\perp},\tau_{z}\right)\vec{Y}_{m'n'}^{\lambda'}\left(\vec{r}_{\perp},k_{z}-\tau_{z}\right)d^{2}r_{\perp}$, $\hat{\chi}\left(\vec{r}_{\perp},\tau_{z}\right)=\sum\limits_{x_{i},y_{i}}\int\hat{\chi}_{cell}\left(x-x_{i},y-y_{i},\zeta\right)e^{-i\tau_{z}\zeta}d\zeta$, m' and n' are found by the conditions like (215), ω_{L} is the Langmuir frequency, $\omega_{L}^{2}=\frac{4\pi e^{2}\rho_{0}}{m}$.

This system of equations coincides in form with that describing the instability of a beam passing through an infinite crystal [51,60]. The difference between them is that the coefficients appearing in these equations are defined differently and that in the case of an infinite crystal, the wave vectors $\vec{k}_{mn}$ have a continuous spectrum of eigenvalues rather than a discrete one.

These equations enable one to define the dependence $k\left(\omega\right)$, thus defining the expressions for the waves propagating in the crystal. By matching the incident wave packet and the set of waves propagating inside the photonic crystal using the boundary conditions, one can obtain the explicit expression describing the solution of the considered equations.

The result obtained is formally analogous to that given in [55].

According to (217), the expression between the square brackets acts as the

dielectric permittivity ε of the crystal under the conditions when diffraction can be neglected:

$$\varepsilon_0 = n^2 = 1 + \chi_{mn}^{\lambda\lambda}(0) - \frac{\omega_L^2\left(k_{mn}^2c^2-\omega^2\right)}{\omega^2\gamma c^2\left(\omega-\vec{k}_{mn}\vec{u}\right)^2}\left\{\frac{1}{2\pi}\left|\int \vec{u}\,\vec{Y}_{mn}^{\lambda}\left(\vec{k}_{\perp},k_z\right)d^2k_{\perp}\right|^2\right\},$$

n is the refractive index.

As is seen, in this case the contribution to the refractive index comes not only from the scattering of waves by the unit cell of the crystal lattice, but also from the scattering of waves by the beam electrons (the term proportional to ω_L^2): the photonic crystal penetrated by a beam of electrons is a medium that can be described by a ceratin refractive index n (or the dielectric permittivity ε_0).

According to (217), the beam contribution increases when $\omega \to \vec{k}\vec{u}$.

Since this system of equations is homogeneous, its solvability condition is the vanishing of the system determinant.

In the beginning, let us assume that the diffraction conditions are not fulfilled. Then the amplitudes of diffracted waves are small. In this case the sum over τ can be dropped, and the conditions for the occurrence of the wave in the system is obtained by the requirement that the expression between the square brackets equal zero.

This expression can be written in the form (the velocity $\vec{u}||oz$)

$$(\omega-k_zu)^2\left(k_{mn}^2-\frac{\omega^2}{c^2}n_0^2\right) = -\frac{\omega_L^2\left(k_{mn}^2c^2-\omega^2\right)}{\gamma c^4}\left\{\frac{1}{2\pi}\left|\int \vec{u}\,\vec{Y}_{mn}^{\lambda}\left(\vec{k}_{\perp},k_z\right)d^2k_{\perp}\right|^2\right\},$$

where n_0 is the refractive index of the photonic crystal in the absence of the

beam $\varepsilon_0 = n_0^2 = 1 + \chi_{mn}^{\lambda\lambda}(0)$,

i.e.,

$$\left(k_z^2 - \left(\frac{\omega^2}{c^2} n_0^2 - \kappa_{mn}^2\right)\right)(\omega - k_z u)^2 = -\frac{\omega_L^2 \left(k_{mn}^2 c^2 - \omega^2\right)}{\gamma c^4} \left\{\frac{1}{2\pi} \left| \int \vec{u}\, \vec{Y}_{mn}^{\lambda}\left(\vec{k}_\perp, k_z\right) d^2 k_\perp \right|^2 \right\} \quad (218)$$

Since the nonlinearity is insignificant, let us consider as the zero approximation the spectrum of the waves of equation (218) with zero right-hand side.

Let us concern with the case when $\omega - k_z u \to 0$ (i.e., the Cherenkov radiation condition can be fulfilled) and $\left(k_z^2 - \left(\frac{\omega^2}{c^2} n_0^2 - \kappa_{mn}^2\right)\right) \to 0$, i.e, the electromagnetic wave can propagate in a photonic crystal without the beam. With zero right-hand side the equation reads

$$\left(k_z^2 - \left(\frac{\omega^2}{c^2} n_0^2 - \kappa_{mn}^2\right)\right) = 0, \quad (\omega - k_z u) = 0 \quad (219)$$

As a consequence, in this case the roots of the equation are

$$k_{1z} = \frac{\omega}{c} \sqrt{n_0^2 - \frac{\kappa_{mn}^2 c^2}{\omega^2}}, \quad k'_{1z} = -k_{1z}, \quad k_{2z} = \frac{\omega}{u}. \quad (220)$$

Since $k_{2z} = \frac{\omega}{u} > 0$ in view of the Cherenkov condition, we are concerned with the propagation of the wave with $k_{1z} > 0$ in the photonic crystal. In this case in the equation for k_z, one can take $(k_z - k_{1z})(k_z + k_{1z}) \approx 2k_{1z}(k_z - k_{1z})$ and rewrite equation (218) as follows:

$$(k_z - k_{1z})(k_z - k_{2z})^2 = -\frac{\omega_L^2 \omega^2 \left(n_0^2 - 1\right)}{2k_{1z} u^2 \gamma c^4} \left\{\frac{1}{2\pi} \left| \int \vec{u}\, \vec{Y}_{mn}^{\lambda}\left(\vec{k}_\perp, k_z\right) d^2 k_\perp \right|^2 \right\} \quad (221)$$

i.e.,

$$(k_z - k_{1z})(k_z - k_{2z})^2 = -A \quad (222)$$

where A is real and $A > 0$ (as for the occurrence of the Cherenkov effect, it is necessary that $n_0^2 > 1$). We have obtained the cubic equation for k_z. Let us consider the case when the roots k_{1z} and k_{2z} coincide $k_{1z} = k_{2z}$. It is possible when the particle velocity satisfies the condition

$$u = \frac{c}{\sqrt{n_0^2 - \frac{\kappa_{mn}^2 c^2}{\omega^2}}}. \tag{223}$$

Introduction of $\xi = k - k_{1z}$ gives for $k_{1z} = k_{2z}$

$$\xi^3 = -A. \tag{224}$$

The solution of equation (224) gives three roots $\xi_1 = -\sqrt[3]{A}$, $\xi_{2,3} = \frac{1}{2}\left(1 \pm i\sqrt{3}\right)\sqrt[3]{A}$.

As a consequence, the state corresponding to the root $\xi_2 = \frac{1}{2}\left(1 + i\sqrt{3}\right)\sqrt[3]{A}$ grows with growing z, which indicates the presence of instability in a beam [189]. In this case $Im\, k_z = Im\, \xi_2 \sim \sqrt[3]{\rho}$.

Note here that the photonic crystal built from metallic threads has the refractive index $n_0 < 1$ for a wave with the electric polarizability parallel to the threads, i.e., in this case the Cherenkov instability of the beam does not exist [87] (but if the electric vector of the wave is orthogonal to the metallic threads, the refractive index is $n_0 > 1$, so for such a wave the Cherenkov instability exists [165]).

It should be pointed out, however, that, unlike an infinite photonic crystal, the field in the crystal placed into the waveguide has a mode character, and so the presence of κ_{mn}^2 in the denominator of equation (223) results in reduction of the radicand in (223) to the magnitude smaller than unity even when $n_0^2 > 1$. Hence, $u > c$, which is impossible. Consequently, the radiative instability of

the above type in the waveguide can arise under the condition $n_0^2 - \frac{\kappa_{mn}^2 c^2}{\omega^2} > 1$ rather than $n_0^2 > 1$.

Suppose now that in the photonic crystal the conditions can be realized under which the wave amplitude $C_{mn}\left(\vec{k}_{mn} + \vec{\tau}\right)$ is comparable with the amplitude $C_{mn}\left(\vec{k}_{mn}\right)$. By analogy with the standard diffraction theory for an infinite crystal [165,15], in the case under consideration, when $\chi << 1$, it is sufficient that only the equations for these amplitudes remain in (217).

To be specific, let us further consider a photonic crystal formed by parallel threads. Also assume that they are parallel to the waveguide boundary (y, z).

Analysis of diffraction of a λ-type wave with the electric vector in the plane (y, z) (a TM-wave) gives

$$\left[k_{mn}^2 - \frac{\omega^2}{c^2}\varepsilon\right] C^{\lambda}\left(\vec{k}_{mn}, \omega\right) - \frac{\omega^2}{c^2}\chi_{mn}^{\lambda\lambda}\left(-\vec{\tau}\right) C^{\lambda}\left(\vec{k}_{mn} + \vec{\tau}, \omega\right) = 0 \qquad (225)$$

$$\left[\left(\vec{k}_{mn} + \vec{\tau}\right) - \frac{\omega^2}{c^2}\varepsilon_0\right] C^{\lambda}\left(\vec{k}_{mn} + \vec{\tau}, \omega\right) - \frac{\omega^2}{c^2}\chi_{mn}^{\lambda\lambda}\left(\vec{\tau}\right) C^{\lambda}\left(\vec{k}_{mn}, \omega\right) = 0.$$

Since the term containing $\left(\omega - \left(\vec{k} + \vec{\tau}\right)\vec{u}\right)^{-1}$ is small when $\left(\omega - \vec{k}\vec{u}\right)$ vanishes, in the second equation it is dropped.

The dispersion equation defining the relation between k_z and ω is obtained by equating to zero the determinant of the system (225) and has a form:

$$\begin{aligned}&\left[\left(k_{mn}^2 - \tfrac{\omega^2}{c^2}\varepsilon_0\right)\left(\left(\vec{k}_{mn} + \vec{\tau}\right)^2 - \tfrac{\omega^2}{c^2}\varepsilon_0\right) - \tfrac{\omega^4}{c^4}\chi_{\tau}\chi_{-\tau}\right](\omega - k_z u)^2 = \\ &-\tfrac{\omega_L^2}{\gamma c^4}\left\{\tfrac{1}{2\pi}\left|\int \vec{u}\,\vec{Y}_{mn}^{\lambda}\left(\vec{k}_{\perp}, k_z\right) d^2 k_{\perp}\right|^2\right\}\left(k_{mn}^2 c^2 - \omega^2\right)\left(\left(\vec{k}_{mn} + \vec{\tau}\right)^2 - \tfrac{\omega^2}{c^2}\varepsilon_0\right).\end{aligned} \qquad (226)$$

Because the right-hand side of the equation is small, one can again seek the solution near the points where the right-hand side is zero that corresponds

the condition of occurrence of the Cherenkov radiation and excitation of the wave which can propagate in the waveguide:

$$\begin{array}{l}\left(k_z^2-\left(\frac{\omega^2}{c^2}\varepsilon_0-\kappa_{mn}^2\right)\right)\left(\left(k_z+\tau\right)^2-\left(\frac{\omega^2}{c^2}\varepsilon_0-\left(\vec{\kappa}_{mn}+\vec{\tau}_\perp\right)^2\right)\right)-\frac{\omega^4}{c^4}\chi_\tau\chi_{-\tau}=0\\ \left(k_z-\frac{\omega}{u}\right)^2=0\end{array} \tag{227}$$

The roots of equations are sought near the conditions $k_{mn}^2\approx\left(\vec{k}_{mn}+\vec{\tau}\right)$,

$$k_z=k_{z0}+\xi,\quad k_z^2=k_{z0}^2+2k_{z0}\xi+\xi^2,\quad k_{z0}^2=\frac{\omega^2}{c^2}\varepsilon_0-\kappa_{mn}^2;\quad k_{z0}=\frac{\omega}{c}\sqrt{\varepsilon_0-\frac{\kappa_{mn}^2c^2}{\omega^2}} \tag{228}$$

$$\left(k_z+\tau_z\right)^2=\left[\left(k_{0z}+\tau_z\right)+\xi\right]^2=\left(k_{0z}+\tau_z\right)^2+2\left(k_{0z}+\tau_z\right)\xi+\xi^2$$

Hence,

$$\begin{array}{l}\left(k_{0z}+\tau_z\right)^2+\left(\vec{\kappa}_{mn}+\vec{\tau}_\perp\right)^2+2\left(k_{0z}+\tau_z\right)+2\left(k_{0z}+\tau_z\right)\xi+\xi^2=\\ \left(\vec{k}_{mn}+\vec{\tau}\right)^2+2\left(k_{0z}+\tau_z\right)\xi+\xi^2=k_{0mn}^2+2\vec{k}_{0mn}\vec{\tau}+\tau^2+2\left(k_{0z}+\tau_z\right)\xi+\xi^2.\end{array} \tag{229}$$

And one can get

$$\begin{array}{l}2k_{0z}\xi\left(2\left(k_{0z}+\tau_z\right)\xi+\left(2\vec{k}_{0mn}\vec{\tau}+\tau^2\right)\right)-\frac{\omega^4}{c^4}\chi_\tau\chi_{-\tau}=0\\ 4k_{0z}\left(k_{0z}+\tau_z\right)\xi^2+2k_{0z}\left(2\vec{k}_{0mn}\vec{\tau}+\tau^2\right)\xi-\frac{\omega^4}{c^4}\chi_\tau\chi_{-\tau}=0\\ \xi^2+\frac{\left(2\vec{k}_{0mn}\vec{\tau}+\tau^2\right)}{\left(k_{0z}+\tau_z\right)}\xi-\frac{\omega^4}{c^4}\frac{\chi_\tau\chi_{-\tau}}{4k_{0z}\left(k_{0z}+\tau_z\right)}=0\\ \xi_{1,2}=-\frac{\left(2\vec{k}_0\vec{\tau}+\tau^2\right)}{4\left(k_{0z}+\tau_z\right)}\pm\sqrt{\left(\frac{2\vec{k}_0\vec{\tau}+\tau^2}{4\left(k_{0z}+\tau_z\right)}\right)^2+\frac{\omega^4}{c^4}\frac{\chi_\tau\chi_{-\tau}}{4k_{0z}\left(k_{0z}+\tau_z\right)}}\end{array} \tag{230}$$

If $\left(k_{0z}+\tau_z\right)=-\left|k_{0z}+\tau_z\right|$, the root can cross the zero point. At the same

time, the second equation should hold

$$\omega - k_z u = \omega - k_{0z} u - \xi u = 0.$$

Consequently,

$$\xi = \frac{\omega - k_{0z} u}{u} = \frac{\omega}{u} - k_{0z} = \frac{\omega}{u} - \frac{\omega}{c}\sqrt{\varepsilon_0 - \frac{\kappa_{mn}^2 c^2}{\omega^2}}.$$

If $\varepsilon_0 < 1$, then $\xi = \frac{\omega}{u}\left(1 - \beta\sqrt{\varepsilon_0 - \frac{\kappa_{mn}^2 c^2}{\omega^2}}\right) > 0$, $\xi = \frac{\omega}{u} - k_{0z}$

Let the roots ξ_1 and ξ_2 coincide ($\xi_1 = \xi_2$). This is possible at point

$$\frac{2\vec{k}_0\vec{\tau} + \tau^2}{4\left(k_{0z} + \tau_z\right)} = \pm\frac{\omega^2}{c^2}\frac{\sqrt{\chi_\tau \chi_{-\tau}}}{\sqrt{4k_{0z}\left|k_{0z} + \tau_z\right|}},$$

here $k_{0z} + \tau_z < 0$.

The roots coincide when the following equality is fulfilled

$$\frac{\omega}{u} - k_{0z} = \mp\frac{\omega^2}{c^2}\frac{\sqrt{\chi_\tau \chi_{-\tau}}}{\sqrt{4k_{0z}\left|k_{0z} + \tau_z\right|}},$$

i.e.,

$$\frac{\omega}{u} = k_{0z} \mp \frac{\omega^2}{c^2}\frac{\sqrt{\chi_\tau \chi_{-\tau}}}{\sqrt{4k_{0z}\left|k_{0z} + \tau_z\right|}} \quad \text{and} \quad k_{0z} = \frac{\omega}{c}\sqrt{\varepsilon_0 - \frac{\kappa_{mn}^2 c^2}{\omega^2}}$$

Let $\varepsilon_0 < 1$, then $\frac{\omega}{u} > k_{0z}$ (since $u < c$), the situation for the solution $\frac{\omega}{u} = k_{0z} - \frac{\omega^2}{c^2}\frac{\sqrt{\chi_\tau \chi_{-\tau}}}{\sqrt{4k_{0z}|k_{0z}+\tau_z|}}$ gets complicated and the Vavilov-Cherenkov condition is not fulfilled.

Now let us consider the solution $\frac{\omega}{u} = k_{0z} + \frac{\omega^2}{c^2}\frac{\sqrt{\chi_\tau \chi_{-\tau}}}{\sqrt{4k_{0z}|k_{0z}+\tau_z|}}$. At $\tau_z < 0$ the difference $k_{0z} + \tau_z$ can be reduced so that the sum on the right would appear to become equal to $\frac{\omega}{u}$, and so one could obtain 4 coinciding roots.

Interestingly enough, for backward diffraction, which is a typical case of frequently used one-dimensional generators with a corrugated metal waveguide (the traveling-wave tube, the backward-wave tube), such a coincidence of roots is impossible.

Indeed, let the roots ξ_1 and ξ_2 coincide. In this case for the backward Bragg diffraction $|\tau_z| \approx 2k_{0z}$, $\tau_z < 0$. Then by substituting the expressions for $k_{0z} = \frac{\omega}{c}\sqrt{\varepsilon_0 - \frac{\kappa_{mn}^2 c^2}{\omega^2}}$ and $\varepsilon_0 = n_0^2 = 1 + \chi_{mn}^{\lambda\lambda}(0)$ and retaining the first-order infinitesimal terms, the relation $\frac{\omega}{u} \approx k_{0z} + \frac{\omega^2}{c^2}\frac{|\chi_\tau|}{2k_{0z}}$ can be reduced to the form $\frac{\omega}{u} \approx \frac{\omega}{c}\left(1 - \frac{\left|\chi_{mn}^{\lambda\lambda}(0)\right|}{2} - \frac{\kappa_{mn}^2 c^2}{2\omega^2} + \frac{\omega}{c}\frac{|\chi_\tau|}{2}\right) < \frac{\omega}{u}$, i.e., the equality does not hold and the four-fold degeneracy is impossible. Only ordinary three-fold degeneration is possible.

However, if $\varepsilon_0 > 1$ and is appreciably large, then in a one-dimensional case, the four-fold degeneracy of roots is also possible in a finite photonic crystal [1].

Thus, the left-hand side of equation (226) has four roots ξ_1, ξ_2, and a double degenerated root ξ_3. Hence, equation (226) can be written as follows:

$$(\xi - \xi_1)(\xi - \xi_2)(\xi - \xi_3)^2 = B.$$

If the roots coincide ($\xi_1 = \xi_2 = \xi_3$), one obtains $(\xi - \xi_1)^4 = B$,, i.e., $\xi - \xi_1 = \sqrt[4]{B}$.

The fourth root of B has imaginary solutions depending on the beam density as $Imk_z \sim \rho_0^{1/4}$ (the parameter $B \sim \omega_L^2$, i.e., $B \sim \rho_0$, see the right-hand side

[1] The authors are grateful to K. Batrakov, who drew our attention to the fact that for an infinite crystal with $\varepsilon_0 > 1$, the intersection of roots is possible in a one-dimensional case.

of (226)). This increment is larger than the one we obtained for the case of the three-fold degeneracy.

The analysis shows that with increasing number of diffracted waves, the law established in [25,49,186] is valid: the instability increment appears to be proportional to $\rho^{\frac{1}{s+3}}$, where s is the number of waves emerging through diffraction. As a result, the abrupt decrease in the threshold generation current also remains in this case (the threshold generation current $j_{th} \sim \frac{1}{(kL)^3(k\chi_\tau L)^{2s}}$, where L is the length of the interaction area).

It is interesting that according to [117], for a photonic crystal made from metallic threads, the coefficients $\chi(\tau)$, defining the threshold current and the growth of the beam instability, are practically independent on τ up to the terahertz range of frequencies because the diameter of the thread can easily be made much smaller than the wavelength. That is why photonic crystals with the period of about 1 mm can be used for lasing in terahertz range at high harmonics (for example, photonic crystal with 3 mm period provides the frequency of the tenth harmonic of about 1 terahertz (λ=300 micron).

The analysis of laser generation in VFEL with a photonic crystal when the beam moves in an undulator (electromagnetic wave) located in a finite crystal, made similarly to the above analysis, shows that in this case the dispersion equation and the law of instability also have the same form as in the case of an infinite crystal. The procedure for going from the dispersion equations describing instability in the infinite case (217) is similar to that discussed earlier in this paper. It consists in replacing the continuous $\vec{k}$ by the quantified values of $\vec{k}_{mn}$ and redefining the coefficients appearing in equations like (217).

It is important to emphasize the general character of the rules found in this

paper for obtaining dispersion equations that describe the radiative instability of the electron beam in a finite photonic crystal. In particular, they are valid for describing the processes of instability of an electromagnetic wave in finite nonlinear photonic crystals.

25 Hybrid systems with virtual cathode for high power microwaves generation ([166])

The interest for high power microwave (HPM) sources has emerged in recent years due to revealing new applications and offering novel approaches to existing ones.

Vacuum electronic sources, which convert the kinetic energy from an electron beam into the electromagnetic field energy, are a natural choice for generating HPM.

The high current density electron beam, once generated, propagates through an interaction region, which converts the beam's kinetic energy to HPM. It is the particular nature of the interaction that distinguishes various classes of sources.

High power HPM sources generating high electromagnetic power density require the high power densities in the electron beams, where space-charge effects are essential.

When the magnitude of the current I_b of an electron beam injected into a drift tube exceeds the space-charge-limiting current I_{limit}, an oscillating virtual cathode (VC) is formed [167,168].

According to [167], the following formula gives a good approximation for the space-charge-limiting current:

$$I_{limit}(kA) = \frac{mc^3}{e} G(\gamma^{2/3} - 1)^{3/2} \tag{231}$$

where m and e are the mass and the charge of an electron, c is the speed of light, γ is the Lorentz factor of the electron beam and G depends on the geometry [167,169]. For example, for an annular electron beam in a cylindrical drift tube G reads as follows [169]:

$$G = \frac{1}{(\frac{r_b - r_b^{in}}{r_b} + 2\ln\frac{R}{r_b})(1 - sech\frac{\mu_1 L}{2R})}, \tag{232}$$

where r_b and r_b^{in} are the outer and inner radius of the electron beam, R and L are the radius and length of the cylindrical drift tube and μ_1 is the first root of the Bessel function $J_0(\mu) = 0$.

When the oscillating virtual cathode is formed, two types of electrons exist: those oscillating in the vircator potential well and passing through the vircator area (see Figure 26).

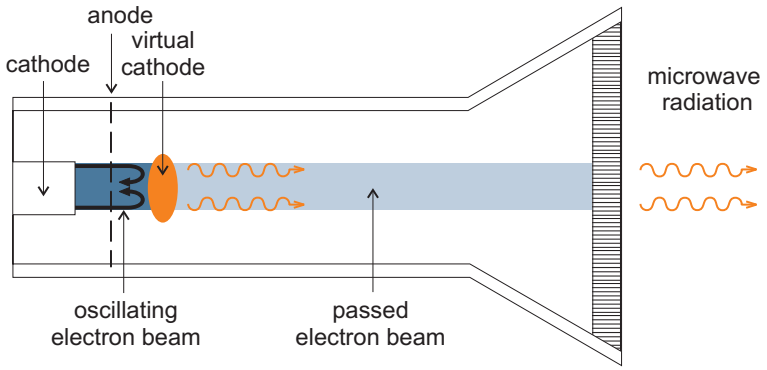

Figure 26. An oscillator with virtual cathode

For electrons oscillating in the area "cathode-anode-virtual cathode", two radiation mechanisms provide a radio-frequency signal [172]:

1. one radiation mechanism originates from the oscillations of the reflected electrons about the anode foil (electron oscillations in the potential well "cathode-anode-virtual cathode"). A microwave signal is generated at a frequency of roughly $\frac{c}{2d_d}$, where d_d is the anode-to-cathode spacing.

2. The other radiation mechanism is the oscillation of the virtual cathode at a frequency near the plasma frequency ω_p of the space charge density that is formed. That is

$$\omega_p = \sqrt{\frac{4\pi n_e e^2}{m}} \tag{233}$$

where n_e is the number density of the electrons in the space charge configuration (in the plane of the anode grid) [172].

The essence of the above radiation mechanisms is bremsstrahlung radiation ensuing from electron deceleration.

It should be emphasized that bremsstrahlung radiation from electrons oscillating in an electron beam with a virtual cathode is accompanied by transition radiation, which is originated by electron velocity rather than acceleration. Use of a photonic crystal enables one to construct several types of hybrid systems with a virtual cathode, which could radiate due to different radiation mechanisms (bremsstrahlung and diffraction (transition) radiation) with different frequencies.

In vircator systems, a grid cathode and anode (or anodes) are commonly used [169,170,171,173]. The electron beam oscillates, making electrons periodically cross the grid anodes and cathode (see, for example [171]). It is transition radiation that occurs when electrons pass through a border between two media

with different indices of refraction. It is worth noting that periodical excitement of transition radiation from electrons oscillating in vircator is similar to diffracted radiation from a charged particle in a periodic structure. As a result, in a system with oscillating virtual cathode, the vircator radiation, which is actually the electron beam bremsstrahlung, is accompanied by radiation excited by the additional mechanism due to transition (diffraction) radiation from oscillating current passing through the grid anodes (cathode).

Let us turn to that part of the beam, which passes through the virtual cathode area. Recall that the oscillation of the virtual cathode can produce a highly modulated electron beam, and, as a result, the energy from the bunched transmitted beam can be recovered using slow-wave structures [174].

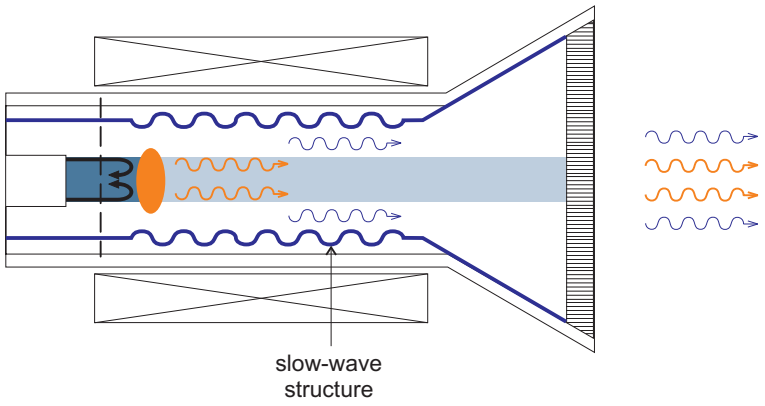

Figure 27. Hybrid system "vircator + travelling wave tube" [174]

Interaction of the electron beam with the slow-wave structure in, for instance, a conventional TWT poses special challenges: interaction is sufficiently effective only for electrons moving at the distance δ from the slow-wave structure surface

$$\delta \leq \frac{\lambda\beta\gamma}{4\pi}, \tag{234}$$

δ is the so-called beam impact parameter, λ is the radiation wavelength, $\beta =$

v/c , v is the electron beam velocity, γ is the electron Lorentz-factor. For example, for electrons with the energy of 250 keV ($\beta = 0.74$ and $\gamma = 1.49$) and the radiation wavelength $\lambda = 10mm$ (frequency 30 GHz), the impact parameter $\delta \approx 0.9mm$. It means that for efficient radiation generation by the annular electron beam with the thickness $\Delta \leq \delta$ only a part of the beam would contribute to radiation.

As we showed in [87,89,103,112,117,175,176,177], this challenge can be overcome by applying a photonic crystal, formed by metal grids (grid traveling wave tube (grid TWT), grid volume free electron laser(grid VFEL)).

What is more, in accordance with [178,179,180], the application of metal inserts (meshes, grids and so on) inside a resonator enables increasing the electron beam limit current.

Therefore, in the grid TWT (grid VFEL), the presence of the metal grid (photonic crystal) serves both for forming the resonator, where interaction of the beam and radiation occurs, and for potential balancing that makes it possible to increase the beam vacuum limit current.

And for the grid TWT (grid VFEL) with the supercritical current, the electron beam executes compound motion exciting two radiation mechanisms contributing to radiation: bremsstrahlung of oscillating electrons and diffraction (transition) radiation from downstream electrons interacting with the periodic grid structure(photonic crystal).

This means that the hybrid system "vircator + grid TWT (grid VFEL)" arise by analogy with the system described in [174], where several vircators could appear due to the presence of several anode grids (see also [169]). But in

contrast to the system [169], the hybrid system "vircator + grid TWT (grid VFEL)" uses periodically placed grids with either constant [112,175,176] or variable period [177].

The frequency of diffracted radiation excited by an electron beam in a periodic structure with the period d is determined by the condition

$$\omega - \vec{k}n(k)\vec{v} = \vec{\tau}\vec{v} \ , \tag{235}$$

where $\vec{v}$ is the electron beam velocity, $\vec{\tau}$ is the reciprocal lattice vector ($|\vec{\tau}| = \frac{2\pi p}{d}$), $n(k)$ is the refraction index of a periodic structure, p is an integer number ($p = 1, 2, 3, ...$).

When the electron beam velocity $\vec{v}$ is parallel to the reciprocal lattice vector $\vec{\tau}$, (235) reads [117]

$$\omega = \frac{2\pi p \cdot v}{d(1 - \beta n(\omega, k)\cos\theta)} \tag{236}$$

Essentially, a photonic crystal in the grid TWT (grid VFEL) is transparent to radiation as well as to an electron beam (see Figure 28). Moreover, several diffracted waves could exist in a photonic crystal (see Figure 28)d, which makes it possible to introduce a feedback in such a system at the frequency of diffracted radiation and, hence, to couple several hybrid "vircator + grid TWT (VFEL)" generators making a phase-locked source, in which diffracted waves from one photonic crystal (grid resonator) excites oscillations in the neighbor resonators.

The proposed grid systems drastically differ from the system described in [169], where several grids serve only for forming several vircators (see Figure

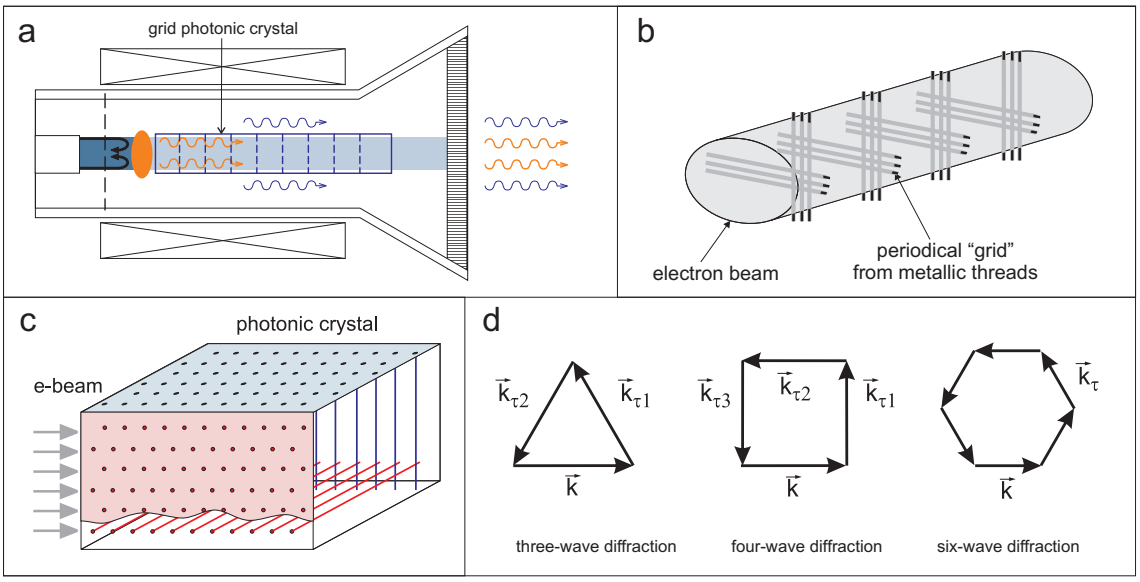

Figure 28. Grid TWT (grid VFEL) and photonic crystal arrangement 29).

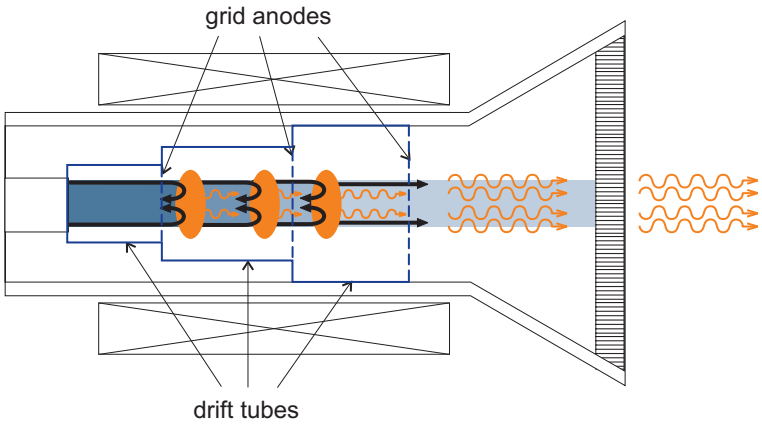

Figure 29. Several vircators [169]

Of course, radiation from a hybrid generator ”vircator + grid TWT (VFEL)” can be excited by several electron beams similar to a phase-locked array.

The bunched electron beam, which has passed through the virtual cathode area, can also be used for excitation of free electron laser (ubitron) (see Figure 30) oscillation contributing to the radiation power.

Thus, the use of a photonic crystal enables one to construct several types

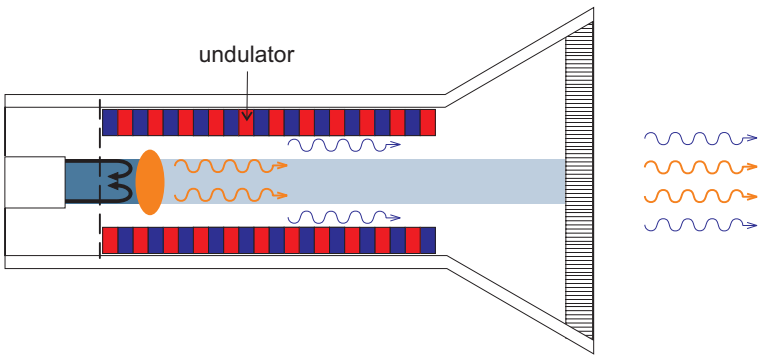

Figure 30. Hybrid system "vircator + undulator FEL"

of hybrid systems with virtual cathode, which could radiate due to different radiation mechanisms (bremsstrahlung and diffraction (transition) radiation) with different frequencies. The photonic crystal makes it possible to create a phase-locked array of generators.

26 Volume Free Electron Laser (VFEL) as a new trend in development of high-power tunable radiation sources: review of theoretical background and experiments in millimeter range

To conclude, let us mark the most important results obtained in investigation of the VFEL. Use of non one-dimensional distributed feedback in vacuum electronic devices enables frequency tuning in a wide range and removes limits for available output power. It also solves a problem of development of highly stable mode-selective overmoded resonators, which open up new avenues for extending the operating frequencies of all classes of microwave vacuum electronic devices.

New advances in different areas require the development of tunable, wideband, high-power sources of coherent electromagnetic radiation in gigahertz, terahertz and higher frequency ranges. Conventional electron vacuum devices

have restricted the possibility of frequency tuning (usually it does not exceed 5-10%) for the certain carrier frequency at certain e-beam energy. They also have power limits because high levels of power density inside the system cause sparkovers and damage of mirrors.

Volume free electron laser (VFEL) [25,87,181] was proposed as a new type of a tunable high-power source of electromagnetic radiation.

The most essential feature of the FEL and other types of generators is a feedback, which is formed by a system of mirrors, or distributed feedback based on diffraction in a spatially periodic medium, when wave vectors of transmitted and reflected waves are colinear. The distinction of volume FEL (VFEL) is non-one-dimensional multi-wave volume distributed feedback (VDFB). Use of a non one-dimensional distributed feedback in vacuum electronic devices gives the possibility of frequency tuning in a wide range and removes limits for available output power. It also solves a problem of development of highly stable mode-selective overmoded resonators, which open up new avenues for extending the operating frequencies of all classes of microwave vacuum electronic devices.

It is well known that each radiative system is defined by its eigenmodes and by the so-called dispersion equation, which in the case of small perturbations (linear regime) describes possible types of waves in a system and relation between frequency and wave number of the system eigenmodes. Thorough analysis of FEL dispersion equation [108] shows that:

1. dispersion equation for FEL in collective regime coincides with that for conventional traveling wave tube amplifier (TWTA) [109];

2. FEL gain (increment of electron beam instability) is proportional to $\rho^{1/3}$,

where ρ is the electron beam density.

But the law of instability of the electron beam can essentially change at passing through a spatially periodic medium. This fact was first indicated in [49]. Dispersion equations were obtained and investigated for conditions of multi-wave diffraction. It was shown that there is a new law of electron beam instability at the points of diffraction roots degeneration. The amplification and generation gain of the electromagnetic wave are sharply changed at these points.

This result is also valid for an electron beam, which moves in vacuum close to the surface of a spatially periodic medium [25] (or in a vacuum slot made inside a periodic medium).

First lasing of the VFEL was reported at FEL 2001 [181].

26.1 Volume FEL distinctive features

The advantages of VFEL are exhibited in a wide spectral range from microwaves to X-rays [55,87,110]. Frequency tuning, possibility to use wide electron beams (several e-beams) and reduction of threshold current density necessary for the start of generation provided by VFEL, make it a basis for development of more compact, high-power and tunable radiation sources than conventional electron vacuum devices could let.

Benefits given by VFEL:

1. Volume FEL provides frequency tuning by rotation of diffraction grating;

2. Use of multi-wave diffraction reduces generation threshold and the size of

the generation zone. The starting current j depends on interaction length L as [55]: $j_{start} \sim 1/\{(kL)^3(k\chi_\tau L)^{2s}\}$, s is the number of surplus waves appearing due to diffraction (for example, in the case of two-wave Bragg diffraction $s = 1$, for three-wave diffraction $s = 2$, and so on).

3. Wide electron beams and diffraction gratings of large volumes can be used in VFEL. Two or three-dimensional diffraction gratings allow one to distribute the interaction over a large volume and to overcome power restrictions in a resonator. Volume distributed feedback provides mode discrimination in a VFEL resonator.

4. VFEL can simultaneously generate radiation at several frequencies.

References

[1] M.L. Goldberger and R.M. Watson *Collision Theory* (Wiley, New York, 1984).

[2] V.G. Baryshevsky *Nuclear Optics of Polarized Media* (Energoatomizdat, Moscow, 1995) [in Russian].

[3] Chang Shih-Lin, *Multiple Diffraction of X-Rays in Crystals* (Springer-Verlag Berlin Heidelberg New-York Tokyo, 1984).

[4] V.G. Baryshevsky, Pis'ma Zh. Tekh. Fiz.**2** (1976) 112-114; V.G. Baryshevsky, Zh.Exp.Teor Fiz. **70** (1976) 430-434[Sov. Phys. JETP].

[5] V.G. Baryshevsky *Nuclear Optics of Polarized Media* (Energoatomizdat, Moscow, 1995) [in Russian].

[6] P.M. Morse, H. Feshbach *Methods of Theoretical Physics* (Mc Graw Hill, New York, 1953),

[7] V.G. Baryshevsky, Zh.Exper.Teor Fiz. **67** (1974) 1651-1659 [Sov. Phys. JETP **40** (1975) 821].

[8] V.G.Baryshevsky, I.D. Feranchuk, J. Physiq. **44** (1983) 913-922.

[9] V.G. Baryshevsky, V.V. Tikhomirov, Sov. Phys.-Uspekhi **32**, 11, (1989) 1013-1032 [Uspekhi Fiz. Nauk **159** (1989) 529-565].

[10] V.G. Baryshevsky, I.Ya. Dubovskaya, Phys. Status Solidi **B 82** (1977) 403.

[11] V.G. Baryshevsky, A.O. Grubich, I.Ya. Dubovskaya, Phys. Status Solidi **B 88** (1978) 351.

[12] V.G. Baryshevsky, A.O. Grubich, I.Ya. Dubovskaya, Phys. Status Solidi **B 99** (1980) 205.

[13] V.G. Baryshevsky, A.O. Grubich, I.Ya. Dubovskaya, Phys. Lett. **A 77** (1980) 61.

[14] M.L. Ter-Mikaelian *High Energy Electromagnetic Processes in Condensed Media* (Interscience Tracts in Physics and Astronomy, Vol 29, Willey, New York, 1972).

[15] R.W. James *The Optical Principles of the Diffraction of X-rays* (Ox Bow Press, 1982)

[16] J.D. Jackson *Classical Electrodynamics*, 3rd ed. (Wiley, 1998)

[17] V.G. Baryshevsky *Channeling, Radiation and Reactions in Crystals at High Energy* (Bel. State Univers., Minsk, 1982)

[18] L.M. Frank *Vavilov-Cherenkov Radiation. Theoretical Questions* (Nauka, Moscow, 1988)

[19] V.G. Baryshevsky and I.Ya. Dubovskaya, Dokl. Akad. Nauk SSSR **231** (1976) 1336.

[20] V.G. Baryshevsky, I.Ya. Dubovskaya, J. Phys. Solid State Phys. **C 16**, 19 (1983) 3663-3672.

[21] V.G. Baryshevsky, O.T. Gradovsky and I.Ya. Dubovskaya, Izv. Akad. Nauk Bel.SSR Ser. Fiz-math., **6** (1987) 77.

[22] O.T. Gradovsky, Phys. Lett. **A 126** (1988) 291.

[23] V. G. Baryshevsky and I. Ya. Dubovskaya, Journal of Physics: Condensed Matter **3**, n 14 (1991) 2421-2430.

[24] A.O. Grubich and O.M. Lugovskaya, Izv. Akad. Nauk Bel.SSR, Ser. Fiz-math., **1** (1991) 61.

[25] V.G. Baryshevsky, Dokl. Akad. Nauk SSSR **299**, 6, (1988) 1363-1365.

[26] V.G. Baryshevsky in : *Some Problems of Modern Physics to 80-th Anniversary of I.M. Frank* (Nauka, Moscow, 1989) 156.

[27] V.G. Baryshevsky and I.Ya. Dubovskaya, Phys. Status Solidi [in Russian] **19** (1977) 597.

[28] A.V. Andreev, Sov. Phys. Usp. **28** (1985) 7084.

[29] A.A. Andriyanchik, I.Ya. Dubovskaya and A.N. Kaminsky, J. Phys. **C 3** (1991) 5579.

[30] A.A. Andriyanchik, V.G. Baryshevsky and A.N. Kaminsky, Pis'ma v zhur. Tekh. Fiziki **17** (1991) 53.

[31] A.A. Andriyanchik, V.G. Baryshevsky and A.N. Kaminsky, Physica Status Solidi (b) **184**, 2, (1994) 543-551.

[32] A.A. Andriyanchik, V.G. Baryshevsky and A.N. Kaminsky, Nucl. Instr. Methods **B 83**, 4, (1993) 482-494.

[33] V.G. Baryshevsky, Izv. Akad. Nauk Bel.SSR, Ser. Fiz-math. **3** (1980) 117-122.

[34] V.G. Baryshevsky in : *Abstr. 16-th Conf. on the Physics of Interaction of Charged Prticles with Crystals* (Moscow, 1986) 53.

[35] V.G. Baryshevsky and I.V. Polikarpov, Izv. Akad. Nauk Bel.SSR, ser. fiz-mat. **2** (1988) 86.

[36] V.G. Baryshevsky and I.V. Polikarpov, Zh. Eksp. Teor. Fiz. **94** (1988) 109.

[37] V.G. Baryshevsky and I.V. Polikarpov, Izv. Bel. Univers. Ser. 1 **1** (1989) 8.

[38] V.G. Baryshevsky and I.V. Polikarpov, Phys. Lett. **A 190** (1989) 205.

[39] V.G. Baryshevsky and I.V. Polikarpov, Izv. Akad. Nauk Bel.SSR, ser. fiz-mat. **2** (1989) 81.

[40] I.V. Polikarpov and V.V. Skadorov, Phys. Status Solidi **B 143** (1987) 11.

[41] I.V. Polikarpov and V.V. Skadorov, Izv. Akad. Nauk Bel.SSR, Ser. Fiz-math. **6** (1978) 95.

[42] I.V. Polikarpov and V.V. Skadorov, Izv. Akad. Nauk Bel.SSR, Ser. Fiz-math. **3** (1988) 83.

[43] I.Ya. Dubovskaya and Truong Ba Ha, Izv. Bel. Univers. Ser. 1 **1** (1988) 11.

[44] A.O. Grubich and O.M. Lugovskaya, Izv. Akad. Nauk Bel.SSR Ser. Fiz-energ. **3** (1991) 61.

[45] A.A. Andriyanchik and A.I. Kaminsky, Izv. Bel. Univers. Ser. 1 **2** (1988) 54.

[46] V.G. Baryshevsky and I.D. Feranchuk in: *Dokl. 11-th Conf. on the Physics of Interaction of Charged Prticles with Crystals* (Moscow, 1982) 208.

[47] V.G. Baryshevsky and I.D. Feranchuk, Dokl. Akad. Nauk Bel.SSR **27** (1983) 995.

[48] V.G. Baryshevsky and I.D. Feranchuk, Dokl. Akad. Nauk Bel.SSR **28** (1984) 336.

[49] V.G. Baryshevsky and I.D. Feranchuk, Phys. Lett. **A 102** (1984) 141.

[50] V.G. Baryshevsky and I.D. Feranchuk, Izv. Akad. Nauk Bel.SSR, Ser. Fiz-math. **2** (1985) 79.

[51] V.G. Baryshevsky, I.Ya. Dubovskaya and I.D. Feranchuk, Izv. Akad. Nauk Bel.SSR, Ser. Fiz-math. **1** (1988) 92-97.

[52] V.G. Baryshevsky, K.G. Batrakov and I.Ya. Dubovskaya in : *Dokl. 19-th Conf. on the Physics of Interaction of Charged Prticles with Crystals* (Moscow, 1990) 105.

[53] K.G. Batrakov and I.Ya. Dubovskaya, Izv. Akad. Nauk Bel.SSR, Ser. Fiz-math. **5** (1990) 82.

[54] V.G. Baryshevsky, K.G. Batrakov and I.Ya. Dubovskaya, Izv. Akad. Nauk Bel.SSR Ser. Fiz-energ. **1** (1991) 53.

[55] V.G. Baryshevsky, K.G. Batrakov and I.Ya. Dubovskaya, J. Phys. Appl. Phys. **D 24** (1991) 1250.

[56] V.G. Baryshevsky, I.Ya. Dubovskaya and A.V. Zege in : *Dokl. 19-th Conf. on the Physics of Interaction of Charged Prticles with Crystals* (Moscow, 1990) 102.

[57] V.G. Baryshevsky, I.Ya. Dubovskaya and A.V. Zege, Nucl. Instr. Methods **A 135** (1990) 368.

[58] V.G. Baryshevsky, I.Ya. Dubovskaya and A.V. Zege, Izv. Akad. Nauk Bel.SSR Ser. Fiz-energ., **3** (1990) 49.

[59] V.G. Baryshevsky, I.Ya. Dubovskaya and A.V. Zege, Phys. Lett. **A 149** (1990) 30-34.

[60] V.G. Baryshevsky and I.Ya. Dubovskaya, Izv. Akad. Nauk Bel.SSR Ser. Fiz-energ., **1** (1990) 30-36.

[61] A. Fridman, A. Gover, G. Kurizki, et. al, Rev. Mod. Phys. **60** (1988) 471.

[62] G. Kurizki in: *Relativistic Channeling*, Eds. R.A. Carrigan and S.A. Ellison (M.Y. Plenum Press, 1987) 505.

[63] S.A. Bogaez and J.B. Ketterson, J. Appl. Phys. **60** (1986) 177.

[64] M. Strauss, P. Amend, N. Rostoker and A. Ron, Appl. Phys. Lett. **52** (1988) 866.

[65] M. Strauss and N. Rostoker, Phys. Rev. **A 39** (1989) 579.

[66] M.A. Piestrup and P.E. Finman, IEEE J. Of Quantum Electronics **QE-19** (1983) 357.

[67] M.A. Piestrup, IEEE J. Of Quantum Electronics **QE-24** (1988) 591.

[68] M.A. Yariv, Appl. Phys. **24** (1974) 105.

[69] R. Kompfner, Wireless World **52** (1946) 369.

[70] R. Pierce, Proc. of the IRE **35**, 2, (1947) 111.

[71] S.J. Smith and E.M. Purcell, Phys. Rev. **92** (1953) 1069.

[72] W.W. Salisbury, US Patent 2,634,372 (1953).

[73] W.W. Salisbury, J.Opt. Soc. Am. **60**, 10, (1970) 1279-1284.

[74] G. Doucas, J.H. Mulvey, M.Omori, J.Walsh and M.F.Kimmit, Phys.Rev.Lett. **69** (1992) 1761.

[75] John E. Walsh US Patent 5,790,585 (1996).

[76] B. M. Bolotovskii and G. V. Voskresenskii, Usp. Fiz. Nauk. **88** (1966) 209. (Sov. Phys. Usp. **9** (1966) 73).

[77] F.S. Rusin and G.D. Bogomolov, JETP Lett. **4** (1966) 160.

[78] F.S. Rusin and G.D. Bogomolov, (USSR inventors certificate no.195557 (1967));

[79] F.S. Rusin and G.D. Bogomolov, Proc. IEEE **57** (1969) 720.

[80] K.Mizuno, S.Ono and Y. Shibata, IEEE Trans. Electron Devices **ED-20** (1973) 749 .

[81] R. P. Leavitt et al., IEEE Jour. Quant. Electr. **QE-17**, no.8, (1981) 1333.

[82] D. E. Wortman et al., IEEE Jour. Quant. Electr. **QE-17**, 8, (1981) 1341.

[83] D. E. Wortman and R. P. Leavitt, *Infrared and Millimeter Waves: Coherent Sources and Applications*, Part II', Vol. 7, chapter 7, 321-375 (editted by K.J. Button, Academic Press, New York, 1983);

[84] D. E. Wortman, C.A. Morrison and R. P. Leavitt, US Patent 4,545,056 (1985).

[85] V.G. Baryshevsky, I.D. Feranchuk, A.P. Ulyanenkov, *Parametric X-Ray Radiation in Crystals: Theory, Experiment and Applications* (Series: Springer Tracts in Modern Physics, Vol. 213 2005).

[86] G.Kurizki, M.Strauss, I.Oreg and N.Rostoker, Phys.Rev. **A 35** (1987) 3427 .

[87] V.G.Baryshevsky, Nucl. Instr. Methods **A 445** (2000) 281-283; LANL e-print archive physics/9806039.

[88] V.G.Baryshevsky, K.G. Batrakov, A.A. Gurinovich et al., Nucl. Instr. Methods **A 507** (2003) 137.

[89] V.G.Baryshevsky, A.A. Gurinovich, LANL e-print arXiv: physics/0409107.

[90] A. L. Pokrovsky and A. L. Efros, Phys. Rev. **B 65** (2002) 045110 .

[91] A. L. Pokrovsky, Phys. Rev. **B 69** (2004) 195108 .

[92] E. I. Smirnova, C. Chen, M. A. Shapiro et al., J. Appl.Phys. **91**, 3 (2002) 960.

[93] E. I. Smirnova and C. Chen, M. A., J. Appl.Phys. **93**, 10, (2003) 5859 .

[94] N.S.Ginzburg, A.S.Sergeev, N.Yu.Peskov et al., Nucl. Instr. Methods **A 375** (1996) 202 .

[95] Iv.V. Konoplev, A.W. Cross, W. He, A.D.R. Phelps, K. Ronald, G. R. M. Robb, C. G. Whyte, N. S. Ginzburg, N. Yu. Peskov and A. S. Sergeev, Nucl. Instr. Methods **A 445** (2000) 236.

[96] A.W. Cross, W. He, I.V. Konoplev, A.D. R. Phelps, K. Ronald, G. R. M. Robb, C. G. Whyte, N. S. Ginzburg, N. Yu. Peskov and A. S. Sergeev, Nucl. Instr. Methods **A 475** (2001) 164.

[97] I.V. Konoplev, A.D.R. Phelps, A.W. Cross, K. Ronald, P. McGrane, W. He, C.G. Whyte, N.S. Ginzburg, N.Yu. Peskov, A.S. Sergeev and M. Thumm, Nucl. Instr. Methods **A 528** (2004) 101.

[98] N.S. Ginzburg, N. Yu. Peskov,A. S. Sergeev, I. V. Konoplev, K. Ronald, A. D. R. Phelps and A. W. Cross, Nucl. Instr. Methods **A 528** (2004) 78.

[99] M.Born, E.Wolf, *Principles of optics: Electromagnetic Theory of Propagation, Interference and Diffraction of Light* (Pergamon Press, 1965)

[100] V.V. Nikolsky, *Electrodynamics and propagation of radio-wave* (Nauka, 1978).

[101] Hönl H., Maue A., Wespfahl K., *Theorie der Beugung* (Berlin:Springer-Verlag, 1961).

[102] K.G.Batrakov and S.N.Sytova, Computational Mathematics and Mathematical Physics **45**, 4, (2005) 666.

[103] V.G. Baryshevsky, N.A. Belous, V.A. Evdokimov, A.A. Gurinovich, A.S. Lobko, P.V. Molchanov, P.F. Sofronov, V.I. Stolyarsky, LANL e-print arXiv: physics/0605122.

[104] T.C. Marshall, *Free-Electron Lasers* (Macmillan Publishing Company, London, 1985).

[105] V.G.Baryshevsky, K.G.Batrakov, I.Ya.Dubovskaya, Nucl. Instr. Methods **A 358** (1995) 493-496.

[106] N. S. Yerokhin, M. V. Kuznetsov, S. S. Moiseev, et al. *Nonequilibrium and Resonance Processes in Plasma Radiophysics* (Nauka, Moscow (1982)) [in Russian].

[107] V.G.Baryshevsky, K.G.Batrakov, V.I.Stolyarsky in : *Proceedings of 21 FEL Conference* (1999) 37-38.

[108] A.Gover, Z. Livni, Optics Commun. **26** (1978) 375.

[109] J.R.Pierci, *Travelling wave tubes* (Van Nostrand, Princeton, 1950);

[110] V.G.Baryshevsky, K.G.Batrakov, I.Ya. Dubovskaya, V.A.Karpovich, V.M.Rodionova, Nucl. Instr. Methods **A 393** (1997) 71-75.

[111] V.L.Granatstein, R.K.Parker and C.M.Armstrong, Proceedings of the IEEE **87**, 5, (1999) 702-716.

[112] V.G. Baryshevsky, K.G. Batrakov, N.A. Belous, A.A. Gurinovich, A.S. Lobko, P.V. Molchanov, P.F. Sofronov, V.I. Stolyarsky, LANL e-print archive: physics/0409125.

[113] S.Takagi, Acta Crystall. **15** (1962) 1311.

[114] M.P.Batura, A.A.Kuraev, A.K.Sinitzyn, *Simulation and optimization of powerful microwave devices* (Minsk, 2006) [in Russian]

[115] T.J.Orzechovsky, B.R.Anderson, J.C.Clark et.al., Phys.Rev.Lett. **57** (1986) 2172.

[116] A. Yariv and P. Yeh, *Optical Waves in Crystals* (Wiley, 1984).

[117] V.G. Baryshevsky, A.A. Gurinovich, Nucl. Instr. and Methods in Physics Research **B 252**, 1, (2006) 92-101.

[118] V.G. Baryshevsky, I.Ya Dubovskaya in : *Abstarcts of reports at 14th All-Union Conference on the Physics of Interaction of Charged Particles with Crystals*, Izd-vo Mosk. Univ., Moscow, 1984, p. 50.

[119] V.G. Baryshevsky, I.Ya Dubovskaya in: *Proceedings of the 15th All-Union Conference on the Physics of Interaction of Charged Particles with Crystals*, Izd-vo Mosk. Univ., Moscow, 1986, pp. 60-62.

[120] A.M. Fedorchenko, I. Ya. Kotzarenko, *Absolute and Convective instability in Plasma and Solids* (Moscow, 1981) [in Russian].

[121] V.I. Fadeeva, I.M. Terentiev, *Value Tables of the Probability Integral of the Complex Argument* (Moscow, 1954) [in Russian].

[122] V.G. Baryshevsky, I.D. Feranchuk, Pis'ma Zh. Tekh. Fiz. **10**, 19, (1984) 1157-1159.

[123] V.G. Baryshevsky, Doklady Akad. Nauk BSSR **15** (1971) 306.

[124] V.G. Baryshevsky, I.D. Feranchuk, Zh. Eksp. Teor. Fiz. **61** (1971) 944 [Sov. Phys. JETP **34**(1972) 50; Errata, ibid **64** (1973) 760 [**37** (1973) 605].

[125] V.G. Baryshevsky, A.O. Grubich, Le Tien Hai, Zh. Eksp. Teor. Fiz. **94** (1988) 51 [Sov. Phys. JETP **67**(1988) 895].

[126] V.G. Baryshevsky, I.D. Feranchuk, Phys. Lett **A 57** (1976) 183.

[127] V.G. Baryshevsky, I.D. Feranchuk, Nucl. Instr. Methods **A 228** (1985) 490.

[128] A. Caticha, Phys. Rev. **A 40**,8 (1989) 4322-4329.

[129] A. Caticha, Phys. Rev. **B 45**, 17 (1992) 9541-9550.

[130] H.Nitta, Phys. Lett. **A 158**, 5(1991) 270-274.

[131] H.Nitta, Phys. Rev. **B 45**, 14(1992) 7621-7626.

[132] R.B. Fiorito, D.W. Rule, M.A. Piestrup, Li Qiang, A.H. Ho, X.K. Maruyama, NIM **B79**, 1-4, (1993) pp. 758-761

[133] R. B. Fiorito, D. W. Rule, M. A. Piestrup, X. K. Maruyama, R. M. Silzer, D. M. Skopik, and A. V. Shchagin Phys. Rev. **E 51** (1995) R2759.

[134] V.G. Baryshevsky et al., Nucl. Instr. Methods **A 249** (1993) 304.

[135] Yu.N. Adishchev et al., Nucl. Instr. Methods **B 44**, 2, (1989) 130-136.

[136] J. Freudenberger, V. B. Gavrikov, M. Galemann, H. Genz, L. Groening1, V. L. Morokhovskii, V. V. Morokhovskii, U. Nething, A. Richter, J. P. F. Sellschop, and N. F. Shul'ga, Phys. Rev. Lett. **74**, 13, (1995) 24872490.

[137] V.G. Baryshevsky, K.G. Batrakov, I.Ya Dubovskaya in : *Proceedings of the All-Union Conference on the Physics of Interaction of Charged Particles with Crystals*, Izd-vo Mosk. Univ., Moscow, 1990.

[138] V.G. Baryshevsky, K.G. Batrakov, I.Ya Dubovskaya in: *Abstracts of the All-Union Conference on the Physics of Interaction of Charged Particles with Crystals*, Izd-vo Mosk. Univ., Moscow, 1990 p. 88.

[139] V.G. Baryshevsky, I.Ya. Dubovskaya, *Diffraction phenomena in spontaneous and stimulated radiation by relativistic particles in crystals* (Review) (1991) Technical Report Lawrence Berkeley Lab., CA (United States) DOI 10.2172/5808050

[140] M.L. Ter-Mikaelian, Usp. Fiz. Nauk **171**, n. 6, (2001) 597 [Sov. Phys. Uspekhi **44** (2001) 571-596].

[141] Ulrik I. Uggerhøj, Rev. Mod. Phys. **77**, 4, (2005) 1131-1171 .

[142] R. Yabuki, H. Nitta, T. Ikeda and Y. H. Ohtsuki, Phys. Rev. **B 63**, 17, (2001) 174112.

[143] T. Ikeda, Y. Matsuda, H. Nitta, Y. H. Ohtsuki, Nucl. Instr. Methods **B 115**, 1-4, (1996) 380.

[144] Y. Matsuda, T. Ikeda, H. Nitta, H. Minowa, Y. H. Ohtsuki, Nucl. Instr. Methods **B 115**, 1-4, (1996) 396-400.

[145] K.B. Korotchenko, Yu.L. Pivovarov, T.A. Tukhfatullin, Nucl. Instr. Methods **B 266**, 17, (2008) 3753-3757.

[146] V. G. Baryshevsky, Nucl. Instr. Methods **B 122**, 1, (1997) 13-18.

[147] V.G. Baryshevsky, Vesti AN BSSR, Ser. phiz-math nauk, **1** (1992) 31-37.

[148] A. Kostyuk, A. V. Korol, A. V. Solov'yov and W. Greiner, Journal of Physics B **43**, 15, (2010) 151001.

[149] V. G. Baryshevsky and K. G. Batrakov, Nucl. Instrum. Methods **A 483** (2002) 531533.

[150] V.G. Baryshevsky, K.G. Batrakov, LANL e-print arXiv:physics/0209028v1 [physics.optics].

[151] V. G. Baryshevsky, K. G. Batrakov and I. Ya. Dubovskaya Nucl. Instr. Methods **A 375**, 1-3,(1996) 292-294.

[152] V.G. Baryshevsky and A.A. Gurinovich, Proc. FEL'06, Berlin, August 2006, TUPPH013, p.335, http://www.JACoW.org; LANL e-print arXiv:physics/0608068v1[physics.acc-ph].

[153] D.A. Baklanov, I.E. Vnukov, V.K. Grishin, Yu.V. Zhandarmov, A.N. Ermakov, G.P. Pokhil, R.A. Shatokhin, Preprint MGU 2008-1/837, 14p.

[154] "Charged and Neutral Particles Channeling Phenomena - Channeling 2008", Proceedings of the 51st Workshop of the INFN Eloisatron (Project S.B. Dabagov and L. Palumbo, Eds., World Scientific, 2010) (The Science and Culture series - Physics, Series Ed. A. Zichichi)

[155] W. Wagner, B. Azadegan, H. Büttig, J. Pawelke, M. Sobiella, L. Sh. Grigoryan, in: "Charged and Neutral Particles Channeling Phenomena - Channeling 2008", Proceedings of the 51st Workshop of the INFN Eloisatron (Project S.B. Dabagov and L. Palumbo, Eds., World Scientific, 2010) (The Science and Culture series - Physics, Series Ed. A. Zichichi) pp. 378-407.

[156] A.V. Korol, A.V. Solov'yov and W. Greiner, Journal of Physics **G 24**, 5 (1998) L45-L53.

[157] A.V. Korol, A.V. Solov'yov and W. Greiner, International Journal of Modern Physics **E 8**, 1 (1999) 49-100.

[158] V. T. Baranov, S. Bellucci, V. M. Biryukov, G. I. Britvich and C. Balasubramanian, et al., JETP Lett. **82**, 9 (2005) 562-564.

[159] V.G. Baryshevsky, Dok. Akad. Nauk BSSR **31**, 12 (1987) 1090-1092.

[160] A. R. Mkrtchyan, H. A. Aslanyan, A. H. Mkrtchian, R. H. Gasparian, A. Kh. Mkhitarian, G. M. Garibian, R. H. Avakian, S. P. Taroyan, A. E. Avetisyan, H. S. Kisogyan, K. R. Dallakyan, V. A. Gyurdzhyan, S. S. Danagulyan, G. M. Elbakyan and, Ye. M. Boyakhchyan, Solid State Commun. **79**, 4 (1991) 287-288.

[161] A. R. Mkrtchyan, A. H. Mkrtchian, H. A. Aslanyan, et al, Izv. Akad. Nauk. Arm. SSR, Fizika **47** (2005) 282.

[162] P.N. Zhukova, M.S. Ladnykh, A. H. Mkrtchian, A. R. Mkrtchyan, N.N. Nasonov, Pis'ma Zh. Tekh. Fiz. **36**, 21 (2010) 29-37.

[163] V.G. Baryshevsky, A.A. Gurinovich LANL e-print arXiv: physics.acc-ph/1011.2983

[164] V.G. Baryshevsky, K.G. Batrakov, V.A. Evdokimov, A.A. Gurinovich, A.S. Lobko, P.V. Molchanov, P.F. Safronov, V.I. Stolyarsky, Nuclear Instruments and Methods **B 252**, 1, (2006) 86-91 .

[165] V.G. Baryshevsky, E.A. Gurnevich The possibility of Cherenkov radiation generation in a photonic crystal formed by parallel metallic threads, in: *Proceedings of 2010 International Kharkov Symposium on Physics and Engineering of Microwaves, Millimeter and Submillimeter Waves (MSMW)*, 21-26 June 2010. DOI: 10.1109/MSMW.2010.554 6019, p. 1-3.

[166] V.G. Baryshevsky, A.A. Gurinovich, LANL e-print arXiv:0903.0300v1 [physics.acc-ph]

[167] L.S. Bogdankevich and A.A. Rukhadze, Sov. Phys.Usp. **14**, 2, (1971) 163-189.

[168] A.E. Dubinov, V.D. Selemir, Radiotekhnika i electronika. **47** (2002) 645.

[169] A.E. Dubinov, I.A.Efimova, Technical Physics **46**, 6, (2001) 723-728.

[170] A.E. Dubinov et al., patent RU 2221306 C2

[171] A.E. Dubinov et al., Izv. VUZov, Fizika **6** 67 (1999)

[172] Clayborne D. Taylor, D.V.Giri, *High-Power Microwave systems and effects* (Taylor and Francis, 1994).

[173] V.D. Selemir, A.E. Dubinov, B.G Ptitsyn, K.S. Shilin, patent RU 2260870 C1

[174] V. D. Selemir, A. E. Dubinov, E. E. Dubinov, I. V. Konovalov and A. V. Tikhonov, Technical Physics Lett. **27**, 7, 583-585 (2001).

[175] Baryshevsky V.G., Belous N.A., Gurinovich A.A. et al, in: *Proceedings of the 28th Intern. Free Electron Laser Conference FEL2006* (2006) 331-334.

[176] Baryshevsky V.G., Gurinovich A.A. in: *Proceedings of the 28th Intern. Free Electron Laser Conference FEL2006* (2006) 335-338.

[177] V.G.Baryshevsky, N.A.Belous, A.A.Gurinovich et al, in: *Proceedings of the 29th Intern. Free Electron Laser Conference FEL2007* (2007) TUPPH012.

[178] D.D. Ryutov, Pis'ma Zh. Tekh. Fiziki **1** (1975) 581.

[179] R.A. Richardson, J. Denavit, M. S. Di Capua, and P. W. Rambo J.Appl.Phys. **69** 6261-6272 (1991).

[180] R.J. Adler, B.Sabol, G.F. Kiuttu, IEEE Trans. **NS-30**, 4, 3198-31200 (1983)

[181] V. Baryshevsky, K. Batrakov, A. Gurinovich, I. Ilienko, A. Lobko, V. Moroz, P. Sofronov, V. Stolyarsky Nucl. Instr. Methods **A 483** (2002) 21-23.

[182] V.G.Baryshevsky et al., Eurasian Patent 004665 B1

[183] D.I.Trubeckov, A.E.Hramov, *Lectures on microwave electronics for physicists* (Moscow, FIZMATLIT, 2004) [in Russian].

[184] R. A. Silin, *Periodic Waveguides* (Phasis, Moscow, 2002) [in Russian].

[185] R.A.Silin, V.P.Sazonov, *Slow-wave structures* (Soviet Radio, Moscow, 1966) [in Russian]; R.A. Silin and V.P. Sazonov, *Slow Wave Structures* National Lending Library for Science and Technology, Boston SPA, Eng (1971).

[186] V.G. Baryshevsky, Doklady Akademy of Science of Belarus SSR, v.31, n.12 (1987) 1089.

[187] L.D. Landau, E.M. Lifshitz, *The Classical Theory of Fields* in: L.D. Landau, E.M. Lifshitz *Course of Theoretical Physics* Vol. 2 (Pergamon Press, 4ed., 1975).

[188] L.D.Landau, E.M.Lifshitz, L.P.Pitaevskii, *Electrodynamics of Continuous Media* in: L.D. Landau, E.M. Lifshitz *Course of Theoretical Physics* Vol. 8 (Butterworth Heinemann, 2ed., 1984).

[189] L.P.Pitaevskii, E.M.Lifshitz, *Physical Kinetics* in: L.D. Landau, E.M. Lifshitz *Course of Theoretical Physics* Vol. 10 (Butterworth Heinemann, 1981).

[190] Z. G., Pinsker, *Dynamical scattering of X-rays in crystals* (Springer-Verlag Berlin, Heidelberg, New York, 1978).